

144
AFAPL-TR-72-74

AD 749131

EXPANDABLE AIRLOCK EXPERIMENT (DO21) AND THE SKYLAB MISSION

Lou Manning

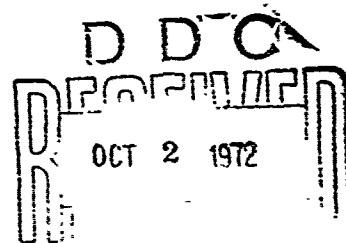
Leo Jurich

Goodyear Aerospace Corporation

TECHNICAL REPORT AFAPL-TR-72-74

September 1972

Report of
NATIONAL TECHNICAL
INFORMATION SERVICE
Springfield, Mass.



Approved for public release;
distribution unlimited

Air Force Aero Propulsion Laboratory
Air Force Systems Command
Wright-Patterson Air Force Base, Ohio

Ras

NOTICE

When Government drawings, specifications, or other data are used for any purpose other than in connection with a definitely related Government procurement operation, the United States Government thereby incurs no responsibility nor any obligation whatsoever; and the fact that the government may have formulated, furnished, or in any way supplied the said drawings, specifications, or other data, is not to be regarded by implication or otherwise as in any manner licensing the holder or any other person or corporation, or conveying any rights or permission to manufacture, use, or sell any patented invention that may in any way be related thereto.

ACCESSION for	
NTIS	WFOC Section <input checked="" type="checkbox"/>
DOC	Est. Section <input type="checkbox"/>
UNANNOUNCED	<input type="checkbox"/>
JUSTIFICATION	
BY	
DISTRIBUTION/AVAILABILITY CODES	
Dist.	AVAIL. 220/50/100
A	

Copies of this report should not be returned unless return is required by security considerations, contractual obligations, or notice on a specific document.

Unclassified

Security Classification

DOCUMENT CONTROL DATA - R & D

(Security classification of title, body of abstract and indexing annotation must be entered when the overall report is classified)

1. ORIGINATING ACTIVITY (Corporate author) Goodyear Aerospace Corporation 1210 Massillon Road Akron, Ohio 44315		2a. REPORT SECURITY CLASSIFICATION Unclassified	
		2b. GROUP	
3. REPORT TITLE Expandable Airlock Experiment (D021) and The Skylab Mission			
4. DESCRIPTIVE NOTES (Type of report and inclusive dates) Final Technical Report, 15 December 1966 - December 1971			
5. AUTHOR(S) (First name, middle initial, last name) Lou Manning and Leo Jurich			
6. REPORT DATE September 1972		7a. TOTAL NO. OF PAGES 283	7b. NO. OF REFS 8
8a. CONTRACT OR GRANT NO. F33615-67-C-1380		9a. ORIGINATOR'S REPORT NUMBER(S) GER-15607	
b. PROJECT NO. 8170			
c. Task No. 817004		9b. OTHER REPORT NUMBER(S) (Any other numbers that may be assigned this report) AFAPL TR-72-74	
d.			
10. DISTRIBUTION STATEMENT Approved for public release; distribution unlimited			
11. SUPPLEMENTARY NOTES		12. SPONSORING MILITARY ACTIVITY Air Force Aero Propulsion Laboratory Wright Patterson Air Force Base, Ohio 45433	
13. ABSTRACT <p>The program was directed at evaluating the potential advantages of expandable structures to serve in certain space applications such as airlocks, crew quarters experiment chambers, emergency escape capsules, and crew transfer tunnels.</p> <p>The human factors characteristics and geometry were established after extensive underwater neutral buoyancy testing by the Air Force Aero Medical Laboratory. The airlock design dimensions were found adequate to accommodate the entry of a fully suited rescuer with back pack to rescue another crewman simulating an incapacitated condition. Hatch size, latching, and opening features, mobility restraints and lighting requirements were also established.</p> <p>The qualification test program was conducted at both GAC-Akron, and Arnold Engineering & Development Center (AEDC), Tullahoma, Tennessee.</p> <p>Material samples of the airlock structure were subjected to simulated micro-meteoroid penetration tests and exposed to simulated space radiation and hard vacuum environments with confirmation of the engineering analyses.</p> <p>The qualification test unit (identical to flight hardware) was subjected to extremes of temperature, vacuum, and solar radiation in both the packaged and deployed state. Functional deployments were conducted in a vacuum chamber at cold temperature. Numerous pressurization cycles were conducted to verify structural adequacy. In the packaged state, the unit was subjected to shock, vibration, and acceleration tests to simulate transportation, handling and launch environments.</p>			

Security Classification

14

KEY WORDS

LINK A

LINX B

LINK C

[illegible]

WT

[illegible]

WT

[illegible]

447

Expandable Structures

Expandable Airlock

Emergency Escape Capsule

Crew Transfer Tunnel

Experiment Chamber

Security Classification

EXPANDABLE AIRLOCK EXPERIMENT (D021)

AND THE SKYLAB MISSION

Lou Manning
Leo Jurich

Approved for public release;
distribution unlimited

FOREWORD

This report was prepared by the Goodyear Aerospace Corporation (GAC), Akron, Ohio under USAF Contract F33615-67-C-1380, Project Number 8170, Task Number 817004. The work was administered under the direction of Mr. F. W. Forbes (DOY) for the Air Force Aero Propulsion Laboratory.

The program was started 15 December 1966 and final delivery of hardware was made December 1971.

Mr. Leo Jurich was the initial project manager for GAC at the start of the program and shortly thereafter turned the assignment over to Lou Manning to complete the effort. The contractor's identification number for this report is GER-15607.

This report was submitted by the authors September 1972.

Publication of this report does not constitute Air Force approval of the report's findings or conclusions. It is published only for the exchange and stimulation of ideas.



Blackwell C. Dunnam
Chief, Technical Operation Office

ABSTRACT

This report presents the results of Goodyear Aerospace Corporation's (CAC) program effort under Contract F33615-67-C-1380 for the Air Force Aero Propulsion Laboratory, Air Force Systems Command, United States Air Force.

The program was directed at evaluating the potential advantages of expandable structures to serve in certain space applications such as airlocks, crew quarters experiment chambers, emergency escape capsules and crew transfer tunnels. A configuration of a one-man expandable airlock was chosen as the candidate design most appropriate for an early evaluation.

The human factors characteristics and geometry were established after extensive underwater neutral buoyancy testing by the Air Force Aero Medical Laboratory. The airlock design dimensions were found adequate to accommodate the entry of a fully suited rescuer with back pack to rescue another crewman simulating an incapacitated condition. Hatch size, latching, and opening features, mobility restraints and lighting requirements were also established

Prototype training hardware was delivered in 1970. The first unit was installed in a KC-135 airplane and evaluated in numerous zero-gravity flight maneuvers by Air Force personnel, as well as NASA astronauts and other interested parties. The one-G realistic trainer was displayed at the Second National Conference on Space Maintenance and Extravehicular Activities held at Los Vegas, Nevada August 6-8, 1968. Later it was delivered to McDonnell-Douglas Astronautics Corporation - E. D. (MDAC). In a subsequent shipment of this unit back to CAC-Akron for a Critical Design Review, the article was badly damaged by the commercial carrier in a loading accident. It later was temporarily repaired and demonstrated at the Skylab Training Hardware Crew Systems Review held at Huntsville, Alabama November 16-20, 1970.

The qualification test program was conducted at both CAC-Akron, and Arnold Engineering & Development Center (AEDC), Tullahoma, Tennessee.

Material samples of the airlock structure were subjected to simulated micrometeoroid penetration tests and exposed to simulated space radiation and hard vacuum environments with confirmation of the engineering analyses.

The qualification test unit (identical to flight hardware) was subjected to extremes of temperature, vacuum, and solar radiation in both the packaged and deployed state. Functional deployments were conducted in a vacuum chamber at cold temperature. Numerous pressurization cycles were conducted to verify structural adequacy. In the packaged state, the unit was subjected to shock, vibration, and acceleration tests to simulate transportation, handling and launch environments.

Flight and backup hardware units were completed and awaiting minor updating changes when the cancellation of the Skylab mission was received.

TABLE OF CONTENTS

<u>Section</u>	<u>Title</u>	<u>Page</u>
I	INTRODUCTION.	1
II	EXPERIMENT DESCRIPTION.	2
	A. General	2
	B. Chronological Evolution	3
	1. Preliminary Design.	3
	2. Operational Airlock Study	5
	3. Miscellaneous Design Improvements	7
	4. Weight Reduction Program.	8
	5. Skylab Impact on D021	9
	6. Critical Design Review.	10
	7. Experimental Integration and Test Requirements Review.	12
	C. Final Design Configuration.	13
	1. Expandable Structure and Equipment Assembly - P/N 66QS1512.	13
	2. Design Analyses and Supporting Data	33
III	TEST PROGRAM.	67
	A. Materials Evaluation and Development Tests.	67
	B. Simulated Micrometeoroid Impact Tests	67
	C. Environmental Qualification Tests	70
	1. Launch Profile Pressure Simulation.	72
	2. Launch Accelerations.	72
	3. Vibration	73
	4. Acoustic Noise.	73
	5. Cold Temperature Deployment	73
	6. Cold Environmental Tests.	73
	7. Solar Environment Tests	73
IV	AEROSPACE GROUND EQUIPMENT (AGE).	75
V	CONCLUSIONS	79
	REFERENCES	269

Appendix		Page
I	List of Attendees and Minutes of D021/D024 Experiments Critical Design Review.	81
II	GAC Action Items Accomplished as Established at Test Requirements Reviews.	91
III	Thermal Analysis.	102
IV	Thermal Analysis Computer Run	114
V	Determination of Organic Off-Gassing Products and Carbon Monoxide for D021 Airlock Nonmetallic Materials	128
VI	D021 Airlock Nonmetallic Materials Compliance With ASPO-RQTD-D67-5A (May 3, 1967).	134
VII	Leak Test Calculations.	143
VIII	Failure Analysis and Corrective Action Report	147
IX	Fungus, Salt Fog and Acoustic Tests	160
X	Illustrations and Tables Extracted from AEDC-TR-70- 262	190
XI	Engineering Reports of Deployment Verification Tests Performed at GAC.	231
XII	D021/D024 Vibration Test Requirements	257

LIST OF ILLUSTRATIONS

Figure		Page
1	D-21 Packaged Configuration	3
2	D-21 Expanded Configuration	4
3	Airlock Located on SSES Trusses.	4
4	Elastic Recovery Materials Technique.	5
5	Functional Sequence Diagram	6
6	Instrumentation-Telemetry	6
7	D021 Skylab Configuration	9
8	D021 and D024 Material Samples - Original Location.	11
9	Dimensional Clearance Envelope Packaged and Deployed - D021	15/16
10	Expandable Structure.	
11	Hatch Assembly.	18
12	Outer Cover	19
13	Pressure Bladder.	19
14	Method of Joining Flexible Structure to Rigid Structure	20
15	Packaging Harness	22
16	Harness Installed	22
17	Harness Released.	23
18	Airlock Deployed.	23
19	Thermal Blanket Installed on Packaged Airlock . . .	24
20	Internal Mobility Aids.	25
21	Qualification Hardware - Exterior Controls and Instrumentation Interface	25
22	Qualification Hardware - Electrical Interface-Base Unit.	26
23	Interior View of Base Section	26
24	System Schematic - Airlock Pressurization	28
25	Electrical System Block Diagram	29
26	Telemetered Instrumentation Schematic	32
27	Optical Deployed and Packaged Properties - D021 Airlock Experiment.	42
28	Original Orientation/Final Location - Thermal Model.	44

Figure		Page
29	Orbital Temperatures.	47
30	Near-Earth Micrometeoroid Environment	48
31	Case 1.	52
32	Case 2.	53
33	Case 3a	55
34	Case 3b	55
35	Case 3c	56
36	Case 4.	57
37	Case 5.	57
38	Case 6.	59
39	Case 7.	60
40	Case 8a	60
41	Case 8b	61
42	Case 8c	61
43	Case 9.	62
44	Case 10	63
45	DO21 Outer Cover and Thermal Control Coating	68
46	Outer Composite Less EPT Foam & Inner Liner	68
47	1 - LB/FT ³ Polyurethane Foam.	69
48	2 - LB/FT ³ Polyurethane Foam.	69
49	Ballistic Limit Test Results.	70
50	Airlock Vibration Profile	71
51	Airlock Control Simulator and Test Panel.	76
52	Drill Fixture Assembly.	77
53	Reusable Shipping Container	78
54	Fusistor Load Cycle Test Circuit.	99
55	Fusing Test Circuit	100
56	Fuse Test - Typical Oscillograph Record	101
57	Proposed Airlock Location	104
58	Temperature Excursions (Packaged Configuration)	106
59	Temperature Excursions (Deployed Configuration)	108
60	Deployed and Packaged Thermal Properties.	111
61	Composite Wall Off-Gassing.	130
62	Pressure Bladder Off-Gassing.	130

Figure		Page
63	Polyester Film Off-Gassing.	131
64	Polyether Foam Off-Gassing.	131
65	Outer Cover Off-Gassing	131
66	D-21 Composite Wall Flammability Test (Upward) - Packaged Configuration.	139
67	D-21 Composite Wall Flammability Test (Upward) - Deployed Configuration.	140
68	D-21 Composite Wall Flammability Test (Outer Cover Side)	141
69	D-21 Composite Wall Flammability Test (Pressure Bladder Side)	142
70	Acoustic Test Spectrum.	172
71	Acoustic Spectrum Plot - Rec. No. 1 - Microphone 1. . .	173
72	Acoustic Spectrum Plot - Rec. No. 2 - Microphone 2. . .	174
73	Acoustic Spectrum Plot - Rec. No. 3 - Microphone 3. . .	175
74	Acoustic Spectrum Plot - Rec. No. 4 - Microphone 1. . .	176
75	Acoustic Spectrum Plot - Rec. No. 5 - Microphone 2. . .	177
76	Acoustic Spectrum Plot - Rec. No. 6 - Microphone 3. . .	178
77	Packaged D-21 Airlock	191
78	Deployed D-21 Airlock	192
79	Airlock Axes Orientation.	193
80	Airlock Pressure System	194
81	Centrifuge Schematic.	195
82	Vibration System Schematic.	196
83	Vibration Equipment	197
84	Aerospace Research Chamber (12V).	198
85	Auxiliary Vacuum Chamber.	199
86	Solar Shield.	200
87	Heat Flux Schematic	201
88	Accelerometer Location.	202
89	Vacuum Test Instrument Schematic.	205
90	Deployment Thermocouple Location.	206
91	Vacuum Environment Thermocouple Location.	207
92	Launch Pressure Simulation.	208
93	Acceleration versus Time.	209
94	Thermal Blanket Separation.	210

Figure		Page
95	Acceleration Windscreen	211
96	Vibration Spectrum.	212
97	Deployment String Snag.	214
98	Deployment Surface Scratch.	215
99	Blister from Photographic Light	216
100	Solar Damage.	217
101	Solar Damage.	218
102	Typical Internal Airlock Pressure Cycle	219
103	Pressure Degradation during 12-Hour Leak Test	220
104	Temperature Change During Solar And Pressure Changes. .	221
105	Pressure During Solar Leak Test	225
106	D-21 Airlock Deployment	235
107	Vacuum Chamber Deployment	236
108	Typical Tear of Outer Cover Caused by Low Temperature Deployment.	238
109	Compressive Load - PSI @ 20% Deflection	239
110	Deployment Test Schematic	241
111	D-21 Airlock Deployment at 150,000 Feet	242
112	D-21 Airlock - Modified Inflation and Pressurization System Schematic.	244
113	Pressurization Cycle.	245
114	Pressurization System and Instrumentation	251
115	Thermocouple Location - Special Test Thermocouples. . .	252
116	Airlock Integral Temperature Sensors.	253
117	D-21 Airlock Deployment	254
118	Low Temperature Vacuum Chamber Deployment - Internal Pressure of Preshaping Bottle	255
119	D-21 Airlock Low Temperature Vacuum Chamber Deployment.	256
120	Materials Samples and Return Container Vibration Test Criteria.	264
121	Airlock Experiment Vibration Profile.	265

LIST OF TABLES

Table		Page
I	Unit Weight Breakdown	14
II	Instrumentation Subsystem	34
III	D021 Airlock Weight Summary (Final Configuration) . . .	43
IV	Power Profile	64
V	D021 Airlock Electrical Load Analysis	65/66
VI	D-21 Fusistor Blow Test (IRC Spec A-0306)	98
VII	Resonance Vibration Response.	226
VIII	Cold Environment Test	227
IX	Solar Cycle Data.	228

LIST OF ABBREVIATIONS

<u>Abbreviation</u>	<u>Nomenclature</u>
SSESM	Spent Stage Experiment Shop Module
OWS	Orbital Work Shop
ATM	Apollo Telescope Mount
A/M	Airlock Module
MDA	Multiple Docking Adapter
AAP	Apollo Applications Program
STS	Structural Transition Section
MOL	Manned Orbital Laboratory
EQT	Environmental Qualification Test
PDA	Pre-Delivery Acceptance
PIA	Pre-Installation Acceptance
AFAPL	Air Force Aero Propulsion Laboratory
MSC	Manned Spacecraft Center
MSFC	George C. Marshall Space Flight Center
KSC	Kennedy Space Center
GAC	Goodyear Aerospace Corporation
MDAC-ED	McDonnell Douglas Astronautics Co. - Eastern Division
MM-DD	Martin Marietta Corp. - Denver Division
GT&R	Goodyear Tire & Rubber Co.

SECTION I

INTRODUCTION

This report covers the Goodyear Aerospace Corporation (GAC) effort conducted under Contract F33615-67-C-1380 for the Air Force Aero-Propulsion Laboratory (AFAPL) of Directorate of Laboratories, Air Force Systems Command, Wright-Patterson Air Force Base, Ohio. The program was aimed toward the advancement of expandable-type structures for certain applications in the National Space Programs where the unique properties of these types of structures offer definite advantages in less volume during launch, lower weight, greater structural efficiency, and functional versatility.

The orbital space stations and the Space Shuttle program will involve extravehicular activity (EVA) for various docking and maintenance activities. Airlocks and crew transfer tunnels are necessary adjuncts to such activities to reduce the atmosphere losses and maintain comfort of other crew members. Wherever such applications can benefit from the reduced launch volume or a flexible extendable section is required, the D021 Expandable Airlock Structural technology is now available to provide practical engineering solutions to the problem.

The original planning called for launching the D021 Experiment on NASA's Orbital Work Shop (OWS), which was an S-IV-B spent stage of the Saturn IB launch vehicle. The spent stage was to be purged and activated in orbit by astronauts rendezvousing from a later launch vehicle and converted to a workshop configuration. NASA's planning eventually progressed to the current version of the Skylab mission. These program evolutions created numerous perturbations in the D021 design requirements and interface restraints which are covered in this report.

The D021 hardware was in the final flight qualification stages when the orbital evaluation of the experiment was deleted by withdrawal of the experiment from the Skylab mission by the action of the Manned Space Flight Experiments Board.

Although the experiment was not flown, flight-type hardware was actually built, and successfully withstood the rigors of simulated launch and orbital environments. The experiment was also favorably evaluated in underwater neutral buoyancy and zero-gravity airplane maneuvers for ingress-egress capabilities. These ingress-egress tests were conducted by crewmen clothed in Apollo-type pressure suits to check out the hatch size, the hatch movement, the latching mechanism, the general size of the airlock, and the type and location of mobility aids. These tests further substantiated the capability of the design to maintain its deployed shape even when unpressurized.

The technology of expandable elastic recovery materials as used in the D021 Airlock Experiment has now been advanced to the point where only orbital testing remains for complete evaluation.

SECTION II

EXPERIMENT DESCRIPTION

A. GENERAL

The D021 Airlock Experiment is composed of the Expandable Airlock and the necessary support systems needed to deploy and pressurize the airlock from within the Skylab and telemeter the desired engineering data to earth.

An operational airlock would require as a minimum the following components:

- (1) The flexible airlock shell which provide: the desired airlock volume
- (2) One airlock ingress-egress hatch and operating mechanisms such as latches, hinges and handles (The hatch at the opposite end would be part of the vehicle and operate within the vehicle)
- (3) A packaging restraint harness and release system
- (4) Internal lighting
- (5) Mobility aids (Webbing handhold provided as required)
- (6) Two manual pressure release valves (one in each hatch)
- (7) A pressure suit umbilical connection for life support and communication lines

As an initial experiment certain additional equipment must be provided to obtain engineering data for adequate functional evaluation. The weight of these latter items is as much as that of the basic airlock. This additional equipment is listed below.

- (1) Pressurization System* - N_2 gas in high pressure containers is provided for 3 complete pressurization cycles. (See Subsection 3 of this section for an early version which provided 5 pressure cycles)
- (2) Pressure and temperature sensing and signal conditioning equipment
- (3) Battery pack power supply for the pyrotechnically operated pressurization sequence valves.
- (4) Pressure bulkhead and support structure for equipment mounting.

* In normal use as an operational airlock, the vehicle atmosphere is bled into the airlock and later discharged to space by means of vent valves.

The specific objectives of the experiment were:

- (1) To validate the airlock design using the elastic recovery materials approach
- (2) To evaluate the packaging and deployment dynamics
- (3) To provide a functional evaluation of the airlock
- (4) To study the effects of the space environments on the expandable structure materials
- (5) To evaluate the airlock structural stiffness during astronaut ingress-egress maneuvering.

These objectives were verified by subjecting materials and flight-type hardware to simulate transportation, storage, launch, and orbital environments as defined in Reference 1, the Skylab Cluster Requirements Specification. Only the actual flight verification of these results has not been performed.

B. CHRONOLOGICAL EVOLUTION

At the Preliminary Design Review held at the George C. Marshall Space Flight Center (MSFC) Orbital Workshop (OWS) Project Office on January 18 and 19, 1967, the experiment was configured as specified below.

1. Preliminary Design

a. Configuration. The airlock was configured as shown on Figure 1 for the packaged state during launch and as shown on Figure 2 in the deployed condition after orbit is achieved.

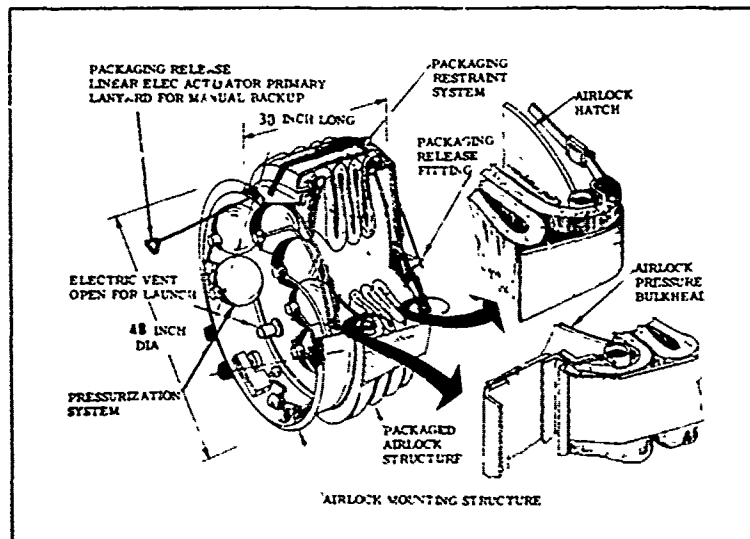


Figure 1. D-21 Packaged Configuration

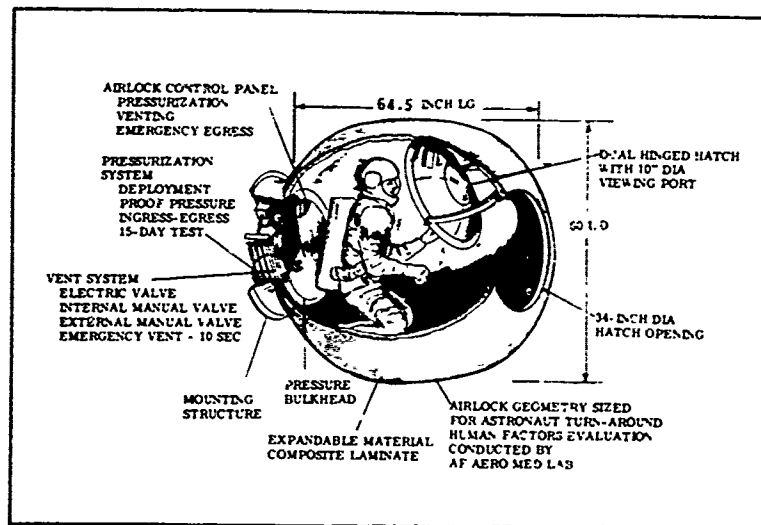


Figure 2. D-21 Expanded Configuration

The airlock was to be located on the Spent Stage Experiment Shop Module (SSESM) trusses as shown on Figure 3. EVA access was achieved by exit from the A/M EVA hatch then through the SSESM thermal curtain to the D021 experiment.



Figure 3. Airlock Located on SSESM Trusses

b. Airlock Materials. The expandable structure layers of the airlock are illustrated in Figure 4. This illustrates the "elastic recovery materials" approach. For packaging, a vacuum is applied to the space between the outer cover and the pressure bladder which collapses the section to approximately 1/4-inch thickness. The airlock is then packaged and the restraint harness is applied. Upon release of the harness, some relaxation of the structure occurs but final shape is achieved by pressurization of the airlock.

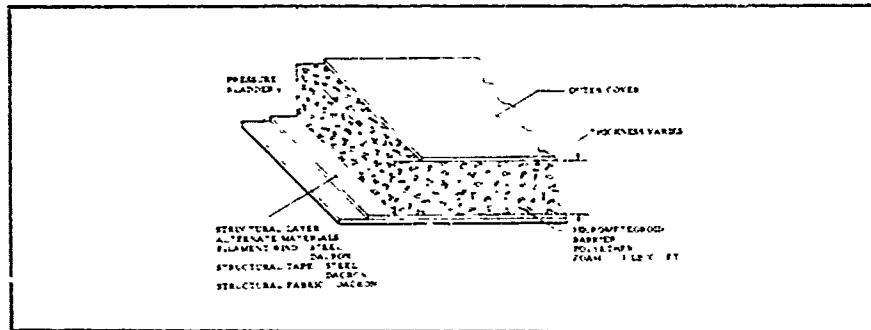


Figure 4. Elastic Recovery Materials Technique

A nominal pressure of approximately 0.1 to 0.2 psi is required to fully shape the airlock. Once deployed, the airlock demonstrates adequate rigidity even in the unpressurized state. After initial shaping, the airlock is pressurized to 3.5 psi working pressure.

Included as part of the experiment, two 6-inch by 6-inch sections of this material construction were attached to the exterior of the cylindrical mounting structure. These were to be recovered at the end of the mission by the astronauts and returned to earth for comparison of physical properties before and after exposure to the space environment.

c. Orbital Experiment. The functional sequence of the experiment as originally planned is shown on Figure 5. This early plan called for up to three EVA periods and involved two pressurization cycles of the airlock with an astronaut on the interior of the D021.

d. Instrumentation. Instrumentation was to be provided to measure inside and outside surface temperatures of the expandable section and monitor the internal pressure of airlock. This data would then be used to evaluate the thermal characteristics of the design and determine the gas tightness of the structure and hatch seals.

The instrumentation system was interfaced with the SSES telemetry system as shown on Figure 6 for transmittal to earth. High pressure transducers are also provided on each high pressure system for connection.

2. Operational Airlock Study

Early in the program, a brief study was performed to consider the possibility of using the D021 airlock in an operational configuration mounted

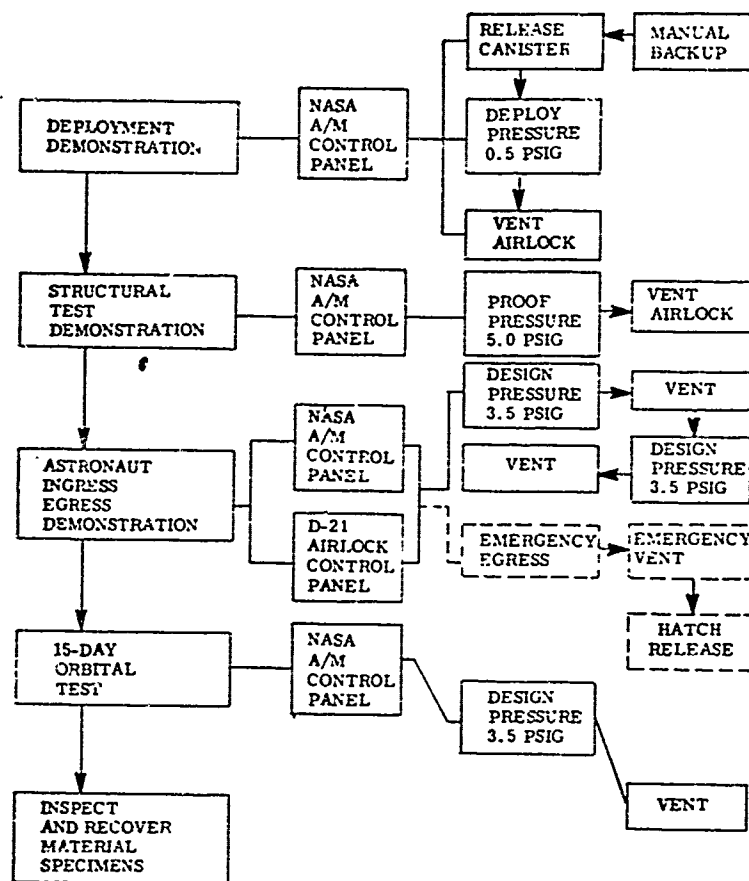


Figure 5. Functional Sequence Diagram

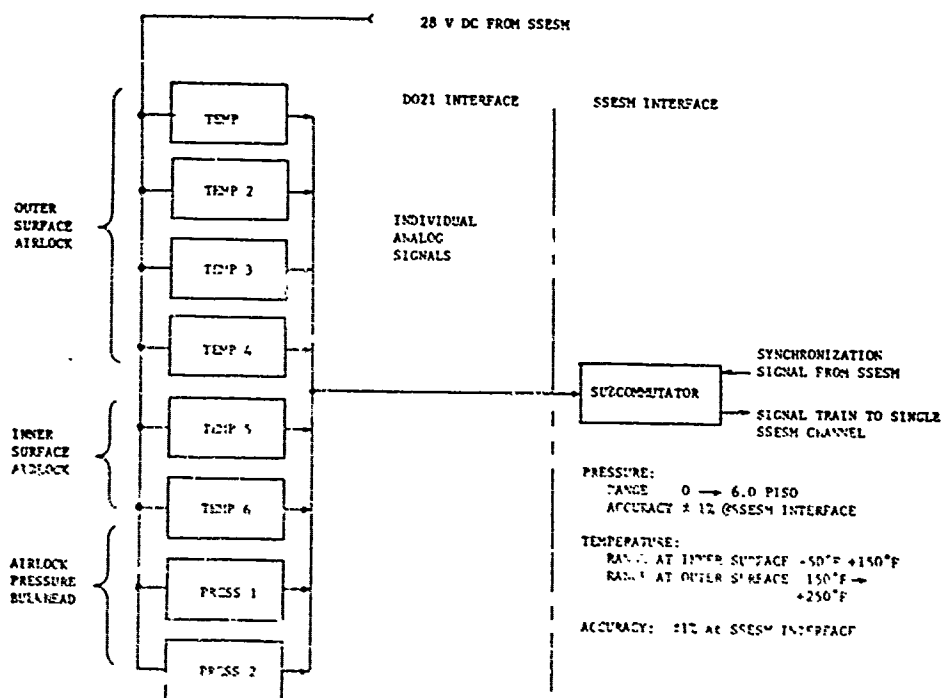


Figure 6. Instrumentation Schematics

on one of the Multiple Docking Adapter (MDA) docking ports. This would have provided a somewhat more realistic functional evaluation of the airlock design.

The study and subsequent reviews established the following major design considerations to be required for this alternate approach:

- (1) The design working pressure would have to be increased from 3.5 psi to 5.5 psi.
- (2) The size of the DO21 airlock would require an increase to a 2-man capacity to be compatible with standard EVA safety procedures.
- (3) Apollo-type probe or drogue connecting hardware would have to be incorporated on the DO21 airlock.
- (4) Provisions for jettisoning the airlock after the experiment was performed would be required in order to make the MDA port available for other purposes.
- (5) The DO21 experiment pressurization system would be replaced by valves opening to the MDA atmosphere.
- (6) Failure modes and safety measures would become more critical to the DO21/MDA relationship.

After reviewing the problem areas at several meetings attended by DOD, NASA and GAC, the alternate approach was dropped because the additional knowledge to be gained was not considered of enough value to warrant the added complexity, expense, and somewhat higher risk factor.

3. Miscellaneous Design Improvements

A number of design improvements were incorporated as the design work progressed and are discussed below.

a. Micrometeoroid Barrier. The original weight estimate for the micro-meteoroid barrier was based on the use of 1.0 lb/ft³ density polyurethane foam. It was found however that this material could not meet the non-flammability requirements stipulated by NASA Spec. MSC-A-D-66-3 Rev. A (issued 5 June 1967). Accordingly, it was necessary to substitute a heavier (2.0 lb/ft³ density) foam material (self-extinguishing in air to meet the specification requirements of "Category I"). The net effect of this material change was an added weight of 6.5 lbs.

b. Improved Bonding of Structural Layer. Subsequent to fabrication of the first two hardware units (qual unit and training unit), new bonding techniques were developed showing substantially improved bonding of the inter-ply structural layer in the composite materials of the airlock wall. Filament wound specimen fabrication of the structural layer indicated substantial bonding improvement between the angular windings. A change in the fabrication process was then initiated to provide this improved inter-ply adhesion through the use of additional bonding material (Taslan[®] yarn plus Vitel adhesive). This change

* T.M. duPont E.I. de Nemours & Co., Inc., Wilmington, Del.

was incorporated on the final two sets of hardware (the flight and backup units) and resulted in a 3 lb. increase to the experiment weight.

c. Locomotion Aids. During underwater neutral buoyancy evaluations, the addition of a rigid handhold ring at the hatch perimeter was found to be a desirable addition to the three internal and external webbing rings already provided. This resulted in a minor weight addition of less than one pound.

d. Thermal Insulation Cover. As a result of low temperature deployment tests and thermodynamic analyses, (see Subsection II. C. 2 and Section III) it was found necessary to add an insulation shroud to the D021 packaged configurations. The purpose of this shroud was to reduce the temperature extremes that would be experienced by the expandable structure portion of the airlock in the orbital environment.

This shroud consisted of a multilayer superinsulation blanket permanently attached at the lower circumference of the airlock and held in place against the surface with snap fasteners. This thermal shroud addition resulted in a weight increase of 3.0 lbs.

4. Weight Reduction Program

As the design progressed, it became apparent that the weight was becoming excessive. This was partially due to the design improvements which were added and partially to underestimating the amount of electrical systems required. In order to return to an acceptable weight, a weight reduction program was invoked to eliminate unnecessary hardware items which would not adversely affect the primary objectives of the experiment.

a. Revision to Pressurization System. Three pressurization bottles and associated plumbing were deleted. This deleted one working pressurization cycle and the proof pressurization cycle.

Deletion of the proof pressurization cycle was judged to be insignificant from a functional standpoint because of the extensive ground pressurization testing to be performed. Since two working cycle pressurizations were still available, the elimination of one was considered immaterial. A weight saving of approximately 21.5 pounds was achieved.

b. Deactivation of Hatch Jettisoning Feature. The need for a hatch jettisoning capability was eliminated when it was established that the astronauts would not be inside the D021 airlock during any pressurization cycle and could not physically close the hatch from the interior because of the umbilical line. This change consisted of deleting the pyrotechnic cartridge portion of the hatch pin pullers as well as the associated wiring. Approximately 11.0 pounds were saved by this deletion. This change was effective on flight units only.

c. Battery Pack Reduction. In connection with the above change, the number of Ni-CAD cells in each battery pack was reduced from 24 to 16 cells because of the reduced power requirements.

The potting compound was changed from an RTV silicone compound to polyurethane foamed in place, material of approximately 2.0 lbs/cu ft density.

A total savings of 6.0 pounds resulted from this change. This change was effective on flight units only.

The final configuration weight summary is given in Table III of Subsection II. C. 2.

5. Skylab Impact on D021

In mid 1969, the D021 Experimenter was informed of drastic changes being made to the OWS program by NASA. The original "wet" stage S-IV-B workshop was to be fully equipped and launched as a "dry" stage. The Apollo Telescope Mount (ATM) was added to the cluster and both payloads launched simultaneously using a Saturn V booster. This had serious impact on McDonnell Douglas Astronautics Company's (MDAC) A/M structure and in turn on the D021 Experiment. Aside from the mechanical interface changes, a number of new problems were created which took considerable time and effort to resolve. The major problems are discussed below.

First, with respect to finding a new location on the A/M structure for the D021, no suitable space near the A/M EVA hatch was available. After a thorough investigation by MDAC and numerous coordination meeting, with AFAPL, NASA and GAC, a location on the ATM support structure between the ATM solar arrays was selected as the only acceptable location available. This is illustrated on Figure 7.

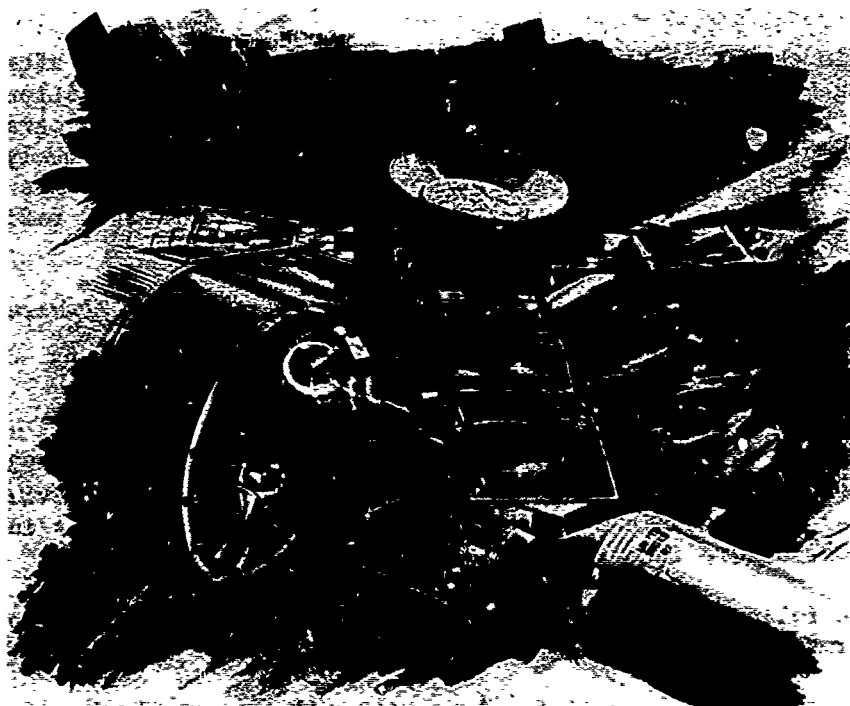


Figure 7. D021 Skylab Configuration

The major design criteria which governed this selection were:

- (1) Adequate space for deployment of the D021
- (2) Reasonable access to the D021 during EVA
- (3) Acceptable line of sight visibility from the Structural Transition Section (STS) windows
- (4) Reasonably unshaded environment with respect to the solar flux.

Second, the location and orientation of the D021 as finally selected resulted in shading of the D021 and D024 material samples which up to now had been attached to the base structure of the D021 as illustrated in Figure 8. Since exposure to solar flux was an important part of these material evaluations, a new location for this part of the experiment had to be established. The spot selected was near the A/M EVA hatch, and by virtue of its physical remoteness from the D021 location, became a separate EVA task.

Third, since both the thermal and launch vibration environments were radically changed, the entire D021 Experiment had to be re-evaluated analytically to establish that design limits would not be exceeded.

Fourth, the presence of the ATM introduced a greater restriction to materials offgassing limits and tests of the D021 expandable materials had to be repeated under the new specification Reference 2.

Fifth, new time lines and tasks sequences had to be established for the revised configuration.

This change to the Skylab configuration was announced after the D021 Training Hardware Unit had been delivered and the Qualification Test Unit had already begun the Environmental Qualification Test (EQT) program. The Flight and Backup units were in the final assembly stage. Fortunately, the new off-gassing and environmental requirements did not require changes to the basic hardware design. However, the test program was revised to reflect these requirements.

The removal of the materials experiment from the D021 base did require minor hardware redesign and rework.

6. Critical Design Review

The Critical Design Review was held at GAC, Akron, Ohio 23 and 24 June 1970. The design and documentation requirements were thoroughly reviewed by the attendees as listed in Appendix I. Documentation changes as authorized by the Review Board were incorporated in subsequent revisions.

The following design changes were also recommended and approved for incorporation by the Review Board:

- (1) Pressure relief valves were added to the high pressure gas storage system to eliminate the chance of overpressurizing the system.

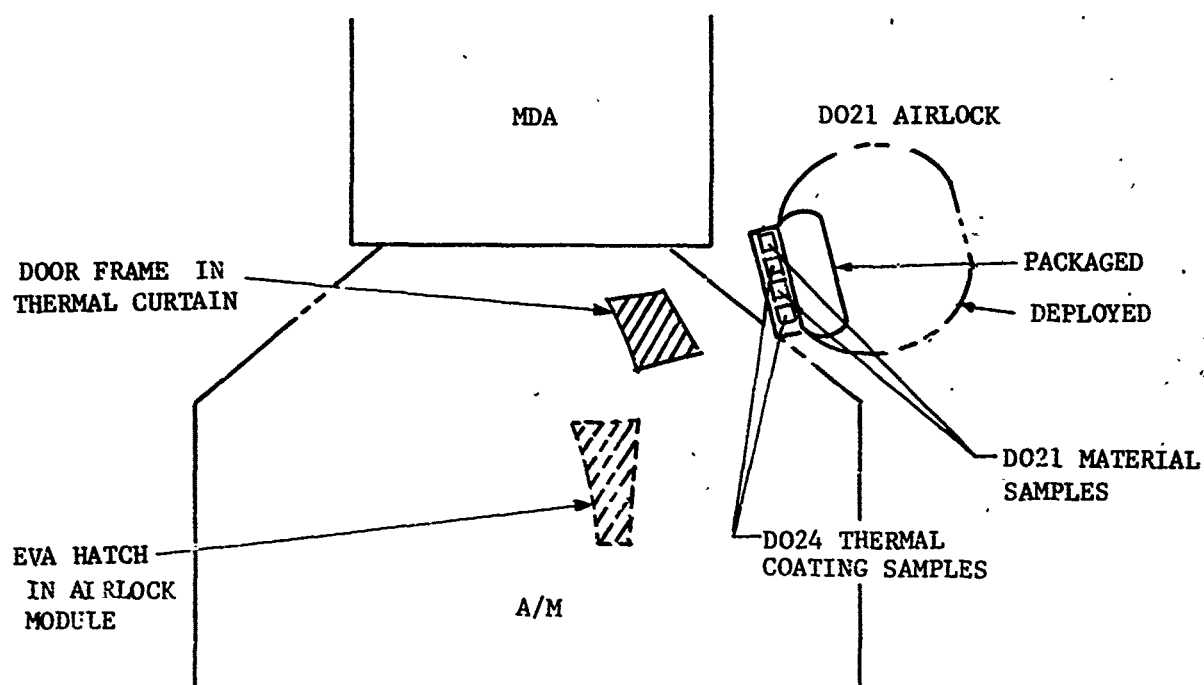


Figure 8. D021 and D024 Material Samples - Original Location

- (2) The restraint harness release was changed from a horseshoe shaped snap ring to a pull pin. It was believed that this would reduce the possibility of accidental release of the harness.
- (3) A detent-type engagement was added to the hatch centering blocks which would provide a catch in closed position of the hatch. This allows closing and latching of the hatch as a one-handed operation.
- (4) The "Hatch Open" restraint was changed from a Velcro* patch to a mechanical snap fastener.
- (5) The D021 internal control panel (which was inactive) was removed and a special bracket added to support the light which was previously mounted to the panel.

7. Experiment Integration and Test Requirements Review

Reviews were held at both GAC-Akron and MSFC Huntsville to discuss the D021 Experiment Integration and Test Requirements.

The subject of end-to-end system checkout was thoroughly discussed. It was established that the logical place to splice into existing circuits for such a check would be on the A/M side of the interface. The D021 system tester (described in Section III) connects directly to the D021 interface and simulates the A/M inputs to the experiment. This does check out the D021 experiment by itself, but once the D021 is mated to the A/M, there is no way to assure that the interconnects have continuity or have been properly made other than actually applying power to the circuits. This is contrary to NASA Test Policies. No final action was established, but it was obviously an NASA/MDAC/MM-DD responsibility to resolve.

The following action items were assigned to GAC. The responsive action is described in detail in Appendix II.

- (1) GAC was asked to establish an acceptable method for positively identifying each temperature and pressure sensor after mating to the A/M. The pressure sensors are accessible and a suction applied to each sensor fitting will provide positive identification. The thermal sensors can be identified by applying heat with 250 watt heat lamps to each sensor location.
- (2) The pyrotechnic circuitry cannot be tested at design load in an end-to-end check without actually firing the cartridges. As the next best approach, a pyrotechnic simulator was designed and built which would plug into the electrical harness in place of the actual pyros and signal the fact that an adequate firing impulse was received when the circuit was activated. This would verify the circuitry all the way from the A/M control panel up to the pyro connectors as well as circuitry to the battery packs. A fusistor cycling test was also performed to verify that this test would not deteriorate the fusistor capability. Sample

*T.M. - Velcro Corp., New York, N. Y.

fusistors were put through 100 cycles of the maximum current impulse applied by the tester and then tested for their fusing characteristics. This is reported in detail in Appendix B.

- (3) Dimensional data for the maximum deployment path of the D021 airlock was requested. This was provided to MDAC with the understanding they would make a clearance check template from this data and use it to establish actual clearance on the ATM support structure.

C. FINAL DESIGN CONFIGURATION

The D021 General Arrangement, external dimensions, C.G.'s and mechanical interfaces are shown on Figure 9. Both the packaged and deployed conditions of the airlock are included.

The two major subassemblies which form one complete airlock unit are described below. These are P/N 66QS1512, the Expandable Structure and Equipment Assembly and P/N 66QS1513, the Base Structure and Equipment Assembly.

1. Expandable Structure and Equipment Assembly - P/N 66QS1512

The Expandable Structure and Equipment Assembly consists of:

- (1) The basic expandable structural shell (see Figure 10)
- (2) The hatch hardware (see Figure 11)
- (3) The rear bulkhead hardware. (In an operational airlock, this bulkhead would be eliminated.)
- (4) The packaging harness and release cables.
- (5) The thermal blanket.
- (6) Mobility aids.

The basic structural shell is composed of the flexible material and the 6061-T6 aluminum alloy terminal rings at each end which form the hatch openings. The rear bulkhead and the hatch retaining ring must be inserted in the layup mold prior to fabricating the expandable structure because they are both larger in diameter than the terminal rings which establish the hatch opening.

The major parts of the expandable structure were previously illustrated in Figure 4. The outer cover consists of a film-fabric laminate of Capran* (nylon) film and 1.0 oz/sq yd nylon fabric as illustrated in Figure 12. The fabric layer forms the outer surface of the airlock. This in turn is sprayed with Ball Bros. 80U paint for thermal control purposes.

* T.M. Allied Chemical Corporation, New York, New York

The micrometeoroid barrier is a flexible polyurethane open cell foam of 2.0 lbs/cu ft density. Fire resistance has been incorporated by special compounding. A 1.0 inch thickness was selected as the required thickness to provide the necessary micrometeoroid protection. The analysis for this is covered in Subsection C 2 and later verified by test as discussed in Section III.

The structural cage is a matrix of filament wound stainless steel wire, "Taslan"* yarn and adhesive. The stainless steel wire is 3.6 mil diameter wound into a three strand cable approximately 8 mils in diameter. This cable and alternate strands of Taslan yarn are fed through the GT&R compound AD913 adhesive and applied to the airlock form at a 30° wrap angle. The Taslan yarn serves to pick up the proper amount of adhesive in order to lock the filament cage into a stable structure.

This results in a double layer of wire with one layer at 60° orientation with respect to the other layer. The spacing is 32 ends per inch in each layer. The center section, which is cylindrical and therefore at a higher unit tensile load than the spherical ends, is reinforced with a third layer which is wound on circumferentially at 34 ends per inch. Ultimate tensile strength of the wire is rated at 300,000 psi. The Instron Tensile tests gave results of 9.2 lbs/end minimum values (300,000 psi tensile strength).

The pressure bladder is a composite of several layers as shown on Figure 13. A triple gas barrier is provided by the two film-fabric laminates and the closed cell EPT foam. The splices of material are staggered so that no two seams are directly over each other. This three-layer composite provides a cushioning effect to achieve greater puncture resistance against sharp object contact. Any single layer can be pierced without making a leak path. The inner foil layer is multifunctional. The primary purpose is to act as a flame barrier against flash ignition sources, but it also provides improved scuff resistance to the bladder and in combination with the alodine coating, provides passive thermal control.

The unit weight breakdown of each component is shown in Table I.

TABLE I. UNIT WEIGHT BREAKDOWN

<u>Construction Component</u>	<u>Weight - PSF</u>
Aluminum Inner Layer	0.004
Adhesive	0.010
Pressure Bladder	0.159
Adhesive	0.010
Structural Layer	0.062
Taslan Interlocking Layer and Adhesive	0.048
Polyurethane Foam	0.167
Adhesive	0.010
Outer Cover and Coating	<u>0.062</u>
Total	0.532 PSF

* T.M. duPont E. I. de Nemours & Co., Inc. Wilmington, Del.

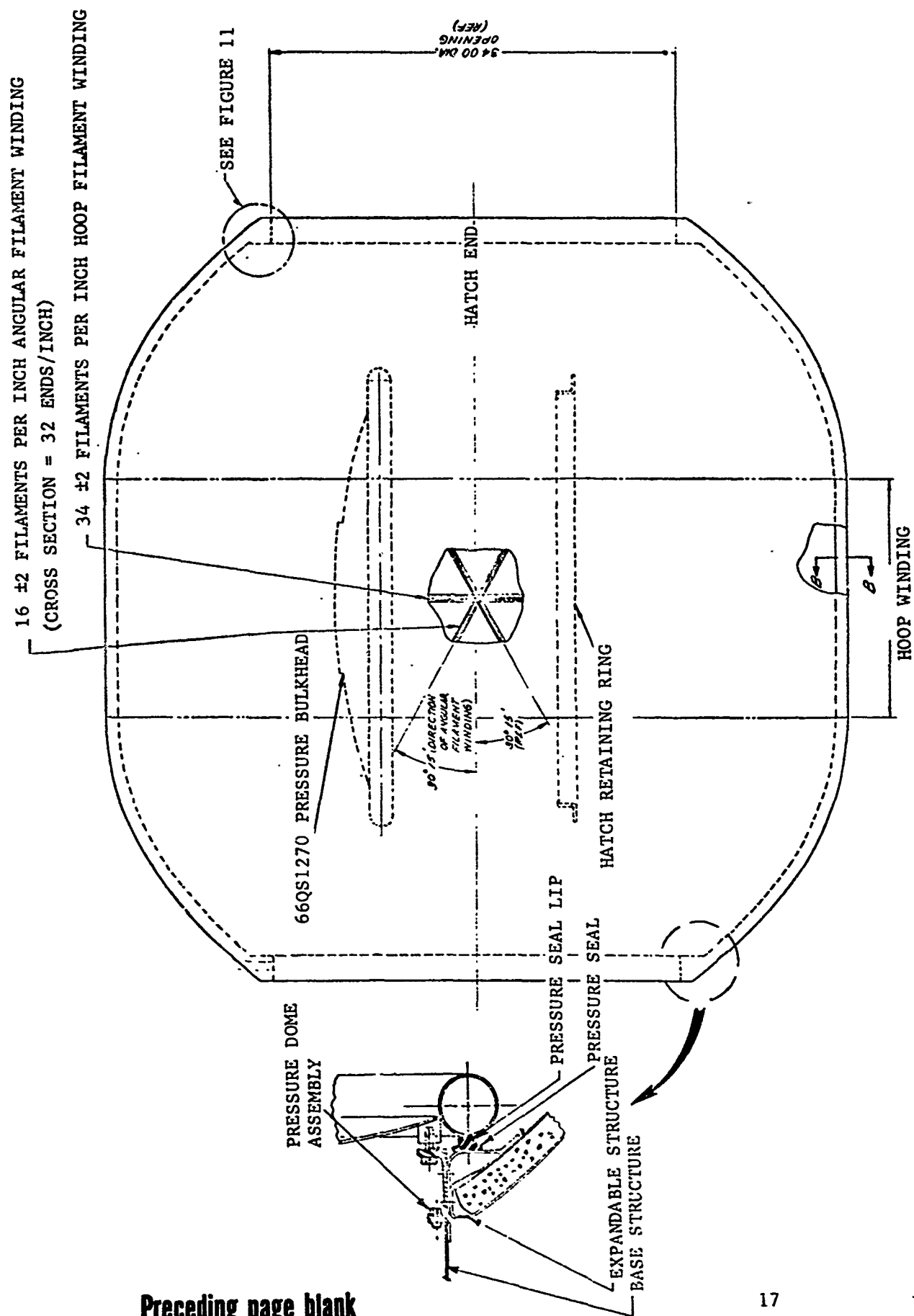


Figure 10. Expandable Structure

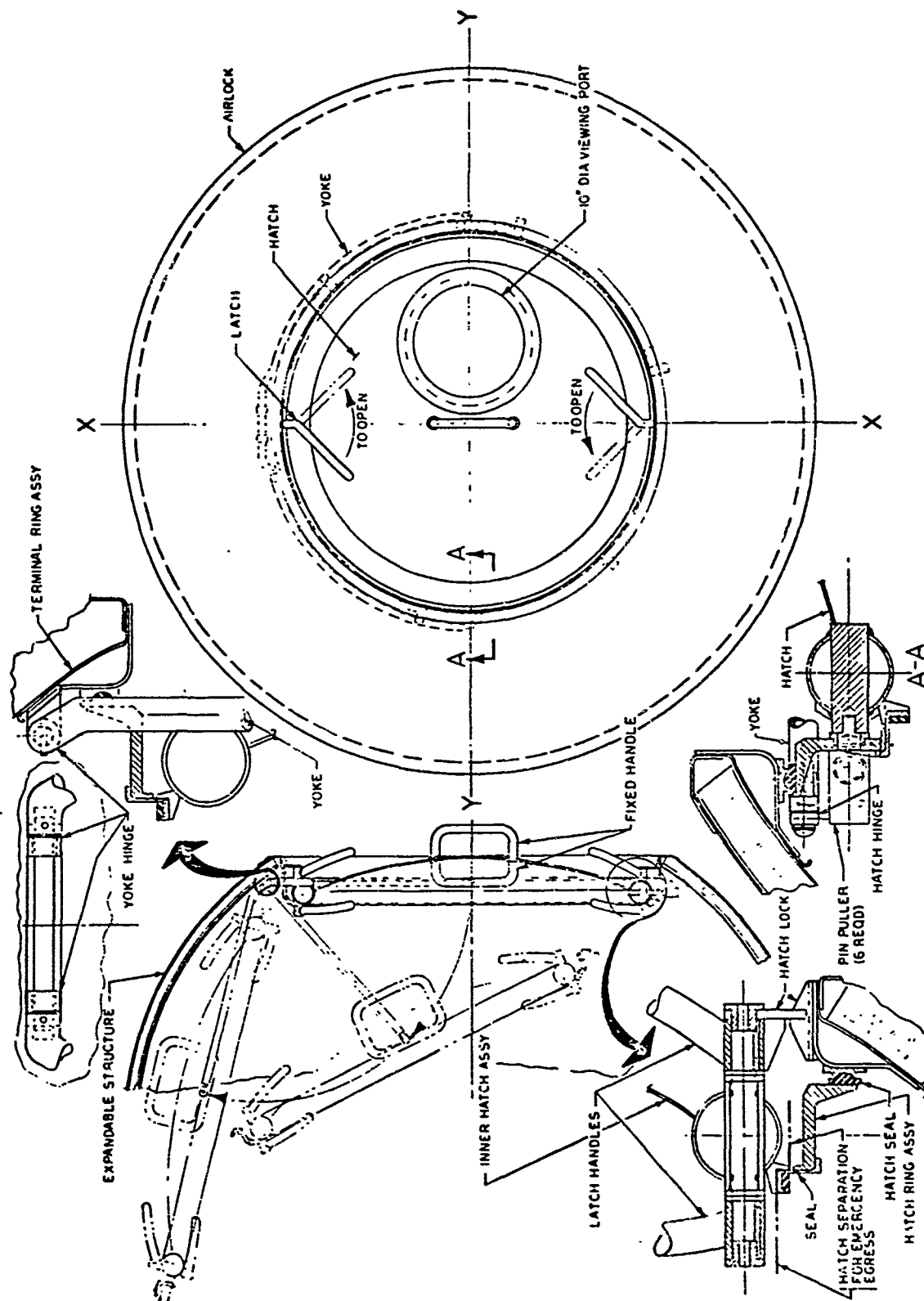


Figure 11 . Hatch Assembly

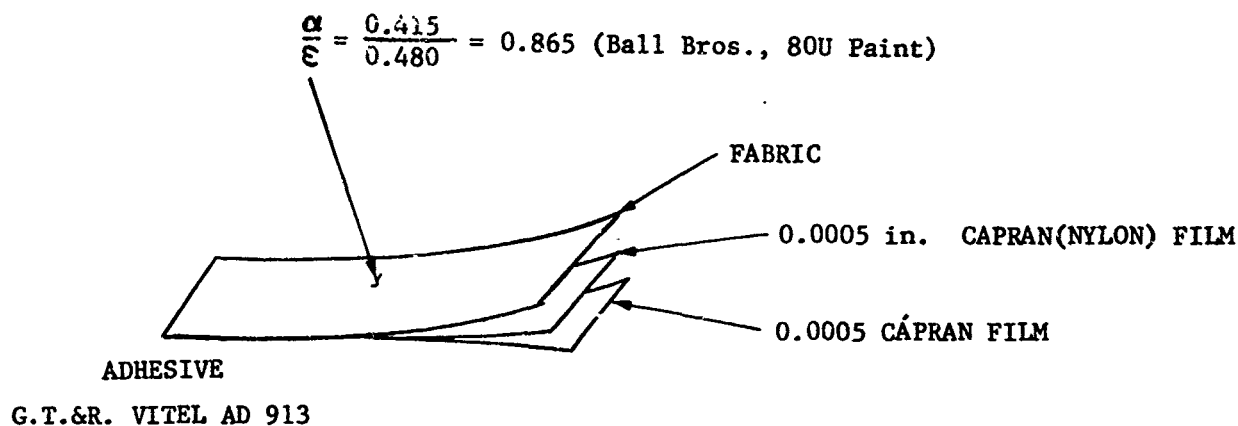


Figure 12. Outer Cover

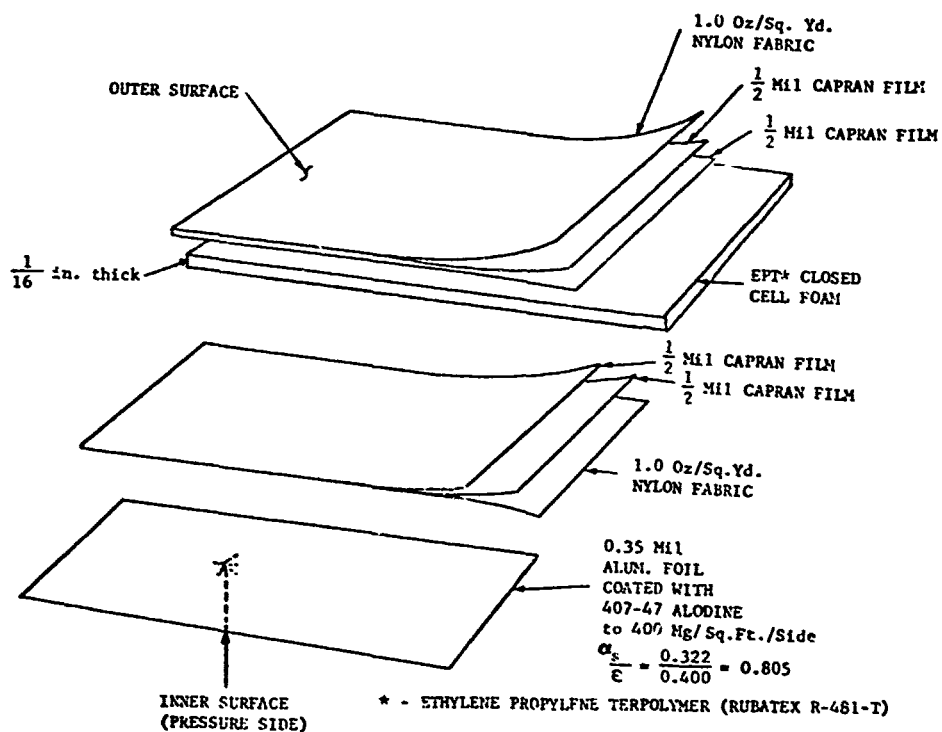


Figure 13. Pressure Bladder

One of the critical design problems is the transfer of pressure loads from the flexible structure to the rigid hatch rings without introducing serious stress concentrations in the flexible structure. Figure 14 illustrates the method used on the D021.

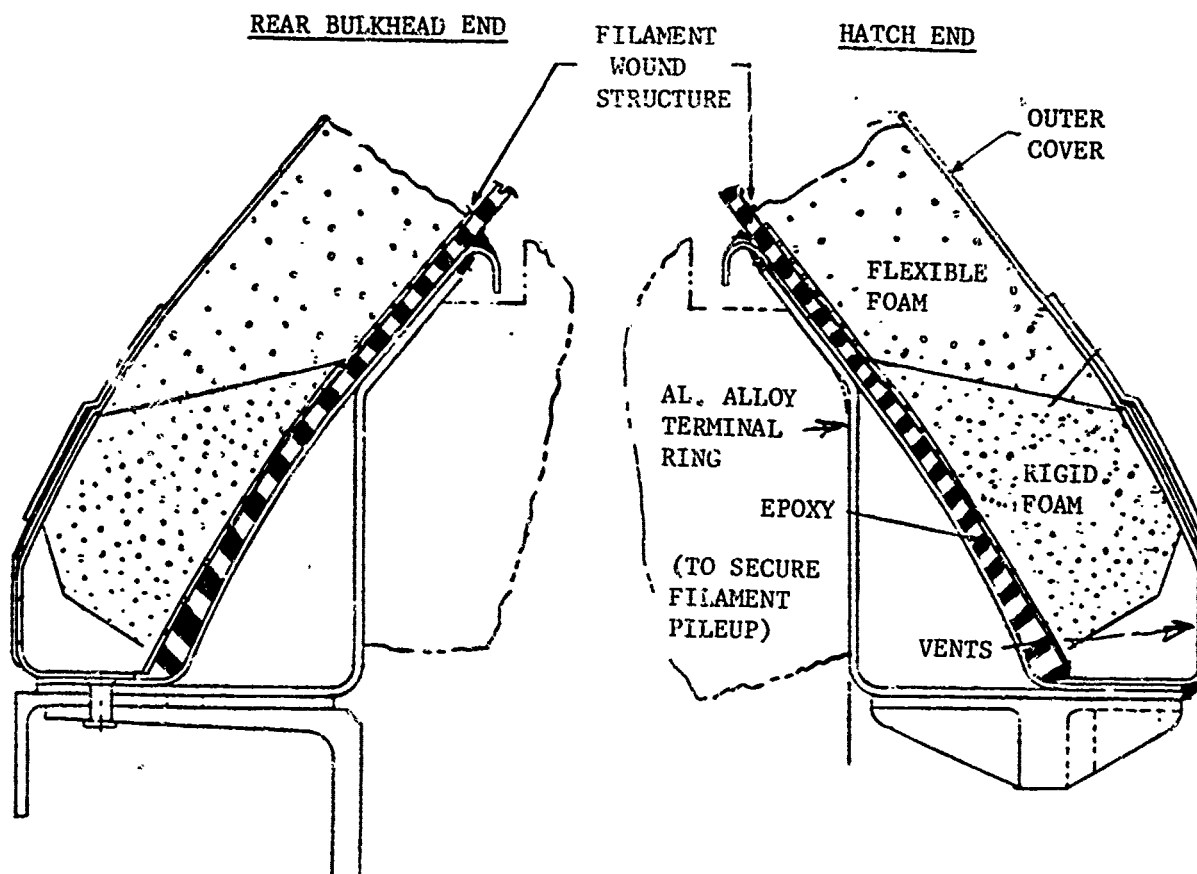


FIGURE 14 - METHOD OF JOINING FLEXIBLE STRUCTURE TO RIGID STRUCTURE

The bladder serves as an elastic cushion between the filament wound structural layer and the hard terminal ring made of 6061-T6 aluminum alloy. There is a pile-up of filament material at this opening due to the inherent nature of the winding process which provides a natural high strength hoop at the hatch openings. It is then only necessary to insert a rigid hoop inside the cage which can withstand the compressive load created by sliding against the taper of the filament cage.

By keeping the intervening surface between these members soft and elastic, the pressure loads are uniformly distributed around the opening and transferred from the soft structure to the hard structure without stress concentrations.

The hatch hardware was illustrated on Figure 11. A compression-type seal made of butyl rubber is used to seal the hatch in the closed position. Butyl demonstrates excellent flexibility at temperatures as low as -65°F and has acceptable offgassing characteristics in vacuum. Two latches are provided at diametrically opposite sides of the hatch to provide the initial clamping pressure. Internal pressure within the airlock adds further compression to the seal. A handle is located directly in the center of the hatch on both the interior and exterior surface for manipulation of the hatch.

The hinge mechanism has been designed to provide maximum unobstructed internal volume in both the closed and open positions. A 10-inch diameter viewing port is provided in the hatch to permit visual observations. The original planning of the experiment called for several pressurization cycles with an astronaut on the interior of the DO21. Therefore, an emergency escape feature was included in the original hatch design. This resulted in a two-piece hatch design with the inner section of the hatch small enough to pass through the terminal rings. The two sections were joined at six equally spaced radial points by means of shear pins. In case of emergency, these pins would be pulled by means of electrically initiated pyrotechnic cartridges.

The basic emergency escape feature was retained even after the astronaut tasks were revised to eliminate this requirement because of potential future need for this capability on an operational airlock. However, the system was deactivated for the flight and backup units by removing the pyrotechnic cartridges and the related electrical system.

The rear pressure bulkhead is a 6061-T6 aluminum alloy dome welded at its periphery to a 6061-T6 aluminum alloy tubular ring. The installation detail was previously shown in the detail of Figure 10. The pressure seal is identical to that used on the hatch opening. The internal control panel was originally mounted on this bulkhead but was removed from Flight and Backup units as a CDR action item.

A pair of GRIMES 32 candlepower lights are mounted to this bulkhead to furnish internal lighting, an electrically actuated vent valve is mounted to the exterior of the bulkhead to depressurize the airlock, between pressure cycles.

An additional vent line is also attached to the bulkhead leading to a manually operated vent valve as a backup system. A cover plate seals off the opening which was originally planned for use as an umbilical feed-through connection. A high capacity vent valve is also mounted on the bulkhead. This was part of the emergency hatch release system but has been deactivated and locked in the closed position.

The packaging harness is shown on Figure 15 and the release system is shown on Figures 16 and 17. The harness restrains the airlock in the packaged state during launch. It consists of six webbing straps which are secured to a circumferential steel tension cable located at the pressure bulkhead end of the airlock. The opposite end of each strap terminates in a steel fitting which is captured by the quick-release collars at the center of the hatch. When the airlock is deployed, the pin is first pulled from this quick release collar by means of a cable leading to an electric actuator located in the base structure. A second release cable is also provided for a manual release backup mode. The six straps are then free to fall away from the airlock except that the ends are attached to the outer surface of the airlock by means of restraining cords. These restraining cords are adjustable in length so that they hold the harness straps and release collar against the outer surface of the airlock in the deployed condition as shown in Figure 18.

The thermal blanket consists of seventeen layers of aluminized "Kapton"* film separated by fiberglass cloth layers to achieve a "super insulation"

*T.M. DuPont E.I. de Nemours & Co., Inc. Wilmington, Del.

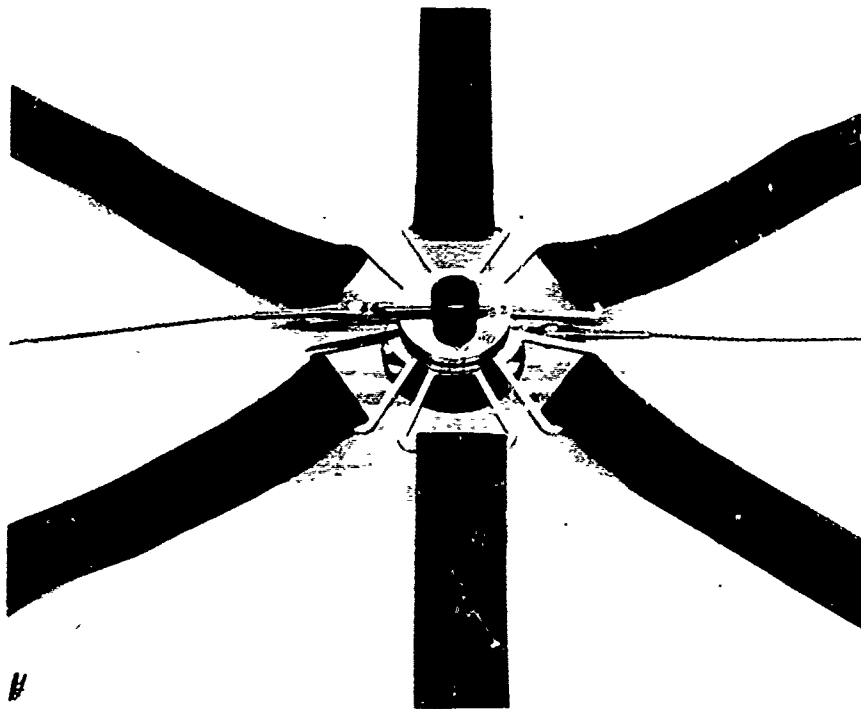


Figure 15. Packaging Harness

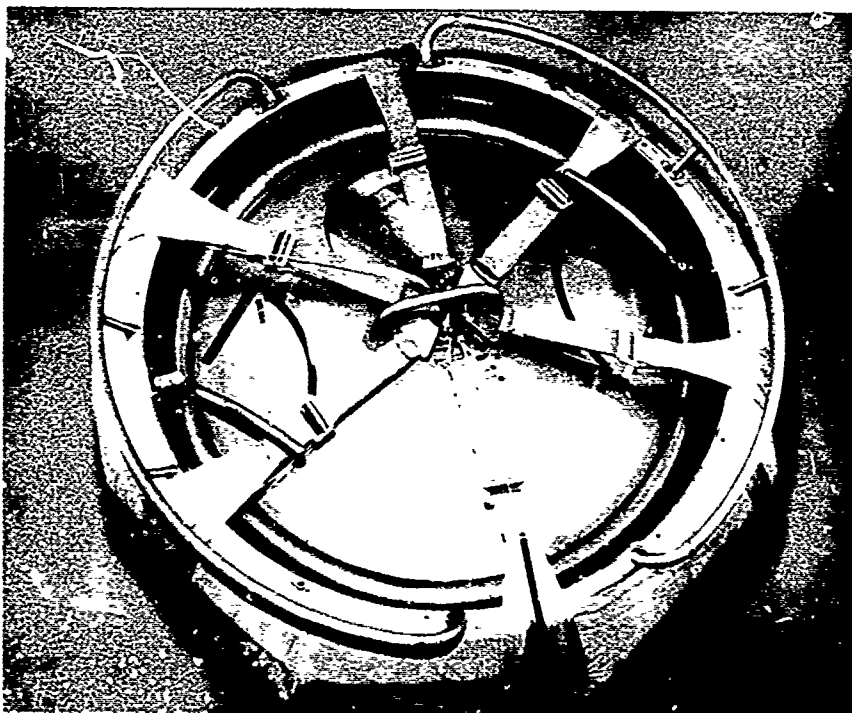


Figure 16. Harness Installed

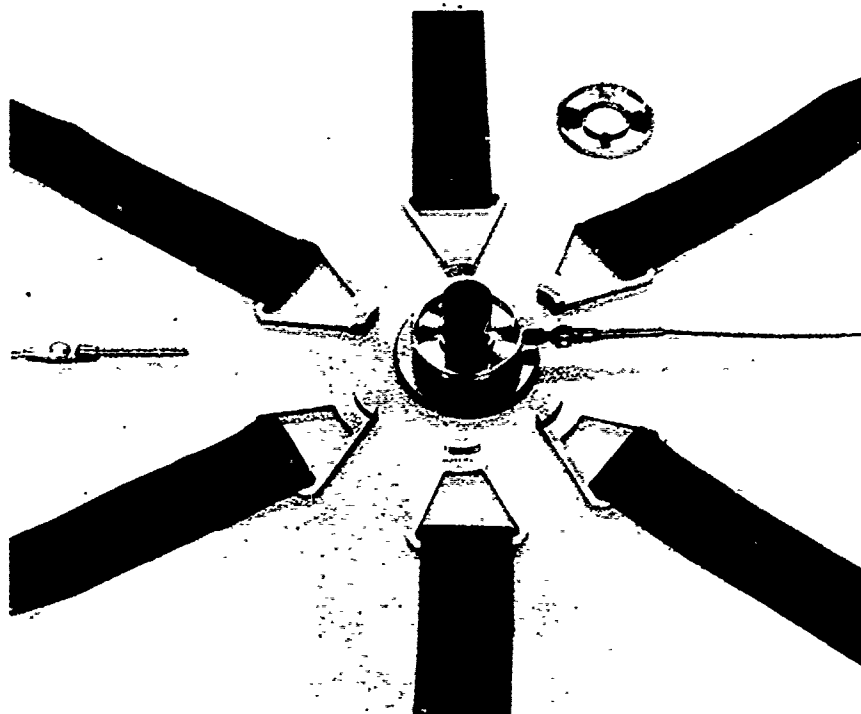


Figure 17. Harness Released



Figure 18. Airlock Deployed

blanket. The blanket is tailored into six sections which are snapped together to cover the expandable portion of the airlock as illustrated in Figure 19. The purpose of the blanket is to moderate the temperature variations experienced by the airlock expandable structure during orbit prior to deployment. The thermal aspects are discussed in detail in Section III.

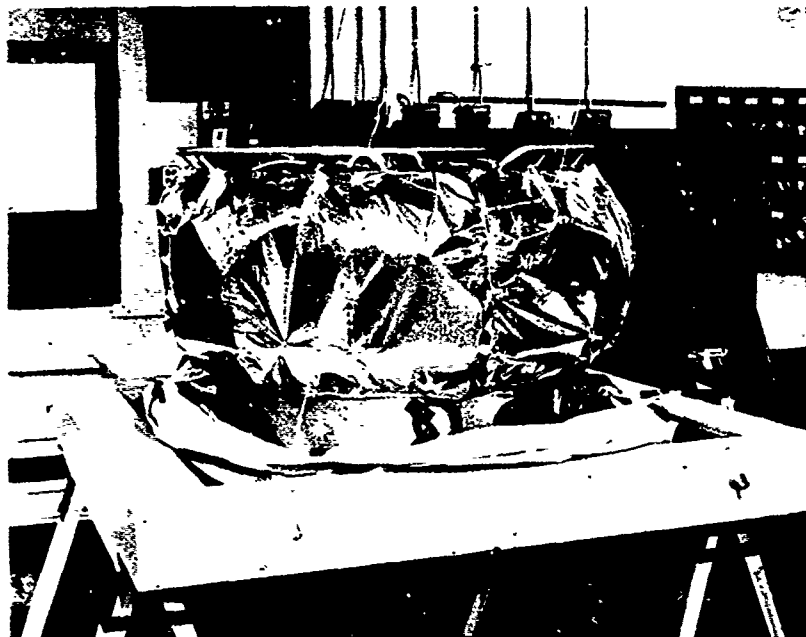


Figure 19. Thermal Blanket Installed on Packaged Airlock

When the airlock is deployed, the cover is forced apart at the snap connections by the action of the expandable section of the airlock. Each blanket gore is attached to one of the harness straps in order to retain each blanket gore in a given position after deployment.

The mobility aids consist of three circumferential webbing handholds located on both the outside and inside surface of the airlock. A rigid handhold ring is also provided at the entrance hatch of the airlock. The external mobility aids are visible on Figure 18 and the internal aids are shown on Figure 20. The hatch handle may also be used as a mobility aid when the hatch is in the latched position.

a. Base Structure Assembly - P/N 66QS1513. The base structural assembly consists of a cylindrical aluminum alloy shell which attaches to the expandable structure at one end and provides the A/M mechanical interface connection at the other end. The A/M electrical and instrumentation interfaces are located on the cylinder exterior. Hardware components for the various systems required by the experiment are located in the interior of this cylindrical section. Appropriate brackets are provided to support these equipments from cylindrical base section. This major subassembly is illustrated in Figures 21, 22 and 23.

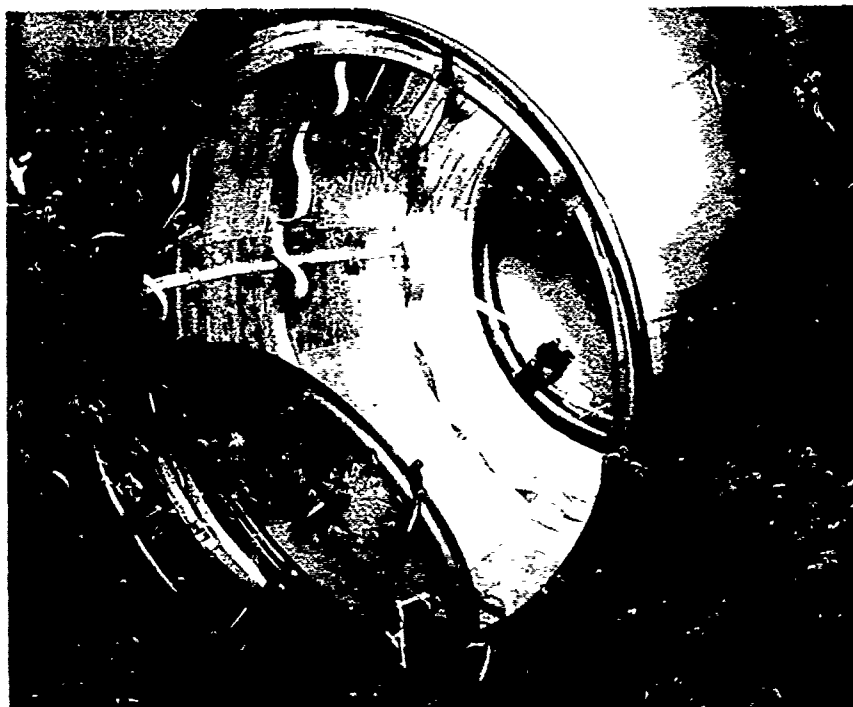


Figure 20. Internal Mobility Aids

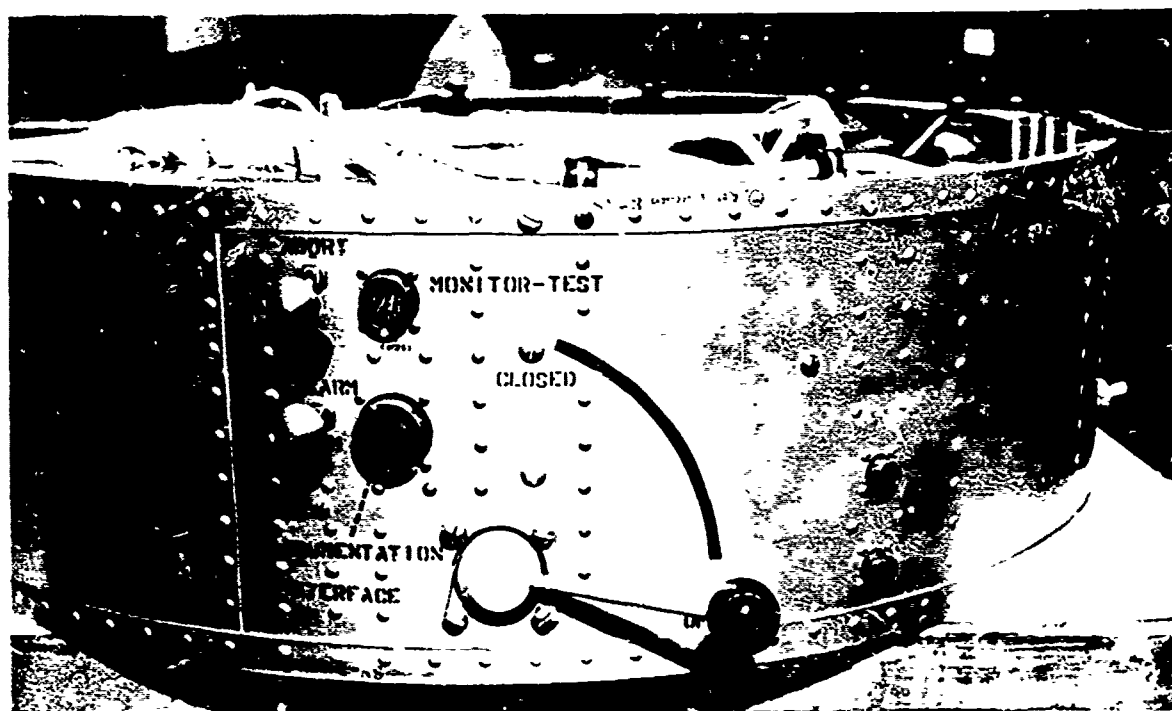


Figure 21. DO-21 Qualification Hardware - Exterior Controls and Instrumentation Interface

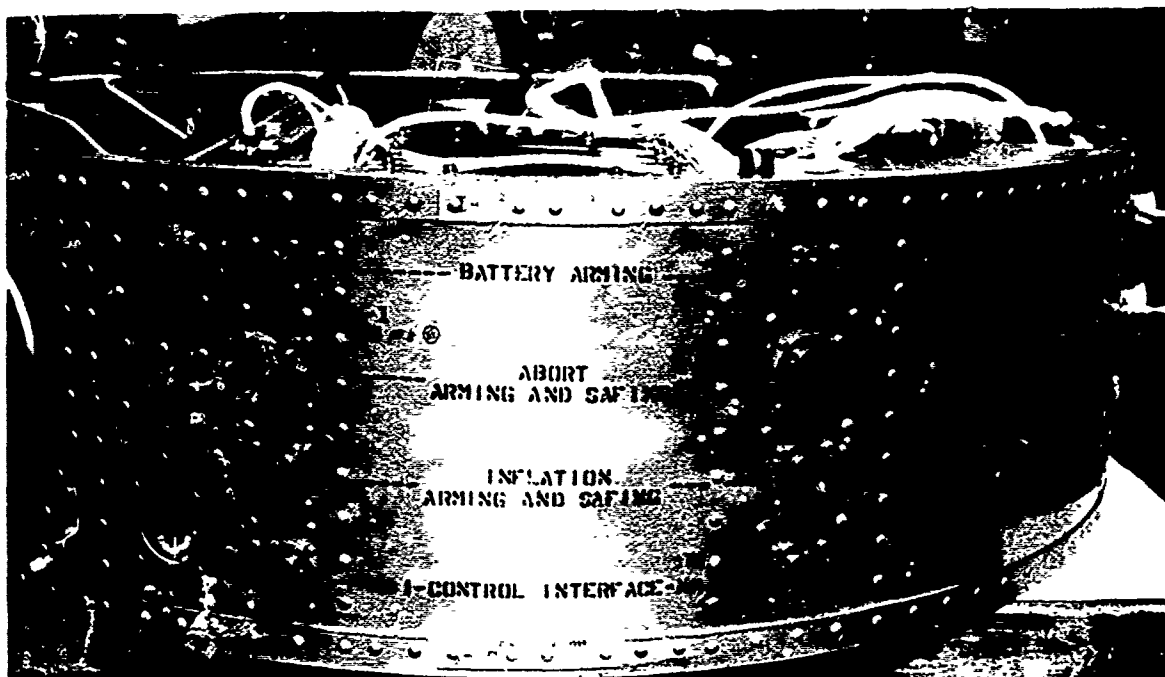


Figure 22. Qualification Hardware - Electrical Interface - Base Unit

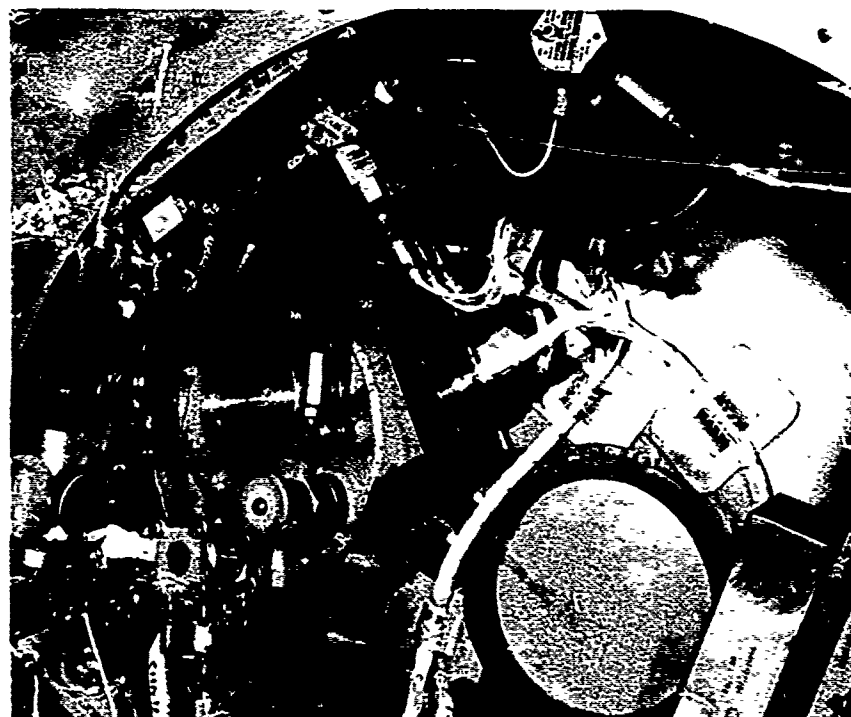


Figure 23. Interior View of Base Section

The major systems and components of the Base Structure assembly are:

- (1) The Base Structure. (Includes all mounting brackets, clips, stiffeners, etc.)
- (2) The Pressurization System.
- (3) The manually operated Vent Valve.
- (4) The Electrical System.
- (5) The Instrumentation System.

(1) Base Structure. The Base Structure is composed of a cylindrical aluminum alloy sheet, 34-inch diameter and 9.5-inch high, with a flanged ring riveted to each end to provide attachment faces. Stiffeners are riveted to the internal surface to reinforce the cylindrical section and carry loads from one flange surface to the other. Six flared holes were put into the cylindrical surface to serve as pockets to locate the spherical high pressure gas storage bottles. Steel straps are used to secure these spherical bottles in these pockets.

(2) Pressurization System. The Pressurization System is schematically shown on Figure 24. There are three steel bottles of 150 cu. in. capacity. The one bottle which is used for preshaping and initial deployment is charged to 250 psi, and the remaining two are charged to 3150 psi. The 250 psig bottle pressurizes the 78 cu. ft. expanded airlock volume to 0.295 psia and each 3150 psig bottle will provide 3.5 psia internal pressure to the airlock. The bottles are charged with N₂ gas through their individual recharging valves which project through the Base Structure. Pressure transducers are mounted to each bottle drain fitting to permit monitoring of the charge pressures. Release of the gas to the airlock is controlled by individually actuated pyrotechnic discharge valves. Upon firing, the pyrotechnic gases are totally contained within the cartridge chamber, operating a sealed plunger which then shears off and retains a tube section allowing the high pressure N₂ to discharge through an accurately sized orifice. A pressure relief valve is located on the pressure bulkhead at a setting of 5.0 psi to prevent inadvertent overpressurization.

A manually operated vent valve is mounted to the interior of the Base Structure with the operating handle protruding through the base structure.

A flexible 1-inch diameter line connects the valve to the Expandable Structure rear bulkhead. This provides a backup system for releasing airlock pressure in case of failure of the electric vent valve described in Section II-C.

(3) Electrical System. The DO21 Airlock electrical system consists of four (4) major subsystems. These are:

- (1) Restraint Harness Release
- (2) Pressurization Control System

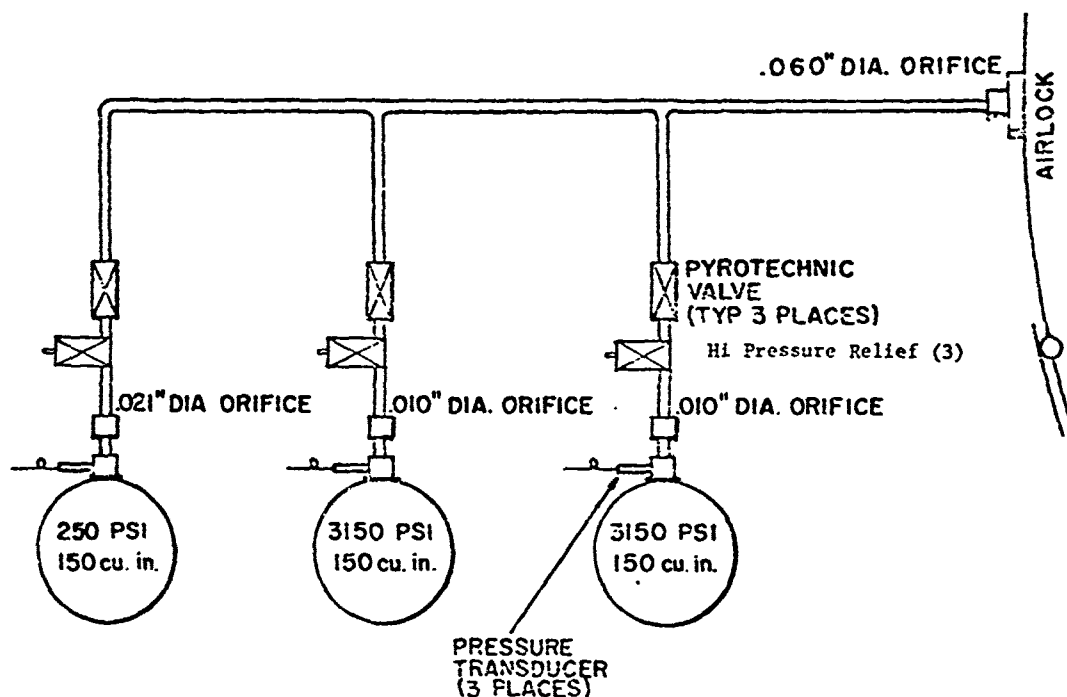


Figure 24. System Schematic - Airlock Pressurization

- (3) Emergency Egress System (Inactive on Flight Hardware)
- (4) Airlock Lighting System

The major subassemblies associated with these systems are:

- (1) The D021 Airlock Control Panel (Deleted on Flight Hardware)
- (2) Pressurization System Relay Box
- (3) The Battery Packs (2) including battery heaters

These systems are integrated with the NASA A/M which provides 28 V.D.C. power and remote control.

This system is shown in functional block form on Figure 25.

To start the D021 Airlock Experiment, a "START EXPERIMENT" switch is provided on the NASA A/M control panel. This switch provides 28 volt DC power to all the control circuits and instrumentation system. It is an on-none-off lever-lock type switch, locked in both positions.

The Restraint Harness Release consists of a 28-volt DC motor driven actuator controlled from a switch on the NASA A/M control panel. When

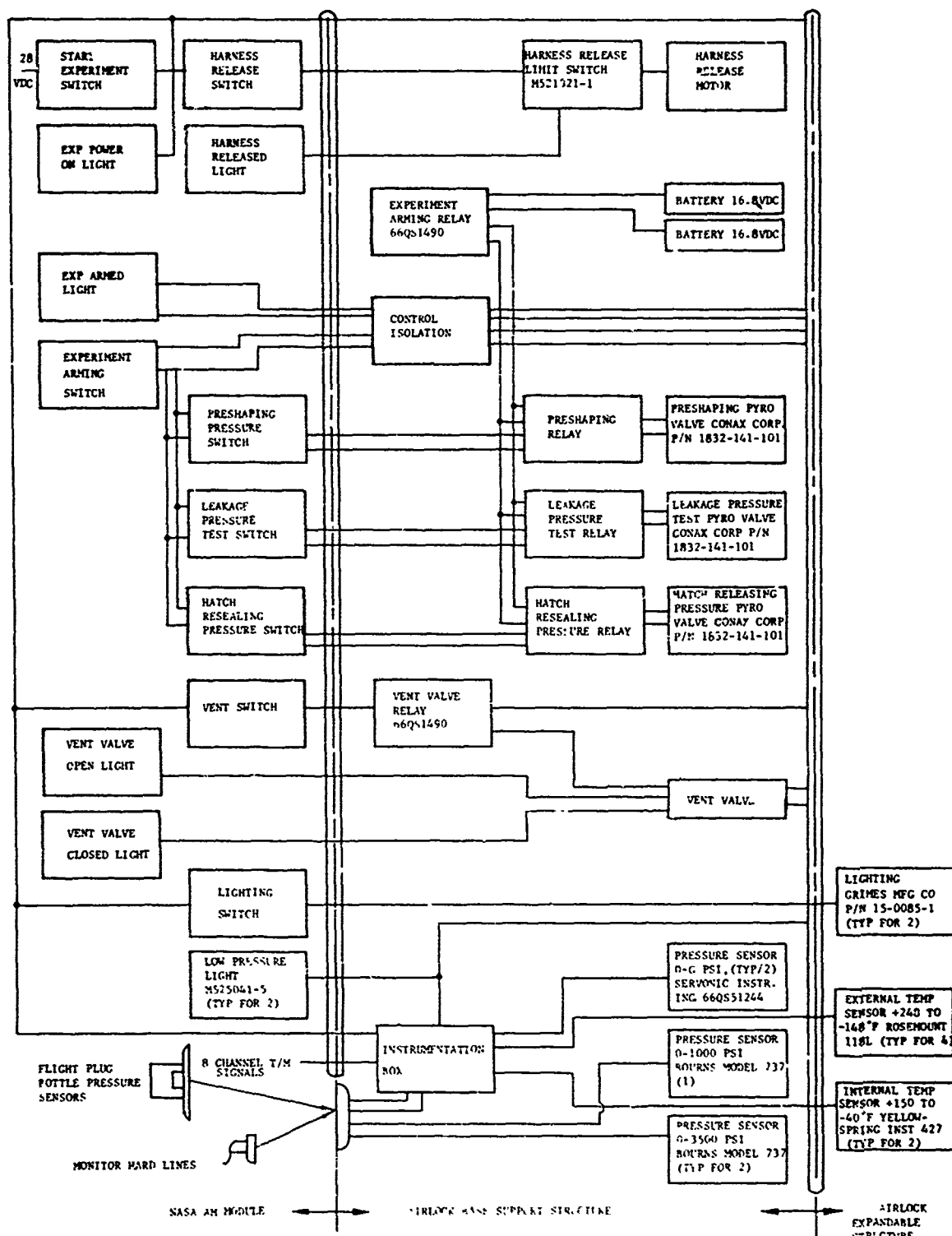


Figure 25. Electrical System Block Diagram

energized, the actuator reels in a cable, which in turn pulls a pin releasing the airlock packaging harness allowing the expandable structure to deploy. When the actuator reaches the end of its travel, it actuates a limit switch which disconnects power from the motor and lights an indicator light of the NASA A/M control panel. Power for the motor is supplied from the NASA A/M and the requirement is 1.0 ampere (3.5 ampere surge) at 28-volt DC. A manual release cable is provided at the airlock base structure as a backup deployment system. The cable routing and termination on the ATM structure is to be determined by MDAC.

The pressurization control system's function is to operate the three (3) pyrotechnic valves to pressurize the airlock and to operate the motorized vent valve to vent the airlock between pressurization cycles. To function, the pyrotechnic valve circuits must first be armed from the NASA A/M control panel.

The arming switches control redundant latching-type arming relays located in the relay box. When the switch is thrown to the ON (arm) position, the arming relays energized and magnetically latched in the armed position. In this position, battery power is supplied to the pyrotechnic valve control circuits. The relays will remain in the armed position until the switch is pressed to the momentary ON (disarm) position. Then the relays are energized and magnetically latched in the disarm position. Indicator lights on the control panel show when the arming relays are in the armed position. The NASA A/M provides 28-volt DC power to operate the arming relays and the indicator lights.

When the pressurization system has been armed from the NASA A/M, the three (3) pyrotechnic valves may be operated from their respective switches on the NASA A/M control panel.

The valve control switches energize redundant firing circuits. Each redundant firing circuit consists of a firing relay located in the relay box; a 16.8 volt nickel cadmium battery pack (Qualification Test Hardware is equipped with 28 VDC battery packs because of the active emergency-egress system) which is common to all firing circuits and one side of the dual bridge wire pyrotechnic power cartridges used for operating the valves. The redundant circuits are routed in separate wire bundles and isolated from each other through redundant connectors except where they terminate in a single dual bridge wire device. The battery packs are redundant and the relay box contains redundant circuitry and components that are separated, inside the box, by a solid aluminum bulkhead.

When one of the firing switches is activated, 28 volt DC from the NASA A/M simultaneously energizes the coils of two firing relays located in the relay box. When the firing relays are energized they connect each of the dual bridge wires in the valve's power cartridge to one of the nickel-cadmium battery packs. The battery packs supply the necessary energy to fire the power cartridges actuating the valve. Current limiting fusistors are provided in series with each bridge wire to remove any fault from the battery in event of a bridge wire short.

A vent valve and control system are provided to decompress the airlock between pressurization cycles. The vent valve may be operated from a control switch on the NASA A/M control panel. The vent valve is left in the "OPEN" position during launch. Moving the vent valve switch to "CLOSE" from the A/M control panel energizes a magnetic latching relay which then supplies 28 VDC power to the vent valve drive motor. When the valve reaches the closed position, a limit switch cuts the motor power and provides a signal to the "CLOSED" status indicator light on the A/M control panel. Moving the switch to "OPEN" initiates a similar sequence until the valve limit switch cuts the power at the valve open position and provides an "OPEN" signal to the status indicator light.

(4) Instrumentation System. The Instrumentation System consists of eight (8) telemetry data channels. There are 6 temperature and 2 pressure monitoring sensors and their associated signal conditioning equipments which provide zero to 5 volts DC analog signals at the DO21 Airlock/NASA Airlock Module (A/M) interface. A schematic of the telemetered "instrumentation" is shown on Figure 26. Four (4) of the temperature sensors are Rosemount Engineering type 118L sensors and are located 90 degrees apart, on the exterior surface of the expandable structure portion of the DO21 Airlock. The range of operation for these sensors has been calibrated from -148 °F to +248 °F.

The remaining two (2) temperature sensors are Yellow Springs Instrument type 427 and are located 180 degrees apart on the inside surface of the expandable structure portion of the DO21 Airlock. These sensors are located directly inside of two of the exterior's sensors so that the temperature different all through the wall material may be observed. The range of operation of these sensors has been calibrated from -40 °F to +150 °F. The accuracy of the temperature data at the DO21 Airlock/NASA A/M interface is ± 1.0 percent of full scale.

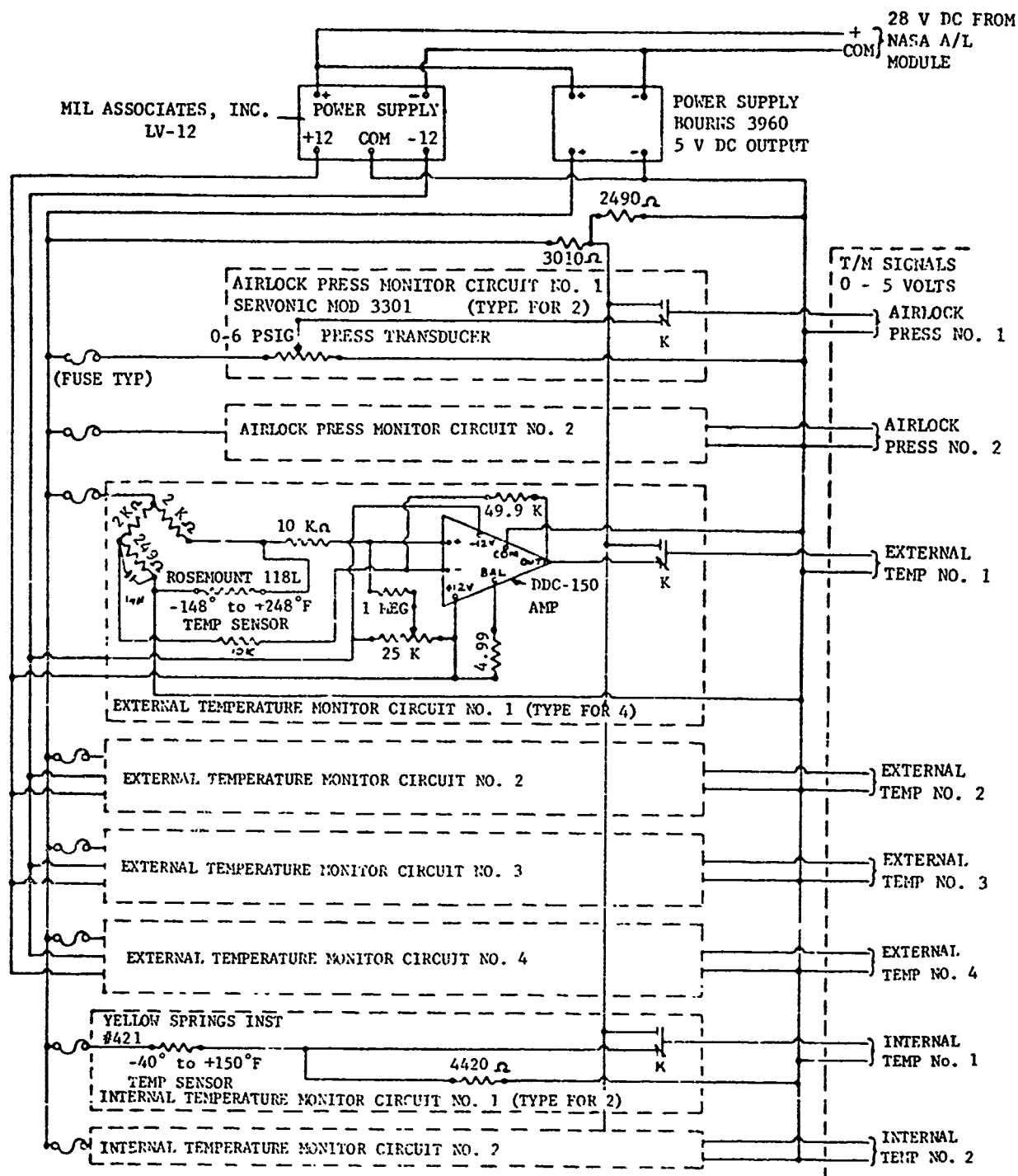


Figure 26. Telemetered Instrumentation Schematic

The two pressure sensors have a 0-6 psig range and are similar to Servonic Instruments Inc., Model 3301. The sensors are used to monitor DO21 Airlock internal pressure. The accuracy of the pressure data at the DO21 Airlock/NASA A/M interface is ± 1.5 percent of full scale.

These 8 data systems are conditioned to zero to 5 volts full range DC signals in an instrumentation box located in the DO21 Airlock base support structure.

The instrumentation box requires 0.34 amperes of 28 volt DC power to be supplied by the NASA A/M. The signal source of all channels is less than 10,000 ohms and the rate change in signal level is such that they can be commutated at a sample rate of 1.25 samples per second.

The data is to be monitored continuously from the start of the DO21 Airlock Experiment until the completion of the initial deployment and pressurization, then for five seconds once every four hours for the first two days, then continuously during the EVA ingress-egress evaluation, and second pressurization, and finally for 5 seconds every 12 hours through the remainder of the test. The necessary data storage and telemetry equipment to accomplish this will be provided on the NASA A/M side of the DO21 Airlock/NASA A/M interface.

In addition to being fed to telemetry, the outputs of the 0-6 psig sensors are fed into detector circuits in the instrumentation box which provides step function signals as the DO21 Airlock internal pressure passes through 0.1 psi. These signals are used to operate an indicator light on the NASA A/M control panel. The low pressure indicator light will come ON with decreasing pressure when the airlock internal pressure drops below 0.1 psi, indicating the pressure is at a safe level to open the hatch. One low pressure detector's circuit with indicator light is used with each 0-6 psig sensor to provide redundant internal airlock pressure indicators at the NASA A/M control panel.

In addition to the telemetered instrumentation described above, one (1) 0-1000 psig transducer and two (2) 0-3500 psig transducers are installed on the high pressure circuits to provide ground monitoring of the bottle pressures via hardline cable.

Upon removal of the hardline monitor, it is replaced with a jumper connector which provides the bottle pressure discharged signals to the DO21 Airlock instrumentation box. Detector circuits are provided in the instrumentation box similar to those provided for the 0-6 psig sensors to operate indicator lights if so desired.

The sensor locations and ranges are tabulated in Table II.

Table II. Instrumentation Subsystem

Sensor		Range	Output To:		
Code No.	Location		Tele-metry	A/M Control Panel	DO21 AGE
T-1	Exterior DO21 Airlock Wall Temperature	-148° F to +248° F $\pm 1\%$	x		x
T-2	Exterior DO21 Airlock Wall Temperature 90° from T-1	-148° F to +248° F $\pm 1\%$	x		x
T-3	Exterior DO21 Airlock Wall Temperature 180° from T-1	-148° F to +248° F $\pm 1\%$	x		x
T-4	Exterior DO21 Airlock Wall Temperature 270° from T-1	-148° F to +248° F $\pm 1\%$	x		x
T-5	Interior DO21 Airlock Wall Temperature	-40° F to +150° F $\pm 1\%$	x		x
T-6	Interior DO21 Airlock Wall Temperature 180° from T-5	-40° F to +150° F $\pm 1\%$	x		x
P-1	Interior DO21 Airlock Pressure	0-6.0 psi $\pm 1.5\%$	x	Indicator Lights <0.1 psi	x
P-2	Interior DO21 Airlock Pressure	0-6.0 psi $\pm 1.5\%$	x	Indicator Lights <0.1 psi	x
P-3	Preshaping Pressurization Bottle	0-1000 psi			x
P-4	Long Term Leakage Test Bottle	0-3500 psi			x
P-5	Hatch Resealing Test Bottle	0-3500 psi			x

2. Design Analyses and Supporting Data

a. General. This section presents the engineering analyses performed in support of the DO21 Airlock Experiment design requirements. A number of times new requirements were imposed or existing requirements increased in severity as a result of NASA's drastic program revisions. This continued, even after DO21 hardware was actually fabricated. In spite of this, only minor modifications were found necessary to adapt the hardware to meet the more stringent requirements.

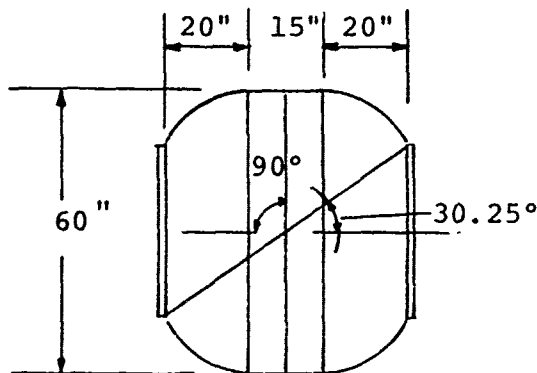
The analyses are grouped in the following categories:

- (1) Stress Analysis
- (2) Weights Summary
- (3) Thermodynamic Analyses
- (4) Fluid Flow and Gasdynamics Computations
- (5) Micrometeoroid Analysis
- (6) Miscellaneous

b. Stress Analysis. Many of the structural analyses performed during the early phase of the program are no longer meaningful as a result of the newer Skylab requirements. However, the hardware has actually been subjected to these increased loading conditions and has survived without failure. These test results are covered in Section III.

c. Pressure Calculations. The design working pressure for the airlock was specified as 3.5 psi with a Factor of Safety of 3.0. The following calculation substantiates the strength of the filament wound structural cage.

STRESS ANALYSIS - DO21 FILAMENT WINDING



The DO21 configuration is as shown. The design load requirement is an internal pressure of 3.5 psi with a safety factor of 3 for a total of 10.5 psi. Ultimate.

The filament-wound pressure vessels are fabricated by applying a specifically oriented pattern of continuous filaments to a properly contoured mandrel. In the cylindrical portion of the pressure vessel, the unidirectional filaments are oriented to meet the requirements of the biaxial force

field. This is accomplished through a combination of longitudinal ($\alpha=30.25^\circ$) and circumferential ($\alpha=90^\circ$) winding patterns. The circumferential load/inch is $N_\theta=pR$ and the axial load/inch is $N_\phi=\frac{pR}{2}$. The axial load is resisted by

the longitudinal windings and the circumferential load by a combination of the longitudinal and circumferential windings. The longitudinal windings also resist the meridional and circumferential forces in the dome. The dome contour has been matched with the longitudinal winding angle (30.25°) to provide a "balanced-in-plane" contour which provides a load condition which matches the winding pattern to maintain the same load throughout the longitudinal windings in the dome and cylinder. These loads are resisted by a continuous high strength steel wire in a three-strand cable. The strength of this cable has been established by test at 9.2 pounds per cable. Because of the large dome openings, 15% reduction is applied to the longitudinal windings to provide for possible variations in winding pattern and load conditions in the dome area. Therefore the cable strengths are

$$\text{Circumferential cable} = 9.2 \text{ pounds/cable}$$

$$\text{Longitudinal cable} = 9.2 \times .85 = 7.82 \text{ pounds/cable.}$$

The loads in the cylinder are

$$N_\theta = 10.5 \times 30 = 315\#/inch$$

$$N_\phi = \frac{10.5 \times 30}{2} = 158\#/inch$$

The number of longitudinal windings required per inch are

$$\text{Long. cables} = \frac{N_\phi}{(\cos 30.25^\circ)^2 \cdot 7.82} = \frac{158}{(.864)^2 \cdot 7.82} = 27 \text{ cables/inch, Req'd}$$

$$\text{Actual No. Used} = 32 \text{ Cables/Inch: M.S.} = \frac{32}{27} = 1.185$$

The number of circumferential windings required per inch are

$$\begin{aligned} \text{Circumferential cables} &= \frac{N_\theta - 32(7.82) \sin^2 30.25^\circ}{9.2} \\ &= \frac{315 - 32(7.82)(.504)^2}{9.2} = 27.3 \text{ Cables/Inch Req'd} \end{aligned}$$

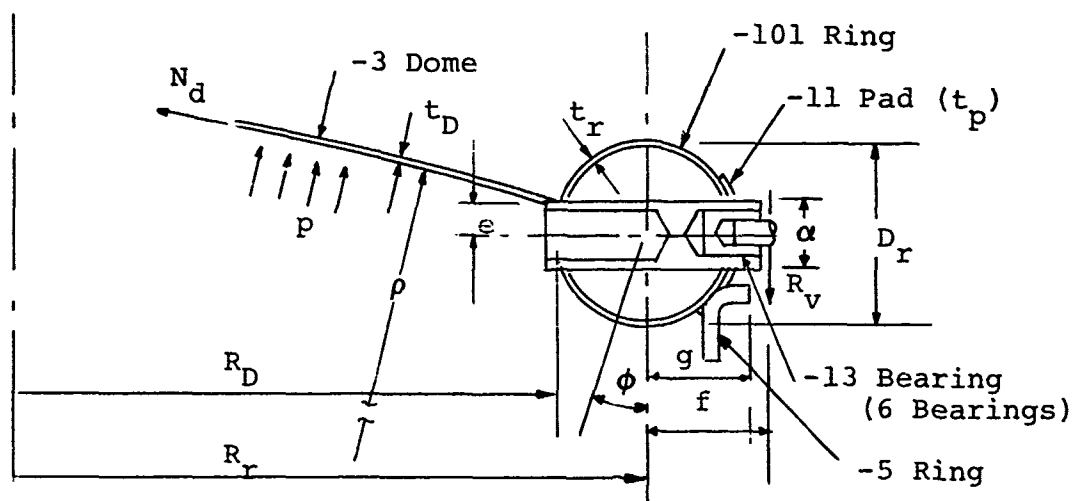
$$\text{Actual No. Used} = 34 \text{ cables/Inch: M.S.} = \frac{34}{27.3} = 1.245$$

Although tests have shown that sharp creasing of individual cables reduces the breaking strength by approximately 15%, no such deterioration was found when the composite layups were folded and unfolded over 100 times then tested. Apparently, the wire is protected against sharp creasing when enclosed by the total composite materials. At any rate, the 18% and 24% margins of safety calculated above are considered more than adequate to cover any packaging effects.

A stress analysis of the hatch assembly subjected to the proof and the ultimate internal pressures is presented below. The minimum margin of safety for the dome was found to be +2.98. The combined stresses in the ring yielded net, circumferential compressive stresses throughout with a conservatively calculated, minimum margin of safety of +0.06.

The structural integrity of this assembly is considered adequate.

d. Stress Calculation of Hatch Assembly (Reference GAC Dwg. #66QS1481).



Design, Pressure Loads:

$$p_l = 3.5 \text{ psi (limit)}$$

$$p_p = 4.9 \text{ psi (proof)}$$

$$p_u = 10.5 \text{ psi (ultimate)}$$

Material - 6061 T-6 AL.

Dimensions: (Inches)

Before Welding

$$F_{tu} = 38 \text{ ksi}$$

$$F_{ty} = 35 \text{ ksi}$$

$$F_{cy} = 35 \text{ ksi}$$

$$F_{su} = 24 \text{ ksi}$$

$$\rho = 45.0$$

$$R_D = 14.294$$

$$R_r = 15.235$$

$$D_r = 2.0$$

$$d = 0.75$$

$$e = 0.27$$

$$f = 1.75$$

$$g = 1.192$$

$$t_o = 0.040$$

$$t_r = 0.049$$

$$t_p = 0.040$$

$$\phi = 19^\circ 48'$$

After Welding (at Weld)

$$F_{tu} = 24 \text{ ksi}$$

$$F_{ty} = \begin{cases} 15 \text{ ksi (across weld)} \\ 11 \text{ ksi (parallel to weld)} \end{cases}$$

-3 Dome

$$f_t = \frac{p\rho}{2 t_D} = \frac{45 p}{(2)(0.040)} = 563 p$$

$$f_{ty} = (563)(4.9) = 2760 \text{ psi}; \text{ M.S.}_y = \frac{11000}{2760} - 1 = \underline{+2.98}$$

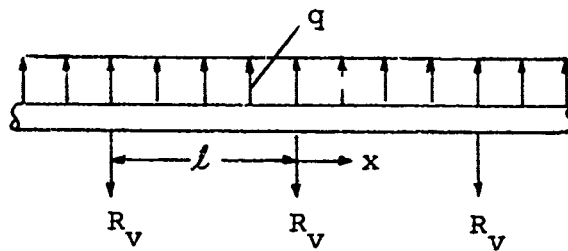
$$f_{tu} = (563)(10.5) = 5910 \text{ psi}; \text{ M.S.}_u = \frac{24000}{5910} - 1 = \underline{+3.05}$$

-101 Ring

$$\ell = \frac{2 \pi R_r}{N} = \frac{2 \pi (15.235)}{6} = 15.954 \text{ in.}$$

$$N_d = \frac{p\rho}{2} = 22.5 p$$

$$N_d \sin \phi = (22.5)(0.3386) p = 7.63 p$$



$$N_d \cos \theta = (22.5) (0.9409) p = 21.2 p$$

$$q = \frac{p}{2 R_r} (R_r + g)^2 = \frac{(15.235) \div 1.195^2}{2 (15.235)} p = 8.86 p$$

$$R_v = q l = (8.86) (15.954) p = 141.3 p$$

Ring Compressive Force, P_c

$$P_c = - R_r N_d \cos \theta = - (15.235) (21.2) p = 323.5 p$$

$$P_{cy} = -(323.5) (4.9) = \underline{-1583 \text{ lbs.}}$$

$$P_{cu} = -(323.5) (10.5) = \underline{-3390 \text{ lbs.}}$$

Ring As A Continuous Beam

$$\text{Shear, } V_x = q \left(\frac{l}{2} - x \right) = 8.86 \left(\frac{15.954}{2} - x \right) p = 70.7 p - 8.86 p x$$

$$V_{\max} = V_o = 70.7 p$$

$$V_{\max y} = (70.7) (4.9) = \underline{346 \text{ lbs.}}$$

$$V_{\max u} = (70.7) (10.5) = \underline{742 \text{ lbs}}$$

$$\text{Moment, } M_x = \frac{q}{12} (6 \ell x - \ell^2 - 6 x^2)$$

$$@ x = 0, M_o = - \frac{q \ell^2}{12} - \left(\frac{8.86}{12} \right) (15.954)^2 p = -188.3 p$$

$$M_{oy} = - (188.3) (4.9) = \underline{-922 \text{ in.-lbs.}}$$

$$M_{ou} = - (188.3) (10.5) = \underline{-1975 \text{ in.-lbs.}}$$

$$@ x = \frac{\ell}{2} \quad M_m = \frac{M_o}{2}$$

$$M_{my} = \underline{461 \text{ in.-lbs.}}$$

$$M_{mu} = \underline{987.5 \text{ in.-lbs.}}$$

Moment Due to Offset Reactions, M_m

$$m = \frac{f R_v}{2 \pi R_r}$$

$$M_m = m R_r = \frac{f R_v}{2} = \frac{(1.75) (141.3)}{2 \pi} p = 39.3 p$$

$$M_{my} = (39.3) (4.9) = \underline{193 \text{ in.-lbs.}}$$

$$M_{mu} = (39.3) (10.5) = \underline{413 \text{ in.-lbs.}}$$

Basic Ring Section Properties

$$A = 0.3003 \text{ In.}^2$$

$$I = 0.1430 \text{ In.}^4$$

$$Q = \frac{A D_r}{2 \pi} = 0.09559 \text{ In.}^3$$

Stresses

$$f_{sy} = \frac{V_y Q}{2 t_r I} = \frac{(346) (0.09559)}{2(0.049)(0.1430)} = \underline{2360 \text{ psi}}$$

$$f_{su} = \frac{10.5}{4.9} (2360) = \underline{5070 \text{ psi}}$$

$$\therefore M.S. S_{\min} = \frac{F_{su}}{f_{su}} - 1 = \frac{24000}{5070} - 1 = \underline{+3.73}$$

$$f_{cy} = \frac{P_{cy}}{A} = - \frac{1583}{0.3003} = \underline{- 5280 \text{ psi}}$$

$$f_{cu} = \frac{P_{cu}}{A} = - \frac{3390}{0.3003} = \underline{- 11300 \text{ psi}}$$

$$@ x = 0$$

$$f_{by_o} = \pm \frac{M_y D_r}{2I} = \pm \frac{(-922 + 193)}{0.1430} = \underline{\pm 5100 \text{ psi}}$$

$$f_{bu_o} = \pm \frac{(-1975 + 413)}{0.1430} = \pm \underline{10940 \text{ psi}}$$

$$@ x = \frac{\ell}{2}$$

$$f_{by_u} = \pm \frac{(461 + 193)}{0.1430} = \pm \underline{4570 \text{ psi}}$$

$$f_{bu_M} = \pm \frac{(987.5 + 413)}{0.1430} = \pm \underline{9800 \text{ psi}}$$

Therefore, the combined stresses are compressive over the entire ring, i.e.,

$$f_{y_o} = -5280 \pm 5100 = \begin{cases} - 10380 \text{ psi} \\ - 180 \text{ psi} \end{cases}$$

$$f_{uo} = -11300 \pm 10940 = \begin{cases} - 22240 \text{ psi} \\ - 360 \text{ psi} \end{cases}$$

$$f_{yu} = - 5280 \pm 4570 = \begin{cases} - 710 \text{ psi} \\ - 9850 \text{ psi} \end{cases}$$

$$f_{uM} = -11300 \pm 9800 = \begin{cases} - 1500 \text{ psi} \\ - 21100 \text{ psi} \end{cases}$$

Conservatively, assume equal compressive and tensile yield strengths of the weld values apply at the maximum "C" distances. The minimum margin is then:

$$M.S._{\min} = \frac{F_{ty}}{f_{yo}} - 1 = \frac{11000}{10380} - 1 = \underline{+0.06}$$

e. Weight Summary. The final weight status representative of the Flight and Backup airlock units is listed in Table III.

f. Thermodynamic Analyses. The finally selected thermodynamic properties of the DO21 Airlock were as shown on Figure 27.

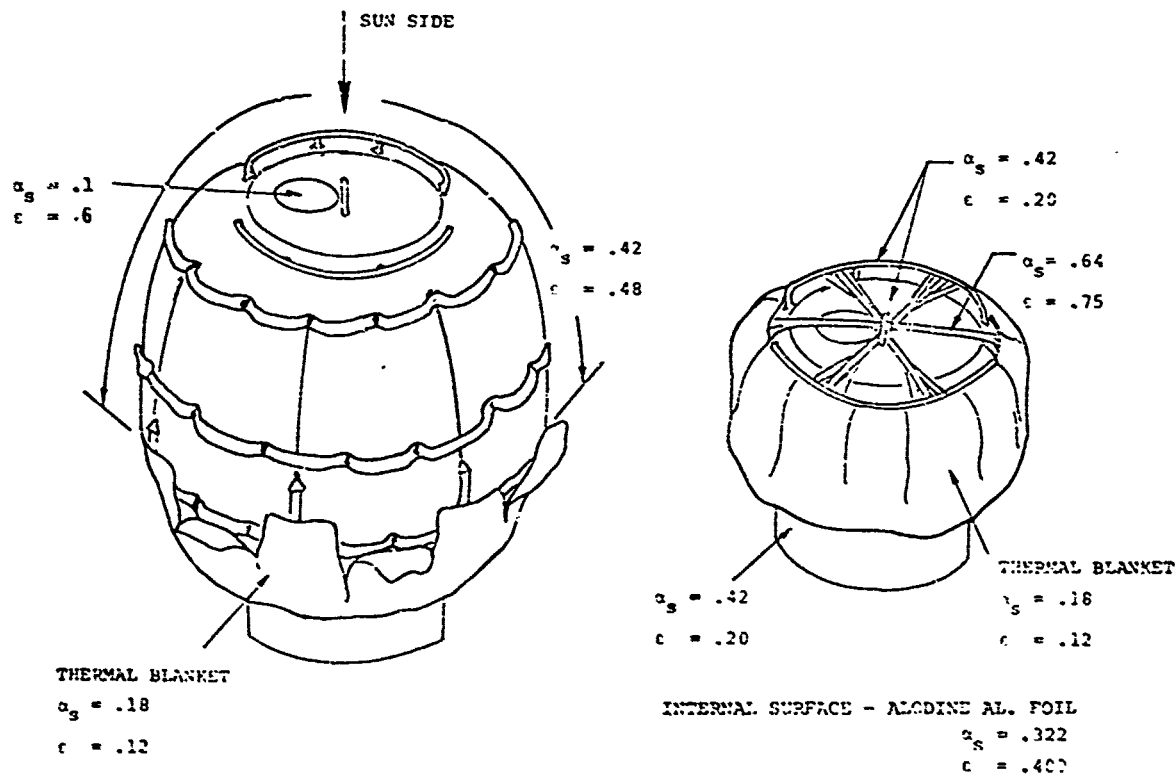


Figure 27. Optical Deployed and Packaged Properties
DO21 Airlock Experiment

Table III. D021 Airlock Weight Summary
(Final Configuration)

	<u>Detail Weight</u>	<u>Assembly Total</u>
Airlock.		114.60
Expandable Material	55.35	
Terminal Ring (2)	15.90	
Closing Rings (2) Outer Surface	3.10	
Hatch Assembly.	19.10	
Pressure Bulkhead	9.15	
Seals (2)	2.50	
Locomotion Aids	9.50	
Packaging.		18.35
Packing Restraint and Release	6.60	
Mounting Structure.	8.75	
Thermal Blanket	3.00	
Pressurization		41.66
150 In. 3 Storage Bottles (3)	15.30	
Inflation Gas N ₂	3.31	
Bottle Supports	3.50	
Pyrotechnic G s Release Valves (3).	0.69	
Drain Fittings (6).	1.14	
Charging Valves (5)	0.36	
Pressure Relief Valve	0.40	
Vent Valve Manual (1)	1.50	
Vent Valve Electrical	5.50	
Vent Valve - Emergency Egress	1.50	
Manifold, Tubing & Fittings	8.46	
Instrumentation and Controls		26.38
Telemetry Sensors (6 Temp, 2 Press)	0.65	
Hard Line Sensors (3)	0.75	
Batteries (2)	6.37	
Control Panel	Deleted	
Printed Circuit Boards (14)	3.34	
Circuit Board Holders	2.93	
Power Supply Wiring (12V)	1.64	
Pyrotechnic Pin Pullers (No cartridges)	2.81	
Wiring and Receptacles.	7.89	
D021 Airlock Assembly - Lbs. Total		200.99
Materials Samples (2)	0.60	
*One Half of Material Return Container	<u>2.30</u>	
Materials Experiment Total	2.90	

* Other Half of Return Container is Chargeable to D024 Experiment

(1) Effect of Apollo Telescope Mount on DO21 Airlock Location. The incorporation of the Apollo Telescope Mount (ATM) on the same vehicle as the DO21 airlock introduced a potential solar shadowing interference which had not existed previously. This location is defined in Reference 3.

A preliminary thermal analysis (See Appendix III) of the DO21 airlock was performed based on a location between ATM solar arrays; however, MDAC design studies indicated this location to be impractical for structural reasons. MDAC investigated a number of alternative locations and finally selected the position defined in Reference 3 and illustrated in Figure 7. This location provides solar exposure to approximately 85 percent of the projected area of the packaged airlock. The only shadows are from the structural members of the inner bay of the solar array. The basic thermal cube model used in the preliminary analysis is rotated from the sun line by 26° in the ecliptic plane and tilted upwards by 15° to simulate the new location (See Figure 28). Comparing each individual surface against the previous orientation of the cube gives the following effects.

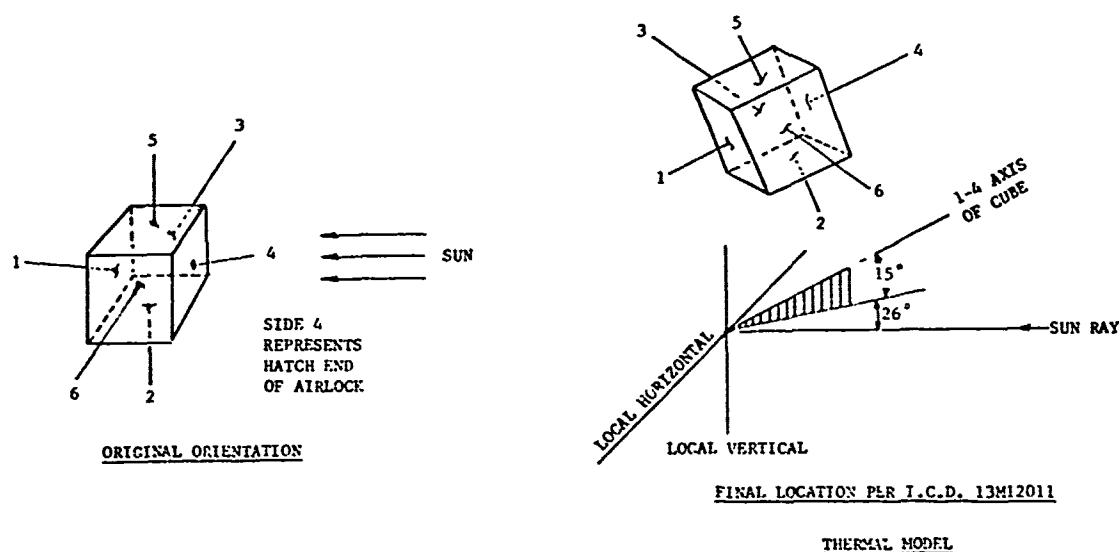


Figure 28. Original Orientation / Final Location - Thermal Model

Side 1. Little or no effect will be noted as this side will continually view the main structure. The view factor of the structure will be decreased slightly but not significantly to affect the average temperature of this surface.

Side 2. The 15° tilting will now cause side 2 to view the sun a majority of the time in orbit. This added solar energy will increase the temperature to a more desirable level.

Side 3. This side of the cube wall will be affected the greatest as it will now view outer space for a majority of the time. This surface must receive its heat by conduction from the outer surfaces and this will be explained later in the report.

Side 3 will obviously experience the coldest temperatures of any of the sides. Since this is considered the critical condition for satisfactory deployment, this side will be studied in detail.

Side 4. No problem exists on this side as it views the sun during the daylight portion of the orbit.

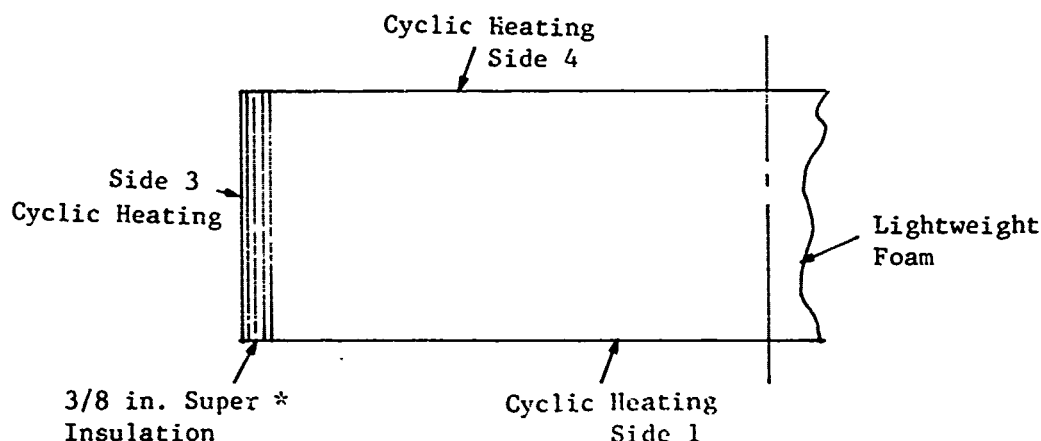
Side 5. Little or no effect will be noted, a slight increase in temperature will be noted if any, due to the increased viewing of the structure.

Side 6. The 26° shift will now allow side 6 to view the sun and will increase its temperature.

The thermal model used in Appendix IV treats each surface as an independent item. In the launch configuration, however, these surfaces are compacted together as one "solid-like" object.

A cube was selected as the thermal model in order to simplify the computer program. It was reasoned this would give a reasonably conservative answer which would bracket the extreme temperature excursion of the hot and cold surfaces. The influence of the temperature differences between adjacent hot and cold surfaces is determined by using the finite difference approach known as the "Relaxation Method." The temperature distribution is determined by dividing the cross section into equal grids and expressing the temperature at each point in terms of its surrounding temperatures.

(2) Two Dimensional Thermal Analysis. The following two-dimensional model was used in the thermal analysis.



* Analysis was based on 3/8-inch thick superinsulation consisting of seventeen fiberglass cloth separators and eighteen shields.

Side 3 was selected as the critical surface because it receives the least solar heat flux. Sides 1, 3, and 4 are subjected to cyclic heating due to the orbital characteristics of the flight vehicle. The above surfaces were treated as semi-infinite slabs and the depth at which the temperature wave is damped to within a small percentage of the outer temperature was determined by

$$\ln \frac{T}{t_{o_i}} = - \sqrt{w/2\alpha} X$$

where

T = average outer temperature

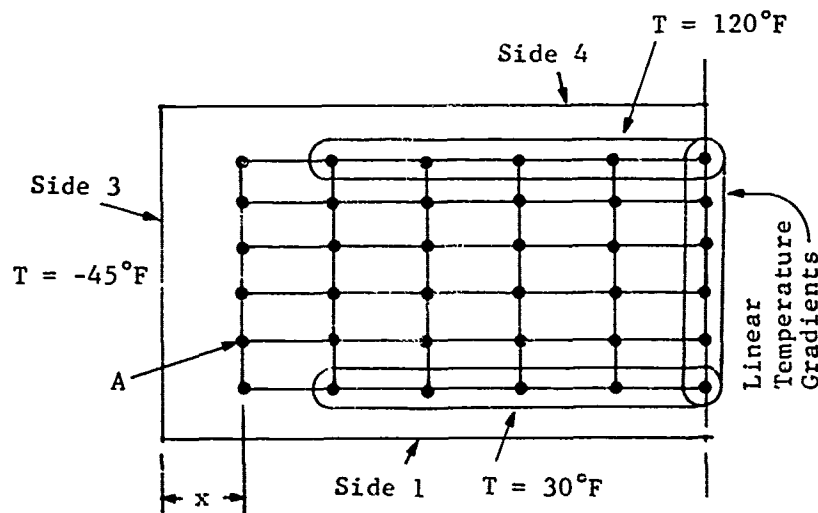
t_{o_i} = average inner temperature @ X

w = frequency

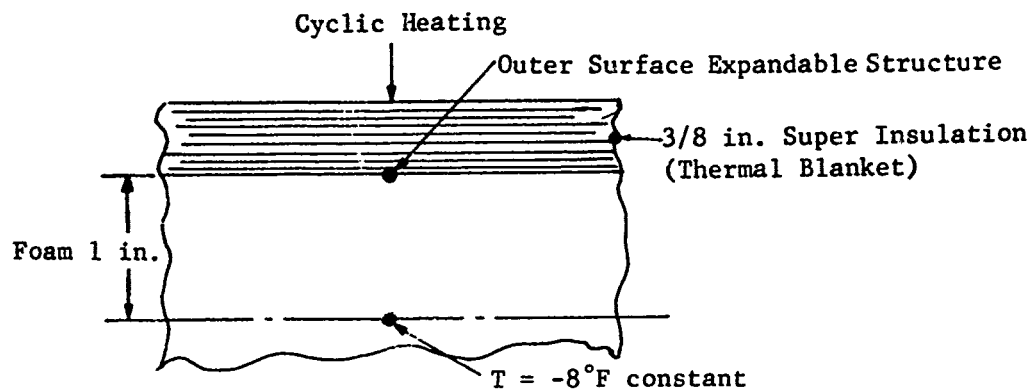
α = thermal diffusivity

X = distance

Based on the properties of the foam, the temperature is dampened within 2-1/2 inches or the surface. Using these fixed internal temperatures for Sides 1 and 4 and assuming a linear gradient down the centerline, the temperature gradients throughout the foam were then determined by the "relaxation method" as shown below.



The minimum constant temperature occurred at point "A" which was -8°F. To complete the analysis, the minimum foam temperature between point "A" and the outer surface must be determined. The distance "X" was 2-1/2 inches and the resistance value of 2-1/2 inches of foam is equivalent to 3/8-inch of superinsulation plus 1 inch foam. A multi-slab one dimensional computer run of this composite was then made based on the following sketch.



ONE DIMENSIONAL MULTI-SLAB THERMAL MODEL

The multi-slab solution showed that the outer surface of the foam at the superinsulation wall will vary cyclicly between -13.0°F and -24.6°F . The analysis shows that energy from the hotter surfaces will be transferred to the colder surface and restrict the minimum temperatures to approximately -25°F . Figure 29 shows the temperatures as a function of time for the above configuration.

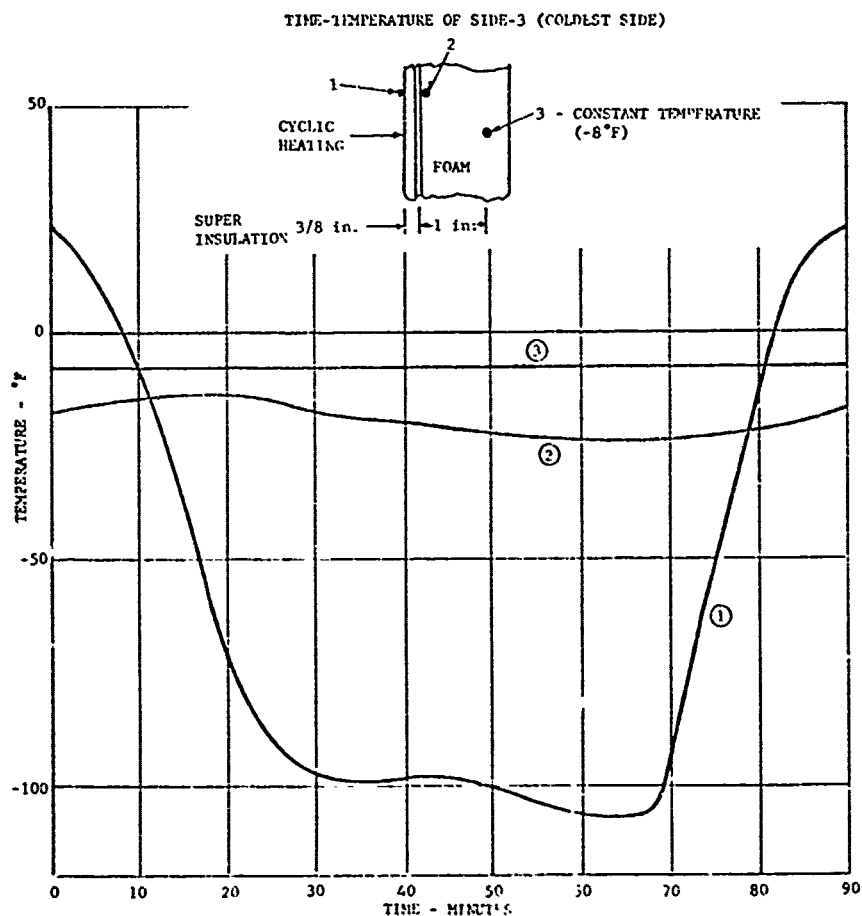


Figure 29. Orbital Temperatures.

g. Micrometeoroid Protection Calculations. The design requirement specified for the D021 Airlock was to provide a micrometeoroid barrier of sufficient thickness to ensure a 30-day exposure probability of zero penetrations of 0.9999.

Using the prior background of experience as reported in Reference 4, the following computations were made. Later, the hypervelocity simulated meteoroid tests (as reported in Section III) substantiated the accuracy of these calculations.

Assumptions:

Mission Duration	30 days
Orbital Altitude	150 to 20 N.M.
Micrometeoroid Flux	Per Figure 30

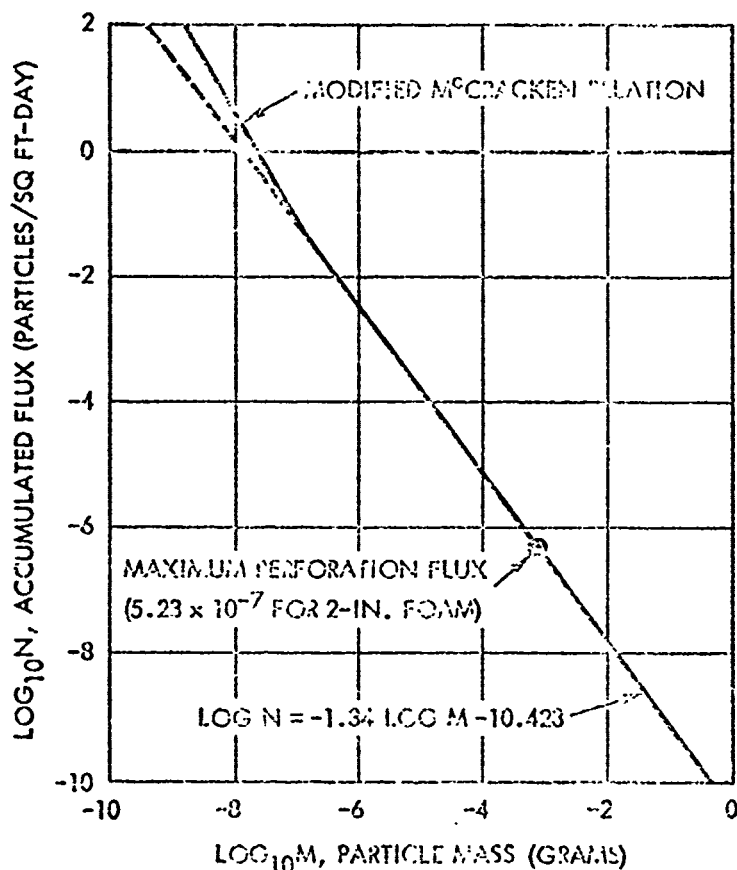


Figure 30. Near-Earth Micrometeoroid Environment

To determine the hazard presented by micrometeoroids, the selection of the flux model is highly significant. The above model was chosen based on wide acceptance by most of the industry. With this model, the total average number of impacts, T , of particles of mass, m , or larger is given as

$$T = SN \tau (FA_p + A_s),$$

where

S = intravehicle shielding X earth shielding,

$N = 10^{-10.423} M_m^{-1.34}$,
 = number of particles of mass ($M \geq 10^{-7}$ grams)
 per sq ft per day,

τ = mission deviation,

F = ratio of shower to sporadic micrometeoroids,
 and

A_p = projected area (sq ft).

Substituting the given value for N results in

$$T = S \tau (F A_p + A_s) 10^{-10.423} M_m^{-1.34}$$

This expression is now substituted into the Poisson distribution to obtain the probability of no impacts, $P_{(0)}$, of particles of mass M_m or larger.

$$\begin{aligned} P_{(0)} &= e^{-T} \approx 1 - T \\ &\approx 1 - S \tau (F A_p + A_s) 10^{-10.423} M_m^{-1.34} \end{aligned}$$

The airlock has the following approximate values for the parameters in this equation:

$$A_s \approx 75 \text{ sq ft}$$

$$A_p \approx 20 \text{ sq ft}$$

$$F \approx 1.0$$

$$\tau = 30 \text{ days}$$

$$S = 0.70 \text{ (earth shielding)} \times 0.5 \text{ (intravehicle shielding)}$$

$$= 0.35$$

The proposed material is felt to have a ballistic limit of about 2 mg. This is based on an extrapolation of the fact that ballistic limit of 2 inches of a similar structure has a ballistic limit of about 17 mg, and 1.5 inch has a ballistic limit of about 5 to 6 mg (Reference 4). Hence, the appropriate value of $M_m = 0.002 \text{ gm}$.

Substituting these values into the above equation results in a $P_{(o)}$ of about 0.9999.

h. Vent and Relief Valve Sizes. The following flow analyses were performed early in the program to evaluate the adequacy of the vents and relief valves under normal operating conditions and to see that the design ultimate burst pressures were not exceeded even under extremely unlikely cases such as accidental discharge of all five pressure bottles simultaneously.

The following difference now exists between the analysis given and the final configuration, but the analyses are still valid with proper interpretation.

The differences are:

- (1) The astronaut is not EVA in the pressurization events.
- (2) O_2 has been changed to N_2 for the pressurization gas.
- (3) The 3.5 psi relief valve has been deleted.

i. Flow Analysis. An airlock, with a volume of 78 ft^3 expanded and 100 in^3 packaged, is connected to a single supply line (orifice diameter - $1/16 \text{ in.}$) which is fed by five pressure bottles of oxygen. Each bottle has a volume of 150 in^3 with pressures of 2250, 2250, 3150, 3150, and 3150 psia respectively. The airlock is provided with two vents: one (orifice diameter = 0.84 in.) is electrically operated, and the second (orifice diameter = 0.75 in.) is manually operated. Also provided are two relief valves (James, Pond, & Clark, Inc. valve D524A-16D-5.5 and D524A-16D-3.5) with cracking pressures of 5.5 psia and 3.5 psia respectively. The following cases were analyzed (pressure-time relations). The ambient pressure is 0.0 psia, and the airlock is expanded unless otherwise specified.

Case 1 - Blow down (both vents open and both valves closed) with an initial pressure of 3.5 psia and an astronaut suit discharging 7.9 lb/hr.

Case 2 - Blow down (only electrical vent open) with initial pressure of 5.0 psia.

Case 3 - With only the 5.5 psia relief valve operating, unless otherwise specified, find the peak pressure in the following cases.

- (a) All five pressure bottles discharge with the airlock initially at 0.0 psia.
- (b) The three 3150 psia bottles discharge with the airlock initially at 5.0 psia.
- (c) All five bottles discharge with the airlock initially at 0.0 psia and the electrical vent open.

Case 4 - Case 3 c) with the airlock packaged.

Case 5 - Find the equilibrium pressure with the 3.5 psia relief valve operating and an astronaut suit discharging 7.9 lb/hr.

Using the equilibrium pressure found in Case 5 as an initial condition, one 3150 psia bottle discharges and the astronaut suit continues to discharge. Find the peak pressure.

Cases 6 through 10 - Repeat Cases 1 to 5 with the airlock in a KC-135 airplane in flight at a pressure altitude of 8000 ft (10.92 psia).

Flow Through an Orifice

<u>SYMBOL</u>	<u>DESCRIPTION</u>	<u>UNITS</u>
A	Area	In ²
C _d	Discharge coefficient	--
g	Standard gravitational acceleration	Ft/Sec ²
K	Specific heat ratio	--
m	Mass	Lb _m
p	Pressure	Psia
p _d	Discharge pressure	Psia
R	Gas constant per unit mass	Ft-Lb _f /Lb _m -°R
T	Temperature	°R
t	Time	Sec
W	Mass flow rate	Lb _m /Sec

Assuming isentropic flow of a perfect gas, the following equation can be derived from the continuity equation.

$$W = C_d A \sqrt{\frac{2 K g}{K - 1} \frac{p^2}{R T} \left[\left(\frac{p_d}{p} \right)^{2/K} - \left(\frac{p_d}{p} \right)^{\frac{K+1}{K}} \right]} \quad (1)$$

For subsonic flow ($\Delta p \ll p$; $C_d = 0.6$; O_2)

$$W = \frac{0.6925 p A}{\sqrt{T}} \sqrt{\frac{\Delta p}{p}} \quad 0 < \frac{\Delta p}{p} < 0.528 \quad (2)$$

For sonic flow $\left(\frac{p_d}{p} = \left(\frac{2}{K+1} \right)^{\frac{K}{K-1}} ; C_d = 0.9 ; O_2 \right)$

$$W = \frac{0.5029 p A}{\sqrt{T}} \quad 0.528 < \frac{\Delta p}{p} < 1 \quad (3)$$

For the following cases, all flows were considered isothermal with a temperature of 529°F.

Analysis

Case 1 - Consider the change in mass of oxygen in the airlock

$$\frac{dm}{dt} = W_{in} - W_{out} \quad (4)$$

W_{in} refers to the discharge of the astronaut suit, and W_{out} refers to flow through the vents. Assuming isothermal, sonic flow of a perfect gas through the vents, a differential equation of the following form expresses the relation between pressure and time in the airlock.

$$\frac{dp}{dt} = a - b p \quad \text{where } a, b = \text{constants} \quad (5)$$

Integrating and evaluating the constants:

$$p = 3.399 e^{-0.0495 t} + 0.101 \quad \text{where } p - \text{psia} \quad (6)$$

$t - \text{sec}$

This equation is graphed in Figure 31.

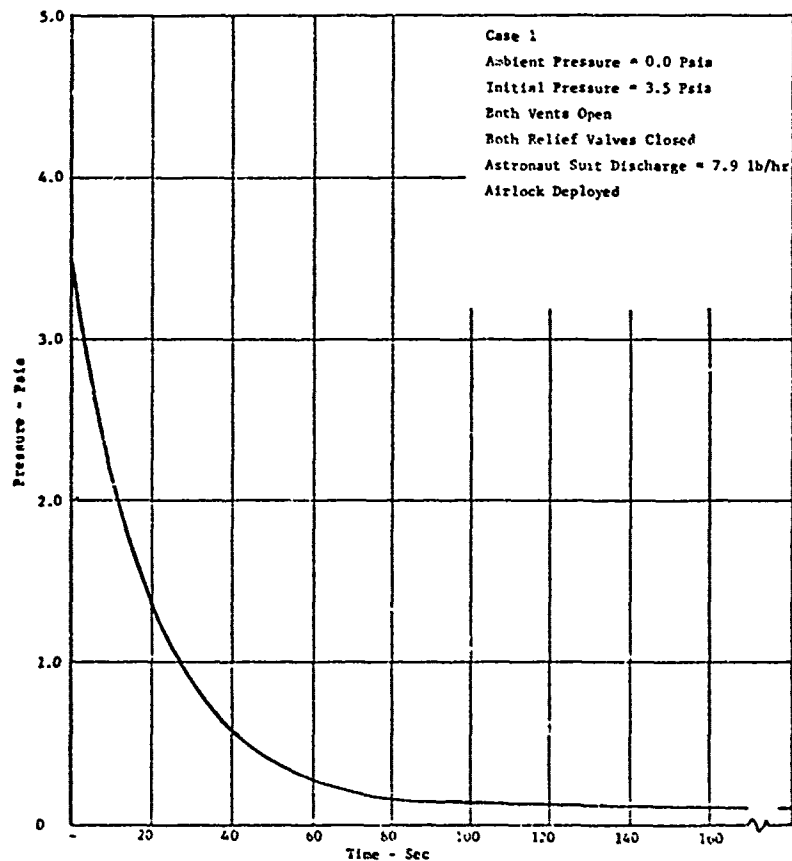


Figure 31

Case 2 - Using the same procedures as outlined in Case 1, the differential equation was derived:

$$\frac{dp}{dt} = -a p \quad \text{where } a = \text{constant} \quad (7)$$

Integrating and evaluating the constants:

$$p = 5. e^{-0.0275 t} \quad \text{where } p = \text{psia} \quad (8)$$

$$t = \text{sec}$$

This equation is graphed in Figure 32.

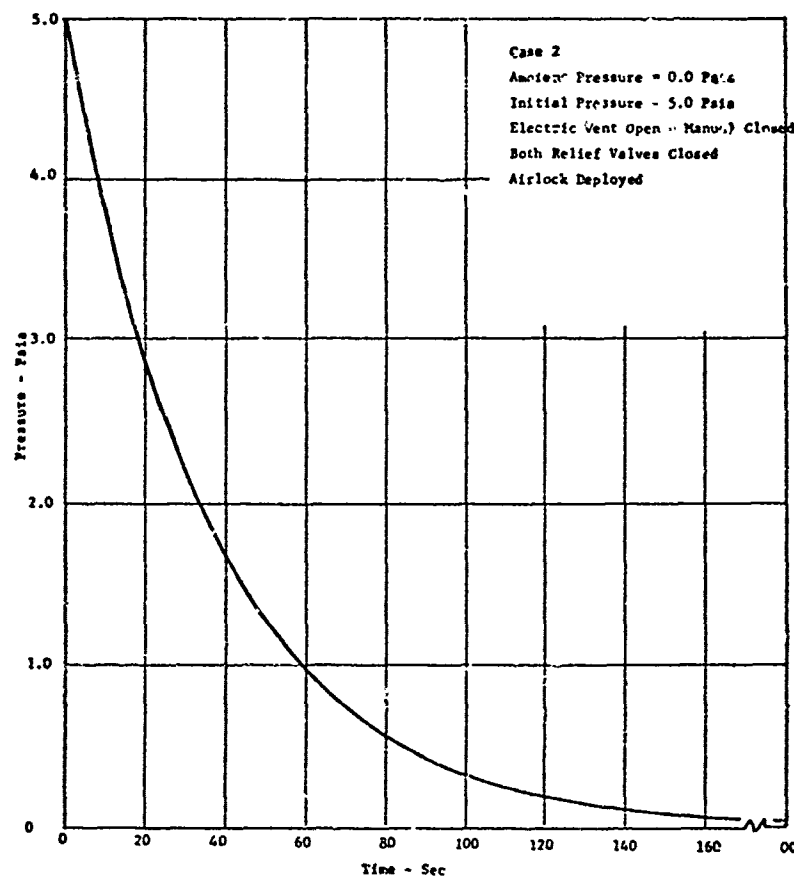


Figure 32

Case 3a - Consider the change in mass of oxygen in the pressure bottles.

$$\frac{dm}{dt} = W_{in} - W_{out} \quad (9)$$

Following the same procedure used in Case 2, an equation which expresses the pressure-time relation for the pressure bottles was derived and integrated.

$$p = 2790 e^{-0.0274 t} \quad \text{where } p = \text{psia} \quad (10)$$

$$t = \text{sec}$$

As pressure decreases in the pressure bottles, the pressure increases in the airlock. Without venting, the pressure in the airlock is equal to the ratio of the volume of the pressure bottles to the volume of the airlock times the decrease in pressure in the pressure bottles. When the pressure reaches 5.5 psia, the relief valve allows a mass flow rate out of the airlock depending on the airlock pressure. Using a graph found in Reference 1 and assuming sonic flow, a graph of pressure drop vs mass flow rate was constructed for the 5.5 psia relief valve.

Vendor data was adjusted for non-standard ambient pressures by presuming flow area is a function of pressure differential and utilizing the above orifice equations.

If the change in mass of oxygen in the airlock is now considered, the following differential equation exists:

$$\frac{dm}{dt} = W_{in} (p_B) - W_{out} (p_A) \quad (11)$$

where:

p_B is the pressure in the pressure bottles

p_A is the pressure in the airlock

Due to the nonlinearity of the relief valve, the IBM 360 computer was used to numerically integrate equation (11).

The result is graphed in Figure 33.

Case 3b - Essentially, the same procedure as explained in Case 3a was followed here. The time-pressure equation for the pressure bottles was found to be:

$$p = 3150 e^{-0.0457 t} \quad \text{where } \begin{matrix} p = \text{psia} \\ t = \text{sec} \end{matrix} \quad (12)$$

Equation (11) was again integrated numerically, and the result is shown in Figure 34.

Case 3c - Again the procedure used in Case 3a was followed. However, the loss of pressure due to the electrical vent must also be included. Assuming isothermal sonic flow through the vent:

$$\bar{W} = 0.0121 p \quad (13)$$

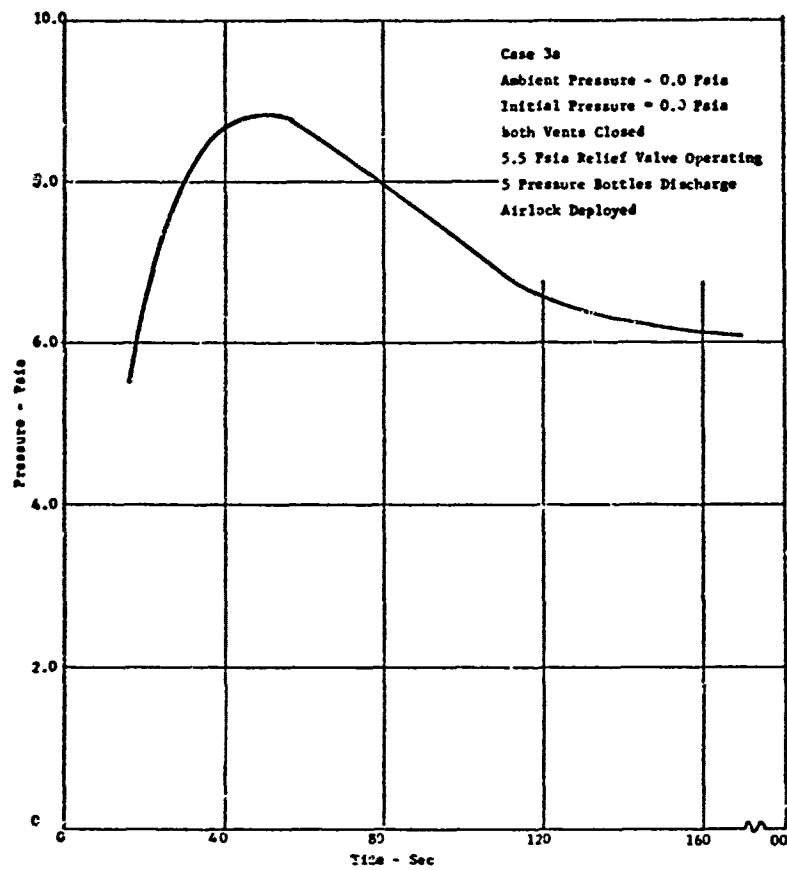


Figure 33

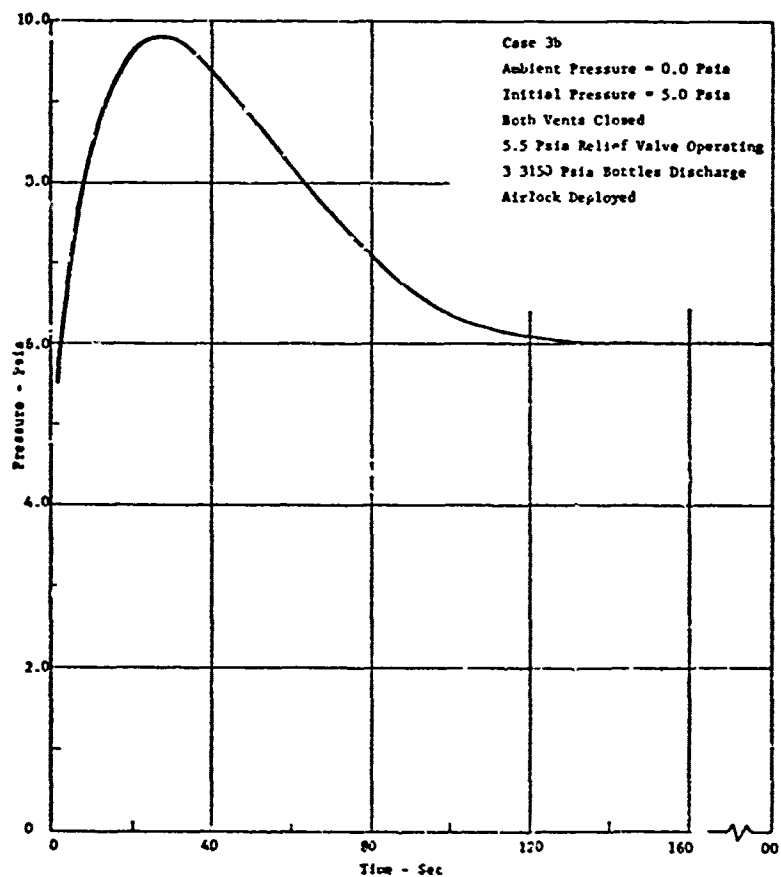


Figure 34

This leads to a revision of equation (11).

$$\frac{dm}{dt} = V_{in} (p_B) - W_{out} (p_A) - \bar{W}_{out} (p_A) \quad (14)$$

The above equation is integrated numerically and the results graphed in Figure 35.

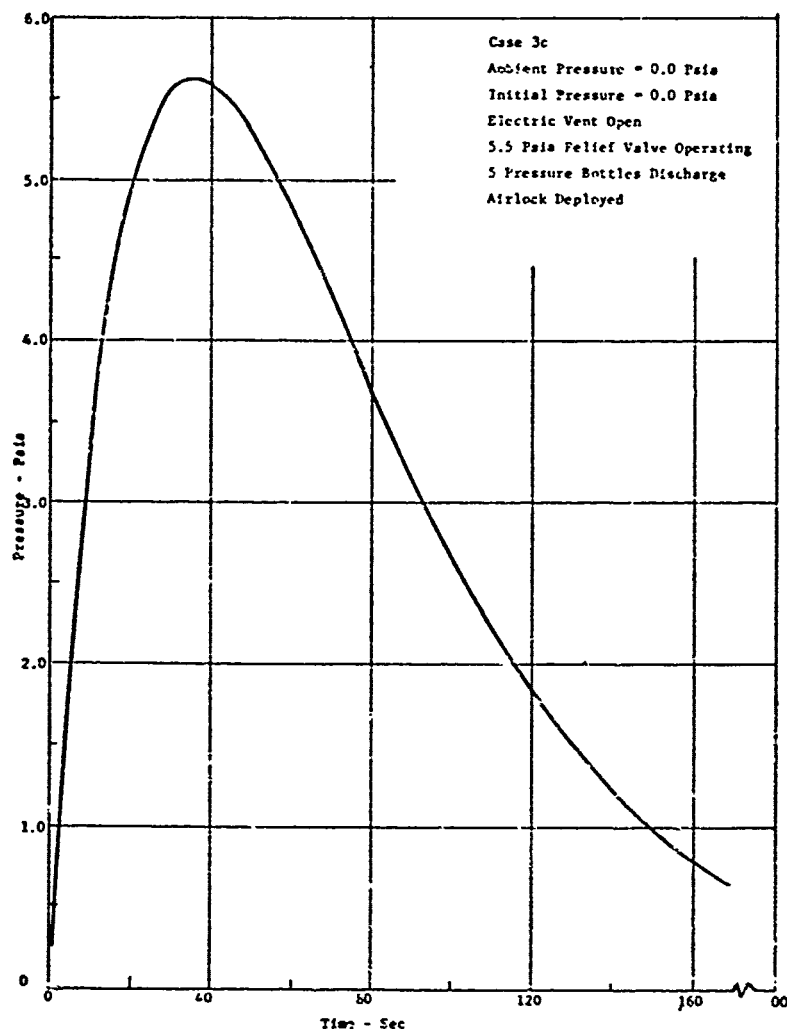


Figure 35

Case 4 - This case was solved in the same way as Case 3c. The change in airlock volume is evident from Figure 36.

Case 5 - Using Reference 1, a graph of mass flow rate vs pressure drop for sonic flow through the 3.5 psia relief valve was constructed. A mass flow rate of 7.9 lb/hr was found to exist at an airlock pressure of 4.02 psia.

Considering the change in mass of oxygen in one pressure bottle, the following pressure-time equation was derived:

$$p = 3150 e^{-0.137 t} \quad \text{where } p = \text{psia} \quad (15)$$

$t = \text{sec}$

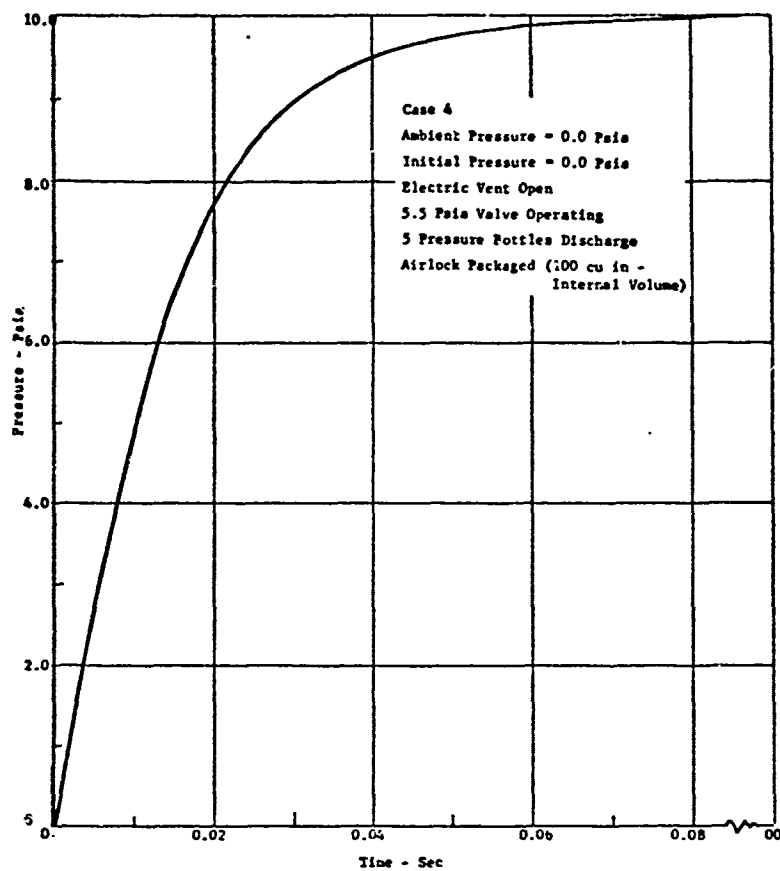


Figure 36

The results of procedures similar to those used above is shown in Figure 37.

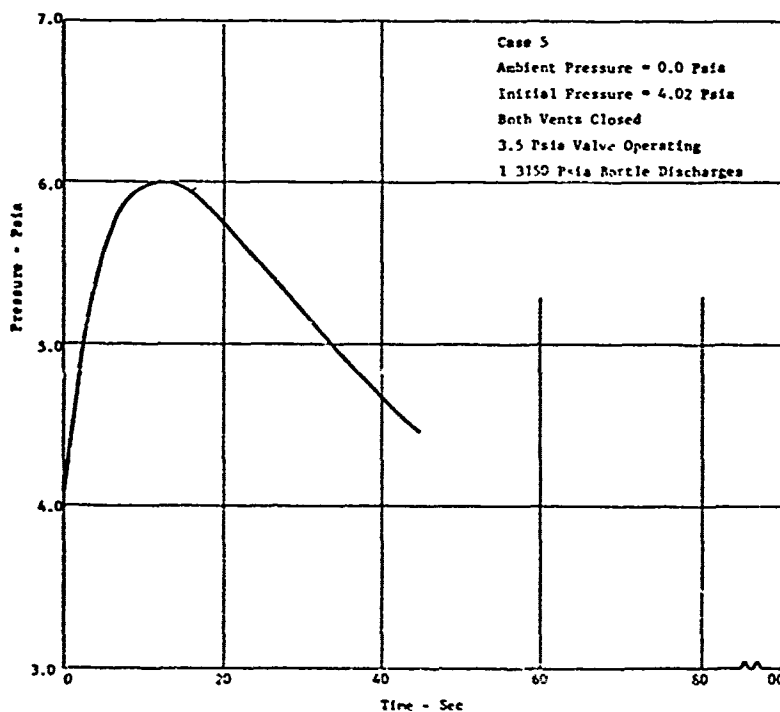


Figure 37

Case 6 - As in Case 1, the change in mass of oxygen in the airlock can be expressed as follows:

$$\frac{dm}{dt} = W_{in} - W_{out} \quad (16)$$

However, the mass flow out is characterized by a subsonic flow equation:

$$W_{out} = 0.6925 A \sqrt{\frac{p^2 - 10.92 p}{T}} \quad (17)$$

This leads to a differential equation of the form:

$$\frac{dp}{dt} = a - b \sqrt{p^2 - C p} \quad \text{where } a, b, c = \text{constants} \quad (18)$$

Integrating this equation and evaluating the constants yields:

$$t = 14.68 \ln \left[\frac{2320}{\sqrt{p^2 - 1573 p + 618,000} + \sqrt{p^2 - 1573 p}} \right] \\ + 0.197 \ln \left[\left(\frac{53.6 \sqrt{p^2 - 1573 p + 618,000} + 42,200 + 0.719 \sqrt{p^2 - 1573 p}}{\sqrt{p^2 - 1573 p} - 10.53} \right) / 100.7 \right] \quad (19)$$

where: $p = \text{lb/ft}^2$

$t = \text{sec}$

A graph of this equation is shown in Figure 38.

Case 7 - This case was solved in the same manner as Case 2 except that the flow through the electrical vent was considered subsonic.

$$W = 0.6925 A \sqrt{\frac{p^2 - 10.92 p}{T}} \quad (20)$$

$$\therefore \frac{dp}{dt} = a \sqrt{p^2 - b p} \quad \text{where } a, b = \text{constants} \quad (21)$$

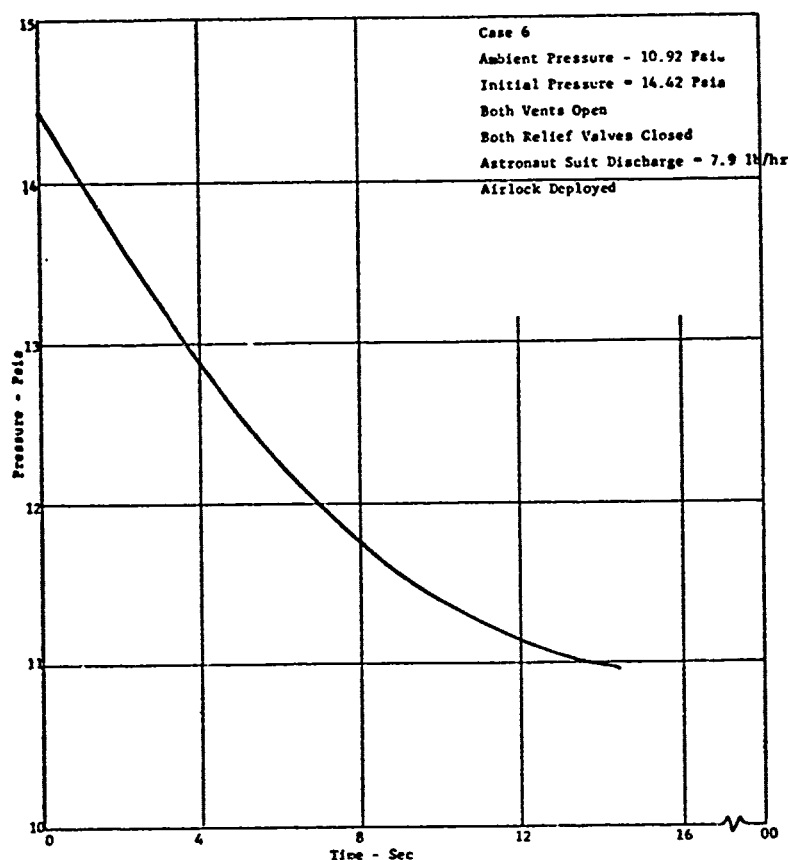


Figure 38

Integrating and evaluating the constants:

$$t = 26.4 \ln \left[\frac{2793}{\sqrt{p^2 - 1573 p} + p - 786.5} \right] \quad (22)$$

where:

$$p = \text{lbf/ft}^2$$

$$t = \text{sec}$$

A graph of this equation is shown in Figure 39.

Cases 8a, 8b, 8c, and 9 - These cases follow the same procedures as Cases 3a, 3b, 3c, and 4 respectively except that the flow out of the airlock through either the relief valve or the electrical vent is subsonic:

$$W = 0.6925 A \sqrt{\frac{p^2 - 10.92 p}{T}} \quad (23)$$

With this correction, a computer study similar to Cases 3a, 3b, 3c, and 4 was run. The results are shown in Figures 40, 41, 42, and 43.

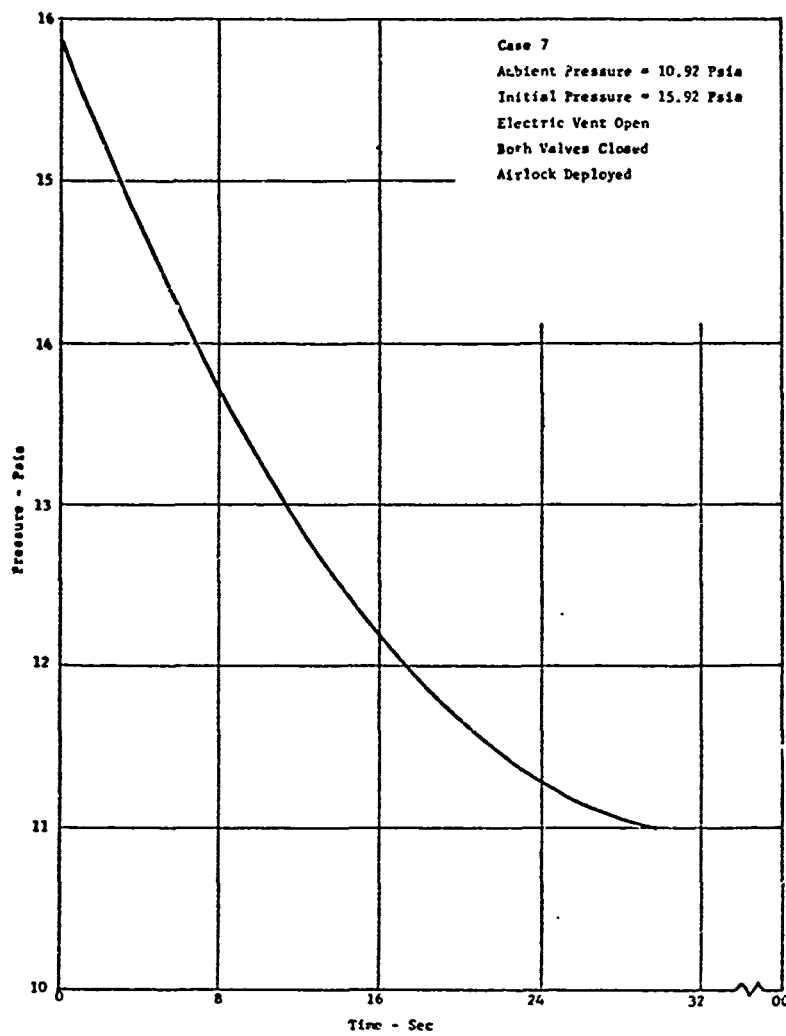


Figure 39

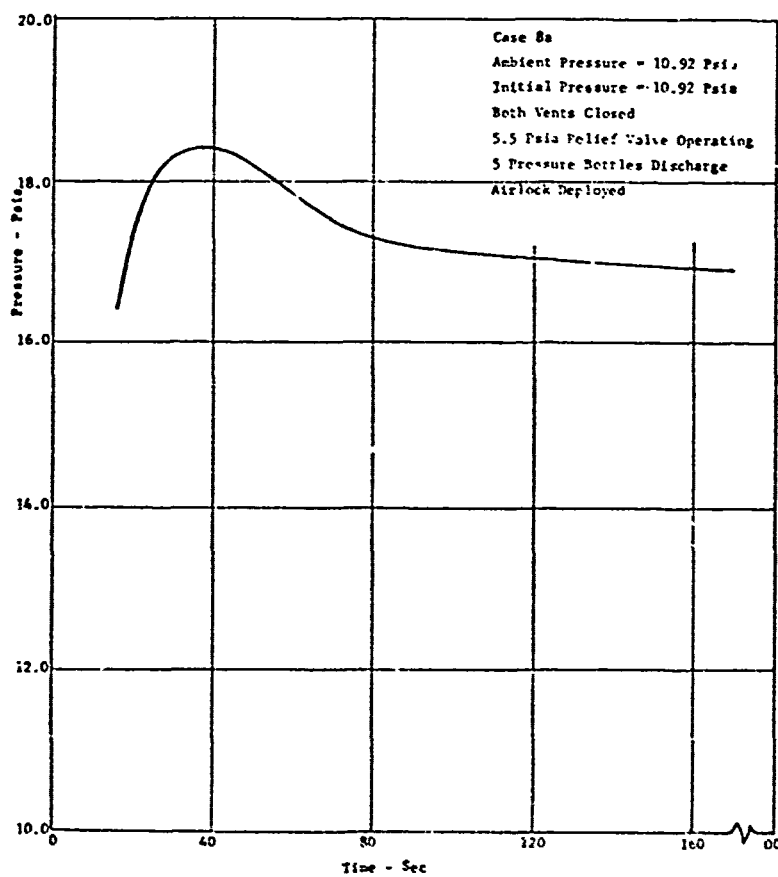


Figure 40

Figure 41

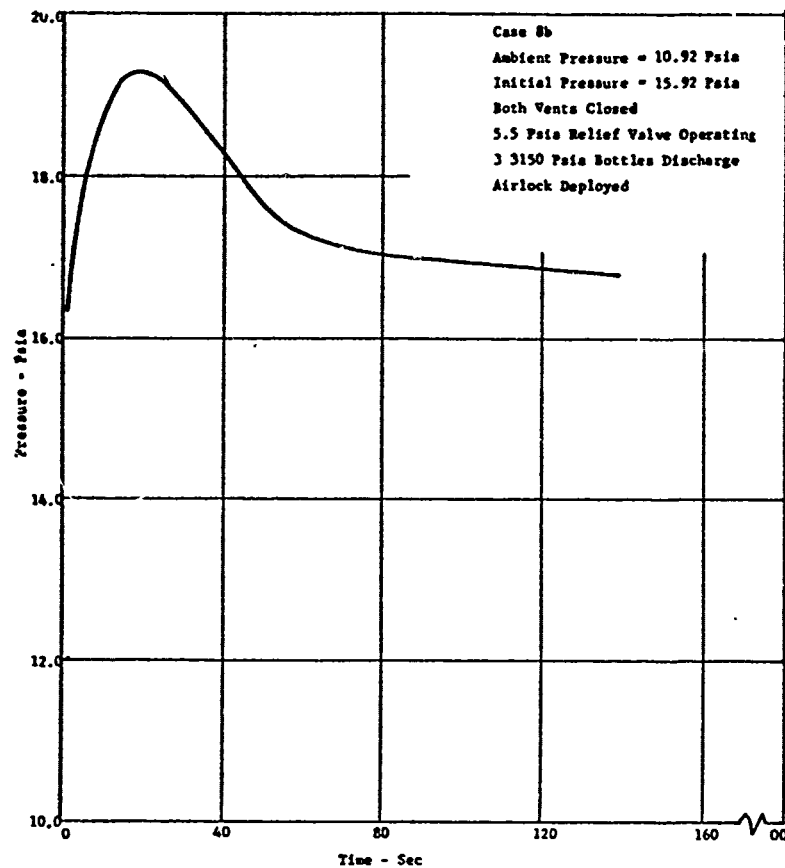
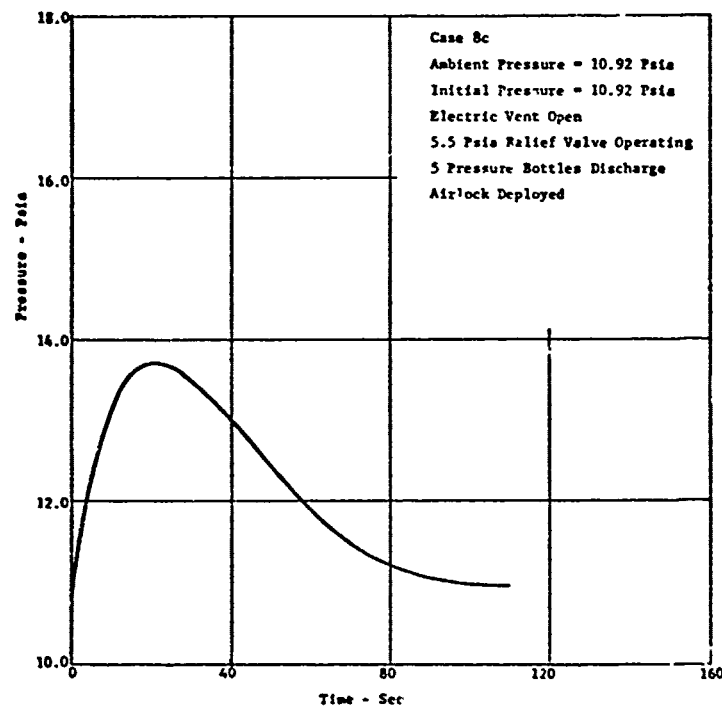


Figure 42



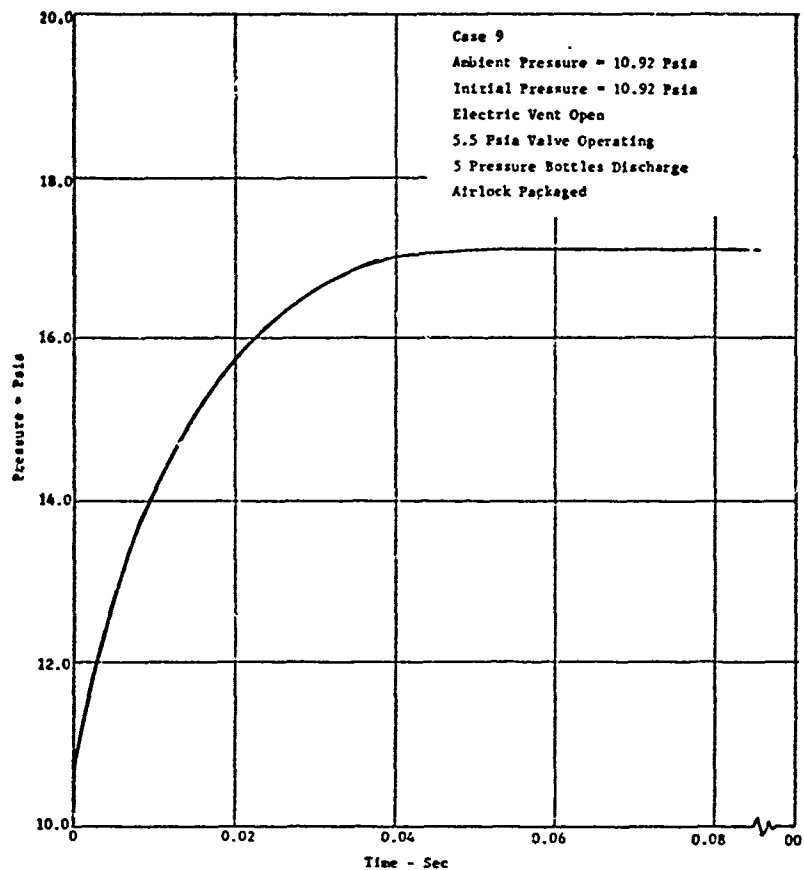


Figure 43

Case 10 - As in Case 5, a graph of mass flow rate vs pressure drop was constructed for the 3.5 psia relief valve. However, the flow through the valve was considered subsonic. A mass flow rate of 7.9 lb/hr was found to exist at an airlock pressure of 14.85 psia or 3.93 psig.

Using the same procedures as used in Case 5 (with subsonic flow through the valve), a pressure-time equation was numerically integrated on the computer. The result is shown in Figure 44.

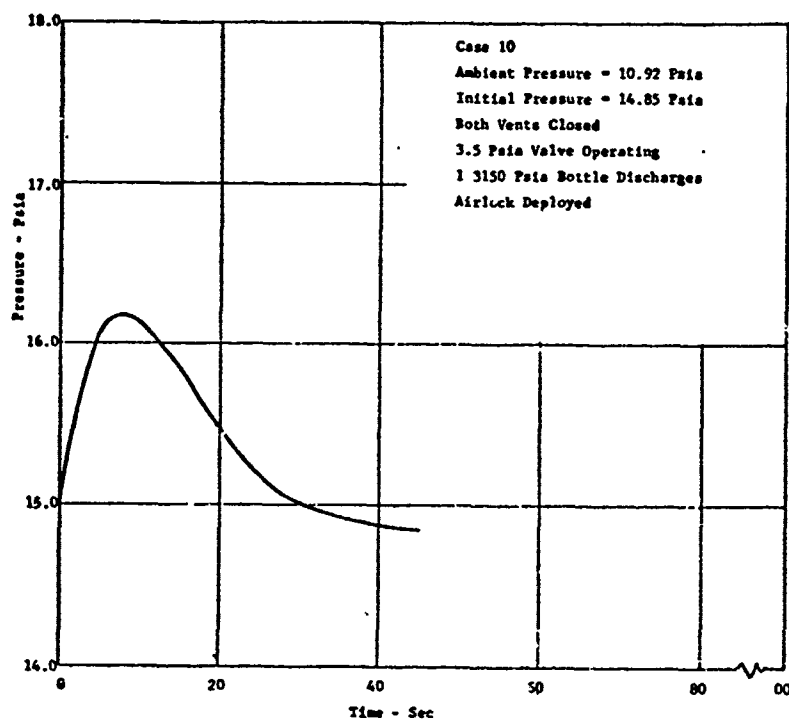


Figure 44

j. Electrical Power Requirements Analysis. The NASA/AM power to be supplied at the D021 electrical interface requires 28 volts DC at a total connected load of 6.3 amperes for the experiment plus a cyclic requirement of 0.83 amperes for the battery heaters on a thermostatically controlled basis. A dual self-contained battery pack is also provided as part of the D021 Airlock to provide power for the pyrotechnically operated gas discharge valves in the pressurization system.

The power profile for the various experiment operating modes is given in Table IV. The detail electrical load analysis by component is given in Table V.

Table IV. Power Profile

Operating Mode	Duration Minutes	Average Load Amps		Total Load - Amps			Peak Duration
		Remote Control Panel Load**	D-21 Airlock Load*	Average	Peak	Peaks/ Mode	
1. Experiment On	6.8	0.24	0.34	0.58	-	-	-
2. T/M Calibration	**	0.24	0.38	0.62	-	-	-
3. Harness Release	3.0 sec	0.28	0.34	0.62	1.62	1	3 sec.
4. Pressure System Armed	5.3	0.32	0.57	0.89	-	-	-
5. Preshaping Pressurization	5.1	0.28	0.65	0.93	2.08	1	1 sec.
6. Vent	1.0 sec	0.24	0.34	0.58	1.70		
7. Long-Term Leakage Pressure Test	Intermittent 15-day (Approx.)	0.24	0.34	0.58	1.72	1	1 sec.
8. Ingress-Egress	29.7	0.28	2.34	2.62			
9. Hatch Re-sealing Pressurization Test	7.	0.32	0.74	1.06	1.18	1	1 sec.
10. Final Vent	1 sec.	0.24	0.34	0.58	1.70	1	1 sec.
Battery Heating***	As Required	--	--	0.83	--	-	-

* Battery Heaters are not included in D-21 Airlock Experiment Loads

** Estimated on basis of suggested schematic - Actual design and equipment selection will be by MDAC

*** Battery Heater load controlled thermostatically to apply 10 watts per pack (2 packs) when temperature is below 85° F

**** TM data readout required. Switching arrangement and timing to be determined by MDAC

TABLE V. D021 AIRLOCK ELECTRICAL LOAD ANALYSIS

Part Name	Connected Load 28 VDC Nom. (Amps)	Start Experiment (Amps) (0.2 min)	Vent (Close) (Amps) (1 sec.)	Harness Release (Amps) (3 sec.)	Press. Sys. Arm (0.2 min.)	Deploy & Front Press. (Amps) (5.0 min.)	15-Day Test Disarm (Amps) (15-days)	Vent (Open) (Amps) (1 sec.)	Ingress/ Egress	Vent (Close) (Amps) (1 sec.)	Pressure System Re-Arm	Working Pressure Test and Disarm	Vent (Open) (Amps) (1 sec.)
Instrument Box Assy Converter #124	0.260	0.260	0.260	0.260	0.260	0.260	0.260	0.260	0.260	0.260	0.260	0.260	0.260
Converter # 34	0.075	0.075	0.075	0.075	0.075	0.075	0.075	0.075	0.075	0.075	0.075	0.075	0.075
7/M Cal. Relay Sub Total	0.004 0.379	0.335	0.335	0.335	0.335	0.335	0.335	0.335	0.335	0.335	0.335	0.335	0.335
Press. Sys. NASA Pol Ind. Lts.	0.040	0.040	0.040	0.040	0.040	0.040	0.040	0.040	0.040	0.040	0.040	0.040	0.040
Arm	0.080	-	-	-	0.040	0.040	-	-	-	-	0.040	-	-
Hi Press(2)	0.080	0.080	0.080	0.080	0.080	0.080	0.080	0.080	0.080	0.080	0.080	0.080	0.080
Lo Press(2)	0.040	0.040	0.040	0.040	0.040	0.040	0.040	0.040	0.040	0.040	0.040	0.040	0.040
Prehype Press	0.040	0.040	0.040	0.040	0.040	0.040	0.040	0.040	0.040	0.040	0.040	0.040	0.040
Warning Press	0.040	0.040	0.040	0.040	0.040	0.040	0.040	0.040	0.040	0.040	0.040	0.040	0.040
Deploy	0.040	0.040	0.040	0.040	0.040	0.040	0.040	0.040	0.040	0.040	0.040	0.040	0.040
Vent (2)	0.080	0.040	0.040	0.040	0.040	0.040	0.040	0.040	0.040	0.040	0.040	0.040	0.040
Light On	0.040	0.040	0.040	0.040	0.040	0.040	0.040	0.040	0.040	0.040	0.040	0.040	0.040
Sub Total	0.480	0.240	0.240	0.280	0.320	0.280	0.240	0.280	0.280	0.280	0.320	0.240	0.240
Lighting	2.04							2.040	2.040	2.040	2.040	2.040	2.040
Relay Box													
Relays													
Arm	0.230	-	-	-	0.230	0.230	-	-	-	-	0.230	0.230	-
Prehype Press	0.068	-	-	-	-	0.068	-	-	-	-	0.068	0.068	-
Leak Test Press	0.068	-	-	-	-	-	-	-	-	-	-	0.068	-
Sub Total	0.466	-	-	-	0.230	0.318	-	-	-	-	0.318	0.406	-
Harness Release Motor	1.0(1 min)(3.5(surge))			1.000									
Vent Valve	1.0(1 sec)(surge)		1.0(1 sec)	-	-	-	-	1.0(1 sec)	-	1.0(1 sec)	-	-	1.0(1 sec)
Relay	1.0(1 sec)(surge)		0.115(1 sec)	-	-	-	-	0.115(1 sec)	-	0.115(1 sec)	-	-	0.115(1 sec)
Sub Total	0.115(1 sec)		1.115(1 sec)	0.615	0.865	0.933	0.975	1.115(1 sec)	-	1.115(1 sec)	-	-	1.115(1 sec)
TOTAL	-	0.575	0.575	1.615(1 sec)	1.693	1.761	1.403	3.770(1 sec)	2.655	2.655	3.013	3.021	2.615
Total (Peak) With Battery Heaters	0.828	1.403	2.518	2.443	1.693	1.761	1.403	4.598	3.483	4.598	3.841	3.849	4.556

65.3

65.2

65.1

See the following pages
for further details

TABLE V. DO21 AIRLOCK ELECTRIC

Part Name	Connected Load 28 VDC Nom. (Amps)	Start Experiment (Amps) (0.2 min)	Vent (Close) (Amps) (1 sec.)	Harness Release (Amps) (3 sec.)	Press. Sys. Armed (Amps) (0.2 min.)	Deploy & Proof Press. (Amps) (5.0 min.)	15-De Di (A) (15-
Instrument Box Assy Converter ±12V	0.260	0.260	0.260	0.260	0.260	0.260	0.2
Converter + 5V	0.075	0.075	0.075	0.075	0.075	0.075	0.0
T/M Cal. Relay	<u>0.044</u>	—	—	—	—	—	—
Sub Total	0.379	0.335	0.335	0.335	0.335	0.335	0.3
Press. Sys. NASA Pnl Ind. Lts.							
Start	0.040	0.040	0.040	0.040	0.040	0.040	0.0
Arm	0.040	-	-	-	0.040	0.040	-
Hi Press(2)	0.080	-	-	-	-	0.080	0.0
Lo Press(2)	0.080	0.080	0.080	0.080	0.080	-	-
Preshape Press	0.040	0.040	0.040	0.040	0.040	-	-
Warning Press	0.040	0.040	0.040	0.040	0.040	0.040	0.0
Deploy	0.040	-	-	0.040	0.040	0.040	0.0
Vent (2)	0.080	0.040	0.040	0.040	0.040	0.040	0.0
Light On	<u>0.040</u>	—	—	—	—	—	—
Sub Total	0.480	0.240	0.240	0.280	0.320	0.280	0.2
Lighting Relay Box Relays							
Arm							
	0.230	-	-	-	0.230	0.230	-
Preshape Press	0.088	-	-	-	-	0.088	-
Leak Test Press	<u>0.088</u>	—	—	—	—	—	—
Sub Total	0.406	-	-	-	0.230	0.318	-
Harness Release Motor							
Vent Valve	1.0(1 min)(3.5(surge)			1.000			
Relay	1.0(1 sec)5.0(surge)		1.0(1 sec)	-	-	-	-
	<u>0.115(Momentary)</u> -		<u>0.115(1 sec)</u>				
Sub Total	1.115(1 sec)		1.115(1 sec)				
TOTAL		0.575	0.575	0.615	0.865	0.933	0.1
	-	-	1.690(1 sec)	1.615(1 sec)	-	-	-
Total (Peak) With Battery Heaters	0.828	1.403	2.518	2.443	1.693	1.761	1.1

65.1

65.2

TABLE V. D021 ATRLOCK ELECTRICAL LOAD ANALYSIS

Vent (Close) (Amps) (1 sec.)	Harness Release (Amps) (3 sec.)	Press. Sys. Armed (Amps) (0.2 min.)	Deploy & Proof Press. (Amps) (5.0 min.)	15-Day Test Disarm (Amps) (15-days)	Vent (Open) (Amps) (1 sec.)	Ingress/ Egress	Vent (Close) (Amps) (1 sec.)	Pressure System Re-Armed
0.260	0.260	0.250	0.260	0.260	0.260	0.260	0.260	0.260
0.075	0.075	0.075	0.075	0.075		0.075	0.075	0.075
0.335	0.335	0.335	0.335	0.335	0.335	0.335	0.335	0.335
0.040	0.040	0.040	0.040	0.040	0.040	0.040	0.040	0.040
-	-	0.040	0.040	-	-	-	-	0.040
-	-	-	0.080	0.080	-	-	-	-
0.080	0.080	0.080	-	-	0.080	0.080	0.080	0.080
0.040	0.040	0.040	-	-	-	-	-	-
0.040	0.040	0.040	0.040	0.040	0.040	0.040	0.040	0.040
-	0.040	0.040	0.040	0.040	0.040	0.040	0.040	0.040
0.040	0.040	0.040	0.040	0.040	0.040	0.040	0.040	0.040
-	-	-	-	-	0.040	0.040	0.040	0.040
0.240	0.280	0.320	0.280	0.240	0.280	0.280	0.280	0.320
					2.040	2.040	2.040	2.040
-	-	0.230	0.230	-	-	-	-	0.230
-	-	-	0.088	-	-	-	-	0.088
-	-	-	-	-	-	-	-	-
-	-	0.230	0.318	-	-	-	-	0.318
1.0(1 sec)	1.000	-	-	-	1.0(1 sec)	-	1.0(1 sec)	-
0.115(1 sec)	-	-	-	-	0.115(1 sec)	-	0.115(1 sec)	-
1.115(1 sec)	-	-	-	-	1.115(1 sec)	-	1.115(1 sec)	-
0.575	0.615	0.865	0.933	0.575	2.655	2.655	2.655	3.013
1.690(1 sec)	1.615(1 sec)	-	-	-	3.770(1 sec)	-	3.770(1 sec)	-
2.518	2.443	1.693	1.761	1.403	4.598	3.483	4.598	3.841

65.2

65.3

INTERLOCK ELECTRICAL LOAD ANALYSIS

Qty & Pr. ss. (Amps) (15 days)	1--Day Test Disarm (Amps) (15-days)	Vent (Open) (Amps) (1 sec.)	Ingress/ Egress	Vent (Close) (Amps) (1 sec.)	Pressure System Re-Armed	Working Pressure Test and Disarm	Vent (Open) (Amps) (1 sec.)
0.260	0.260	0.260	0.260	0.260	0.260	0.260	0.260
0.075	0.075		0.075	0.075	0.075	0.075	0.075
0.335	0.335	0.335	0.335	0.335	0.335	0.335	0.335
0.040	0.040	0.040	0.040	0.040	0.040	0.040	0.040
0.040	-	-	-	-	0.040	-	-
0.080	0.080	-	-	-	-	0.080	-
-	-	0.080	0.080	0.080	0.080	-	0.080
-	-	-	-	-	-	-	-
0.040	0.040	0.040	0.040	0.040	0.040	-	-
0.040	0.040	0.040	0.040	0.040	0.040	0.040	0.040
0.040	0.040	0.040	0.040	0.040	0.040	0.040	0.040
-	-	0.040	0.040	0.040	0.040	0.040	0.040
0.280	0.240	0.280	0.280	0.280	0.320	0.240	0.240
		2.040	2.040	2.040	2.040	2.040	2.040
0.230	-	-	-	-	0.230	0.230	-
0.088	-	-	-	-	0.088	0.088	-
-	-	-	-	-	-	0.088	-
0.318	-	-	-	-	0.318	0.406	-
	-	1.0(1 sec)	-	1.0(1 sec)	-	-	1.0(1 sec)
		0.115(1 sec)	-	0.115(1 sec)	-	-	0.115(1 sec)
		1.115(1 sec)	-	1.115(1 sec)	-	-	1.115(1 sec)
0.575	0.575	2.655	2.655	2.655	3.013	3.021	2.615
-	-	3.770(1 sec)	-	3.770(1 sec)	-	-	3.730(1 sec)
1.403	1.403	4.598	3.483	4.598	3.841	3.849	4.558

65.3

SECTION III

TEST PROGRAM

A. MATERIALS EVALUATION AND DEVELOPMENT TESTS

Material off-gassing tests were performed to establish weight loss and level of toxic by-products as reported in Appendix V. These tests were made at room temperature and the results were considered acceptable for the early orbital workshop configuration. More stringent requirements were added by Reference 2 when the ATM experiment was added to the same mission.

The off-gassing tests were then repeated at 212°F and 10^{-6} TORR vacuum for the outer composite of the expandable structure. (The outer cover, micrometeoroid layer and the filament wound structure.) The bladder composite was not retested because it is not exposed to the space environment and therefore will not be subject to off-gassings.

The outer cover and thermal control coating were retested to 275°F and 10^{-6} TORR vacuum. The results given in Figures 45 and 46 are well within the maximum allowable limit of 0.04 %/sq cm/hr. These materials were also qualified as "self-extinguishing in air" to meet Category "H" requirements for "Materials in Uninhabited Portions of the Spacecraft" (Reference 5). The results of these tests are reported in Appendix VI.

One effect of achieving this fire-resistant capability resulted in the selection of 2.0 pcf foam for the micrometeoroid barrier instead of the 1.0 pcf foam as originally planned. (The 1.0 pcf foam was not available in fire-resistant quality.)

One less desirable feature of this change became apparent during subsequent deployment tests at low temperature. It was discovered that the stiffness of the 2.0 pcf foam was an order of magnitude higher at -65°F than that of 1.0 pcf foam, whereas they are reasonably close at room temperature. This difference made the thermal superinsulating blanket a necessary addition to the airlock in the packaged state. The low temperature flexibility characteristics of both foams are shown in Figures 47 and 48.

B. SIMULATED MICROMETEOROID IMPACT TESTS

A comprehensive series of hypervelocity particle impact tests were performed at Arnold Engineering Development Center, Arnold Air Force Station, Tennessee. Samples of composite material duplicating the D021 expandable structure were provided for the testing. Results of the tests were reported in Reference 6.

The ballistic mass limit of the projectile was found to be close to four (4) milligrams as illustrated on Figure 49. This verifies that the analytical value of two (2) milligrams mass used in the calculations of Section II C 2 was a conservative assumption.

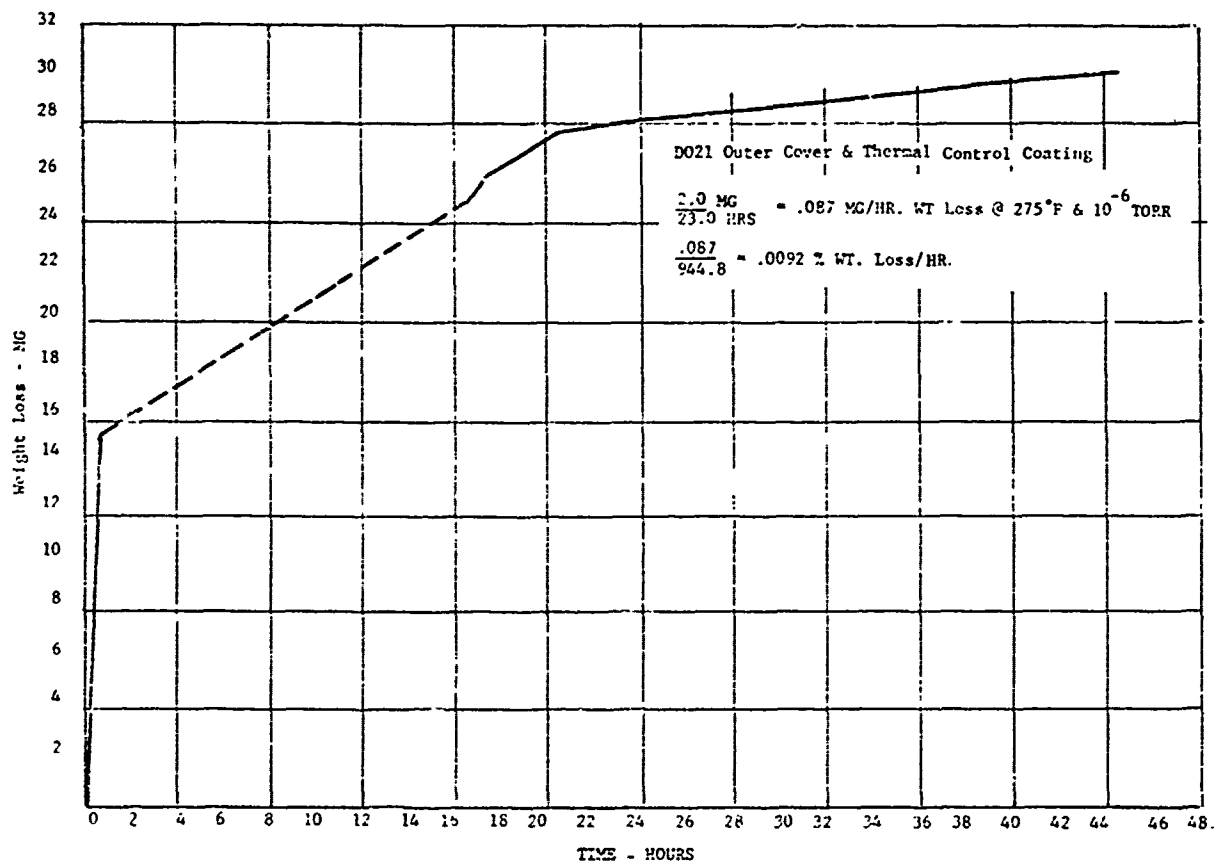


Figure 45

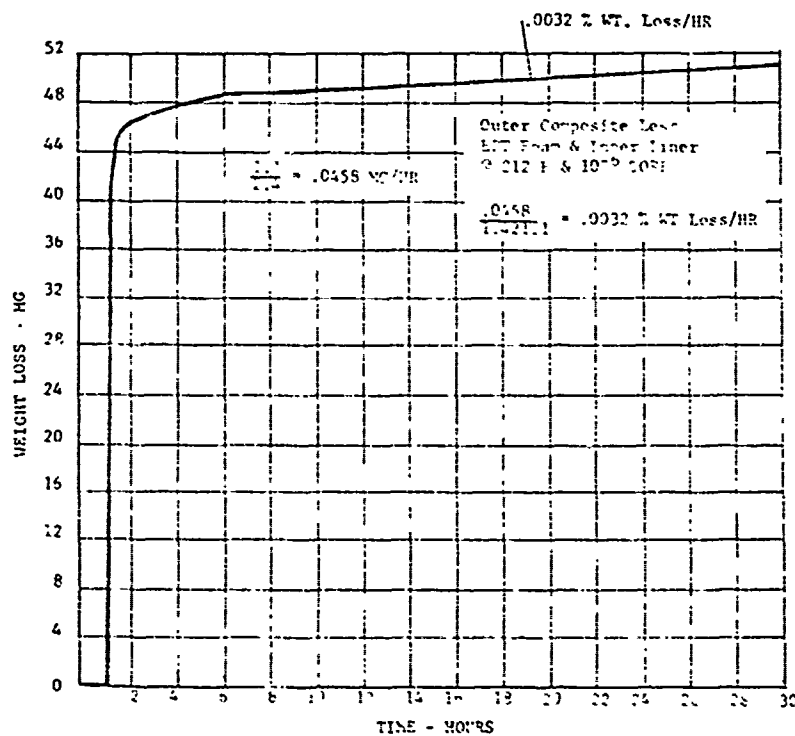


Figure 46

Figure 47

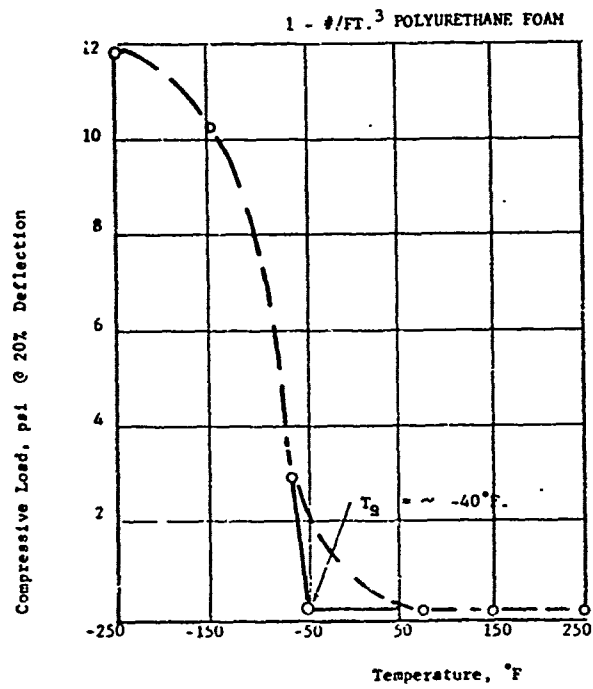
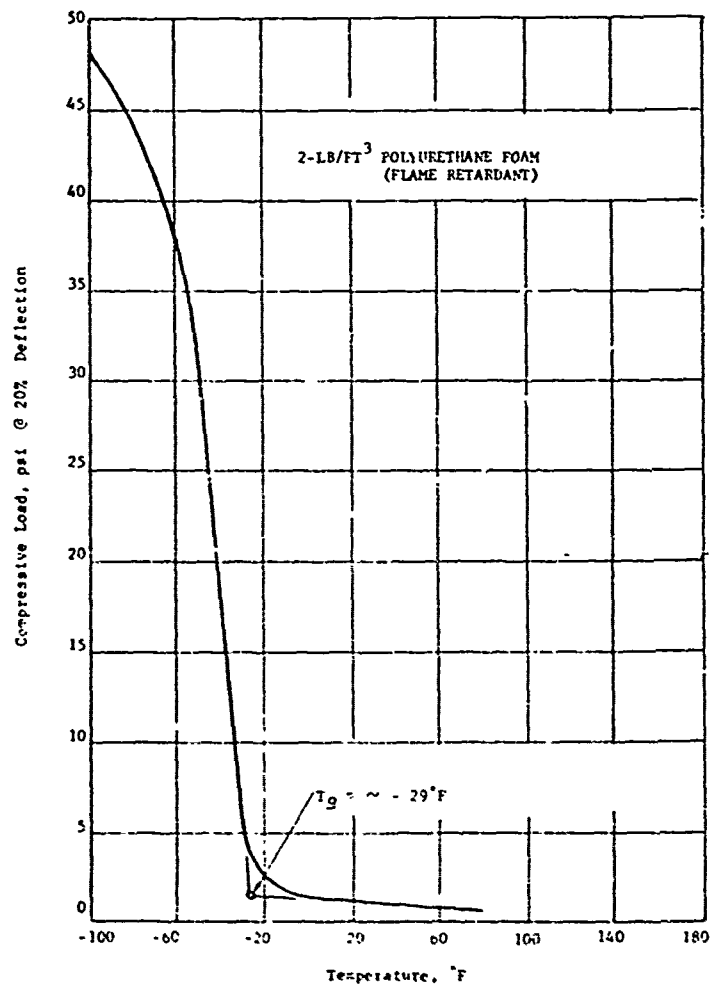


Figure 48



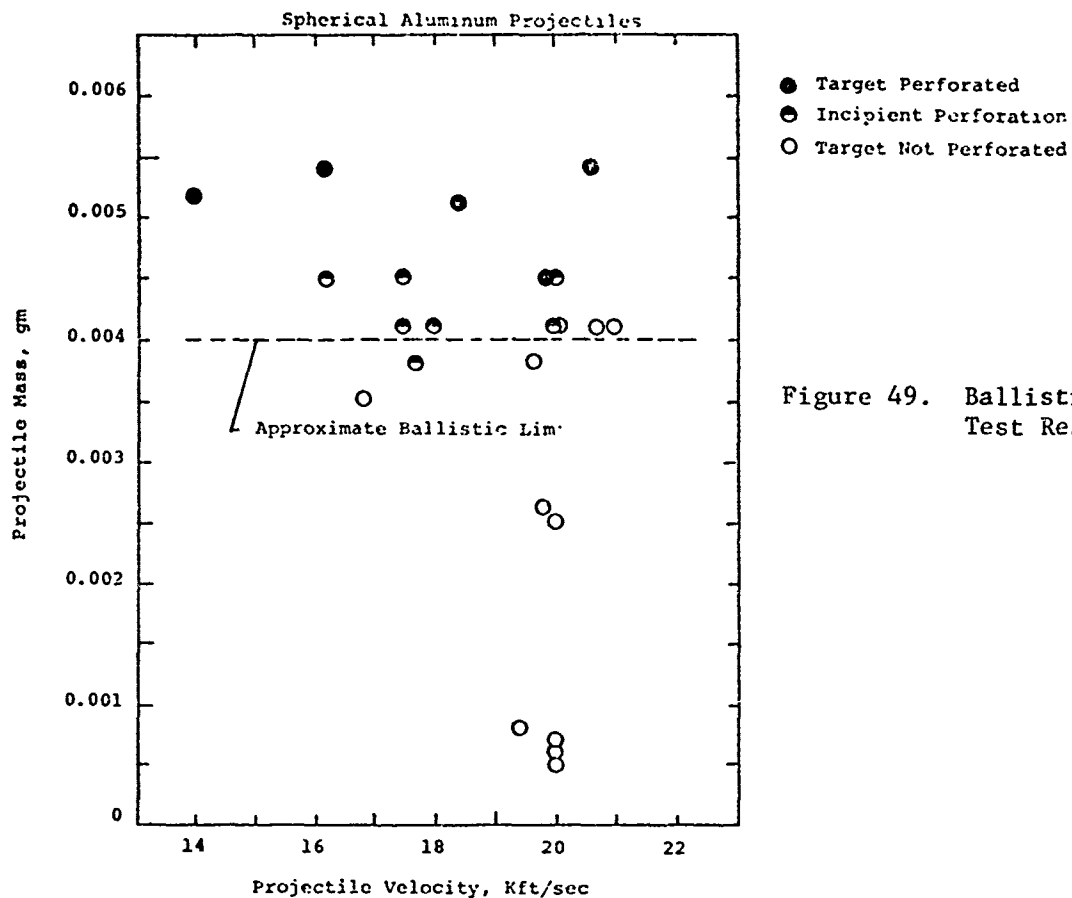


Figure 49. Ballistic Limit Test Results

Results of tests with 5 psia O_2 on the bladder side instead of vacuum were also gratifying. The ballistic limit was found to be the same in either case, (after improving the specimen clamping method) and furthermore, the material did not burn except in the region of the particle path even when complete penetration of the wall occurred with the higher mass projectiles.

C. ENVIRONMENTAL QUALIFICATION TESTS

Prior to starting the Environmental Qualification Tests the test unit was subjected to the following acceptance testing in order to assure that the article was ready for the formal test program. (The results of these Acceptance Tests were reported in Reference 7)

- (1) Leak Test, Preliminary. The unit is pressurized to 3.5 psi and pressure monitored for two (2) hours to verify that no gross leakage is present.
- (2) The unit is then packaged, weighed, and the center of gravity established.
- (3) The test article is then mounted on the MB Model C-210 Vibration Exciter and subject to a low level, one minute duration, Random Vibration Test in each of the three (3) axes. The vibration spectrum is shown on Figure 50. After the test, a complete check of the electrical circuitry is conducted to verify that no damage has occurred. A thorough visual inspection is also performed.

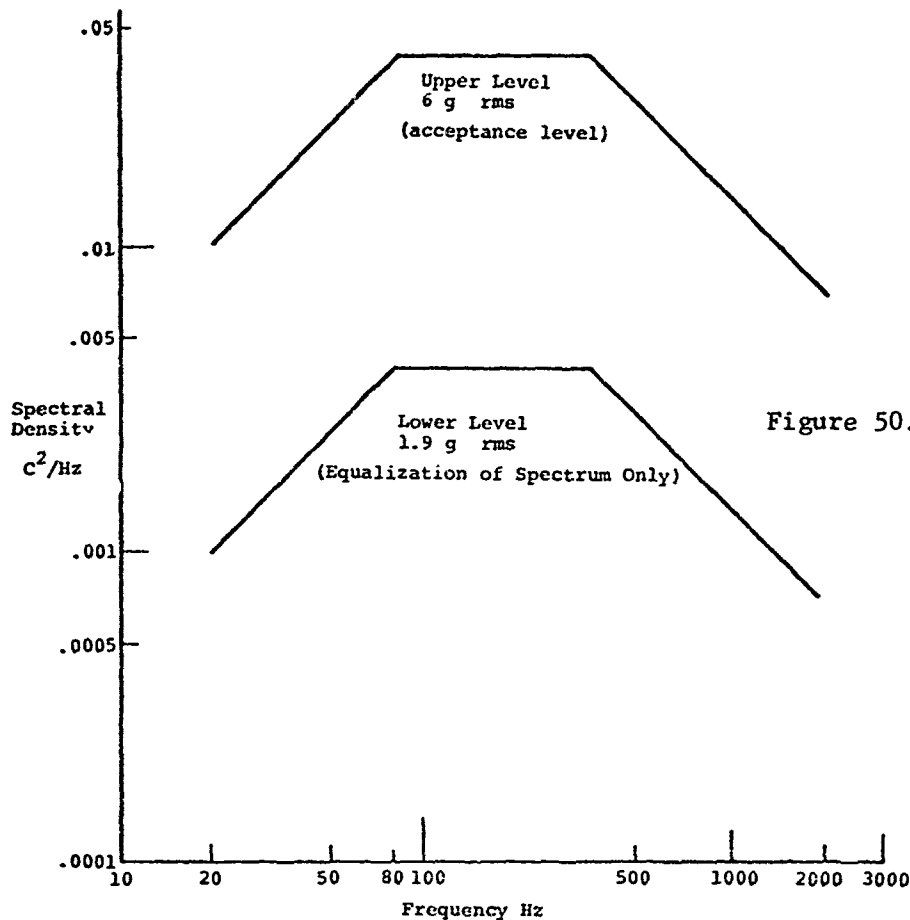


Figure 50. Airlock Vibration Profile

- (4) The unit is then deployed and pressurized to 5.0 psi proof pressure for 30 minutes. Pressure is then relieved to 3.5 psi and monitored for a 24-hour period to establish leak rate. The results of this leakage test are reported in Appendix VII.

After the above tests, the airlock was checked to see that all electrical circuits were still functioning and visually inspected for any evidence of deterioration. Upon passing this inspection, it was packaged and began the Environmental Qualification Test Program.

The qualification testing falls into two general categories

- (1) the ground environments, and
- (2) the launch and space mission environments.

Under the first category of tests, the unit was subject to 100 percent relative humidity, temperature cycling, salt fog exposure, and fungus growth. In addition, several shipments were made by air, and commercial truck between Akron, Ohio, Tullahoma, Tennessee, and Huntsville, Alabama with no special precautions taken other than being packed in the special shipping container.

During the humidity testing, an initial weakness was discovered in the printed circuit boards and power supplies which was corrected as described in Appendix VIII. Subsequently, the unit was repaired and was retested without repetition of this difficulty.

The fungus, salt fog and acoustic tests were subcontracted to Wyle Laboratories, Huntsville, Alabama. The results of these tests are presented in Appendix IX.

Under the second category of tests, the airlock was exposed to simulated launch pressure changes, accelerations, vibrations, acoustic noise, solar exposure, combined low temperature and vacuum, functional deployment at low temperature and vacuum, and cyclic endurance testing from 0 to 5.0 psi under simulated space environments.

With the exception of "Acoustic Noise" which was performed by Wyle Laboratories, Inc., the remainder of these tests were conducted by the Arnold Engineering and Development Center, Air Force Systems Command at Arnold Air Force Station, Tennessee. The test procedures and results were officially reported in Reference 8. These test procedures and objectives are summarized below.

The illustrations and tables from this Reference 8 report are reproduced herein in their entirety as Appendix X in order to illustrate the testing equipment and facilities used.

The initial attempt to deploy the airlock after a cold soak to temperatures as low as -85°F , resulted in damage to the structure. This was attributed to the stiffening of the expandable structure as a result of the low temperature. A rigorous thermal analysis was then initiated to establish more realistically what actual temperatures might be expected. At about the same time, the change to the Skylab Mission impacted the D021 experiment location and the thermal analysis had to be updated to include the shadowing effects of the ATM solar arrays.

As a result of the evaluation, it was found desirable to add a thermal superinsulation protective blanket to the exterior of the D021 airlock which was previously described in Section II B. The Qualification Test Unit was then modified to incorporate this blanket as well as further restricting the discharge rate in the deployment pressurization system. Subsequent deployments were then conducted in GAC's vacuum chamber to prove the effectiveness of these changes. This effort is described in Appendix XI. Verification of these results was then made at Arnold Engineering Development Center in their 12-V chamber.

1. Launch Profile Pressure Simulation

The vacuum chamber in which the packaged airlock was placed was evacuated from ambient pressure to 1.0 TORR in two minutes time. The airlock electric vent valve left in the open position was demonstrated to have adequate flow capacity for launch.

2. Launch Accelerations

The airlock was mounted on a centrifuge and subjected to 4.0 g acceleration in the X and Z axes and 6.0 g acceleration in the Y axis to simulate the launch acceleration. The peak accelerations were maintained for one minute in each axis.

The structural adequacy of the airlock to withstand launch accelerations was thereby demonstrated.

3. Vibration

A resonance search was conducted over the frequency range of 20 to 2000 Hz. The resonance response values are listed in Appendix X. The airlock was then subjected to random vibration simulating the lift-off and boost vibration levels. The vibration spectrum imposed is given graphically in Appendix X. The vibration spectrum requirements were subsequently changed by NASA but a comparative dynamics analysis of the old and new requirements indicated that the test as performed was adequate. This analysis is presented in Appendix XII.

These tests demonstrated the capability of the airlock to withstand the launch and boost phase vibration forces without damage.

4. Acoustic Noise

These tests were reported in Appendix IX. They demonstrated the capability of the airlock to withstand the launch noise environment without damage.

5. Cold Temperature Deployment

As mentioned previously, the packaged airlock was placed in the AEDC - 12 V vacuum chamber. The chamber was evacuated to less than 1×10^{-4} TORR and the airlock subjected to the minimum cold temperature condition of -20°F on the outer cover (inner surface of the insulation blanket). The airlock was then successfully deployed. One minor incident occurred when the harness retaining cord fouled on the hatch latching handle and tore loose its retaining patch. However, this was traced to an improper routing of the cord during packaging. Corrective inspection procedures were instituted to prevent reoccurrence.

This demonstration verified the capability of the airlock to be deployed under the coldest environment anticipated during the orbital portion of the mission.

6. Cold Environmental Tests

The deployed airlock was subjected to -65°F temperature and 10^{-5} TORR vacuum. In this state the airlock pressure was cycled from 0 to 4.8 psia for 30 times.

This was a demonstration of the capability of the airlock to withstand numerous proof pressurizations under orbital night environments.

7. Solar Environment Tests

With the same vacuum and temperature conditions as above, a solar simulation of one sun was added for repetitive cycles of one hour "on" and 0.5 hour "off". The sun's angle of impingement and the shadow effects of the solar arrays were simulated to duplicate the Skylab installation geometry.

Under these conditions the airlock was again proof pressurized from 0 to 4.8 psia for 30 cycles.

This demonstrated the capability of the airlock to withstand numerous proof pressurizations without failure under night-day orbital cycling environments. (The 4.8 psia proof pressure was 1.37 times the 3.5 psia design working pressure.)

SECTION IV

AEROSPACE GROUND EQUIPMENT (AGE)

An airlock control simulator and test panel as illustrated in Figure 51 was the major AGE item required for this program. It was used to verify the functional integrity of the DO21 airlock electrical circuits as well as providing a control panel to simulate the A/M control panel and thereby verify the DO21 side of the DO21/AM Electric and Instrumentation Interface.

The DO21/AM mechanical interface was assured by means of the Drill Fixture Assembly illustrated in Figure 52. A matched pair of these drill fixtures was produced. One fixture was forwarded to MDAC for locating the mounting bolt circle on the A/M and the other retained at GAC to locate the mating interface mounting holes on the airlock.

A reusable shipping container was also provided as illustrated in Figures 53a through 53d. The Ethafoam shock mitigation pads are visible in the corners of the container in Figure 53b. These pads have been designed to limit maximum shock to 25 g's for full deflection of the internal mounting platform. Figure 53c shows the internal mounting platform removed. Clearance is provided within the container so that the airlock will not contact the container walls under full deflection of the platform in the mounting pads.

Figure 53d shows the dust and vapor-tight packaging envelope removed to expose the airlock for detachment from the platform. The attachment to the platform is by means of the same 24 bolt flange surface as the DO21/AM mechanical interface.

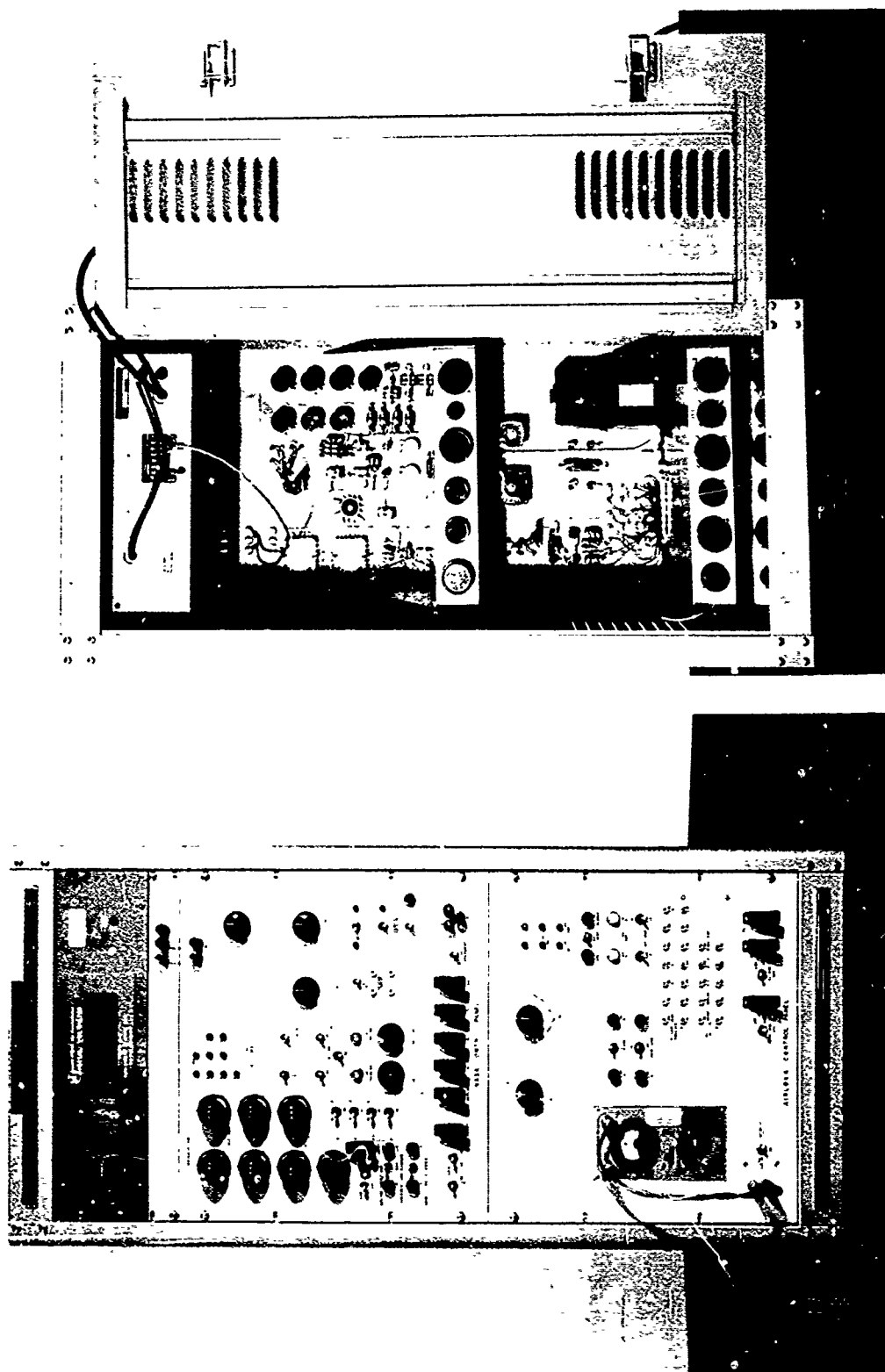
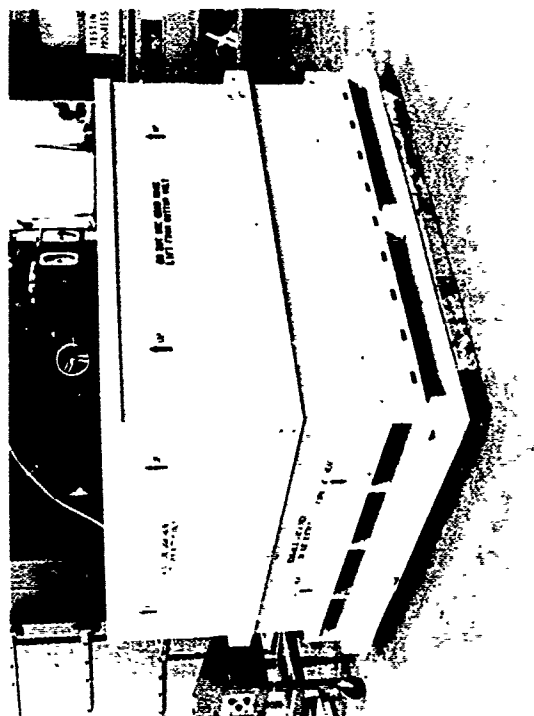


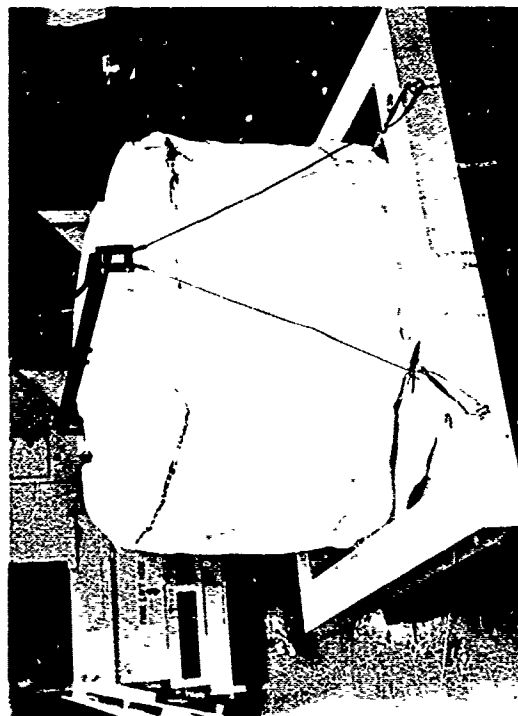
Figure 51. Airlock Control Simulator and Test Panel



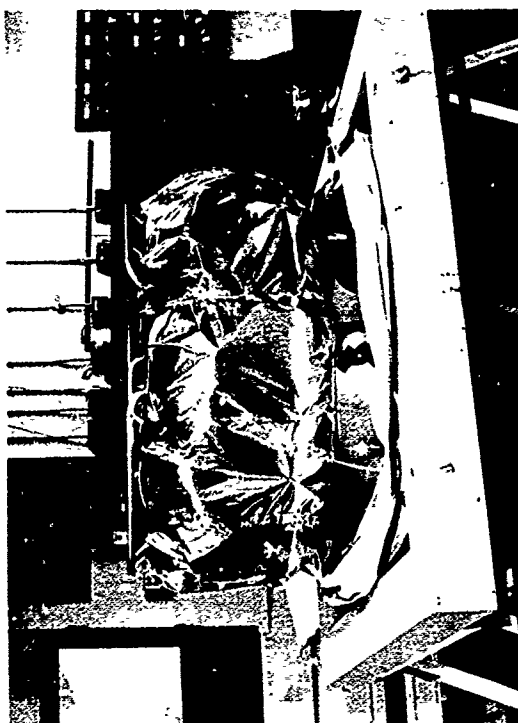
(a)



(b)



(c)



(d)

Figure 53. Reusable Shipping Container

SECTION V

CONCLUSIONS

This program has provided concrete evidence to support the conclusion that an expandable structure airlock is entirely practical for operational use on manned space vehicles. Although valuable supporting evidence would have been supplied if the Skylab flight test of the experiment had not been cancelled, there has been adequate materials and flight-type hardware Environmental Qualification Testing to verify feasibility of the basic expandable airlock design.

As an experiment, the configuration required special instrumentation, individual pressurization systems, extra controls, and the necessary structure to house these additional components. The weight of this added equipment was approximately one half of the total experiment weight of 201.0 pounds.

All these extra systems were provided with "fail-safe" and 100 percent redundancy to meet reliability requirements. The problems associated with developing and testing these special equipments required as much, if not more effort than that of the basic airlock itself.

With respect to the expandable structure, the one major problem encountered was the low temperature deployment difficulty. This was resolved by incorporating a superinsulating thermal protection cover for the packaged condition. On any future application, it is believed a better solution would be the use of newer materials with the proper low temperature characteristics and an improved pressure regulation to control the rate of deployment. It must be realized that the D021 airlock was produced with CY-1966 state-of-the-art materials and that considerable advancement has been made since then. Corollary programs have developed non-flammable bladder composites compatible with 100 percent oxygen environments and significant progress has been made in practical rigidization techniques. This latter property is highly desirable in structures somewhat larger than the D021 airlock to maintain shape in the unpressurized state.

The durability of the airlock to withstand ground handling, shipping, storage, and simulated launch and space environments has been demonstrated. The useful life of the expandable structure in space still needs to be verified in the total space environment although all current evidence indicates several years life without drastic degradation may be expected.

APPENDIX I

**LIST OF ATTENDEES AND MINUTES
OF
D021/D024 EXPERIMENTS CRITICAL DESIGN REVIEW**

**HELD AT
GOODYEAR AEROSPACE CORPORATION
AKRON, OHIO**

June 23 and 24, 1970

D021/D024 Expandable Airlock Experiment Critical Design Review

Attendees

23 June 1970

Name	Organization
Carl Boebel	AFML-WPAFB
Fred Forbes	AFAPL-WPAFB
Maj. Gary Mirar	USAF-HFO-NASA MSC
J. R. Porter	NASA-Hqs/MLS
E. O. Walker	NASA-FM-SL-DP
John P. Boggess	NASA-MSFC-S&E Qual - J
Ernest Balarzs	NASA/BECO MSFC - SMH
Alvin W. Bearskin	NASA/MSFC/S&E - ASTN - SDI
A. F. Smith	NASA/MSFC CF 5
J. W. Neal	Martin Marietta/NASA/MSFC
P. D. Feemster	NASA/MSFC/S&E - Qual - P
Gene Bell	McDonnell-Douglas
Robert X. Tansey	McDonnell-Douglas
Will Roberts	NASA-MSFC - S&E - Qual/FEC
C. R. Chubb	McDonnell-Douglas ED
H. H. Grace	McDonnell-Douglas ED
W. F. Walkenhorst	McDonnell-Douglas ED
R. H. Hostmeyer	McDonnell-Douglas ED
J. C. Van Hooser Jr.	NASA-KSC/LS-ENG-53
M. R. Van Slyke	NASA(MSC) Boeing
D. L. Bailey	NASA KSC AA-SVO-1
J. T. Schneider	NASA KSC LO-PLN-2
L. S. Bourgeois	NASA MSC FC6
W. Beeson	NASA MSC FC6
Paul R. Ilgen	MMC-Denver
I. M. Jaremenko	MMC-Denver
R. V. Danner	MMC-Denver
A. H. Hale	MMC-Denver
Clifford Titus	MMC-Denver
J. Kirby Thomas	Martin-Denver
Nelson E. Brown	Matrix (MSFC Huntsville)
Larry P. Chambers	NASA-Headquarters
William E. Pruett	NASA-Headquarters
Edward G. Gibson	NASA-MSFC/CB
Rusty Schweickart	NASA-MSFC CB

2-10-15(3-70)77-10
REF: ENGINEERING PROCEDURE 3-017

DO21/DO24 Expandable Airlock Experiment Critical Design Review

Attendees

24 June 1970

Name	Organization
John P. Boggess	NASA/MSFC/S&E - Qual - J
Maj. Gary H. Minar	USAF MSC AF FIELD OFC
Fred Forbes	AFAPL - WPAFB
Edward O. Walker	NASA-FM-SL-DP
Carl Boebel	USAF (AFML) - WPAFB
A. Smith	MSC
J. Neal	MSC
E. Balarzs	NASA/BECC S&E ASTN - SMH/SD
Alvin W. Bearskin	NASA/MSFC/S&E ASTN - SD1
William E. Pruett	NASA/Headquarters/MLT
Larry P. Chambers	NASA/Headquarters MLR
Donald Bailey	NASA KSC
J. R. Porter	NASA-HQS-MLS
J. T. Schneider	NASA-KSC-IO-PLN-2
W. F. Walkenhorst	MDAC-ED
R. X. Tansey	MDAC-ED
C. R. Chubb	MDAC-ED
I. M. Jaremenko	MMC-D
R. H. Hostmeyer	MDAC-ED
H. H. Grace	MDAC-ED
C. r. Titus	MMC-D
Nelson Brown	Matrix (MSFC)
R. V. Danner	MMC-D
Paul R. Ilgen	MMC-D
J. Kirby Thomas	MMC-Denver
A. H. Hale	MMC-Denver
P. D. Feemster	NASA/MSFC/S&E - Qual - P
W. Beeson	NASA/MSFC
L. S. Bourgeois	NASA-MSFC
W. Roberts	NASA/MSFC-S&E-Qual/FED
J. C. Van Hooser Jr.	NASA/KSC/LS-Eng-SE

2-ID-15(3-70)77-10
REF: ENGINEERING PROCEDURE 9-017

Goodyear Aerospace Attendees

Robert I. Scoville

Leo Jurich

Joe Apisa

W. A. Murray

J. E. Rice

Herman A. Monaco

James E. Houmard

T. R. Williamson

H. E. Kerber

Walter Haines

Ed Long

Lou Manning

R. T. Madden

D. Neman

Test Operations

Program Management

Thermal Analysis

Reliability

Dynamics & Vibration

Design

Structural Analysis

Human Factors

Human Factors

Quality Assurance

Quality Assurance

Program Management

Marketing

Contract Administration

R. L. James

NavPlant Rep Office - Akron

E-ID-16(3-70)77-10
REF: ENGINEERING PROCEDURE 8-017

Minutes of D021/D024 Experiments Critical Design Review (CDR)

June 23 and 24, 1970

After the welcome talk by Mr. E. A. Brittenham, Major Gary Minar opened the CDR with general remarks regarding the impact of the Skylab Program on the D021/D024 experiments. He also reviewed the rules for governing the conduct of the CDR.

Mr. E. O. Walker then presented the latest configuration of the Skylab illustrating the combined cluster with an excellent pictorial viewgraph.

Mr. Fred Forbes reviewed the long history of the D021 experiment and its association to the organization of the Skylab program. He reviewed the major events and numerous changes that have occurred since the Expandable Airlock Experiment and the original "Orbital Work Shop" programs were initiated.

Mr. Carl Boebel, AFML, described the philosophy behind the D024 Thermal Coatings Materials Experiment and the approach to be followed to more accurately establish the degradation effects on these materials due to space environment exposure.

L. Manning reviewed the current status of the D021/D024 hardware and the Qualification Test Program.

Viewgraph photos of the actual hardware were presented as well as a brief movie of the hardware development and deployment tests. (Later in the day the D021 Qualification Test Unit was deployed and made available for inspection by the attendees.)

Major Minar then organized the CDR into working groups and started the RFD review. (See attached copies of viewgraphs for group disciplines) After the initial session of the separate working groups, it was found desirable to combine Groups 1 and 2 and 3 and 4. This new arrangement was then maintained until the final session of all attendees at the Preboard activity. A total of 163 RIDs were reviewed by the Preboard. In addition, a number of RIDs were withdrawn by the issuer prior to Preboard action.

Final CDR Board action is planned for July 1970. Actual date will be established by Mr. E. Walker.

Agenda for DO21/DO24 CDR

23 June 70

- 0900-0905 - Seating
- 0905-0915 - Welcoming remarks by Goodyear Aerospace Corporation
- 0915-0930 - Program Management Overview
 - Program Status/Experiment Impact
 - CDR Instructions
- 0930-1000 - P.I. Comments, DO21 & DO24
 - History & present status of hardware
 - Detailed agenda
- 1000-1015 - Coffee
- 1015-1230 - Group meetings, prepare RID's
- 1230-1315 - Lunch
- 1315-as required - Continue group meetings

24 June 70

- 0900-0930 - Assemble and coordinate RID's
- 0930-1200 - Pre-board discussions and intergroup coordination
- 1300-1700 - Pre-board activity

July 70 (Date to be announced by MSFC)

Formal Board - Telecon

Management Structure D021 & D024

Experiment Development

D021 Principal Investigator: AFAPL (APO-1/Mr. F.W. Forbes)
Wright-Patterson AFB, OH 45433

D024 Principal Investigator: AFML (MANE/Mr. Carl Boebel)
Wright-Patterson AFB, OH 45433

NASA Skylab Program Management

PM-SL-DP - Skylab Program Office, MSFC
Mr. Ed Walker

Manned Spacecraft Center responsibilities focus under MSC
Skylab Office, Mr. Kleinknecht.

Contractor for D021 & D024

Goodyear Aerospace Corporation
Akron, Ohio
Mr. Lou Manning

Experiment Carrier

Airlock Module - Developed by NASA MSFC
Contractor MDAC
St. Louis, Missouri

DO21/DO24 CDR Functional Groups

1. Structural/Mechanical/Thermal Environment & Fluids
2. Materials/R&QA/GSE/Test/Safety/Launch Operations
3. Mission Operations, Human Factors/Training
4. Instr./Elsec./Comm./
5. P. I. Management/Technical

SPECIAL INSTRUCTIONS

1. D024 RID's should be identified separately from D021.
2. Please cite applicable requirements document on RID as required.

APPENDIX II

**GAC ACTION ITEMS ACCOMPLISHED AS ESTABLISHED
AT
TEST REQUIREMENTS REVIEWS**

DO21/DO24 EITRSS MEETING

GAC - AKRON, OHIO
July 29, 1970

<u>Attendee's Name</u>	<u>Organization</u>
Lou Manning	Goodyear Aerospace Corporation
Harry M. Flake	NASA-MSFC
Roger Chassay	NASA-MSFC
Pat Feemster	NASA-MSFC
Robert Scoville	Goodyear Aerospace Corporation
Roland Danner	Martin Marietta
C. Chubb	McDonnell Douglas
J. J. Hall	General Electric - Huntsville
Lanny R. Taliaferro	NASA-MSFC
Ed Tagliaferri	MMC/Systems Integration (GSE)
Dick Hose	Goodyear Aerospace Corporation
Denny Neman	Goodyear Aerospace Corporation
Jack Altekruze	Goodyear Aerospace Corporation
Fred Fairbanks	McDonnell-Douglas (I /DT)
Ralph Morris	McDonnell-Douglas (LO/DT)
A. L. Hoover	NASA-MSFC - PM-SL-DP
Darrell Moore	NASA-MSFC - S&E-ASTR-EAE
Don Ritchart	MMC/Exp. Test
Paul Ilgen	MMC/Exp. Test
Alex Madyda	NASA-MSFC - PM-SL-DP

DO21 PATRS MEETING

NASA-MSFC - Huntsville, Alabama
August 27, 1970

<u>Attendee's Name</u>	<u>Organization</u>
D. C. Ritchart	MMC-Test Engr. & Op.
A. L. Hoover	MSFC/PM-SL-DP
E. O. Walker	MSFC/PM-SL-DP
P. D. Feemster	MSFC/S&E-Qual-P1
Lou Manning	GAC - P.E.
R. V. Danner	MMC-Exper. Integra.
Roger Chassay	MSFC/PM-SL-AL
Alvin W. Bearskin	MSFC/S&E-ASTN-SD1
Paul Ilgen	MMC-D/Test Engr. & Opr.
O. V. Ruhl	McDonnell-Douglas

M E M O R A N D U M

9 September 1970
SP-7524

To: L. Manning

Subject: End-to-End Telemetry Check of D-21 Temperature Sensors

To determine the feasibility of an end-to-end T/M checkout of the temperature sensors the thermal blanket was removed uncovering the exterior temperature sensors on the Qualification Unit S/N #1. A 250-watt heat lamp was placed approximately 8 to 10 inches from External Temperature Sensor No. 2 (RT2), Internal Temperature Sensor No. 1 (RT5). The D-21 instrumentation system was turned on and the temperature channel outputs read out on a digital voltmeter. The heat lamp was turned on and as the D-21 surface temperature allowed to come up to approximately 200°F. The lamp to surface distance was adjusted to maintain approximately 200°F at the external temperature sensor.

The following table shows the external and internal temperature profile.

	Start	+5 Min.	+10	+15	+20	+25
Ext. Temp. #2 (RT2)	3.246 V 82°F	4.344 V 190°F	4.497 V 210°F	4.487V 207°F	4.504 V 213°F	4.503 V 213°F
Int. Temp. #1 (RT5)	3.723 V 82°F	3.783 V 84°F	3.928 V 89°F	4.020 V 93°F	4.056 V 94°F	4.085 V 95°F

These temperature excursions should be sufficient to perform end-to-end checks for the purpose of identifying T/M channels. This is GAC's recommended method.

R. L. Hose

R. L. Hose

RLH/emg

MEMORANDUM

13 October 1970

SP-7485

To: L. Manning
D-21 Project Engineer

Subject: Fusistor Testing

The D-21 Airlock Simulator and Test Unit (66QS575) has the capability of performing a resistance test of all the D-21 pyrotechnic circuits. It does not have the capability of testing the circuits continuity under the design load, 5 ampere minimum for 10 milliseconds. A resistance test is the only test, short of firing the device, that can safely be conducted on the pyrotechnic device and demonstrates the continuity of the device's initiating bridge wires. However, it is desirable to test the firing circuit under load, demonstrating the ability of the circuit elements to deliver the necessary firing current to the pyrotechnic. One of the circuit elements is a one ohm fusistor (IRC Spec. A-0306) designed to fuse in greater than 1 and less than 5 seconds at 5 amps, limiting the duration of any load test which can be performed.

A self-contained solid state simulator (70QS1640) has been designed and fabricated to perform this load test. This simulator is designed to be substituted for the pyrotechnics and plugs into the connectors which normally connect to the three (3) D-21 pyrotechnic valves. The simulator turns itself on at the application of the firing voltage and applies a 5.5 amp load for 10 milliseconds at 28 volts. (The D-21 pyrotechnics are designed to blow in 10 milliseconds maximum at 5 amps.) The simulator then turns the load off and draws a quiescent current of 0.052 amp until the firing switch is turned off opening the circuit. An indicator on the simulator illuminates only if the current reaches 5 amps or more. There is an indicator for each pyrotechnic circuit. The load current will vary between 5 and

8 amps depending upon the charge conditions of the D-21 battery packs at the time the test is performed. The load duration is stable, 10 milliseconds, for all voltages.

Prior to fabricating and using the Pyrotechnic Simulator it was deemed necessary to determine the effects, if any, the repeated application of high currents (5 amp) has on the fusistor fusing characteristics. This was done by selecting ten (10) IRC Spec. A-0306 fustors from the D-21 stock. Five of the fustors were cycled at 5 amps for 10 milliseconds. The test circuit schematic is shown in Figure 54 and consists of a motor driven cam operated switch which triggers a transistorized circuit allowing 5 amp to flow through the five fustors connected in series. The transistorized circuit turns the current off after 10 milliseconds and is recycled every 3.17 minutes by the motor drive cam. After 100 cycles two of the fustors were removed and replaced with two one-ohm resistors. The remaining three fustors were cycled another 100 cycles for a total of 200 cycles.

After cycling, the five fustors plus the five that were not cycled were subject to a continuous 5 amp load and fused. The fuse times were recorded on an oscillograph. A schematic of the test circuit is shown in Figure 55. Figure 56 is a typical record of the fuse time. Table VI shows the respective fuse times for the 10 fustors. To perform the test the circuit was set up using a one-ohm resistor in place of the fusistor. The power supply voltage was adjusted until the current was 5 amps with the shunting switch (S_1) open. After the current was adjusted S_1 was closed and a fusistor inserted in place of the one-ohm resistor. The power switch (S_2) was closed and the shunting switch (S_1) opened and the changes in current recorded on the oscillograph (see Figure 56).

Examination of the data in Table VI indicates that the fusing characteristics of the fustors were not changed as a result of a short duration high load current being placed on the fusistor. The 200 cycles is far in excess of the number of times the D-21 pyrotechnic circuits will be tested using the Pyrotechnic Simulator.

As discussed earlier, the test current delivered by the Pyrotechnic Simulator is somewhat dependent on the charge condition of the D-21 battery packs and may approach 8 amps. To demonstrate the fusing characteristics of the A-0306 fusistor at higher currents, another fusistor (Number 11) was fused using the same circuit and recording equipment shown in Figure 55. The power supply voltage was adjusted, prior to the test, to produce a fusing current of 10 amps. The resulting fuse time is shown in Table VI. The fusing time at 10 amps is shown to be more than an order of magnitude greater than the 10 millisecond time the simulator will apply the test load. Therefore, no damage to the fuses should result from using the Pyrotechnic Simulator, even if the D-21 battery packs are at their maximum charge. It is therefore concluded that the simulator is a safe and efficient device for testing the D-21 pyrotechnic circuits.

Richard L. Hose

Richard L. Hose
Space Systems Engineering

RLH/emg

cc: Manning - 3
B. B. Carpenter

TABLE VI - D-21 FUSISTOR BLOW TEST (IRC SPEC. A-0306)

Fusistor Number	Times Cycled (5 amps for 10 milliseconds)	Fuse Time at 5 amps
1	0	1.938 sec
2	0	1.669 sec
3	0	1.713 sec
4	0	1.646 sec
5	0	1.668 sec
6	100	1.723 sec
7	100	1.782 sec
8	200	1.922 sec
9	200	1.840 sec
10	200	1.683 sec
11	0	0.17 $\frac{1}{2}$ (10 amp)
Ambient Temperature 75°F for all tests		

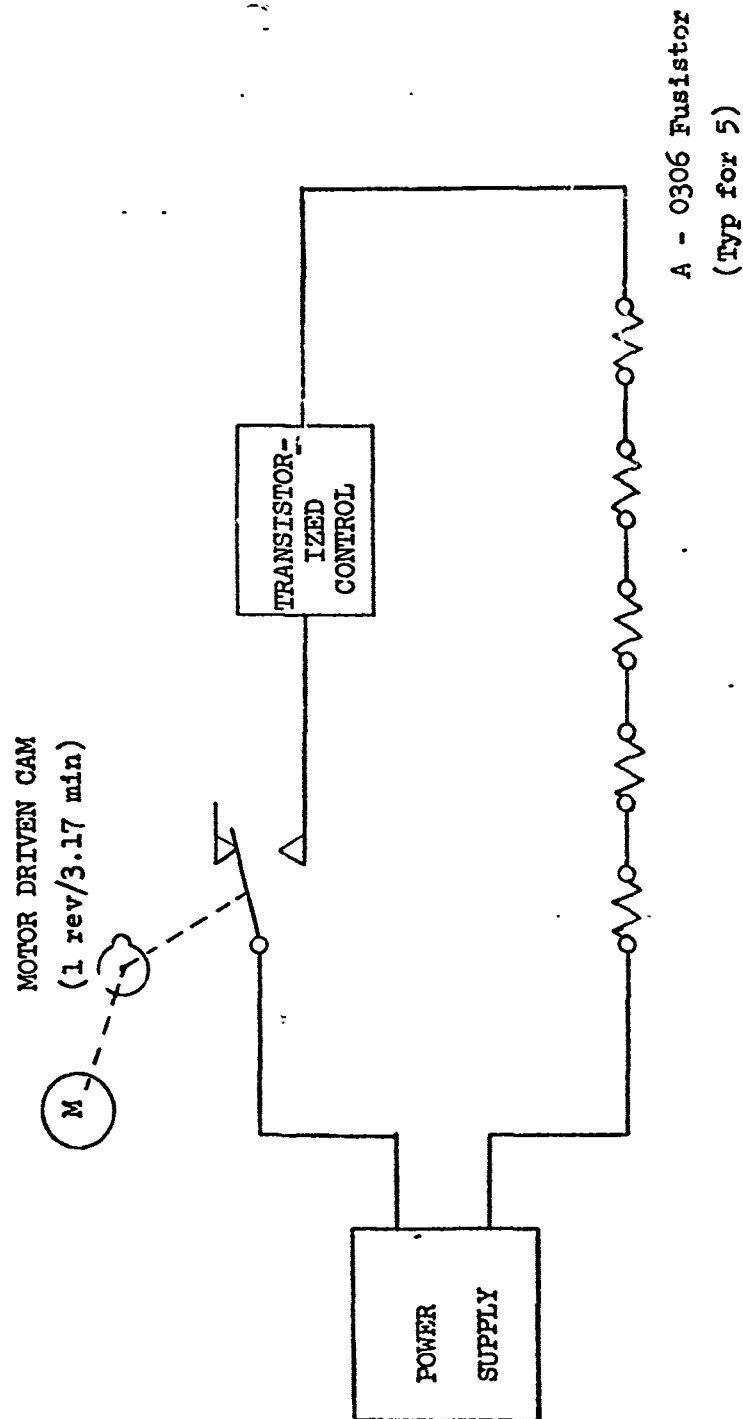


Figure 54. Fusistor Load Cycle Test Circuit

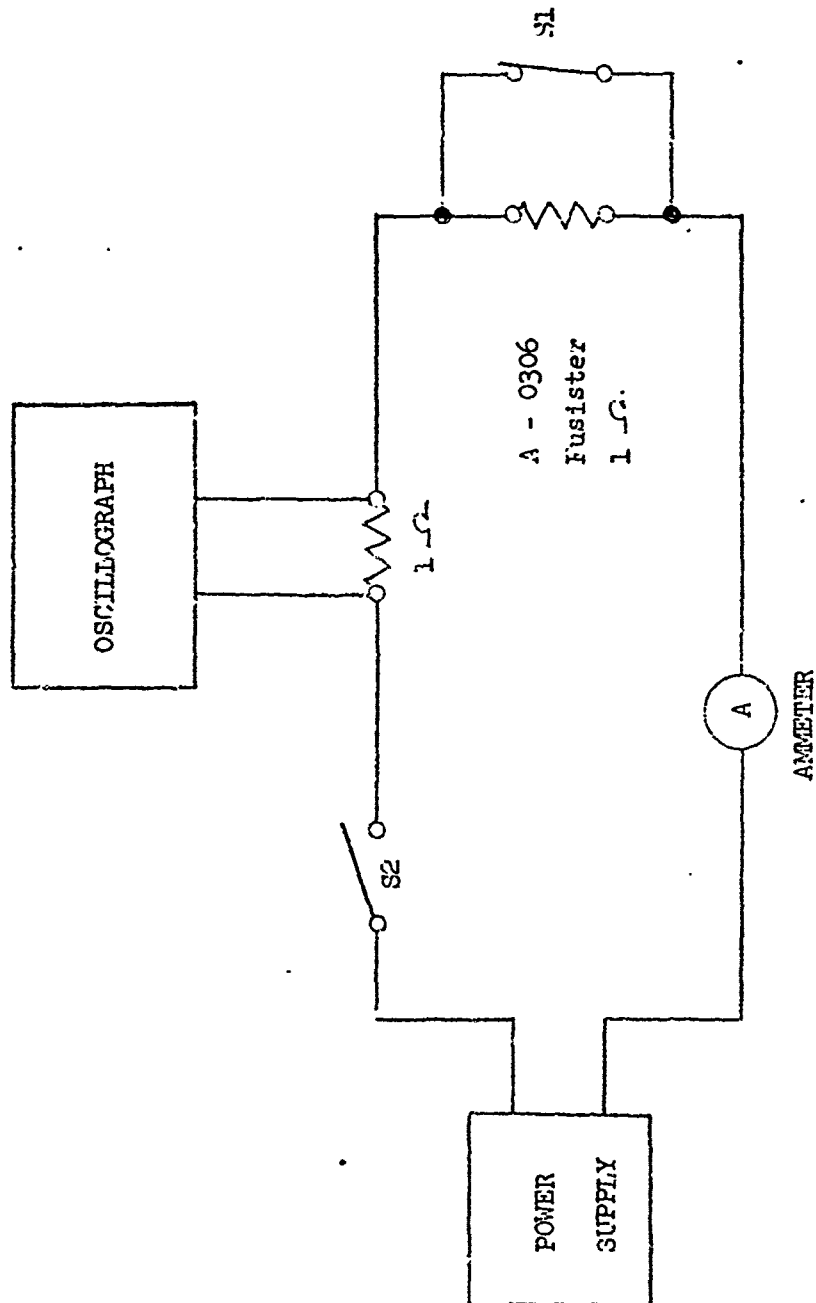


Figure 55. Fusing Test Circuit

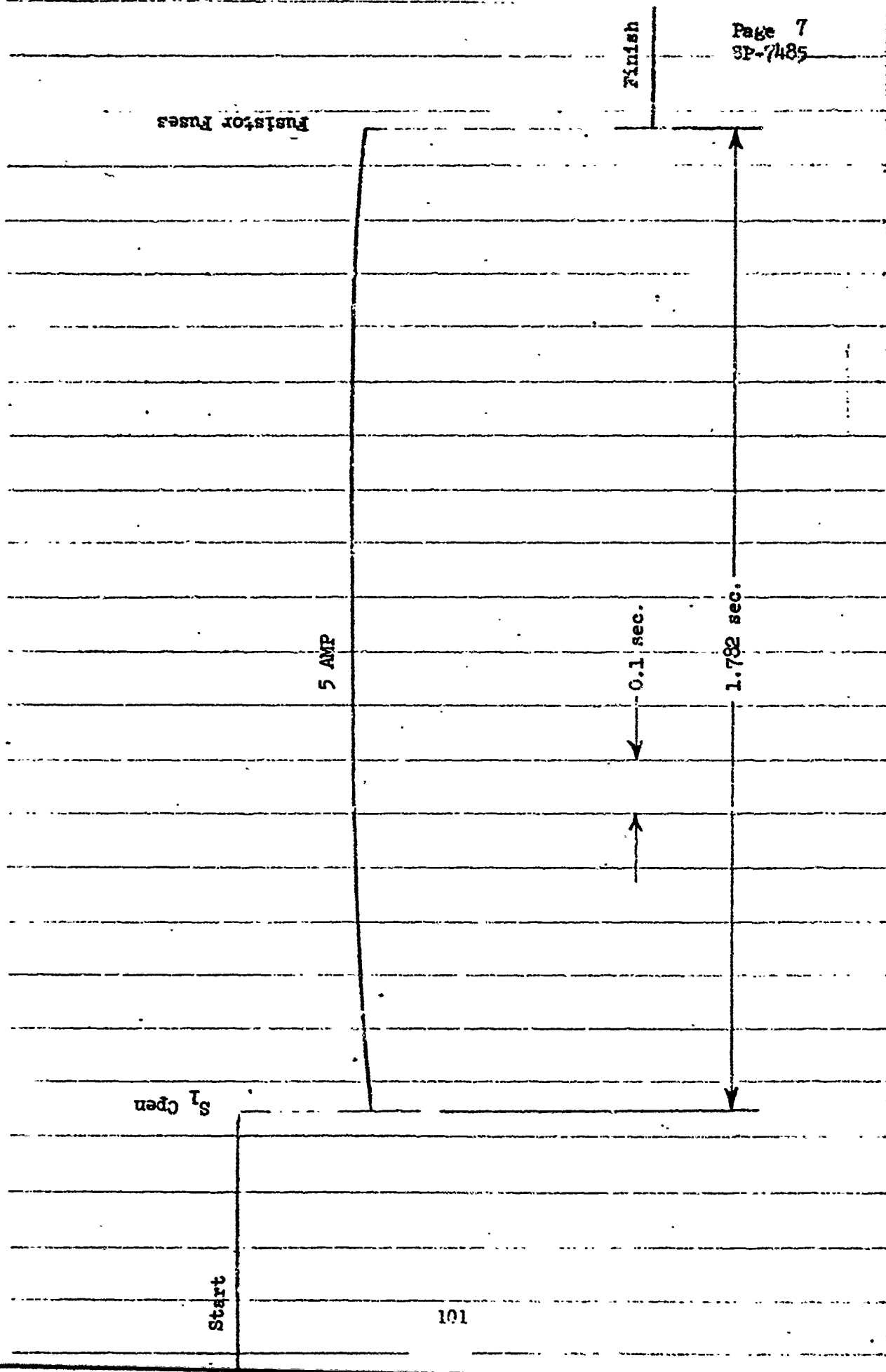


Figure 56. Fuse Test - Typical Oscillograph Record

APPENDIX III

THERMAL ANALYSIS

ENGINEERING MEMORANDUM

4 September 1969
SP-7087

Subject: Thermal Analysis - Effect of Apollo Telescope Mount on
D-21 Airlock Location

INTRODUCTION

The new concept of the NASA SIVB "Dry" Workshop includes the Apollo Telescope Mount (ATM) as part of the payload launched with a single Saturn V booster. This arrangement places the current location of the D-21 airlock behind one of the ATM solar cell arrays when the array is deployed. A thermal analysis was made to determine the effect of this shadowing on the airlock temperatures. An alternate location of the airlock between the ATM solar cell arrays was also studied and found to be more favorable. See Figure 57.

SUMMARY

The present location of the D-21 airlock in the shadow of the ATM solar array imposes severe extremes of thermal environment. If a thermal coating with "hot" properties is selected to keep the airlock warm in the shade, it proves to be too hot during those periods the airlock is exposed to the sun prior to ATM deployment or during random orientation periods. A cooler thermal coating which is suitable to control the heat flux in the sun, is found to be too cold to be satisfactory in the shade.

Although this problem exists to some degree regardless of the airlock location, there is a spot between solar cell arrays which has less extreme fluctuations in thermal flux. The D-21 is currently located on the McDonnell Douglas airlock module (AM) Strut No. 3. Relocation of the D-21 airlock to Strut No. 4 of the AM appears practical and will provide a more suitable thermal environment.

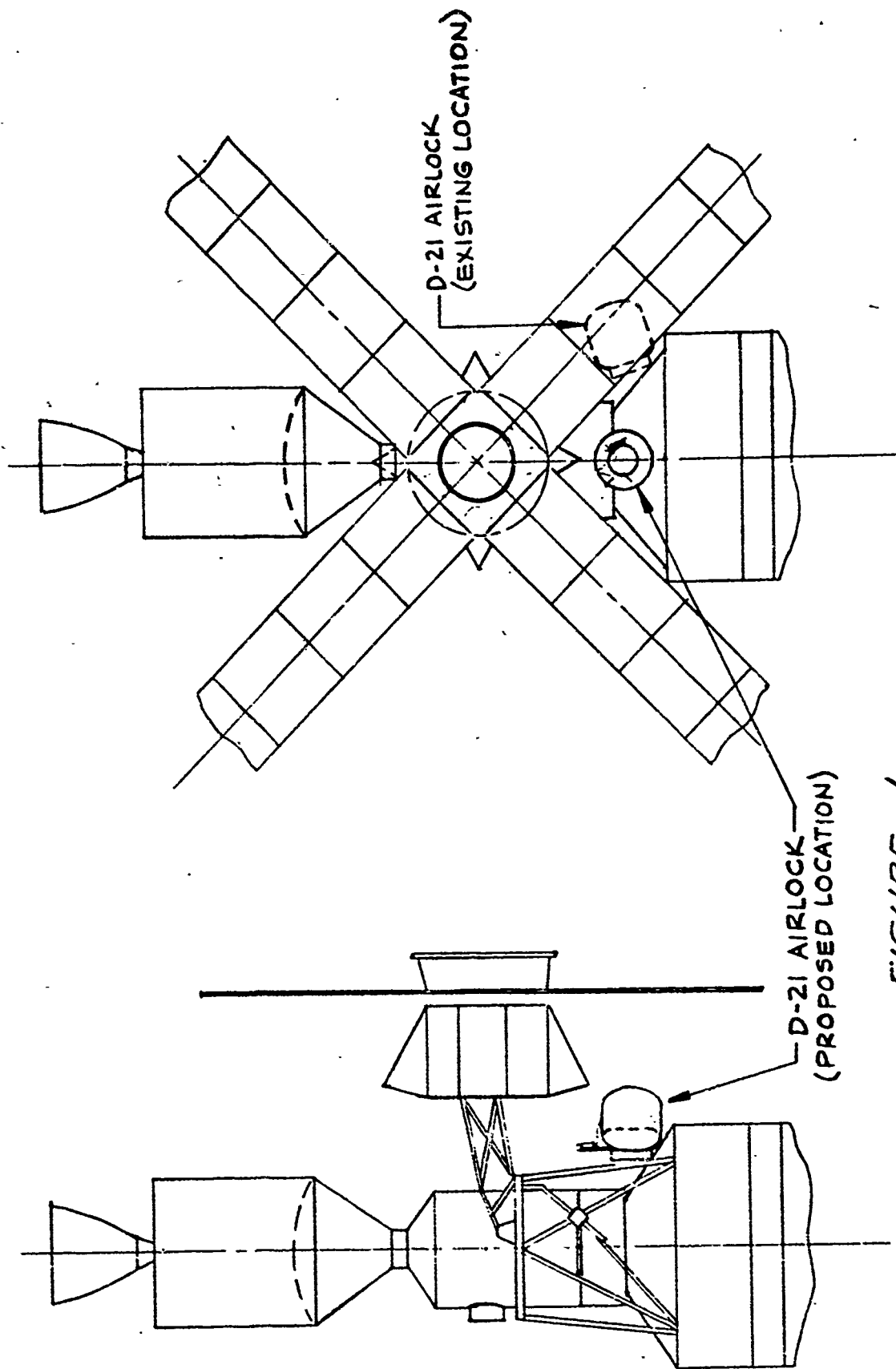


FIGURE 1
PROPOSED AIRLOCK LOCATION

Figure 57. Proposed Airlock Location

ANALYTICAL APPROACH

The D-21 airlock was simulated thermally as a cube with one side always sun oriented. A heat flux program was established where the total heat flux subjected to each side of the cube was determined. The coordinates of the perpendicular to each surface are inputs to the program and by knowing these values, the relative location of each surface with respect to the sun and earth is known for any position in any desired orbit. Solar, reflected and earth heating effects were computed for 24 locations in a 500-mile orbit having an inclination of 10 degrees. In the temperature calculations, the time increments must be considerably smaller to ensure computational stability, and these values were obtained by linear interpolation between computed points. With the above heat flux program, the study was divided into two separate phases namely; packaged and deployed configurations. The IBM Model 360 digital computer was used for this analysis.

Packaged Configuration - Maximum Temperature Case

The heat fluxes on the sun-oriented side of the cube were used for the maximum temperature calculations. Optical properties for the surface were varied through a range of emissivities from 0.04 to 0.12 and corresponding solar absorptances. The heat fluxes obtained from the orbital heat flux program were modified by these surface properties, then used with a transient one-dimensional temperature program to obtain temperatures through the structure. This program divides any homogeneous material into a number of slabs and by conducting a heat balance on each slab, computes the temperature gradient through the foam structure. For the particular case investigated, 13 slabs were used, 3 for the multi-layer insulation and 10 slabs for the foam varying in thickness from 1/8 inch to 1/2 inch giving a total thickness of 2-7/8 inches. The results of this run (with the final coating) are shown in Figure 58 where temperature (1) is the outside surface of the thermal blanket and temperature (4) is the surface of the foam structure adjacent to the protective multi-layer insulation.

Packaged Configuration - Minimum Temperature Case

For the minimum temperature case, the same optical surface properties were assumed to now be on side (3) of the cube and the orbital heat flux program modified

DATE _____
 REV DATE _____
 REV DATE _____

GOODYEAR AEROSPACE
 CORPORATION
 AKRON 11, OHIO

PAGE Page 4
 GER. SP-7087
 CODE IDENT NO. 25500

TEMPERATURE EXCURSIONS (PACKAGED CONFIGURATION)

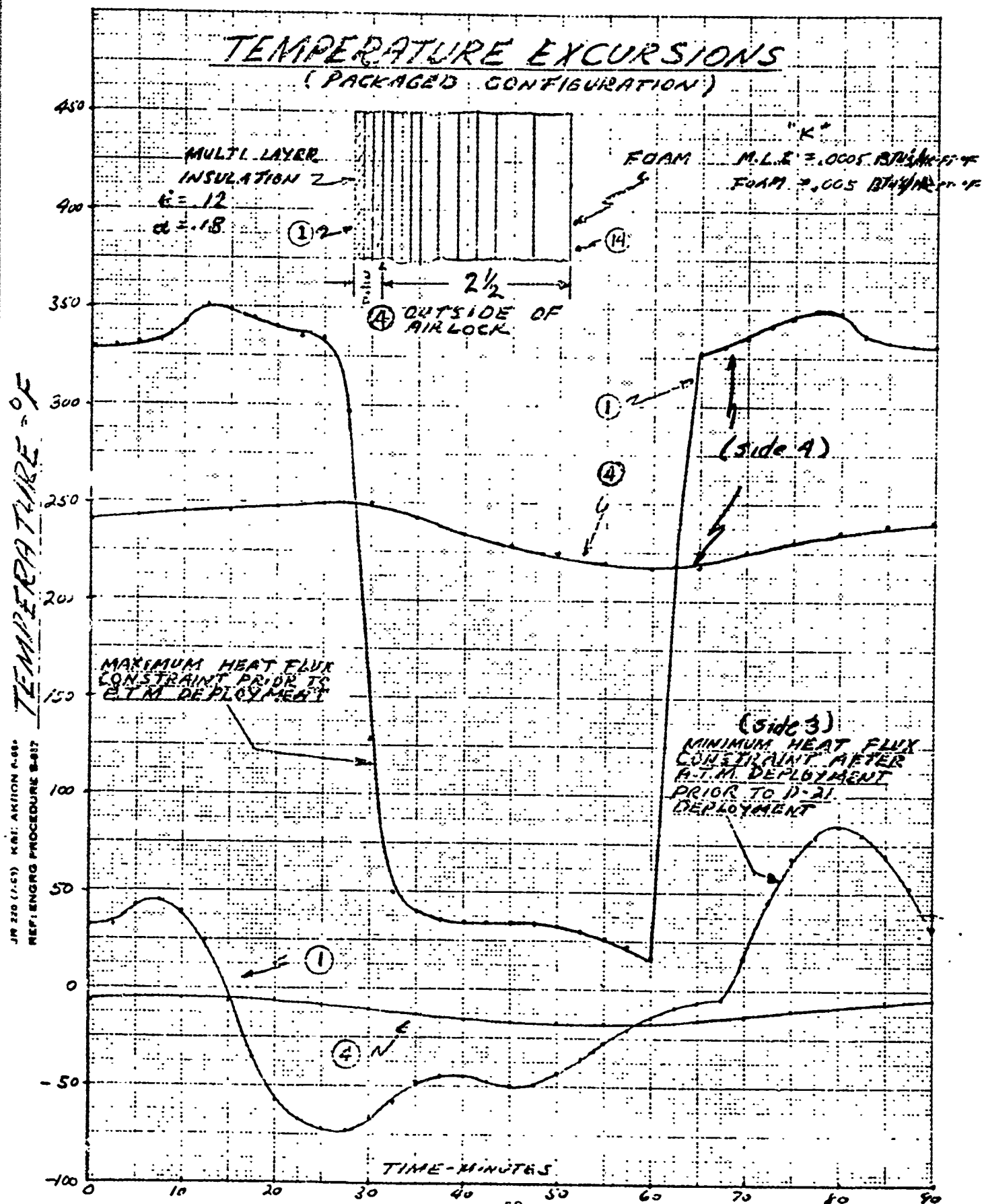


Figure 58
 106

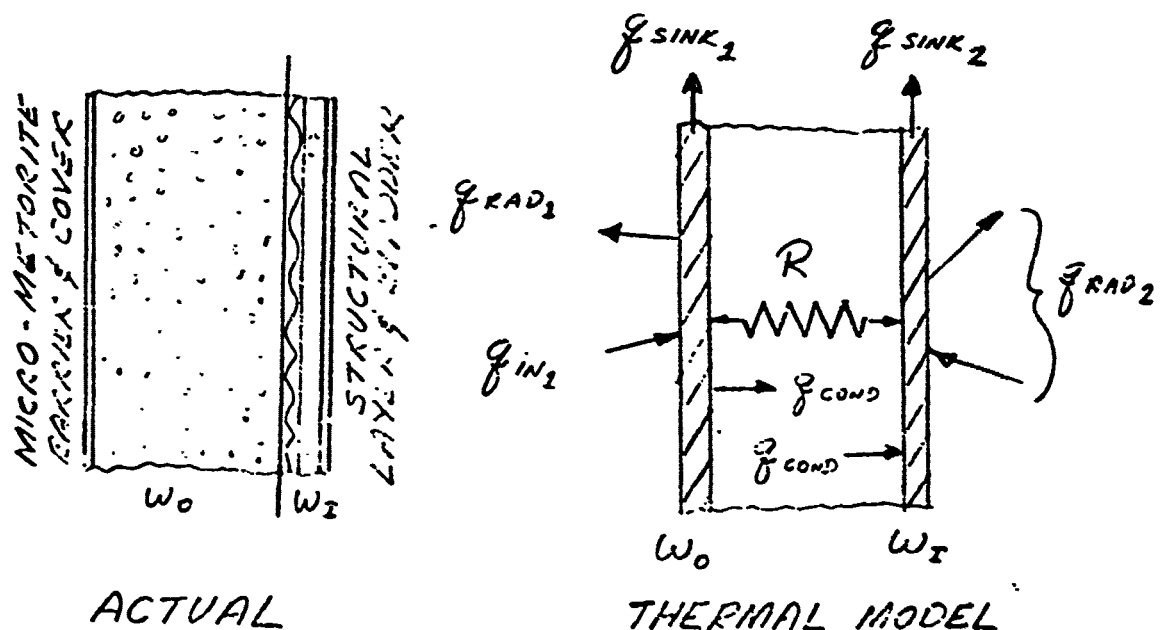
accordingly. (See Figure 59 for cube identification) Side (3) is assumed to receive the minimum overall heat flux. Sides (2) and (5) actually are subjected to a lesser heat flux based on solar, reflected and earth heating but are expected to be warmer due to effects of the surrounding structure. The re-radiation of sides (2) and (5) will be reduced since these surfaces will be viewing a much warmer surface than absolute zero. No study was made to determine these effects since the properties and pertinent information on the structure is unknown and it is expected that side (3) will be the surface receiving the minimum heat flux.

Heat fluxes obtained from the above program for side (3) were modified slightly to include the view factor effects of the solar paddles and ATM structure.

A view factor was computed between side (3) and the structure and assuming the structure temperature is constant at 60° F and having a surface emittance of 0.60, the radiation interchange between these surfaces were computed. The multi-slab solution was again used and temperatures obtained for the modified coating and the results are shown on Figure 58.

Deployed Configuration

The thermal model for the deployed configuration was assumed to be a hollow cube with walls one inch thick. The wall of the cube was simulated thermally by the model shown below:



TEMPERATURE EXCURSIONS (DEPLOYED CONFIGURATION)

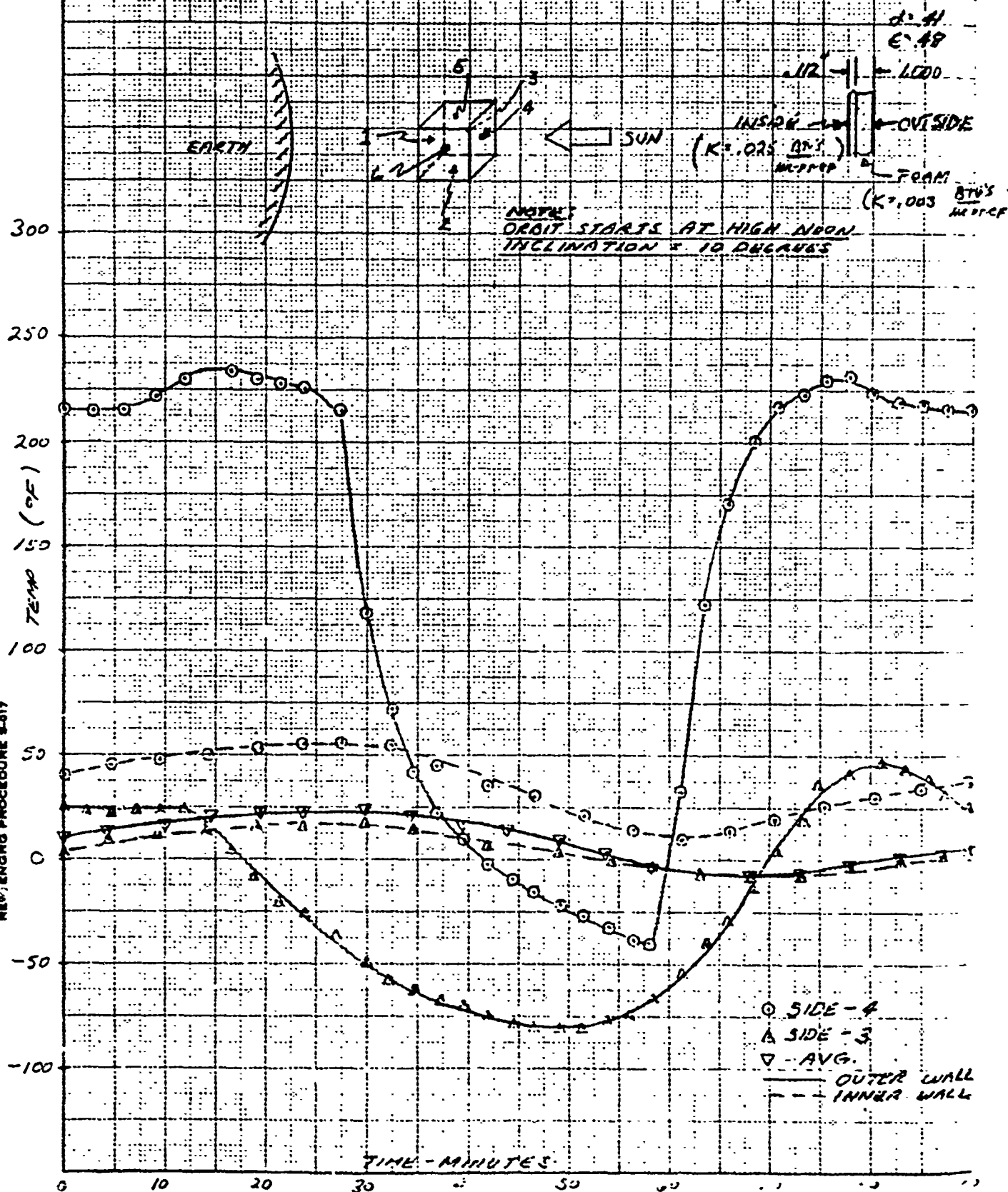
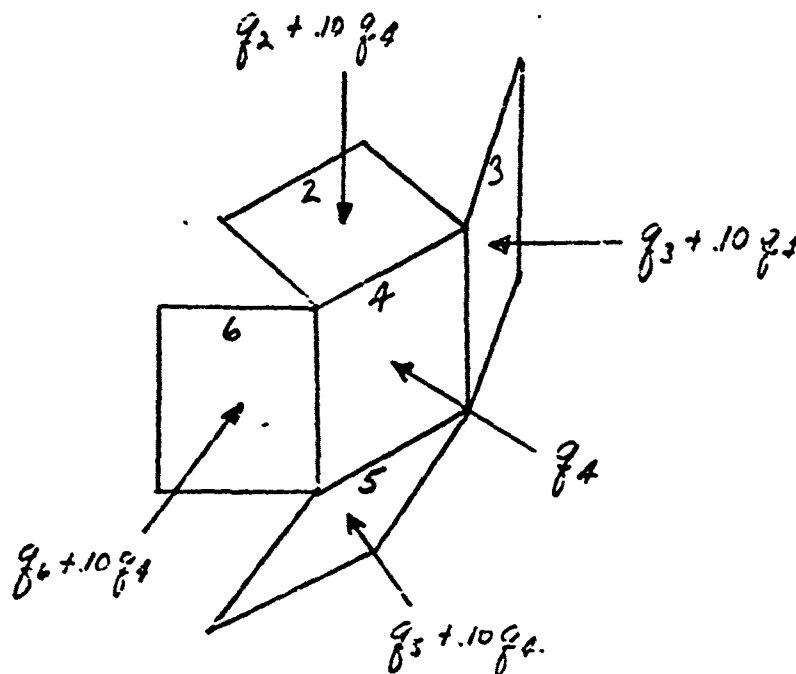


Figure 59.
108

A transient temperature analysis was then conducted between each node to obtain inner and outer temperatures. This program calculates the temperatures of all six sides of the cube, and also incorporates internal radiation between surfaces. By knowing the surface properties, materials and heat fluxes on each surface, a time-temperature history can be obtained for each side of the cube throughout the flight.

The D-21 airlock configuration is basically a spherical shape and is simulated thermally by a cube. If we look at the radiating area to heating area ratios it can be seen that the cube simulation will yield lower overall temperature results. A spherical shape configuration has a radiating to heating area of 4 compared to 6 for the cube. In order to obtain more realistic answers, we must increase our heating area or decrease our radiation area to more closely simulate the spherical shape. The temperature program was then modified by using the first approach. A sketch is shown below indicating how the heat fluxes were increased to give more realistic results.



The results of this temperature analysis are shown in Figure 59 where side (4) and side (3) temperatures are shown indicating the maximum and minimum orbital temperatures respectively of the D-21 airlock. Side (4) represents the hatch end and side (3) represents the coldest part of the airlock expandable structure in the sun-orientation mode. The average internal surface temperature is also shown in this figure.

RESULTS

On the basis of materials tests the following temperature limits were established as design criteria.

- (1) Outside surface of airlock $+275^{\circ}$ F Max. -20° F Min.
- (2) Outside surface of thermal blanket $+350^{\circ}$ F Max., -150° F Min.

The thermal analysis indicates that relocation of the D-21 airlock to the NASA Airlock Module (AM) Strut No. 4 position is required to avoid exceeding these design temperature limitations.

The primary problem is selection of a coating which will not degrade the surface materials during the orbital phase prior to ATM deployment and yet be warm enough after ATM deployment and orientation to the sun to allow proper deployment of the D-21 airlock.

The thermal coatings selected as optimum for both the packaged and deployed airlock are defined on Figure 60.

As can be seen from the thermal plots of Figure 58, the maximum temperature that the outer layer of the thermal blanket will achieve is $+350^{\circ}$ F prior to deployment of the ATM. The outer surface of the airlock will be kept below $+250^{\circ}$ F, under these conditions. After ATM deployment and orientation to the sun, the D-21 airlock minimum temperature will be no less than -15° F. (The micrometeoroid barrier material of the airlock increases rapidly in stiffness as the temperature is lowered below -20° F.) The outer surface of the insulative blanket will of course cycle from from a maximum of $+350^{\circ}$ F to a minimum of -75° F, during this period but low temperature

SUN SIDE

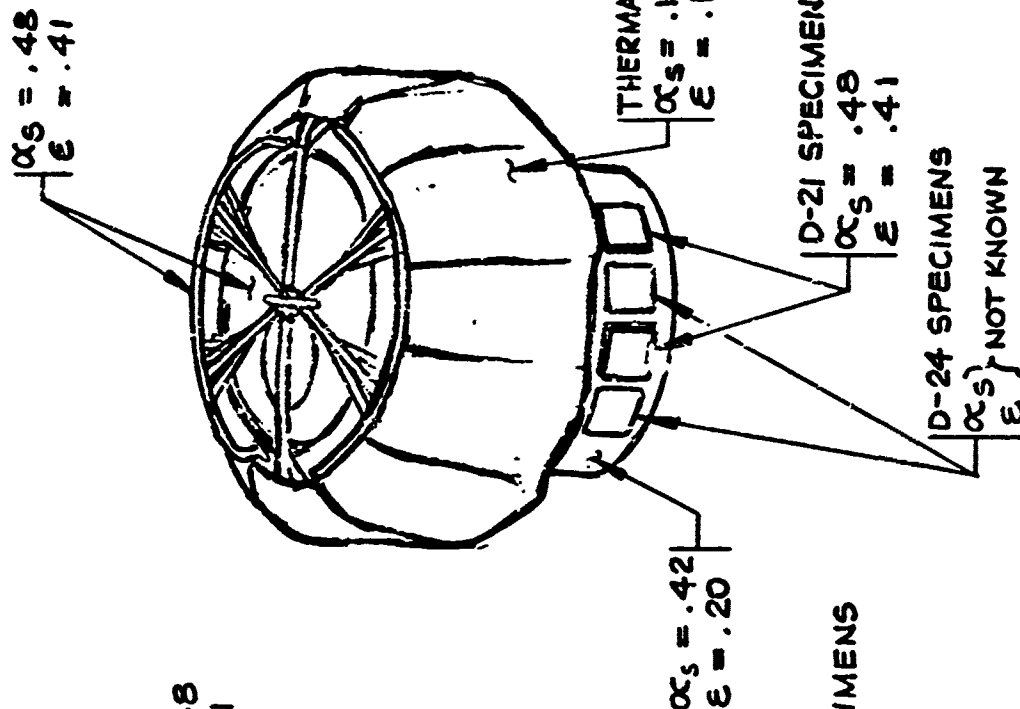
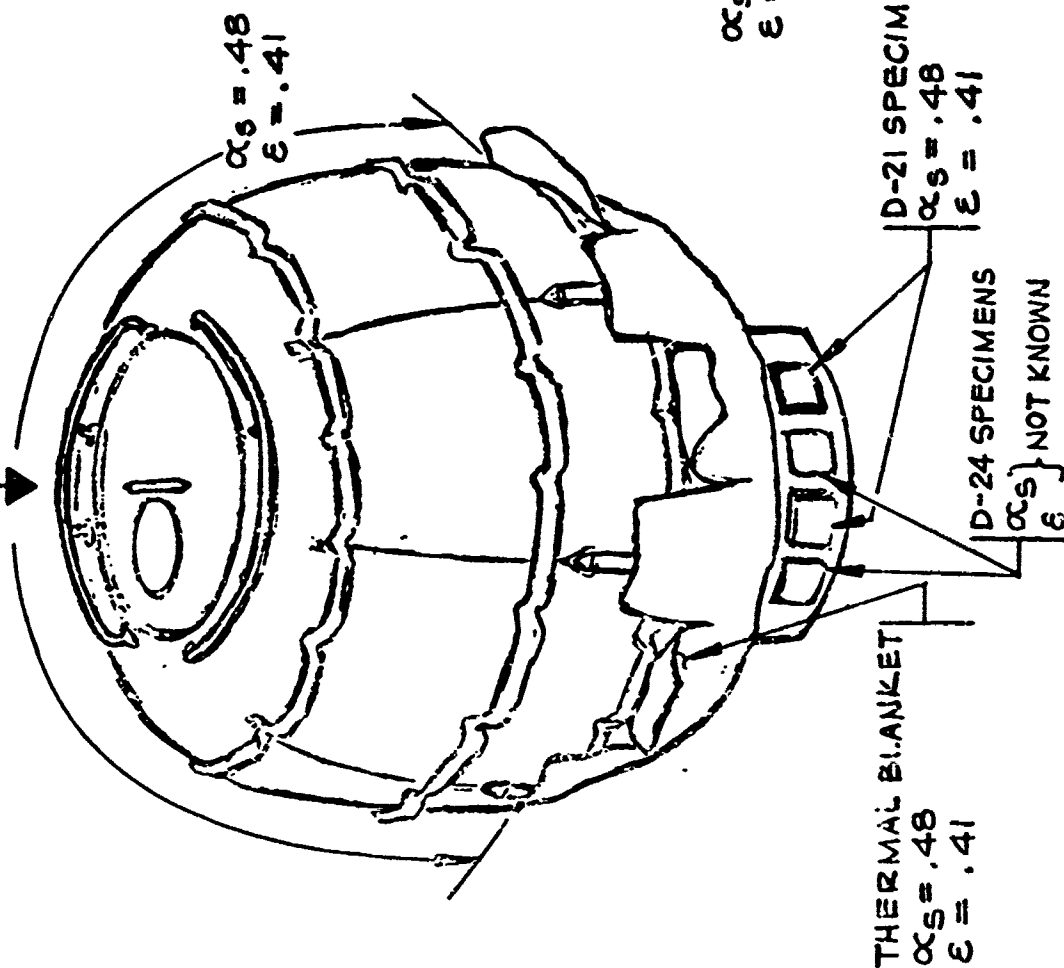


Figure 60. Deployed & Packaged Thermal Properties

tests show the materials of the super insulation thermal blanket are not subject to increased stiffness even as low as -150° F.

After deployment of the D-21 airlock, the thermal model becomes a hollow shell with internal radiation effects. The results of this analysis are shown on Figure 59. The maximum-minimum temperature of the outer surface ranges from $+235^{\circ}$ F to -84° F. The inner surface varies from $+55^{\circ}$ F to -5° F.

For the location behind the solar array of the ATM, there was no single surface coating which would not exceed the limits of $+350^{\circ}$ F in the sun and also maintain the cold condition above -20° F prior to deployment.

DESIGN APPROACH

The hatch end of the airlock is to be painted with Ball Brothers Incorporated 80U Silicone base paint loaded with aluminum flake pigment to achieve values of

$\alpha_s = 0.41$ and $\epsilon = 0.48$. The outer layer of the super-insulation blanket will be aluminized mylar laminated to dacron cloth with surface properties of

$\alpha_s = 0.12$, and $\epsilon = 0.04$. This will be modified by pierced holes to achieve an effective $\alpha_s = 0.18$, and $\epsilon = 0.12$. The super insulation will consist of 18 layers of $1/4$ -mil aluminized mylar separated with dacron cloth.

This should achieve a conductivity of approximately 0.0005 BTU/HR-FT- $^{\circ}$ R.

The thermal insulation blanket surrounds the expandable materials portion of the airlock prior to deployment and tempers the thermal environment during this period.

After deployment, it lies against the lower surface of the airlock and continues to serve as thermal moderator in this area, although it is no longer required. The remainder of the exposed expandable structure is coated with the same silicone base paint as used on the hatch.

CONCLUSIONS

1. The D-21 airlock should be relocated from its current position on Strut No. 3 of the NASA AM to the Strut No. 4 position in order to provide an acceptable thermal environment. (See Figure 60)
2. A thermal insulation blanket is required to protect the expandable structure section of airlock from extremes of the thermal environment in the packaged state.
3. The thermal blanket is not required after airlock deployment, but it need not be jettisoned.
4. The Qualification Test Program procedures should be revised to reflect realistic thermal environment corresponding to this thermal analysis.

APPENDIX IV

THERMAL ANALYSIS COMPUTER RUN


```

0005 004:RAM 1V 360J-F0-479 J-1      HAINPGM      DATE 04/08/70      TIME 11.40.58      PAGE 0001
C      PROG'NAM Z5490-ONE DIMENSIONAL TRANSIENT HEAT CONDUCTION IN A
C      MULTI LAYER SLAB EXPOSED TO CONVECTIVE AND RADIANT HEATING
C      ENVIRONMENT AT EITHER OR BOTH OUTER SURFACES
C      MULTIPLE SLAB TEMP DETERMINATION
C
0001      DIMENSION A(35,10),XK(35),C(35),RHO(35),DELTX(35),T(35),Z(35)
0002      ,ABC(100),HCD(35),TAW(80),T(135),T(100),T(180)
0003      900 FORMAT(2F10.5,E10.3,F10.5,E10.5)
0004      901 FORMAT(8F10.5)
0005      902 FORMAT(3I2)
0006      903 FORMAT(26X,76H      XK(1)      C(1)      RHO(1)      DELTX(1)
0007      ,1
0008      904 FORMAT(26X,75H      EPI      SIGMA      ZR      ZL
0009      ,1,ALPHA      BETA      DELT      //24X,2F10.3,F10.6//)
0010      905 FORMAT(27H,35H      HCL      //24X,2F10.3,F10.3,E10.3,E10.3//)
0011      906 FORMAT(110X,40H      HCL      EPS      //27X,8E10.3//)
0012      907 FORMAT(110X,40H      HCL      EPS      //27X,8E10.3//)
0013      908 FORMAT(110X,40H      HCL      EPS      //27X,8E10.3//)
0014      909 FORMAT(110X,40H      HCL      EPS      //27X,8E10.3//)
0015      910 FORMAT(110X,40H      HCL      EPS      //27X,8E10.3//)
0016      911 FORMAT(110X,40H      HCL      EPS      //27X,8E10.3//)
0017      912 FORMAT(110X,40H      HCL      EPS      //27X,8E10.3//)
0018      913 FORMAT(110X,40H      HCL      EPS      //27X,8E10.3//)
0019      914 FORMAT(110X,40H      HCL      EPS      //27X,8E10.3//)
0020      915 FORMAT(110X,40H      HCL      EPS      //27X,8E10.3//)
0021      916 FORMAT(110X,40H      HCL      EPS      //27X,8E10.3//)
0022      917 FORMAT(110X,40H      HCL      EPS      //27X,8E10.3//)
0023      918 FORMAT(110X,40H      HCL      EPS      //27X,8E10.3//)
0024      919 FORMAT(110X,40H      HCL      EPS      //27X,8E10.3//)
0025      920 FORMAT(110X,40H      HCL      EPS      //27X,8E10.3//)
0026      921 FORMAT(110X,40H      HCL      EPS      //27X,8E10.3//)
0027      922 FORMAT(110X,40H      HCL      EPS      //27X,8E10.3//)
0028      923 FORMAT(110X,40H      HCL      EPS      //27X,8E10.3//)
0029      924 FORMAT(110X,40H      HCL      EPS      //27X,8E10.3//)
0030      925 FORMAT(110X,40H      HCL      EPS      //27X,8E10.3//)
0031      926 FORMAT(110X,40H      HCL      EPS      //27X,8E10.3//)
0032      927 FORMAT(110X,40H      HCL      EPS      //27X,8E10.3//)
0033      928 FORMAT(110X,40H      HCL      EPS      //27X,8E10.3//)
0034      929 FORMAT(110X,40H      HCL      EPS      //27X,8E10.3//)
0035      930 FORMAT(110X,40H      HCL      EPS      //27X,8E10.3//)
0036      931 FORMAT(110X,40H      HCL      EPS      //27X,8E10.3//)
0037      932 FORMAT(110X,40H      HCL      EPS      //27X,8E10.3//)
0038      933 FORMAT(110X,40H      HCL      EPS      //27X,8E10.3//)
0039      934 FORMAT(110X,40H      HCL      EPS      //27X,8E10.3//)
0040      935 FORMAT(110X,40H      HCL      EPS      //27X,8E10.3//)
0041      936 FORMAT(110X,40H      HCL      EPS      //27X,8E10.3//)
0042      937 FORMAT(110X,40H      HCL      EPS      //27X,8E10.3//)
0043      938 FORMAT(110X,40H      HCL      EPS      //27X,8E10.3//)
0044      939 FORMAT(110X,40H      HCL      EPS      //27X,8E10.3//)
0045      940 FORMAT(110X,40H      HCL      EPS      //27X,8E10.3//)
0046      941 FORMAT(110X,40H      HCL      EPS      //27X,8E10.3//)
0047      942 FORMAT(110X,40H      HCL      EPS      //27X,8E10.3//)
0048      943 FORMAT(110X,40H      HCL      EPS      //27X,8E10.3//)
0049      944 FORMAT(110X,40H      HCL      EPS      //27X,8E10.3//)
0050      945 FORMAT(110X,40H      HCL      EPS      //27X,8E10.3//)
0051      946 FORMAT(110X,40H      HCL      EPS      //27X,8E10.3//)
0052      947 FORMAT(110X,40H      HCL      EPS      //27X,8E10.3//)
0053      948 FORMAT(110X,40H      HCL      EPS      //27X,8E10.3//)
0054      949 FORMAT(110X,40H      HCL      EPS      //27X,8E10.3//)
0055      950 FORMAT(110X,40H      HCL      EPS      //27X,8E10.3//)
0056      951 FORMAT(110X,40H      HCL      EPS      //27X,8E10.3//)
0057      952 FORMAT(110X,40H      HCL      EPS      //27X,8E10.3//)
0058      953 FORMAT(110X,40H      HCL      EPS      //27X,8E10.3//)
0059      954 FORMAT(110X,40H      HCL      EPS      //27X,8E10.3//)
0060      955 FORMAT(110X,40H      HCL      EPS      //27X,8E10.3//)
0061      956 FORMAT(110X,40H      HCL      EPS      //27X,8E10.3//)
0062      957 FORMAT(110X,40H      HCL      EPS      //27X,8E10.3//)
0063      958 FORMAT(110X,40H      HCL      EPS      //27X,8E10.3//)
0064      959 FORMAT(110X,40H      HCL      EPS      //27X,8E10.3//)
0065      960 FORMAT(110X,40H      HCL      EPS      //27X,8E10.3//)
0066      961 FORMAT(110X,40H      HCL      EPS      //27X,8E10.3//)
0067      962 FORMAT(110X,40H      HCL      EPS      //27X,8E10.3//)
0068      963 FORMAT(110X,40H      HCL      EPS      //27X,8E10.3//)
0069      964 FORMAT(110X,40H      HCL      EPS      //27X,8E10.3//)
0070      965 FORMAT(110X,40H      HCL      EPS      //27X,8E10.3//)
0071      966 FORMAT(110X,40H      HCL      EPS      //27X,8E10.3//)
0072      967 FORMAT(110X,40H      HCL      EPS      //27X,8E10.3//)
0073      968 FORMAT(110X,40H      HCL      EPS      //27X,8E10.3//)
0074      969 FORMAT(110X,40H      HCL      EPS      //27X,8E10.3//)
0075      970 FORMAT(110X,40H      HCL      EPS      //27X,8E10.3//)
0076      971 FORMAT(110X,40H      HCL      EPS      //27X,8E10.3//)
0077      972 FORMAT(110X,40H      HCL      EPS      //27X,8E10.3//)
0078      973 FORMAT(110X,40H      HCL      EPS      //27X,8E10.3//)
0079      974 FORMAT(110X,40H      HCL      EPS      //27X,8E10.3//)
0080      975 FORMAT(110X,40H      HCL      EPS      //27X,8E10.3//)
0081      976 FORMAT(110X,40H      HCL      EPS      //27X,8E10.3//)
0082      977 FORMAT(110X,40H      HCL      EPS      //27X,8E10.3//)
0083      978 FORMAT(110X,40H      HCL      EPS      //27X,8E10.3//)
0084      979 FORMAT(110X,40H      HCL      EPS      //27X,8E10.3//)
0085      980 FORMAT(110X,40H      HCL      EPS      //27X,8E10.3//)
0086      981 FORMAT(110X,40H      HCL      EPS      //27X,8E10.3//)
0087      982 FORMAT(110X,40H      HCL      EPS      //27X,8E10.3//)
0088      983 FORMAT(110X,40H      HCL      EPS      //27X,8E10.3//)
0089      984 FORMAT(110X,40H      HCL      EPS      //27X,8E10.3//)
0090      985 FORMAT(110X,40H      HCL      EPS      //27X,8E10.3//)
0091      986 FORMAT(110X,40H      HCL      EPS      //27X,8E10.3//)
0092      987 FORMAT(110X,40H      HCL      EPS      //27X,8E10.3//)
0093      988 FORMAT(110X,40H      HCL      EPS      //27X,8E10.3//)
0094      989 FORMAT(110X,40H      HCL      EPS      //27X,8E10.3//)
0095      990 FORMAT(110X,40H      HCL      EPS      //27X,8E10.3//)
0096      991 FORMAT(110X,40H      HCL      EPS      //27X,8E10.3//)
0097      992 FORMAT(110X,40H      HCL      EPS      //27X,8E10.3//)
0098      993 FORMAT(110X,40H      HCL      EPS      //27X,8E10.3//)
0099      994 FORMAT(110X,40H      HCL      EPS      //27X,8E10.3//)
0100      995 FORMAT(110X,40H      HCL      EPS      //27X,8E10.3//)
0101      996 FORMAT(110X,40H      HCL      EPS      //27X,8E10.3//)
0102      997 FORMAT(110X,40H      HCL      EPS      //27X,8E10.3//)
0103      998 FORMAT(110X,40H      HCL      EPS      //27X,8E10.3//)
010
```


// EXEC

04/08/70

11.43.23
MULTIPLE SLAB TEMPERATURE DISTRIBUTION

MATERIAL PROPERTIES

KK(1)	C(1)	RHO(1)	DELTX(1)
0.0005	0.240	1.000	0.010400
KK(1)	C(1)	RHO(1)	DELTX(1)
0.0005	0.240	1.000	0.010400
KK(1)	C(1)	RHO(1)	DELTX(1)
0.0005	0.240	1.000	0.010400
KK(1)	C(1)	RHO(1)	DELTX(1)
0.0050	0.240	6.000	0.010400
KK(1)	C(1)	RHO(1)	DELTX(1)
0.0050	0.240	6.000	0.010400
KK(1)	C(1)	RHO(1)	DELTX(1)
0.0050	0.240	6.000	0.010400
KK(1)	C(1)	RHO(1)	DELTX(1)
0.0050	0.240	6.000	0.010400
KK(1)	C(1)	RHO(1)	DELTX(1)
0.0050	0.240	6.000	0.010400
KK(1)	C(1)	RHO(1)	DELTX(1)
0.0050	0.240	6.000	0.010400
KK(1)	C(1)	RHO(1)	DELTX(1)
0.0050	0.240	6.000	0.010400
KK(1)	C(1)	RHO(1)	DELTX(1)
0.0050	0.240	6.000	0.010400

EPI	EP2	SIGMA	ZK	ZL	ALPHA	BETA	DELT
0.120	0.0	0.173E-04	0.0	432.000	2.000	0.0	3.417E-02

HCL EPS
0.0 0.100E 07 0.130E 01

INITIAL TEMPERATURES

TIME	NODE1	2	3	4	5	6	7	8	9	10	11
0.2000E 00 TIME	-100.991 NODE1	-74.447 2	-51.115 3	-30.702 4	-25.992 5	-24.497 6	-22.740 7	-20.740 8	-13.111 9	-8.000 10	11
0.2030E 02 TIME	-49.877 NODE1	-71.385 2	-51.220 3	-29.255 4	-26.945 5	-24.659 6	-22.740 7	-20.773 8	-16.457 9	-8.000 10	11
0.2300E 02 TIME	-49.546 NODE1	-73.073 2	-50.949 3	-29.175 4	-27.003 5	-24.838 6	-22.721 7	-20.575 8	-15.437 9	-8.000 10	11
0.2550E 02 TIME	-103.214 NODE1	-76.115 2	-51.010 3	-29.248 4	-27.031 5	-24.829 6	-22.584 7	-20.219 8	-14.833 9	-8.000 10	11
0.2000E 02 TIME	-105.656 NODE1	-77.667 2	-52.977 3	-29.370 4	-27.059 5	-24.766 6	-22.420 7	-19.951 8	-14.431 9	-8.000 10	11
0.2050E 02 TIME	-103.456 NODE1	-78.306 2	-53.604 3	-29.463 4	-27.079 5	-24.699 6	-22.266 7	-19.729 8	-14.194 9	-8.000 10	11
0.3300E 02 TIME	-103.123 NODE1	-78.474 2	-53.890 3	-29.506 4	-27.076 5	-24.633 6	-22.138 7	-19.551 8	-14.012 9	-8.000 10	11
0.3550E 02 TIME	-102.774 NODE1	-78.553 2	-53.962 3	-29.504 4	-27.049 5	-24.565 6	-22.037 7	-19.409 8	-13.880 9	-8.000 10	11
0.3800E 02 TIME	-102.517 NODE1	-78.304 2	-53.927 3	-29.470 4	-27.003 5	-24.494 6	-21.729 7	-19.294 8	-13.781 9	-8.000 10	11
0.4050E 02 TIME	-102.455 NODE1	-78.205 2	-53.854 3	-29.415 4	-26.944 5	-24.421 6	-21.842 7	-19.198 8	-13.783 9	-8.000 10	11
0.4300E 02 TIME	-102.560 NODE1	-78.370 2	-53.794 3	-29.351 4	-26.876 5	-24.348 6	-21.762 7	-19.111 8	-13.644 9	-8.000 10	11
0.4550E 02 TIME	-102.811 NODE1	-78.511 2	-53.770 3	-29.215 4	-26.807 5	-24.275 6	-21.637 7	-19.000 8	-13.594 9	-8.000 10	11
0.4800E 02 TIME	-103.488 NODE1	-78.466 2	-53.805 3	-29.224 4	-26.740 5	-24.205 6	-21.617 7	-19.974 8	-13.552 9	-8.000 10	11
0.5050E 02 TIME	-104.342 NODE1	-79.143 2	-53.918 3	-29.175 4	-26.680 5	-24.141 6	-21.556 7	-19.117 8	-13.516 9	-8.000 10	11
0.5300E 02 TIME	-105.437 NODE1	-79.407 2	-54.123 3	-29.141 4	-26.630 5	-24.084 6	-21.525 7	-19.155 8	-13.483 9	-8.000 10	11
0.5550E 02 TIME	-106.991 NODE1	-80.171 2	-54.422 3	-29.127 4	-26.594 5	-24.037 6	-21.446 7	-18.817 8	-13.454 9	-8.000 10	11
0.5800E 02 TIME	-108.442 NODE1	-81.094 2	-54.842 3	-29.137 4	-26.574 5	-24.001 6	-21.401 7	-18.775 8	-13.428 9	-8.000 10	11
0.6050E 02 TIME	-109.690 NODE1	-81.972 2	-55.133 3	-29.161 4	-26.571 5	-23.977 6	-21.377 7	-19.711 8	-13.437 9	-8.000 10	11
0.6300E 02 TIME	-110.200 NODE1	-82.000 2	-55.706 3	-29.216 4	-26.507 5	-23.971 6	-21.350 7	-19.115 8	-13.337 9	-8.000 10	11
0.6550E 02 TIME	-109.951 NODE1	-82.135 2	-55.994 3	-29.265 4	-26.611 5	-23.974 6	-21.317 7	-19.000 8	-13.372 9	-8.000 10	11
0.6800E 02 TIME	-107.864 NODE1	-82.555 2	-56.016 3	-29.293 4	-26.634 5	-23.982 6	-21.335 7	-19.085 8	-13.366 9	-8.000 10	11

0.7051E 02 TIME	-91.503 NODE1	-77.167 2	-54.952 3	-29.259 4	-26.634 5	-23.987 6	-21.334 7	-18.679 8	-13.353 9	-8.000 10	11
0.7301E 02 TIME	-68.970 NODE1	-67.677 2	-51.310 3	-28.962 4	-26.528 5	-23.951 6	-21.323 7	-18.673 8	-13.348 9	-8.000 10	11
0.7551E 02 TIME	-45.572 NODE1	-54.283 2	-45.420 3	-28.295 4	-26.216 5	-23.817 6	-21.268 7	-18.653 8	-13.342 9	-8.000 10	11
0.7801E 02 TIME	-24.531 NODE1	-40.142 2	-38.300 3	-27.267 4	-25.652 5	-23.529 6	-21.131 7	-18.594 8	-13.329 9	-8.000 10	11
0.8051E 02 TIME	-6.811 NODE1	-26.714 2	-30.890 3	-25.958 4	-24.850 5	-23.069 6	-20.884 7	-18.473 8	-13.299 9	-8.000 10	11
0.8302E 02 TIME	7.123 NODE1	-15.122 2	-23.935 3	-24.474 4	-23.857 5	-22.446 6	-20.518 7	-18.273 8	-13.244 9	-8.000 10	11
0.8552E 02 TIME	15.882 NODE1	-5.464 2	-17.881 3	-22.916 4	-22.737 5	-21.689 6	-20.036 7	-17.987 8	-13.155 9	-8.000 10	11
0.8802E 02 TIME	20.843 NODE1	0.658 2	-13.021 3	-21.377 4	-21.554 5	-20.837 6	-19.458 7	-17.618 8	-13.028 9	-8.000 10	11
0.5001E 00 TIME	21.883 NODE1	4.443 2	-9.441 3	-19.934 4	-20.371 5	-19.933 6	-18.808 7	-17.178 8	-12.864 9	-8.000 10	11
0.3001E 01 TIME	18.207 NODE1	5.490 2	-7.461 3	-18.648 4	-19.242 5	-19.019 6	-18.115 7	-16.883 8	-12.644 9	-8.000 10	11
0.5501E 01 TIME	11.524 NODE1	4.029 2	-6.798 3	-17.566 4	-18.214 5	-18.135 6	-17.409 7	-16.155 8	-12.437 9	-8.000 10	11
0.8002E 01 TIME	1.621 NODE1	0.176 2	-7.516 3	-16.723 4	-17.325 5	-17.315 6	-16.719 7	-15.615 8	-12.190 9	-8.000 10	11
0.1050E 02 TIME	-11.268 NODE1	-7.116 2	-9.532 3	-16.142 4	-16.606 5	-16.591 6	-16.071 7	-15.083 8	-11.933 9	-8.000 10	11
0.1300E 02 TIME	-26.106 NODE1	-13.369 2	-12.650 3	-15.838 4	-16.077 5	-15.987 6	-15.487 7	-14.581 8	-11.675 9	-8.000 10	11
0.1550E 02 TIME	-42.660 NODE1	-23.469 2	-16.803 3	-15.811 4	-15.754 5	-15.524 6	-14.994 7	-14.126 8	-11.427 9	-8.000 10	11
0.1800E 02 TIME	-56.751 NODE1	-31.251 2	-21.607 3	-16.047 4	-15.640 5	-15.213 6	-14.603 7	-13.737 8	-11.118 9	-8.000 10	11
0.2050E 02 TIME	-71.164 NODE1	-42.775 2	-26.531 3	-16.494 4	-15.719 5	-15.057 6	-14.326 7	-13.424 8	-10.997 9	-8.000 10	11
0.2301E 02 TIME	-87.296 NODE1	-53.000 2	-31.718 3	-17.117 4	-15.964 5	-15.045 6	-14.163 7	-13.195 8	-10.824 9	-8.000 10	11
0.2551E 02 TIME	-94.195 NODE1	-61.197 2	-36.797 3	-17.898 4	-16.364 5	-15.171 6	-14.113 7	-13.053 8	-10.696 9	-8.000 10	11
0.2801E 02 TIME	-96.756 NODE1	-66.304 2	-40.564 3	-18.709 4	-16.866 5	-15.413 6	-14.169 7	-12.998 8	-10.609 9	-8.000 10	11
0.3051E 02 TIME	-97.961 NODE1	-67.142 2	-43.043 3	-19.451 4	-17.394 5	-15.729 6	-14.312 7	-13.022 8	-10.561 9	-8.000 10	11
0.3301E 02 TIME	-98.581 NODE1	-70.307 2	-44.619 3	-20.096 4	-17.903 5	-16.076 6	-14.512 7	-13.110 8	-10.551 9	-8.000 10	11

0.3551E 02 TIME	NOU1	-11.791 2	-15.5 3	-20.651 4	-18.373 5	-16.433 6	-14.747 7	-13.245 8	-10.573 9	-8.000 10	11
0.3801E 02 TIME	NOU1	-72.430 2	-46.401 3	-21.132 4	-18.801 5	-16.774 6	-14.998 7	-13.410 8	-10.622 9	-8.000 10	11
0.4051E 02 TIME	NOU1	-72.497 2	-46.432 3	-21.555 4	-19.191 5	-17.104 6	-15.234 7	-13.594 8	-10.690 9	-8.000 10	11
0.4301E 02 TIME	NOU1	-73.310 2	-47.367 3	-21.934 4	-19.547 5	-17.415 6	-15.508 7	-13.785 8	-10.770 9	-8.000 10	11
0.4551E 02 TIME	NOU1	-73.754 2	-47.771 3	-22.281 4	-19.877 5	-17.709 6	-15.754 7	-13.979 8	-10.838 9	-8.000 10	11
0.4801E 02 TIME	NOU1	-74.279 2	-48.191 3	-22.606 4	-20.186 5	-17.989 6	-15.993 7	-14.171 8	-10.930 9	-8.000 10	11
0.5051E 02 TIME	NOU1	-74.921 2	-48.628 3	-22.918 4	-20.460 5	-18.255 6	-16.214 7	-14.360 8	-11.044 9	-8.000 10	11
0.5301E 02 TIME	NOU1	-75.718 2	-49.337 3	-23.223 4	-20.764 5	-18.512 6	-16.417 7	-14.543 8	-11.137 9	-8.000 10	11
0.5551E 02 TIME	NOU1	-76.691 2	-49.722 3	-23.529 4	-21.042 5	-18.761 6	-16.663 7	-14.722 8	-11.229 9	-8.000 10	11
0.5801E 02 TIME	NOU1	-77.803 2	-50.392 3	-23.840 4	-21.321 5	-19.007 6	-16.874 7	-14.895 8	-11.318 9	-8.000 10	11
0.6051E 02 TIME	NOU1	-78.955 2	-51.083 3	-24.156 4	-21.600 5	-19.251 6	-17.083 7	-15.066 8	-11.406 9	-8.000 10	11
0.6302E 02 TIME	NOU1	-79.694 2	-51.720 3	-24.470 4	-21.880 5	-19.494 6	-17.498 7	-15.234 8	-11.493 9	-8.000 10	11
0.6552E 02 TIME	NOU1	-80.165 2	-52.220 3	-24.772 4	-22.154 5	-19.735 6	-17.491 7	-15.179 8	-11.578 9	-8.000 10	11
0.6802E 02 TIME	NOU1	-79.893 2	-52.441 3	-25.040 4	-22.415 5	-19.967 6	-17.691 7	-15.561 8	-11.661 9	-8.000 10	11
0.7052E 02 TIME	NOU1	-75.462 2	-51.508 3	-25.232 4	-22.640 5	-20.181 6	-17.411 7	-15.721 8	-11.711 9	-8.000 10	11
0.7302E 02 TIME	NOU1	-65.346 2	-48.117 3	-25.151 4	-22.747 5	-20.355 6	-19.151 7	-15.875 8	-11.424 9	-8.000 10	11
0.7552E 02 TIME	NOU1	-52.146 2	-42.425 3	-24.889 4	-22.636 5	-20.412 6	-18.178 7	-16.803 8	-11.896 9	-8.000 10	11
0.7802E 02 TIME	NOU1	-38.195 2	-35.501 3	-23.857 4	-22.265 5	-20.306 6	-18.205 7	-16.085 8	-11.963 9	-8.000 10	11
0.8052E 02 TIME	NOU1	-24.944 2	-28.281 3	-22.736 4	-21.647 5	-20.019 6	-19.115 7	-18.078 8	-11.006 9	-8.000 10	11
0.8302E 02 TIME	NOU1	-13.504 2	-21.500 3	-21.430 4	-20.830 5	-19.562 6	-17.307 7	-16.011 8	-12.020 9	-8.000 10	11
0.8552E 02 TIME	NOU1	-4.481 2	-13.606 3	-20.042 4	-19.875 5	-18.782 6	-17.151 7	-15.760 8	-11.996 9	-8.000 10	11
0.8802E 02 TIME	NOU1	2.026 2	-10.893 3	-18.664 4	-18.951 5	-18.259 6	-17.114 7	-15.606 8	-11.931 9	-8.000 10	11

0.5001E 00 TIME	22.323 NODE1	5.717 2	-7.544 3	-17.333 4	-17.817 5	-17.696 6	-16.592 7	-15.275 8	-11.825 9	-8.000 10	11
0.3001E 01 TIME	18.074 NODE1	6.695 2	-5.543 3	-16.223 4	-16.930 5	-16.716 6	-16.020 7	-14.884 8	-11.683 9	-8.000 10	11
0.5501E 01 TIME	11.926 NODE1	5.154 2	-5.030 3	-15.282 4	-15.936 5	-15.958 6	-15.428 7	-14.453 8	-11.508 9	-8.000 10	11
0.8002E 01 TIME	2.017 NODE1	1.144 2	-5.845 3	-14.565 4	-15.172 5	-15.259 6	-14.846 7	-14.006 8	-11.312 9	-8.000 10	11
0.1050E 02 TIME	-10.872 NODE1	-6.999 2	-7.920 3	-14.104 4	-14.572 5	-14.648 6	-14.301 7	-13.562 8	-11.103 9	-8.000 10	11
0.1300E 02 TIME	-25.704 NODE1	-12.994 2	-11.150 3	-13.911 4	-14.156 5	-14.152 6	-13.811 7	-13.144 8	10.891 9	-8.000 10	11
0.1550E 02 TIME	-42.247 NODE1	-22.529 2	-15.378 3	-13.990 4	-13.938 5	-13.789 6	-13.414 7	-12.769 8	-10.686 9	-8.000 10	11
0.1800E 02 TIME	-56.127 NODE1	-12.142 2	-20.450 3	-14.327 4	-13.924 5	-13.573 6	-13.110 7	-12.453 8	-10.497 9	-8.000 10	11
0.2050E 02 TIME	-70.731 NODE1	-41.895 2	-25.238 3	-13.865 4	-14.095 5	-13.506 6	-12.915 7	-12.211 8	-10.334 9	-8.000 10	11
0.2301E 02 TIME	-86.050 NODE1	-52.146 2	-20.484 3	-15.575 4	-14.428 5	-13.579 6	-12.829 7	-12.049 8	-10.202 9	-8.000 10	11
0.2551E 02 TIME	-93.744 NODE1	-60.567 2	-35.619 3	-16.438 4	-14.911 5	-13.784 6	-12.852 7	-11.969 8	-10.108 9	-8.000 10	11
0.2801E 02 TIME	-96.314 NODE1	-65.502 2	-39.438 3	-17.326 4	-15.491 5	-14.101 6	-12.976 7	-11.873 8	-10.049 9	-8.000 10	11
0.3051E 02 TIME	-97.534 NODE1	-68.171 2	-41.969 3	-18.141 4	-16.092 5	-14.488 6	-13.183 7	-12.052 8	-10.011 9	-8.000 10	11
0.3301E 02 TIME	-98.169 NODE1	-70.064 2	-43.617 3	-18.855 4	-16.670 5	-14.901 6	-13.444 7	-12.192 8	-10.049 9	-8.000 10	11
0.3551E 02 TIME	-98.477 NODE1	-71.707 2	-44.714 3	-19.477 4	-17.200 5	-15.318 6	-13.737 7	-12.177 8	-10.110 9	-8.000 10	11
0.3801E 02 TIME	-98.736 NODE1	-71.760 2	-45.480 3	-20.020 4	-17.696 5	-15.722 6	-14.042 7	-12.589 8	-10.174 9	-8.000 10	11
0.4051E 02 TIME	-99.041 NODE1	-72.260 2	-46.057 3	-20.501 4	-18.145 5	-16.107 6	-14.349 7	-12.817 8	-10.266 9	-8.000 10	11
0.4301E 02 TIME	-99.434 NODE1	-72.706 2	-46.539 3	-20.936 4	-18.556 5	-16.472 6	-14.651 7	-13.051 8	-10.370 9	-8.000 10	11
0.4551E 02 TIME	-99.987 NODE1	-73.140 2	-46.985 3	-21.336 4	-18.939 5	-16.816 6	-14.944 7	-13.284 8	-10.480 9	-8.000 10	11
0.4801E 02 TIME	-100.716 NODE1	-73.736 2	-47.437 3	-21.712 4	-19.298 5	-17.144 6	-15.226 7	-13.513 8	-10.592 9	-8.000 10	11
0.5051E 02 TIME	-101.803 NODE1	-74.405 2	-47.923 3	-22.071 4	-19.640 5	-17.455 6	-15.497 7	-13.717 8	-10.705 9	-8.000 10	11
0.5301E 02 TIME	-103.007 NODE1	-75.229 2	-48.470 3	-22.422 4	-19.969 5	-17.754 6	-15.754 7	-13.954 8	-10.816 9	-8.000 10	11

0.5551E 02 TIME	-104.111 NODE1	-76.227 2	-49.090 3	-22.771 4	-20.290 5	-18.045 6	-16.012 7	-14.163 8	-10.925 9	-8.000 10	11
0.5801E 02 TIME	-106.331 NODE1	-77.163 2	-49.773 3	-23.122 4	-20.603 5	-18.328 6	-16.258 7	-14.167 8	-11.031 9	-8.000 10	11
0.6051E 02 TIME	-107.633 NODE1	-78.436 2	-50.514 3	-23.476 4	-20.925 5	-18.609 6	-16.499 7	-14.565 8	-11.134 9	-8.000 10	11
0.6302E 02 TIME	-108.305 NODE1	-79.295 2	-51.180 3	-23.826 4	-21.240 5	-18.886 6	-16.736 7	-14.760 8	-11.235 9	-8.000 10	11
0.6552E 02 TIME	-108.092 NODE1	-79.787 2	-51.708 3	-24.162 4	-21.548 5	-19.159 6	-16.969 7	-14.951 8	-11.338 9	-8.000 10	11
0.6802E 02 TIME	-106.098 NODE1	-79.535 2	-51.957 3	-24.467 4	-21.841 5	-17.424 6	-17.191 7	-15.138 8	-11.430 9	-8.000 10	11
0.7052E 02 TIME	-89.189 NODE1	-75.125 2	-51.109 3	-24.684 4	-22.096 5	-19.671 6	-17.417 7	-15.321 8	-11.575 9	-8.000 10	11
0.7302E 02 TIME	-67.571 NODE1	-65.033 2	-47.685 3	-24.633 4	-22.232 5	-19.866 6	-17.615 7	-15.494 8	-11.616 9	-8.000 10	11
0.7552E 02 TIME	-44.400 NODE1	-51.899 2	-42.020 3	-24.199 4	-22.149 5	-19.949 6	-17.757 7	-15.642 8	-11.702 9	-8.000 10	11
0.7802E 02 TIME	-23.554 NODE1	-37.334 2	-35.123 3	-23.393 4	-21.805 5	-19.868 6	-17.807 7	-15.745 8	-11.774 9	-8.000 10	11
0.8052E 02 TIME	-5.993 NODE1	-24.706 2	-27.927 3	-22.298 4	-21.212 5	-19.604 6	-17.738 7	-15.775 8	-11.829 9	-8.000 10	11
0.8302E 02 TIME	7.822 NODE1	-13.287 2	-21.170 3	-21.017 4	-20.418 5	-19.169 6	-17.541 7	-15.719 8	-11.853 9	-8.000 10	11
0.8552E 02 TIME	16.494 NODE1	-4.281 2	-15.799 3	-19.651 4	-19.487 5	-18.591 6	-17.220 7	-15.370 8	-11.838 9	-8.000 10	11
0.8802E 02 TIME	21.386 NODE1	2.212 2	-10.604 3	-18.295 4	-18.484 5	-17.708 6	-16.795 7	-15.112 8	-11.782 9	-8.000 10	11
0.9051E 00 TIME	22.383 NODE1	5.889 2	-7.274 3	-17.025 4	-17.470 5	-17.165 6	-16.290 7	-15.011 8	-11.684 9	-8.000 10	11
0.9301E 01 TIME	18.681 NODE1	6.446 2	-5.329 3	-15.901 4	-16.502 5	-16.403 6	-15.735 7	-14.637 8	-11.549 9	-8.065 10	11
0.9501E 01 TIME	11.981 NODE1	5.307 2	-4.789 3	-14.971 4	-15.626 5	-15.463 6	-15.159 7	-14.222 8	-11.532 9	-8.854 10	11
0.9802E 01 TIME	2.070 NODE1	1.288 2	-5.619 3	-14.272 4	-14.880 5	-14.979 6	-14.592 7	-13.767 8	-11.192 9	-8.650 10	11
0.1050E 02 TIME	-10.818 NODE1	-4.861 2	-7.706 3	-13.827 4	-14.296 5	-14.384 6	-14.061 7	-13.356 8	-12.770 9	-8.000 10	11
0.1300E 02 TIME	-25.649 NODE1	-12.862 2	-10.968 3	-13.649 4	-13.994 5	-13.902 6	-13.590 7	-12.948 8	-10.784 9	-8.000 10	11
0.1550E 02 TIME	-42.191 NODE1	-22.402 2	-15.184 3	-13.743 4	-13.691 5	-13.553 6	-13.201 7	-12.584 8	-10.585 9	-8.000 10	11
0.1800E 02 TIME	-56.270 NODE1	-32.219 2	-20.066 3	-14.092 4	-13.690 5	-13.350 6	-12.907 7	-12.279 8	-10.402 9	-8.000 10	11

0.2050E 02 TIME	-70.672 NODE1	-61.176 2	-25.062 3	-16.641 4	-13.874 5	-13.296 6	-12.723 7	-12.046 8	-10.244 9	-8.000 10	11
0.2301E 02 TIME	-86.739 NODE1	-52.029 2	-30.316 3	-15.365 4	-14.211 5	-13.380 6	-12.648 7	-11.893 8	-10.117 9	-8.000 10	11
0.2551E 02 TIME	-93.603 NODE1	-60.450 2	-35.458 3	-16.240 4	-14.713 5	-13.596 6	-12.680 7	-11.822 8	-10.025 9	-8.000 10	11
0.2801E 02 TIME	-96.254 NODE1	-65.393 2	-39.285 3	-17.138 4	-15.304 5	-13.524 6	-12.814 7	-11.833 8	-9.973 9	-8.000 10	11
0.3051E 02 TIME	-97.476 NODE1	-68.266 2	-41.074 3	-17.963 4	-15.914 5	-14.315 6	-13.030 7	-11.920 8	-9.959 9	-8.000 10	11
0.3301E 02 TIME	-98.214 NODE1	-69.964 2	-43.479 3	-18.687 4	-16.503 5	-14.742 6	-13.299 7	-11.048 8	-9.981 9	-8.000 10	11
0.3551E 02 TIME	-98.444 NODE1	-70.144 2	-44.582 3	-19.318 4	-17.048 5	-15.168 6	-13.519 7	-11.259 8	-10.033 9	-8.000 10	11
0.3801E 02 TIME	-99.685 NODE1	-71.669 2	-45.355 3	-19.869 4	-17.547 5	-15.550 6	-13.912 7	-12.470 8	-10.113 9	-8.000 10	11
0.4051E 02 TIME	-98.993 NODE1	-72.175 2	-45.339 3	-20.114 4	-18.002 5	-15.972 6	-14.226 7	-12.711 8	-10.208 9	-8.000 10	11
0.4301E 02 TIME	-99.388 NODE1	-72.425 2	-46.427 3	-20.801 4	-18.422 5	-16.344 6	-14.534 7	-12.950 8	-10.314 9	-8.000 10	11
0.4551E 02 TIME	-99.953 NODE1	-73.103 2	-46.879 3	-21.208 4	-18.812 5	-16.696 6	-14.833 7	-13.189 8	-10.427 9	-8.000 10	11
0.4801E 02 TIME	-100.745 NODE1	-73.662 2	-47.333 3	-21.590 4	-19.177 5	-17.029 6	-15.122 7	-13.423 8	-10.543 9	-8.000 10	11
0.5051E 02 TIME	-101.766 NODE1	-74.136 2	-47.928 3	-21.954 4	-19.575 5	-17.147 6	-15.199 7	-13.551 8	-10.658 9	-8.000 10	11
0.5301E 02 TIME	-103.054 NODE1	-75.163 2	-48.379 3	-22.313 4	-19.850 5	-17.652 6	-15.500 7	-13.174 8	-10.772 9	-8.000 10	11
0.5551E 02 TIME	-104.575 NODE1	-76.164 2	-49.004 3	-22.667 4	-20.187 5	-17.947 6	-15.774 7	-14.013 8	-10.813 9	-8.000 10	11
0.5801E 02 TIME	-104.216 NODE1	-77.303 2	-49.712 3	-23.024 4	-20.511 5	-18.226 6	-16.174 7	-14.295 8	-10.992 9	-8.000 10	11
0.6051E 02 TIME	-107.600 NODE1	-78.379 2	-50.437 3	-23.383 4	-20.833 5	-18.521 6	-16.419 7	-14.498 8	-11.047 9	-8.000 10	11
0.6302E 02 TIME	-108.273 NODE1	-79.342 2	-51.107 3	-23.736 4	-21.155 5	-18.803 6	-16.661 7	-14.696 8	-11.200 9	-8.000 10	11
0.6552E 02 TIME	-108.042 NODE1	-79.736 2	-51.639 3	-24.077 4	-21.466 5	-19.061 6	-16.898 7	-14.811 8	-11.308 9	-8.000 10	11
0.6802E 02 TIME	-104.070 NODE1	-79.496 2	-51.190 3	-24.343 4	-21.751 5	-19.350 6	-17.131 7	-15.041 8	-11.379 9	-8.000 10	11
0.7052E 02 TIME	-89.664 NODE1	-75.080 2	-51.047 3	-24.610 4	-22.023 5	-17.604 6	-17.354 7	-15.247 8	-11.475 9	-8.000 10	11
0.7302E 02 TIME	-97.544 NODE1	-84.391 2	-47.626 3	-24.561 4	-22.143 5	-19.800 6	-17.554 7	-15.140 8	-11.594 9	-8.000 10	11

0.7492Z 02 TIME	MODE1	-44.382	-21.821	-41.905	-24.132	-22.083	-19.885	-17.699	-15.593	-11.676	-8.000	11
0.7804Z 02 TIME	MODE1	-23.534	-17.394	-15.011	-23.330	-21.742	-19.808	-17.733	-15.608	-11.742	-8.000	11
0.8052Z 02 TIME	MODE1	-5.940	-24.673	-27.870	-22.238	-21.152	-19.548	-17.687	-15.731	-11.806	-8.000	11
0.8302Z 02 TIME	MODE1	7.132	-12.256	-21.125	-20.960	-20.202	-19.115	-17.492	-15.678	-11.830	-8.000	11
0.8552Z 02 TIME	MODE1	16.503	-4.254	-15.256	-19.598	-19.433	-18.540	-17.174	-15.531	-11.817	-8.000	11
0.8802Z 02 TIME	MODE1	21.394	2.237	-10.565	-18.245	-18.433	-17.861	-16.731	-15.295	-11.762	-8.000	11
0.9001E 00 TIME	MODE1	22.391	5.913	-7.237	-16.979	-17.423	-17.120	-16.250	-14.981	-11.665	-8.000	11
0.93001E 01 TIME	MODE1	18.689	6.867	-5.294	-15.856	-16.458	-16.381	-15.697	-14.606	-11.531	-8.000	11
0.9501E 01 TIME	MODE1	11.988	5.127	-4.757	-14.930	-15.584	-15.623	-15.121	-14.191	-11.365	-8.000	11
0.9802E 01 TIME	MODE1	2.078	1.608	-5.588	-14.232	-14.840	-14.941	-14.557	-13.757	-11.176	-8.000	11
0.1050E 02 TIME	MODE1	10.811	-4.842	-7.677	-13.789	-14.258	-14.348	-14.028	-13.327	-10.974	-8.000	11
0.1300E 02 TIME	MODE1	-25.642	-12.844	-10.920	-13.614	-13.859	-13.868	-13.559	-12.922	-10.769	-8.000	11
0.1550E 02 TIME	MODE1	-42.181	-24.115	-15.500	-11.709	-11.657	1.521	-11.171	-10.571	-8.000	-8.000	11
0.1800E 02 TIME	MODE1	-56.262	-37.203	-20.741	-14.061	-13.659	-13.321	-12.880	-11.256	-10.189	-8.000	11
0.2050E 02 TIME	MODE1	-70.664	-41.754	-25.037	-14.613	-13.844	-13.287	-12.177	-12.001	-10.111	-8.000	11
0.2301E 02 TIME	MODE1	-86.781	-52.013	-30.293	-15.337	-14.191	-13.353	-12.623	-11.871	-10.105	-8.000	11
0.2551E 02 TIME	MODE1	-73.675	-60.439	-35.436	-16.213	-14.687	-13.570	-12.657	-11.802	-10.015	-8.000	11
0.2801E 02 TIME	MODE1	-46.246	-65.378	-37.264	-17.113	-15.278	-13.899	-12.792	-11.815	-9.963	-8.000	11
0.3051E 02 TIME	MODE1	-77.468	-68.252	-41.804	-17.918	-15.891	-14.294	-13.178	-11.903	-9.949	-8.000	11
0.3301E 02 TIME	MODE1	-48.106	-69.951	-43.460	-18.664	-16.480	-14.720	-13.279	-12.052	-9.972	-8.000	11
0.3551E 02 TIME	MODE1	-98.417	-70.791	-44.565	-19.236	-17.027	-15.117	-13.540	-11.241	-10.026	-8.000	11
0.3801E 02 TIME	MODE1	-98.674	-71.657	-45.339	-17.849	-17.526	-15.560	-13.774	-12.462	-10.104	-8.000	11

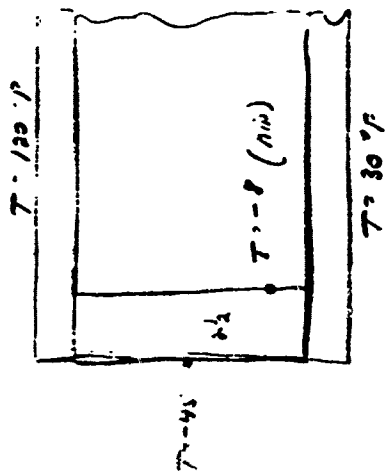
0.4051E 02 TIME	-18.286 NODE1	-72.163 2	-45.023 3	-20.311 4	-17.983 5	-15.954 6	-14.209 7	-12.697 8	-10.200 9	-8.000 10	11
0.4301E 02 TIME	-17.162 NODE1	-72.014 2	-46.412 3	-20.783 4	-18.404 5	-16.327 6	-14.519 7	-12.937 8	-10.307 9	-8.000 10	11
0.4551E 02 TIME	-19.938 NODE1	-73.093 2	-46.805 3	-21.131 4	-18.795 5	-16.679 6	-14.819 7	-13.177 8	-10.420 9	-8.000 10	11
0.4801E 02 TIME	-100.740 NODE1	-73.652 2	-47.323 3	-21.574 4	-19.161 5	-17.014 6	-15.108 7	-13.412 8	-10.536 9	-8.000 10	11
0.5051E 02 TIME	-101.760 NODE1	-74.326 2	-47.815 3	-21.941 4	-19.310 5	-17.332 6	-15.385 7	-13.641 8	-10.655 9	-8.000 10	11
0.5301E 02 TIME	-103.049 NODE1	-75.154 2	-48.366 3	-22.298 4	-19.846 5	-17.638 6	-15.553 7	-13.863 8	-10.767 9	-8.000 10	11
0.5551E 02 TIME	-104.670 NODE1	-76.155 2	-48.992 3	-22.654 4	-20.173 5	-17.934 6	-15.911 7	-14.077 8	-10.878 9	-8.000 10	11
0.5801E 02 TIME	-106.292 NODE1	-77.294 2	-49.700 3	-23.011 4	-20.497 5	-18.224 6	-16.162 7	-14.185 8	-10.986 9	-8.000 10	11
0.6051E 02 TIME	-107.515 NODE1	-78.371 2	-50.427 3	-23.370 4	-20.821 5	-18.509 6	-16.408 7	-14.488 8	-11.092 9	-8.000 10	11
0.6302E 02 TIME	-108.269 NODE1	-79.234 2	-51.098 3	-23.727 4	-21.141 5	-18.792 6	-16.651 7	-14.687 8	-11.195 9	-8.000 10	11
0.6552E 02 TIME	-108.058 NODE1	-79.729 2	-51.630 3	-24.064 4	-21.455 5	-19.071 6	-16.889 7	-14.882 8	-11.295 9	-8.000 10	11
0.6802E 02 TIME	-106.005 NODE1	-79.479 2	-51.882 3	-24.378 4	-21.753 5	-19.340 6	-17.122 7	-15.073 8	-11.374 9	-8.000 10	11
0.7052E 02 TIME	-108.81 NODE1	-79.14 2	-51.039 3	-24.611 4	-22.014 5	-19.592 6	-17.375 7	-15.149 8	-11.490 9	-8.000 10	11
0.7302E 02 TIME	-67.546 NODE1	-64.916 2	-47.619 3	-24.553 4	-22.154 5	-19.792 6	-17.576 7	-15.411 8	-11.504 9	-8.000 10	11
0.7552E 02 TIME	-44.379 NODE1	-51.115 2	-41.703 3	-24.124 4	-22.075 5	-19.878 6	-17.072 7	-15.38 8	-11.672 9	-8.000 10	11
0.7802E 02 TIME	-23.537 NODE1	-37.175 2	-35.065 3	-23.321 4	-21.734 5	-19.800 6	-17.746 7	-15.691 8	-11.749 9	-8.000 10	11
0.8052E 02 TIME	-5.979 NODE1	-24.670 2	-27.873 3	-22.230 4	-21.145 5	-19.541 6	-17.680 7	-15.725 8	-11.803 9	-8.000 10	11
0.8302E 02 TIME	7.834 NODE1	-13.754 2	-21.119 3	-20.953 4	-20.355 5	-19.108 6	-17.486 7	-15.672 8	-11.827 9	-8.000 10	11
0.8552E 02 TIME	16.504 NODE1	-4.250 2	-15.250 3	-17.420 4	-17.420 5	-15.533 6	-17.163 7	-15.526 8	-11.814 9	-8.000 10	11
0.8802E 02 TIME	21.336 NODE1	2.240 2	-10.560 3	-18.238 4	-18.427 5	-17.854 6	-16.746 7	-15.290 8	-11.759 9	-8.000 10	11
0.9001E 00 TIME	22.392 NODE1	5.917 2	-7.231 3	-16.971 4	-17.417 5	-16.114 6	-16.244 7	-14.777 8	-11.663 9	-8.000 10	11
0.9001E 01 TIME	18.689 NODE1	1.071 2	-5.290 3	-15.851 4	-16.451 5	-16.355 6	-15.691 7	-14.601 8	-11.528 9	-8.000 10	11

0.5501E 01 TIME	11.989 NODE1	5.330 2	-4.752 3	-14.924 4	-15.578 5	-15.617 6	-15.117 7	-14.186 8	-11.263 9	-8.000 10	11
0.8002E 01 TIME	2.079 NODE1	1.111 2	-5.514 3	-14.227 4	-14.835 5	-14.416 6	-14.552 7	-13.753 8	-11.174 9	-8.000 10	11
0.1050E 02 TIME	-10.810 NODE1	-4.440 2	-7.673 3	-13.784 4	-14.252 5	-14.343 6	-14.024 7	-13.324 8	-10.972 9	-8.000 10	11
0.1300E 02 TIME	-25.641 NODE1	-12.442 2	-10.916 3	-13.609 4	-13.854 5	-13.863 6	-13.555 7	-12.912 8	-10.768 9	-8.000 10	11
0.1550E 02 TIME	-42.182 NODE1	-22.383 2	-15.154 3	-13.704 4	-13.652 5	-13.516 6	-13.167 7	-12.556 8	-10.569 9	-8.000 10	11
0.1800E 02 TIME	-56.261 NODE1	-17.200 2	-20.038 3	-14.056 4	-13.654 5	-13.315 6	-12.876 7	-12.252 8	-10.388 9	-8.000 10	11
0.2050E 02 TIME	-70.663 NODE1	-41.757 2	-25.036 3	-14.608 4	-13.839 5	-13.261 6	-12.693 7	-12.021 8	-10.230 9	-8.000 10	11
0.2301E 02 TIME	-86.780 NODE1	-52.012 2	-30.290 3	-15.333 4	-14.187 5	-13.349 6	-12.619 7	-11.869 8	-10.104 9	-8.000 10	11
0.2551E 02 TIME	-93.674 NODE1	-60.437 2	-35.433 3	-16.209 4	-14.683 5	-13.567 6	-12.653 7	-11.799 8	-10.013 9	-8.000 10	11
0.2801E 02 TIME	-96.244 NODE1	-65.376 2	-39.262 3	-17.109 4	-15.275 5	-13.896 6	-12.787 7	-11.812 8	-9.961 9	-8.000 10	11
0.3051E 02 TIME	-97.467 NODE1	-68.250 2	-41.802 3	-17.935 4	-15.888 5	-14.293 6	-13.006 7	-11.906 8	-9.935 9	-8.000 10	11
0.3301E 02 TIME	-98.105 NODE1	-69.248 2	-41.458 3	-18.661 4	-16.477 5	-14.718 6	-13.277 7	-12.049 8	-9.971 9	-8.000 10	11
0.3551E 02 TIME	-98.436 NODE1	-70.979 2	-44.562 3	-19.293 4	-17.024 5	-15.144 6	-13.578 7	-12.241 8	-10.026 9	-8.000 10	11
0.3801E 02 TIME	-98.677 NODE1	-71.656 2	-45.336 3	-19.846 4	-17.524 5	-15.558 6	-13.892 7	-12.461 8	-10.104 9	-8.000 10	11
0.4051E 02 TIME	-98.985 NODE1	-72.162 2	-45.922 3	-20.337 4	-17.981 5	-15.952 6	-14.207 7	-12.695 8	-10.290 9	-8.000 10	11
0.4301E 02 TIME	-99.381 NODE1	-72.612 2	-46.410 3	-20.780 4	-18.402 5	-16.324 6	-14.517 7	-12.936 8	-10.307 9	-8.000 10	11
0.4551E 02 TIME	-99.937 NODE1	-73.092 2	-46.863 3	-21.189 4	-18.793 5	-16.677 6	-14.817 7	-13.175 8	-10.420 9	-8.000 10	11
0.4801E 02 TIME	-100.739 NODE1	-73.651 2	-47.321 3	-21.572 4	-19.159 5	-17.012 6	-15.106 7	-13.411 8	-10.535 9	-8.000 10	11
0.5051E 02 TIME	-101.760 NODE1	-74.125 2	-47.113 3	-21.739 4	-19.508 5	-17.330 6	-15.364 7	-13.640 8	-10.653 9	-8.000 10	11
0.5301E 02 TIME	-103.048 NODE1	-75.153 2	-48.166 3	-22.297 4	-19.844 5	-17.636 6	-15.652 7	-13.862 8	-10.766 9	-8.000 10	11
0.5551E 02 TIME	-104.679 NODE1	-76.154 2	-48.991 3	-22.652 4	-20.172 5	-17.931 6	-15.911 7	-14.016 8	-10.977 9	-8.000 10	11
0.5801E 02 TIME	-106.241 NODE1	-77.193 2	-49.644 3	-23.009 4	-20.496 5	-18.222 6	-16.162 7	-14.285 8	-10.986 9	-8.000 10	11

0.6051E 02 TIME	-107.595 MODEL	-78.370 2	-50.426 3	-23.370 4	-20.020 5	-18.501 6	-16.408 7	-14.498 8	-11.017 9	-8.000 10	11
0.6302E 02 TIME	-130.770 MODEL	-79.733 2	-51.076 3	-25.776 4	-21.181 5	-18.791 6	-16.650 7	-14.687 8	-11.195 9	-8.000 10	11
0.6552E 02 TIME	-100.059 MODEL	-79.728 2	-51.629 3	-24.067 4	-21.454 5	-19.070 6	-16.888 7	-14.882 8	-11.295 9	-8.000 10	11
0.6802E 02 TIME	-106.066 MODEL	-77.679 2	-51.881 3	-24.377 4	-21.752 5	-19.339 6	-17.122 7	-15.073 8	-11.394 9	-8.000 10	11
0.7052E 02 TIME	-89.050 MODEL	-77.072 2	-51.038 3	-24.599 4	-22.012 5	-19.591 6	-17.345 7	-15.259 8	-11.490 9	-8.000 10	11
0.7302E 02 TIME	-67.545 MODEL	-64.044 2	-47.617 3	-24.552 4	-22.153 5	-19.791 6	-17.546 7	-15.435 8	-11.594 9	-8.000 10	11
0.7552E 02 TIME	-44.379 MODEL	-51.014 2	-41.056 3	-24.123 4	-22.074 5	-19.877 6	-17.691 7	-15.586 8	-11.672 9	-8.000 10	11
0.7802E 02 TIME	-23.536 MODEL	-37.174 2	-35.064 3	-24.322 4	-21.733 5	-19.793 6	-17.747 7	-15.691 8	-11.748 9	-8.000 10	11
0.8052E 02 TIME	-5.973 MODEL	-10.570 2	-27.072 3	-22.229 4	-21.144 5	-19.540 6	-17.674 7	-15.725 8	-11.833 9	-8.000 10	11
0.8302E 02 TIME	7.034 MODEL	-13.254 2	-21.113 3	-20.952 4	-20.354 5	-19.108 6	-17.485 7	-15.672 8	-11.827 9	-8.000 10	11
0.8552E 02 TIME	16.504 MODEL	-4.250 2	-15.250 3	-19.591 4	-19.426 5	-18.533 6	-17.168 7	-15.526 8	-11.814 9	-8.000 10	11
0.8802E 02 TIME	21.396 MODEL	2.240 2	-10.560 3	-18.134 4	-18.426 5	-17.854 6	-16.746 7	-15.290 8	-11.759 9	-8.000 10	11
0.9052E 02 TIME	26.111 MODEL	7.111 2	-6.111 3	-16.771 4	-17.411 5	17.111 6	-16.244 7	-14.011 8	-11.663 9	-8.000 10	11
0.9302E 01 TIME	18.689 MODEL	6.871 2	-5.289 3	-15.950 4	-16.451 5	-16.354 6	-15.691 7	-14.601 8	-11.528 9	-8.000 10	11
0.9502E 01 TIME	11.799 MODEL	5.311 2	-4.752 3	-14.673 4	-15.574 5	-15.617 6	-15.117 7	-14.106 8	-11.363 9	-8.000 10	11
0.9802E 01 TIME	2.077 MODEL	1.412 2	-5.283 3	-14.127 4	-14.935 5	14.136 6	-14.327 7	-13.753 8	11.174 9	-8.000 10	11
0.1050E 02 TIME	-10.810 MODEL	-4.939 2	-7.072 3	-13.783 4	-14.257 5	-14.343 6	-14.024 7	-13.324 8	-10.972 9	-8.000 10	11
0.1300E 02 TIME	-25.640 MODEL	-17.041 2	-10.916 3	-13.609 4	-13.853 5	-13.863 6	-13.554 7	-12.919 8	-10.768 9	-8.000 10	11
0.1550E 02 TIME	-42.187 MODEL	-22.111 2	-15.114 3	-13.777 4	-13.657 5	-13.516 6	-13.167 7	-12.556 8	-10.569 9	-8.000 10	11
0.1800E 02 TIME	-56.261 MODEL	-32.200 2	-20.037 3	-14.056 4	-13.654 5	-13.315 6	-12.876 7	-12.252 8	-10.388 9	-8.000 10	11

11.45.57 DURATION 00.05.11 04/08/70

W. 11.45.57
R. 10.00.00
P. 11.45.57



26' 1.000 26 36.5.24 1" F. 1000

11.45.57 10.00.00 10.00.00



APPENDIX V

DETERMINATION OF ORGANIC OFF-GASSING PRODUCTS AND
CARBON MONOXIDE FOR DO21 AIRLOCK NONMETALLIC MATERIALS

30 June 1967

Subject: DETERMINATION OF ORGANIC OFF-GASSING PRODUCTS AND
CARBON MONOXIDE FOR D021 AIRLOCK NONMETALLIC MATERIALS

A. SUMMARY

Tests were made on the D021 nonmetallic composite wall material and its component layers under vacuum conditions (10^{-6} TORR) to evaluate weight loss due to off-gassing effect. An initial off-gassing is encountered, resulting from boil-off of plasticizers and volatile solvents, with a negligible weight loss, which subsequently levels off. Curves of off-gassing versus time are shown in Figures 61 thru 65.

Tests were also made to determine what level of toxic by-products, such as those used in the pressure bladder face ply materials, are given off while under the deployment environment of 5 psia O_2 atmosphere. A survey of toxic materials known to be used in the pressure bladder face ply construction was made, and found to be halogenated hydrocarbons (methylene chloride), aromatic hydrocarbons (toluene, xylene), ketones (MEK) and toluene-diisocyanate (TDI).

Tests were also made for carbon monoxide. The test procedure for collecting traces of toxic gases was to place the test material in a pressure vessel that was evacuated and subsequently pressurized to 5 psia with O_2 at 155 degrees F. The test material was exposed for 24 hours prior to chemical analysis of the toxic gases. The test values were determined using a Mine Safety Appliances Company Universal colorimeter type tester for all constituents tested, except TDI, for which test a Uni-Jet Air Sampler (Union Industrial Equipment Corporation) was used for determining the presence of TDI.

2-10-55(7-44)(77-23)
REF. ENGINEERING PROCEDURE 5-017

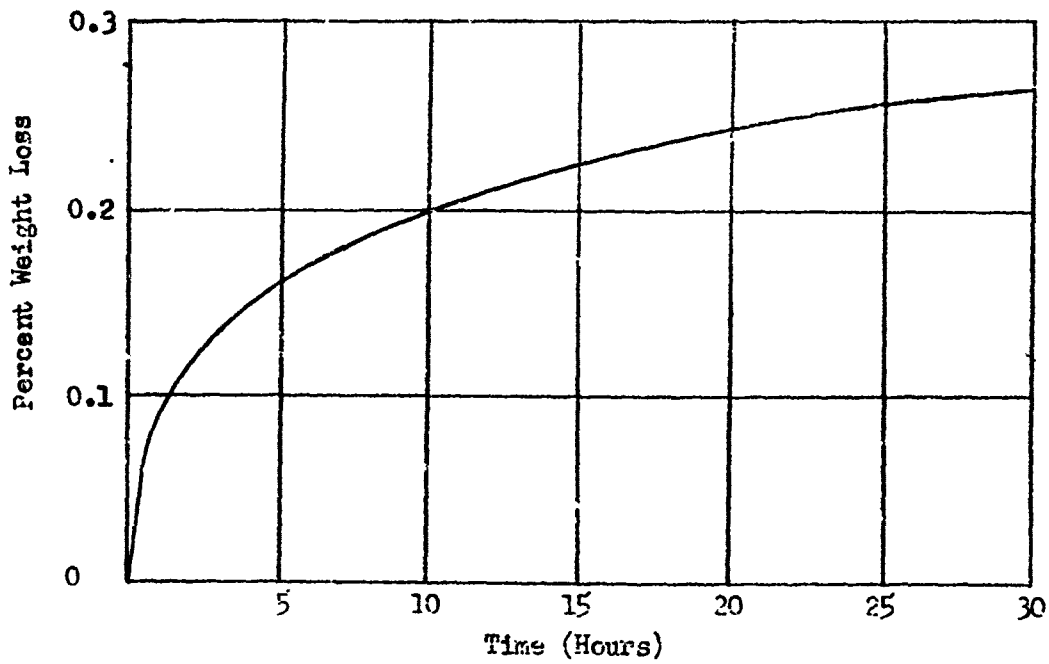


Figure 61. Composite Wall Off-Gassing

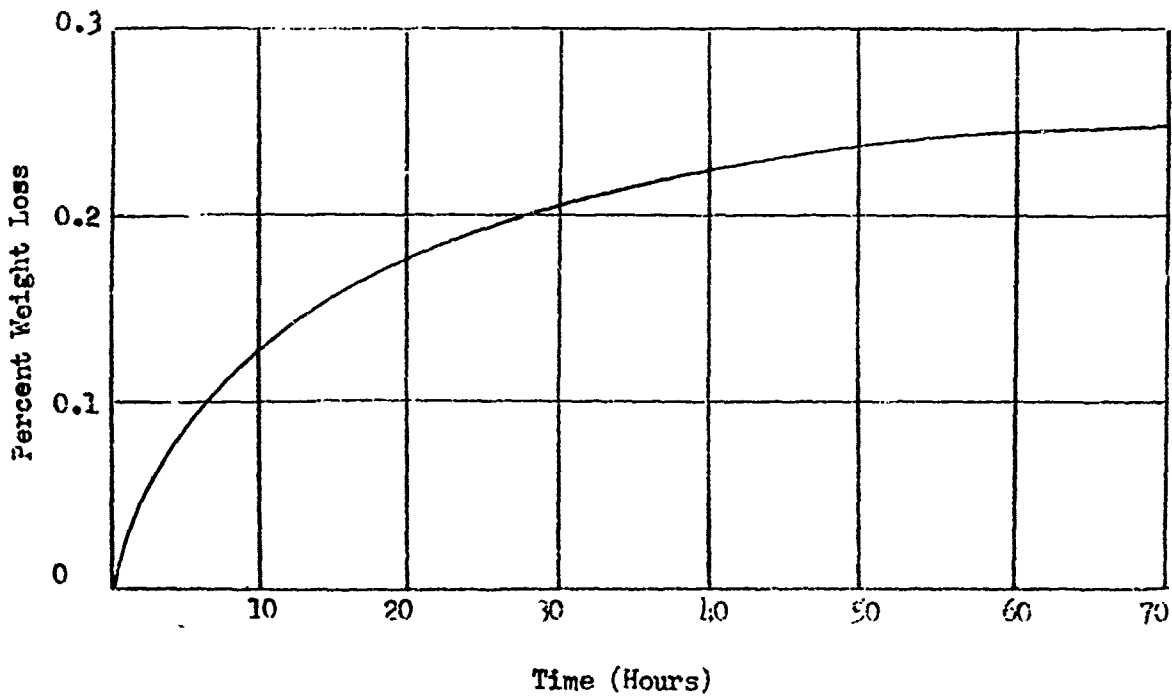


Figure 62. Pressure Bladder Off-Gassing

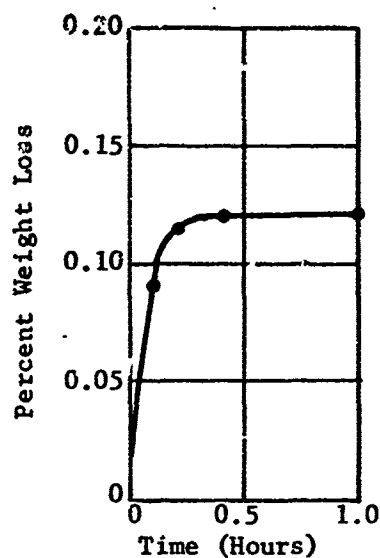


Figure 63. Polyester Film Off-Gassing

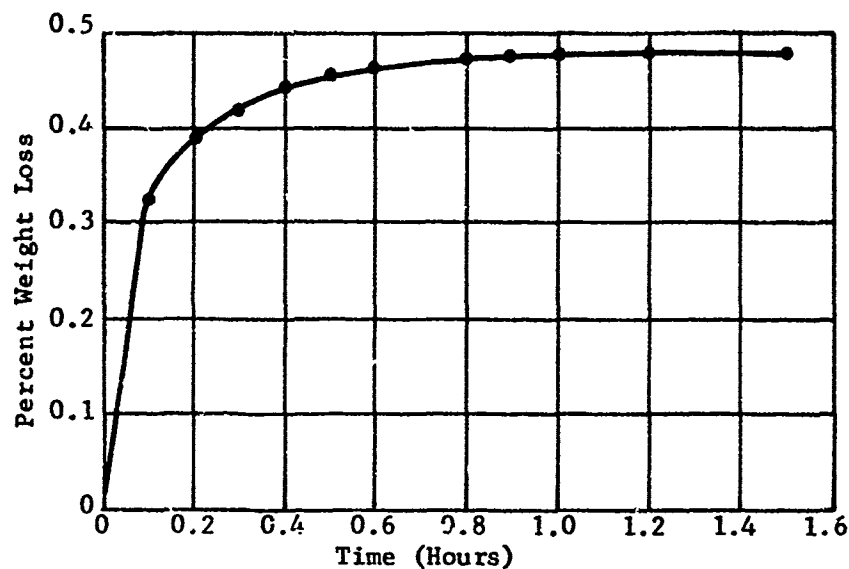


Figure 64. Polyether Foam Off-Gassing

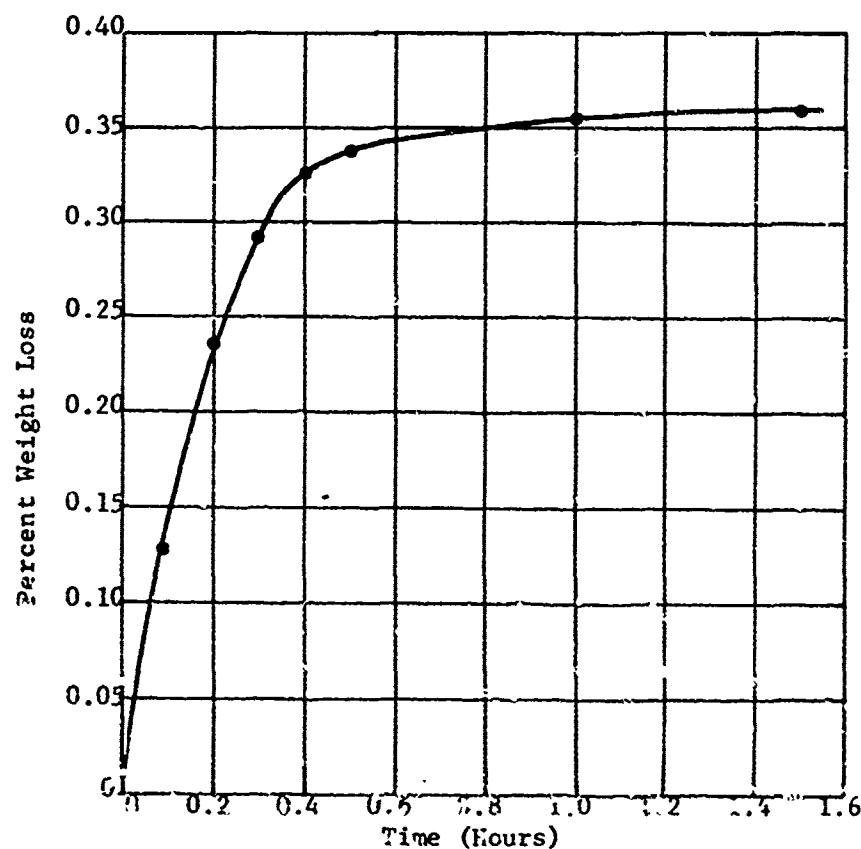


Figure 65. Outer Cover Off-Gassing

B. REPORTING DATA - TOXIC BY-PRODUCTS

1. Type of Material - Test material consisting of pressure bladder face ply (Laminated nylon film, nylon fabric and aluminum foil with ALODINE thermal coating. Interplies laminated with polyester adhesive).
2. Material Usage - Pressure bladder face ply. Aluminum foil ALODINE coated side is exposed to the oxygen pressure. There is approximately 77 square feet of pressure bladder surface area. Airlock expanded volume is approximately 78 ft³. The pressure bladder face ply maximum service temperature is 100 degrees F.
3. Test Material - The test for determination of toxic by-products was conducted on a test sample of pressure bladder face ply material measuring 12 inches square and tested in a chamber of 0.4 ft³.

4. <u>Test Results</u>	TEST CHAMBER	AIRLOCK
	<u>PPM-ft³/ft²</u>	<u>PPM</u>
Carbon Monoxide	2	2
Halogenated Hydrocarbons	0	0
Aromatic Hydrocarbons	20	20
Ketones	12	12
Toluene-Diisocyanate	.004	.004

C. D021 COMPOSITE MATERIAL SUMMARY

<u>ITEM</u>	<u>TYPE</u>
1. Pressure Bladder	
a. Face Ply	
Thermal Coating	ALODINE
Foil Flame Barrier	Alumirum
Fabric	Nylon
Film	Nylon
b. Foam	EPT
c. Face Ply	
Film	Nylon
Fabric	Nylon
2. Structural Layer	
Filament Wire	Stainless Steel
Filament Yarn	Rayon
3. Micrometeoroid Layer	
Foam	Polyether
4. Outer Cover	
Film	Nylon
Fabric	Nylon
Thermal Coating	Aluminized Silicone
5. Interply Adhesive Layers	Polyester

Prepared by:

K. L. Gordier
 K. L. Gordier
 Materials Technology, D/457-G

KLC/het

APPENDIX VI

DO21 AIRLOCK NONMETALLIC MATERIALS COMPLIANCE
WITH ASPO-RQTD-D67-5A (MAY 3, 1967)

14 August 1967

ENGINEERING MEMORANDUM

- Subject: D-21 Airlock Nonmetallic Materials Compliance
With ASPO-RQTD-D67-5A (May 3, 1967)
- Reference: (1) Apollo Spacecraft Program Office,
Nonmetallic Materials Selection Guidelines,
ASPO-RQTD-D67-5A, dated May 3, 1967.
- (2) Procedures and Requirements for the
Evaluation of Spacecraft Nonmetallic Materials,
MSC-A-D-66-3-Rev.-A, dated June 5, 1967

A. GENERAL

The D-21 Airlock Experiment is an in-orbit evaluation of the expandable structures technique applied to an airlock design. The experiment D-21 Airlock package is externally mounted in the uninhabited portion of the NASA Airlock Module, as a corollary experiment aboard the S-IV-B Spent Stage Orbital Workshop, Saturn-Apollo Flight 209.

To interpret the Reference (1) document with regard to the D-21 structure, requires a definition of the elements involved. The interior of the D-21 Airlock is an aluminum foil shell. Outside of this aluminum shell is an atmosphere-retaining pressure bladder. The aluminum shell and pressure bladder are surrounded by a structural filament-wound cage. This basic structure is protected from thermal and micrometeoroid effects by a layer of foam and an external thermal cover.

Review of the Reference (1) document in regard to categorizing the D-21 Airlock nonmetallic materials according to their usage, indicates the materials should qualify in accordance with the test requirements of usage Category "H", titled "Materials in Uninhabited Portions of the Spacecraft."

Goodyear Aerospace Corporation in-house tests of the D-21 nonmetallic materials were made in accordance with the test requirements of Reference (2), Test No. 1, and successfully met the criteria of acceptability that major exposed materials be self-extinguishing in air.

B. REPORTING DATA

The following data are submitted in accordance with the procedures defined in Reference (2), Section 9.0 of Test No. 1.

1. D-21 Composite Material Summary

<u>USAGE</u>	<u>NAME (GENERIC)</u>	<u>MFGS. CODE</u>	<u>MANUFACTURER</u>
<u>Pressure Bladder</u>			
Thermal Coating	ALODINE	407/47	Anchem Prod.
Foil Flame Barrier	Aluminum	1100-0	Alcoa
Fabric	Nylon	A4787	Stern & Stern
Film	Nylon	Capran 77C	Allied Chemical
Foam	EPT	R481T	Rubatex
<u>Structural Layer</u>			
Filament Wire	Stainless Steel	T-302	National Standard
Filament Yarn	Rayon	Taslan	Kahn & Feldman
<u>Micrometeoroid Layer</u>			
Foam	Polyether	UU44FR	Bernel Foam Prod.
<u>Outer Cover</u>			
Film	Nylon	Capran 77C	Allied Chemical
Fabric	Nylon	A4787	Stern & Stern
Thermal Coating	Aluminized Silicone	80U	Ball Brs. Res.
<u>Interply Adhesive Layers</u>			
Coating	Neoprene	1473C	Goodyear
Coating	Polyester	AD917	Goodyear

2. D-21 Expandable Material Physical Characteristics

Total Nonmetallic Material	39.5 pounds
Packaged Volume (Launch)	17.5 cubic feet
Expanded Volume (Orbit)	78.0 cubic feet
Surface Area (Expanded)	77.0 square feet
Maximum Service Temperature	100° F.

3. Self Extinguishing In Air - Yes.

4. Combustion Characteristics

Four configurations of the D-21 nonmetallic composite wall material were tested and in all instances, as illustrated in Figures 66 through 69, the material proved self-extinguishing with negligible flame progression.

5. Test Procedure

Self-extinguishing in air criteria was demonstrated for four configurations of the D-21 nonmetallic composite wall material when tested in accordance with Reference (2) requirements for sample size and ignition source.

Figure 66 illustrates a test sample simulation of the material packaged configuration. A vertical sample, two inches wide by five inches long, held by vertically mounted steel clamps, was ignited at the bottom of the test specimen.

Figure 67 illustrates a test sample simulation of the material deployed configuration. A vertical sample, two inches wide by five inches long, was held in a relaxed condition when ignited at the bottom of the test specimen.

Figure 68 illustrates a test sample where the ignition source was applied at an area with one-inch slits cut through the outer cover.

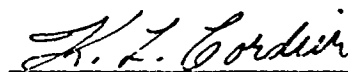
Figure 69 illustrates a test sample where the ignition source was applied at an area with one-inch slits cut through the film-fabric face ply of the pressure bladder.

The figures show the test sequence before, during, and after ignition.

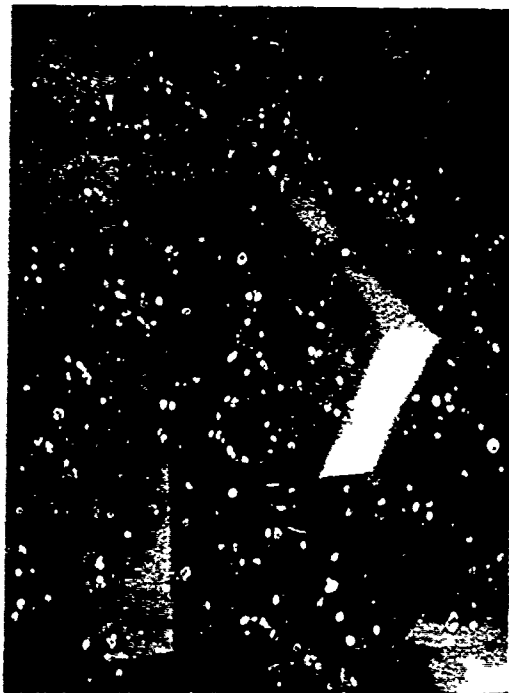
6. Date of Test

August 10, 1967.

7. Tests conducted by GAC Advanced Material Laboratory.

A handwritten signature in cursive script, reading "K. L. Cordier", is written over a horizontal line.

K. L. Cordier, D/457



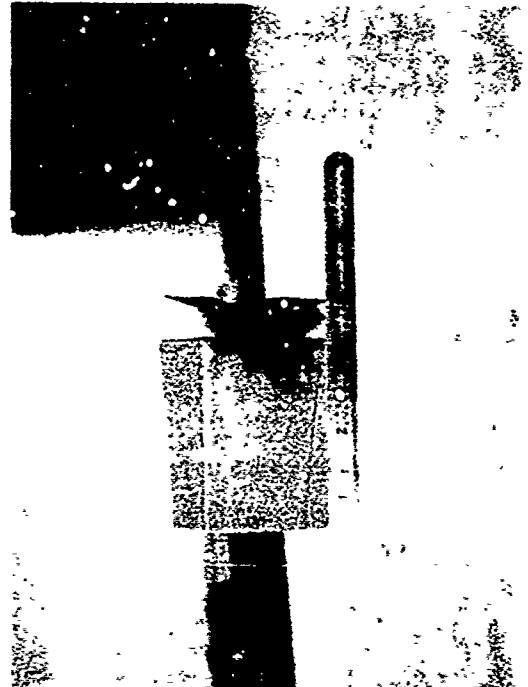
(A)



(B)



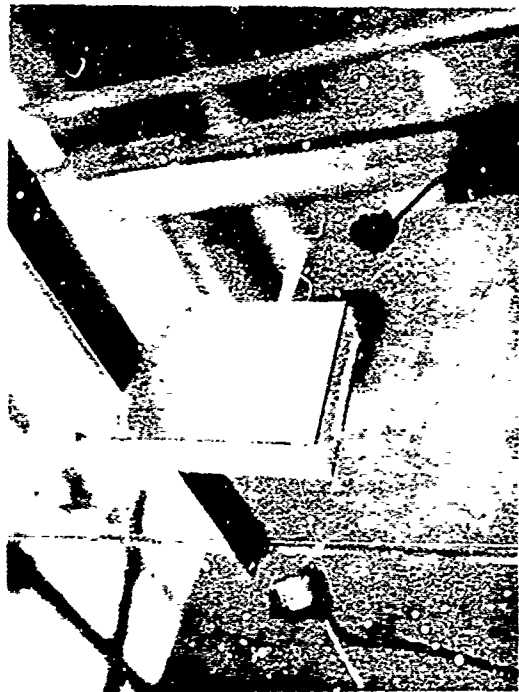
(C)



(D)



(A)



(B)

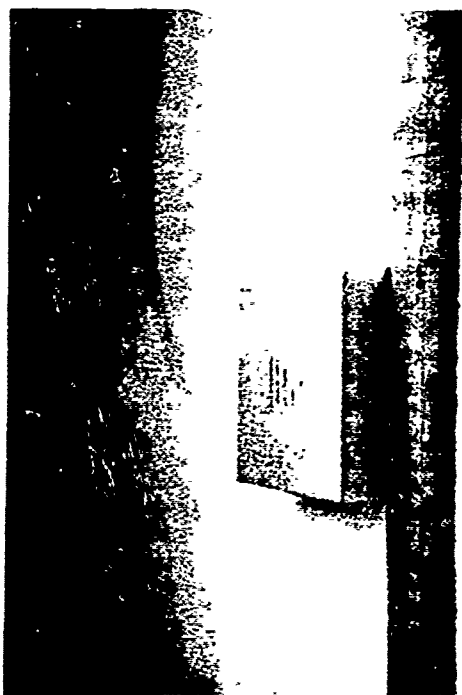


(C)



(D)

Figure 67. D-21 Composite Wall Flammability Test (Upward) - Deployed Configuration



(A)



(B)



(C)

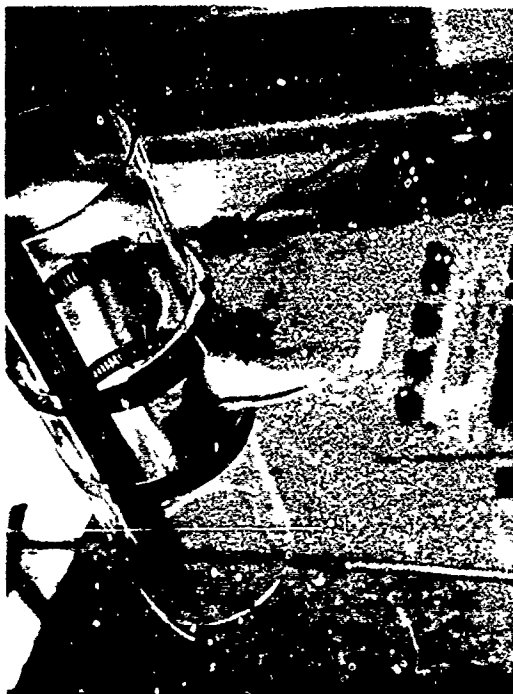


(D)

Figure 68. D-21 Composite Wall Flammability Test (Outer Cover Side)



(A)



(B)



(C)

Figure 69.. D-11 Composite Wall Flammability Test (Pressure Bladder Side)

APPENDIX VII

LEAK TEST CALCULATIONS

LEAK TEST CALCULATIONS

A test was conducted to determine the amount of leakage from the D-21 Airlock configuration in a 24-hour period. From the results of that test, a calculation was made to determine the amount of leakage to be expected under vacuum conditions.

The test was conducted at an internal pressure of 36.363 in/Hg at the beginning of the 24-hour period and ended with an internal pressure of 36.291 in/Hg. The initial outside pressure was 29.243 in/Hg and at the end of test this pressure was 29.311 in/Hg. The amount of nitrogen that escaped during this 24-hour period was calculated to be 0.013 lb.

The area available for leakage was calculated from the following equation:

$$A_L = \frac{\dot{u}}{\dot{u}/A_L} \quad (1)$$

where

$$\begin{aligned} \dot{u} &= \text{leak rate, lb/sec} \\ A_L &= \text{leak area, in.}^2 \end{aligned}$$

The leak rate per unit leak area was calculated from the following equation:

$$\frac{\dot{u}}{A_L} = \frac{P_1}{R} \sqrt{2 g J} \left\{ \frac{C_D}{F_1} \left[\frac{P_X}{F_1} \right]^{2/k} - \left(\frac{P_X}{P_1} \right)^{\frac{k+1}{k}} \right\}^{1/2} \quad (2)$$

where

$$\begin{aligned} p_1 &= \text{internal pressure} \\ p_X &= \text{outside pressure} \\ R &= \text{Nitrogen gas constant, 55.16 ft lb/lb-}^\circ\text{F} \end{aligned}$$

- g = gravitational constant, 32.2 ft/sec^2
 J = heat equivalent, $778 \text{ ft} \cdot \text{lb/BTU}$
 C_p = specific heat of nitrogen, $0.247 \text{ BTU/lb} \cdot ^\circ\text{R}$
 k = ratio of specific heats, 1.4

Solving equation (2) yields a flow rate per unit leak area of

$$\frac{\dot{w}}{A_L} = 0.327 \text{ lb/sec} \cdot \text{in}^2$$

Equation (1) then yields a leak area of

$$A_L = 4.63 \times 10^{-7} \text{ in}^2$$

In a vacuum, where the outside pressure is near zero, the following equation defines the leak rate per unit leak area:

$$\frac{\dot{w}}{A_L} = \frac{p_1 g k \sqrt{\frac{k+1}{k-1}} (2/k + 1)}{\sqrt{g k R T_1}} \quad (3)$$

Solving equation (3) for the leak rate per unit leak area yields

$$\frac{\dot{w}}{A_L} = .0785 \text{ lb/sec} \cdot \text{in}^2$$

In a 24-hour period, the weight loss was calculated to be

$$w = 0.0031 \text{ lb.}$$

on a volume flow rate basis

$$Q = \frac{\dot{w}}{F} \quad (4)$$

The volume flow rates are equal for both cases, estimated to be 11 CFM. The difference in the two weight losses are entirely due to the density of the two situations. In the laboratory, the gas was contained at about 17.8 psia while in a vacuum, the gas pressure is expected to be 3.5 psia, thus for the same contained volume and temperature, the densities are considerably different.

APPENDIX VIII

FAILURE ANALYSIS AND CORRECTIVE ACTION REPORT

Reference GAC Failure Action Report - Serial No. 75773

Corrective Action

The following corrective action has been taken on the Qualification Test Unit and will also be incorporated on the flight units prior to delivery.

1. The terminal board connectors have been re-examined and meticulously cleaned. Conformal coating has been added to cover all exposed solder terminals.
2. The instrumentation box wire harness was removed, cleaned and reinstalled. All exposed solder connections were conformally coated.
3. All unused printed circuit card connectors were potted.
4. Three unused detector board assemblies (2 of 66QS1497-105 and one of 66QS1497-101) were removed to reduce load on the 12 Volt power supply.
5. Defective Electra RN55D type resistors have been replaced with RNR55C type resistors.
6. Conformal coatings on the printed circuit boards have been stripped and new coatings reapplied in strict compliance with GAC Process Specification E-11 Type III conformal coating application procedure.
7. An electrical load analysis shows the maximum current drain on either the plus or minus 12 Volt terminals of the power supply to be 100 ma. This is 66 percent of the 150 ma rating of the power supply. No action required.

8. The corroded areas on the metal shell were due to loss of surface protective coating during several disassembly and assembly operations. Surface areas were buffed to remove corrosion and alodine coatings reapplied.
9. Subsequent to the above corrective action, the 66QSL502-101 Instrumentation Box Assembly was subjected to the 10-day temperature and humidity environments in accord with GER-13088B paragraph 4.0. Unit was found to be in excellent mechanical and electrical condition after this exposure.

L. Manning

L. Manning
Project Engineer
D-21 Airlock
Department 453

FAILURE ANALYSIS REPORT

RETURN TO DEPT. 479

GOODYEAR AEROSPACE

CORPORATION

AKRON, OHIO 44318

PHOTOGRAPHS ☒ TEST ANALYSIS REPORT ☒ X-rays ☒ Vendor F/A ☒ 205
MFR: Mil Associates Inc. STR NO. 7,5,7,7,3
MARKINGS: Mil Associates Inc. Hudson, New Hampshire, Low Voltage Supply (Airlock)
Serial Number 293, Model LV-12, Input 28V + 3V output -12V, common, +12V.
NCR: 66Q51502-101 Instrumentation Box failed ETI-GA597-21, section 1, para. 2A.
There was no 12V output after the ten (10) day humidity test.

Analysis: The failure was verified. The power supply had been returned to the vendor for Failure Analysis (see NCR 75776). The vendor's report (S/N 00216) dated 2-14-69 stated that the discrepancy was the result of an overload external to the supply or a random failure of Q5.

The supply was returned to GAC for further analysis.

The emitter leads of Q3 & Q5 were fused. The emitter wire of Q3 was almost totally disintegrated. The wire of Q5 was fused open but stayed in place (see attached photographs).

The Instrumentation Assembly, test circuits and the wiring were examined to determine the possibility of an external overload being applied to the failed supply.

The following observations, pertinent to the power supply failure, are noted:

- 1) The Instrumentation Assembly circuit board's passivation coating was bubbled.
- 2) The boards had an accumulation of flux contamination that had caused formation of some corrosion.
- 3) The load currents of the failed power supply were not monitored during the post environmental tests.

Continued on Page 2 and 3

BY ES Zeigler DATE 4-4-69

RECOMMENDED ACTION 1) Engineering/Tech Service to investigate the integrity of the passivation coating used on the boards. 2) QC to check the board cleaning procedures and make sure the process is adequate. 3) The test specification GA597-21 should be changed to require adequate monitoring of the test system to allow isolation of failure inducing discrepancies. 4) All Electra resistors type RN55D should be replaced with RNR types to MIL-R-55182 ($\lambda=S$). 5) Use a conformal coating to protect the connector terminations from moisture. 6) Engineering to conduct an analysis of the loading of the +12V supply. The supply should be operating at approximately 66% of its rated output current.

BY JJ Droll DATE 4-4-69

CORRECTIVE ACTION

BY L. Manning

DATE 5/19/69

DISTRIBUTION:

L. Manning (6)
M. Lahr
R. Nuss
W. Murray

CORRECTIVE ACTION

PART NAME

PART SERIAL NO.

POWER SUPPLY

293

PART VENDOR

PART DWG. NO.

MIL ASSOCIATES

LV12-12

REFERENCE DESIGNATION

FAILURE CLASSIFICATION

SECONDARY FAILURE

- 4) The instrumentation package was oscillating. The oscillation ($\approx 50\text{KC}$) were feeding back into the power supply. It was noted that the current drain increased approximately 40% during the periods of oscillation. Current during oscillation was 140 ma and 80 to 100 ma with no oscillations.
- 5) A globule of solder was partially bridging the + and - 12 volt connector terminals in the instrumentation package. An accumulation of corrosion was noted around the solder bridge.

The wiring harness (including the connectors) was tested separately to determine the loading it presents to the + 12 VDC supply (see item 5 above).

Although the solder bridge was probed and the oscillations stopped, the open circuit current of the + and - 12 v supply harness was 5 to 15 ma after ≈ 2 hours at temperature and humidity.

- 6) The pH of the water used in the humidity test was 6.95 (if the pH is 7.0 the hydrogen - and hydroxyl-ion concentrations are equal and the solution is neutral, pH less than 7 the solution is acid, pH greater than 7 the solution is alkaline). This however would not contribute to materials corrosion.
- 7) Ten of the instrumentation package boards did not pass the card test. Threshold levels were out of tolerance. The board failures were Electra RN55D type resistors. The resistors exhibited poor metallization adhesion to the ceramic bobbin, poor spiralling and damaged end caps.
- 8) A spare power supply S/N 313 was subjected to a temperature and humidity test to determine the capability of the supply to operate at full rated load without destroying itself by going into a thermal runaway condition. The unit operated within the procurement specification limits. The supply was operated at full rated load during the temperature and humidity test.

The results of the test are shown in the Environmental Test Lab Analysis Report.

Conclusions

- 1) The power supply apparently failed as a result of an overload. Analysis indicates that an excess current drain caused the power supply switching transistor Q5 to go into thermal runaway and eventually destroying itself and the series regulator transistor (Q3). The overload current was caused by an improperly processed solder joint and oscillations in the detector board assemblies.
- 2) The + and - 12 volt output bus lines are on adjacent terminals on the connector. The improperly processed solder joint was partially bridging these two terminals causing an additional load current to be drawn.
- 3) The detector board failures were caused by defective RN55D type resistors. The Electra RN55D type resistors that failed exhibited defects which indicated that the entire lot should be rejected. Evaluation of stock resistors (RN55D4992F) exhibited poor processing control of the element spiralling.
- 4) Evaluation of the power supply application indicates that the design is marginal. The required load current from the + 12VDC supply is 140ma. The maximum rated output current of the supply is 150 ma.
- 5) The amount of corrosion observed following the T & H test indicates that some of the materials and/or material finishes are not adequate.

Enclosure to FAR-75773
Env. Lab
4-3-69

Power Supply MIL Assoc. LV-12 S/N 313

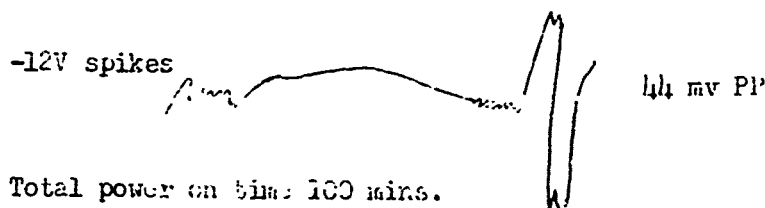
Room Ambient Temperature

Input Voltage 28 VDC
Input Current 300 ma
Output Voltage +11.999 to +12.008 @ 150 ma load
-11.505 to -11.507 @ 148 ma load
Ripple Voltage (+12V) 8 mv with 19 mv spikes
(-12V) 10 mv with 20 mv spikes
Power on Time 10 minutes
Frequency 250 KHz

Temperature 160°F (71°C) RH = 95% f_o = 250 KHz

Time(Minutes)	10	20	30	40	50	60	75	90	Units
Input Voltage	23	28	28	23	28	28	28	23	Volts
Input Current	320	330	350	355	360	360	358	353	ma dc
+12V Output	12.109	12.152	12.192	12.208	12.214	12.213	12.205	12.201	+ Volts
+12V Load I	150	150	150	150	150	150	150	150	+ ma dc
-12V Output	11.601	11.651	11.685	11.706	11.711	11.709	11.704	11.699	- Volts
-12V Load I	148	148	149	149	149	149	149	149	- ma dc
+12V Ripple	10	10	12	13	14	18	14	15	mv PP
-12V Ripple	8	8	9	9	10	11	10	11	mv PP

+12V output $\Delta E/46^{\circ}\text{C} = 206 \text{ mv}$ Spec Limit = 230 mv (5 mv/°C)
-12V output $\Delta E/46^{\circ}\text{C} = 204 \text{ mv}$ Spec Limit = 230 mv (5 mv/°C)
+12V Ripple Spec limit = 40 mv PP



Total power on time 100 mins.

FAILURE ANALYSIS REPORT

RETURN TO DEPT. 479

GOODYEAR AEROSPACE

CORPORATION

AKRON, OHIO 44315

PHOTOGRAPHS ☐ TEST ANALYSIS REPORT ☐

MFR: Electra

MARKINGS: RN55D4992F

205
STR
OTHER

NO. _____

Airlock

Resistor open

Failure verified, resistance measures ∞ .

The passivation appeared only partially accomplished and the resistive element did not adhere completely to the ceramic core of the resistor. (contamination on sub-strate).

One end cap swedged on crooked.

The end cap on the "open" end of the resistor was cut by the spiral cutting operation of the metal film and the spiral cut appeared abnormally wide at this end.

Failure mode: open resistor

Failure mechanism: film deposit and spiral cut.

BY E Zeigler DATE 3-31-69

RECOMMENDED ACTION

See FAR-75773

BY JJ Droll DATE 4-8-69

CORRECTIVE ACTION

BY _____ DATE _____

DISTRIBUTION:

CORRECTIVE ACTION

PART NAME

PART SERIAL NO.

RESISTOR-FIXED FILM

PART VENDOR

PART DWG. NO.

ELECTRA

RN55D4992F

REFERENCE DESIGNATION

FAILURE CLASSIFICATION

R

VENDOR PROCESSING

Enclosure to
FAR-75773

AIRLOCK PARTS EVALUATION

<u>Part Number</u>	<u>Part Name</u>	<u>Manufacturer</u>	<u>P.O. Number</u>	<u>R.S.</u>	<u>Qty.</u>	<u>Sample</u>
RN55D4992F	Resistor	Electra	7H1237EA			2

Markings

G.A.C. blue dot

Vendor RN55D4992F

Discrepancies, process deviations and/or general notes

external 1. hard light blue case
2. markings and leads o.k.

internal 1. passivation thin
2. ragged edges on spiral cut
3. end caps on both units on crooked

Short term overload

#1 49.693K 49.696K	#2 49.612K pre-overload 49.611.56 post-short term overload @ 208V for 5 sec.
-----------------------	---

Data part received

3-26-69

Evaluation performed by

E. S. Zeigler

M.T.C. Number

128042

Date

3-31-69

QC-015

• FAILURE REPORT FORM •

ORIGINATOR

F.R. SERIAL NO.

RAC

00216

QUALITY CONTROL

DATE OF ORIGIN

RAC.

2-14-69

ORIGINALLY Shipped on 5-17-67

PART NO.

SERIAL NO.

CUSTOMER NAME

CUSTOMER ORDER NO.

PAGE

OF

LV-12

293

Goodyear

7E1364-EA (501018)

1

1

NAME OF FAILED ITEM

DESCRIPTION OF FAILURE

Low Voltage Power Supply

No output Voltage

GIVE ENVIRONMENTAL CONDITIONS AT FAILURE TIME

Unknown

GIVE TEST CONDITIONS AT FAILURE TIME

Unknown

REPAIR OR REWORK REQUIRED TO FIX UNIT

LOCATION OF FAILURE: IN PROCESS

FINAL TEST

FIELD

Replace unit

TECHNICAL ANALYSIS OF FAILURE

- (1) Failed components Q3 and Q5 indicate that the unit failed due to a severe overload condition or an extended short circuit across the output.
- (2) A random failure of Q5 could possibly cause the failure mode experienced by the supply.

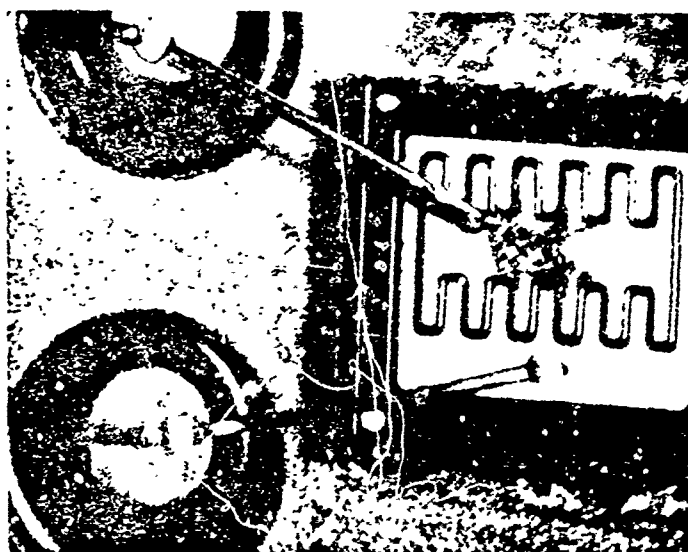
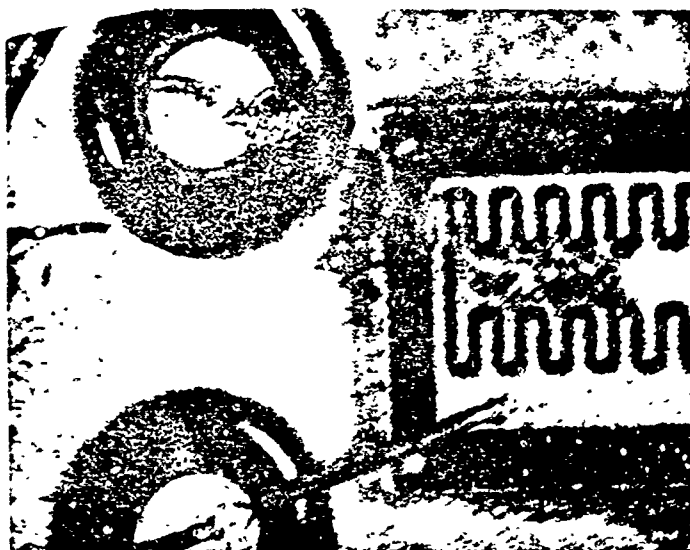
CORRECTIVE ACTION TAKEN TO PREVENT RECURRENCE OF ABOVE FAILURE

MIL ASSOC
LV-12
2-10-69
S/N 293



MIL ASSOC
LV-12
2-10-69
S/N 293





25 X

FEL. LAB. - Q.A.C.

REPORT NO. 75773

PART NO. Q3

VENDOR Selkirk Electric

MAGNIFICATION 25X

FEL. LAB. - Q.A.C.

REPORT NO. 75773

PART NO. Q5

VENDOR Selkirk Electric

MAGNIFICATION 25X

APPENDIX IX

FUNGUS, SALT FOG AND ACOUSTIC TESTS

TEST REPORT

WYLE LABORATORIES TESTING DIVISION HUNTSVILLE FACILITY, 7800 Governors Drive West, Huntsville, Alabama 35800:

Goodyear Aerospace Corporation

Akron, Ohio 44315

REPORT NO. 41062-1

OUR JOB. NO. 41062

YOUR P. O. NO. 7B0058-YX

CONTRACT E33615-67-C-1380

28 Page Report

DATE June 29, 1970

ENVIRONMENTAL QUALIFICATION TEST PROGRAM

ON

ONE EXPANDABLE AIRLOCK
PART NUMBER D-21

FOR

GOODYEAR AEROSPACE CORPORATION
AKRON, OHIO

161

STATE OF ALABAMA
COUNTY OF MADISON

William W. Holbrook

being duly sworn,
deposes and says: That the information contained in this report is the result of complete and
carefully conducted tests and is to the best of his knowledge true and correct in all respects

SUBSCRIBED and sworn to before me this 1st day of July, 1970
Agnes Zielinski
Notary Public in and for the County of Madison, State of Alabama.

My Commission expires Oct. 17, 1972

TEST BY Commerical Projects

MS Darwyn D Hyter

TEST WITNESS N. Kearns

QAR DCAS William W. Holbrook
Partial Evaluation
Tests Witness Are Stamped WJ

TABLE OF CONTENTS

	<u>Page Number</u>
TABLE OF CONTENTS	
1.0 SUMMARY	163
2.0 REFERENCES	163
3.0 MANUFACTURER	163
4.0 TEST CONDITIONS AND TEST EQUIPMENT	163
5.0 REQUIREMENTS, PROCEDURES, AND RESULTS	165
5.1 Fungus Test	165
5.2 Acoustic Test	168
5.3 Salt Fog Test	170
FIGURE 70 ACOUSTIC TEST SPECTRUM	172
FIGURES 71 THROUGH 76 - ACOUSTIC SPECTRUM PLOTS	173 thru 178
PHOTOGRAPH 1 - FUNGUS TEST SETUP	179
PHOTOGRAPH 2 - ACOUSTIC TEST SETUP	180
PHOTOGRAPH 3 - SALT FOG TEST SETUP	181
APPENDIX I - TEST DATA AND TEST EQUIPMENT LISTS	182

WYLE LABORATORIES/TESTING DIVISION HUNTSVILLE FACILITY

1.0 SUMMARY

One Expandable Airlock Experiment (D-21) was subjected to Fungus, Acoustic, and Salt Fog Tests in accordance with References 2.1 and 2.2 of this report.

The test specimen successfully completed the Environmental Test Program without any visual evidence of degradation. The post functional test was performed by the Goodyear Representative.

2.0 REFERENCES

- 2.1 Goodyear Aerospace Corporation Purchase Order Number 7B0058-YX.
- 2.2 Goodyear Aerospace Corporation Document GER 13060, entitled: Environmental Qualification Test Specification for Expandable Airlock Experiment (D-21) GER-13060, Revision F.
- 2.3 Wyile Laboratories Test Procedure Number 41062-1, entitled: Environmental Qualification Test Program on one Expandable Airlock, dated April 1967.
- 2.4 Military Specification MIL-STD-810A, dated 23 June 1964, entitled: Environmental Test Methods for Aerospace and Ground Equipment.

3.0 MANUFACTURER

Goodyear Aerospace Corporation
Akron, Ohio 44315

4.0 TEST CONDITIONS AND TEST EQUIPMENT

4.1 Ambient Conditions

Unless otherwise specified herein, all tests were performed, at an atmospheric pressure of 29.38 ± 0.50 inches of mercury absolute, a temperature of $77 \pm 20^{\circ}\text{F}$. and a relative humidity of less than 95 percent.

REPORT NO. 41062-1

PAGE NO. 3A

WYLE LABORATORIES/TESTING DIVISION HUNTSVILLE FACILITY

4.0 TEST CONDITIONS AND TEST EQUIPMENT (Continued)

4.2 Test Equipment and Instrumentation

All test equipment and instrumentation used for the performance of this test program complies with the requirements of Wyle Laboratories Quality Control Manual which conforms to the applicable portions of Military Specification MIL-C-45662A. The equipment and instrumentation used for each test are presented in Appendix I of this report.

REPORT NO. 41062-1PAGE NO. 4

WYLE LABORATORIES/TESTING DIVISION HUNTSVILLE FACILITY

5.0 REQUIREMENTS, PROCEDURES, AND RESULTS5.1 Fungus Test5.1.1 Requirements

Three material samples shall be subjected to a Fungus Test in accordance with Military Standard MIL-STD-810A, Method 508.1, Procedure II.

5.1.2 Procedures

The ingredients listed below were placed in a flask, plugged with cotton, and the medium was melted in an autoclave.

<u>Ingredients</u>	<u>Quantity</u>
NH ₄ NO ₃	3.0 g
K ₂ HPO ₄	1.0 g
MgSO ₄ · 7H ₂ O	0.25 g
KCl	0.25 g
Agar	15-20.0 g
Distilled Water	1000.0 ml

Approximately 60 ml of the culture medium was poured into three 6-inch petri dishes, and allowed to harden.

Using the spare fungi listed below, a spore suspension was mixed by introducing approximately 10 ml of sterile distilled water into each tube culture of the fungi. The fungi spores were brought into suspension by vigorously shaking each tube of fungi. The separate spore suspensions were mixed together from the three types of fungi to provide a composite suspension.

WYLE LABORATORIES/TESTING DIVISION HUNTSVILLE FACILITY

5.0 REQUIREMENTS, PROCEDURES, AND RESULTS (Continued)5.1 Fungus Test , ontinued)5.1.2 Procedure (Continued)

Aspergillus niger QM 386

Aspergillus flavus QM 380

Trichoderma T-1 QM 365

Each of the 2-inch square dust free specimens were placed on the center of the hardened Agar medium in each of the three petri dishes.

Several strands of heavy sterilized cotton twine 2 to 3 inches long were placed approximately 1 inch from the test specimens.

Using a pipette, the test specimens were inoculated with approximately 0.3 ml of spore suspension. The inocula were distributed evenly, lengthwise, and around the edges of the specimen without flooding the Agar medium.

The cotton twine was inoculated as described above.

The three petri dishes were placed in the fungus chamber and the chamber temperature adjusted to $30 \pm 2^{\circ}\text{C}$. The relative humidity was maintained at 95 ± 5 percent.

The above temperature and relative humidity were maintained for a minimum period of 14 days.

Upon completion of the Fungus Test, a photograph of the test setup was taken.



WYLE LABORATORIES/TESTING DIVISION HUNTSVILLE FACILITY

REPORT NO. 41062-1

PAGE NO. 6

5.0 REQUIREMENTS, PROCEDURES, AND RESULTS (Continued)

5.1 Fungus Test (Continued)

5.1.3 Results

A visual examination of the four samples revealed that the fungus was growing on the cotton twine, but there was no evidence of growth on the specimens.

The test data are presented in Appendix I of this report.

A photograph of the test specimens is presented in Photograph 1.

5.0 REQUIREMENTS, PROCEDURES, AND RESULTS (Continued)5.2 Acoustic Test5.2.1 Requirements

The test specimen shall be subjected to an Acoustic Test using the general procedures of Military Standard MIL-STD-810A. The test spectrum shall be as shown in Figure 9-1 as the proposed test spectrum, or alternatively, as close to the spectrum required by Goodyear Specification GER 13060 as can be attained in a Wyle Acoustic Facility. The acoustic test time shall not exceed 10 minutes.

Upon completion of the Acoustic Test, a visual inspection shall be performed.

A Functional Test shall be performed by the Goodyear Representative upon completion of the Acoustic Test.

5.2.2 Procedures

Three microphones were installed in the acoustic chamber to monitor the sound field of the area the specimen was occupying.

A preliminary spectrum investigation was performed and approval of Quality Control and Government Source Inspection was obtained.

The test specimen was installed in the test setup as shown on the acoustic test data sheets.

A microphone calibration was performed prior to the start of the Acoustic Test.

A photograph was taken of the test setup prior to the start of the Acoustic Test.

The ambient test conditions were measured and recorded on the applicable test data sheets.



5.0 REQUIREMENTS, PROCEDURES, AND RESULTS (Continued)

5.2 Acoustic Test (Continued)

5.2.2 Procedures (Continued)

The output of the three microphones was recorded on the level recorder.

The test specimen was subjected to the "proposed" test spectrum, or alternatively, as close to the "requested" test spectrum as shown in Figure 70 of this test procedure.

Upon completion of the Acoustic Test, a visual inspection was performed.

The Goodyear Representative performed a post Functional Test.

5.2.3 Results

A visual examination of the test specimen revealed no visual evidence of damage or degradation as a result of the Acoustic Test.

The test data are presented in Appendix I of this report.

A photograph of the Acoustic Test setup is shown in Photograph 2 of this report.

The Acoustic Test Spectrum Plots are presented in Figures 71 through 76.

The Functional Test data were retained by the customer representative.

WYLE LABORATORIES/TESTING DIVISION HUNTSVILLE FACILITY

5.0 REQUIREMENTS, PROCEDURES, AND RESULTS (Continued)5.3 Salt Fog Test5.3.1 Requirements

The test specimen shall be subjected to the Salt Fog Test in accordance with Military Standard MIL-STD-810A, Method 509.1.

Upon completion of the Salt Fog Test, the test specimen shall be visually inspected for corrosion of metals and binding of moving parts.

A Functional Test shall be performed by the Goodyear Representative upon completion of the above test.

5.3.2 Procedures

The test specimen was installed in the test setup.

A 5 percent salt solution was mixed by dissolving 5 ± 0.1 parts by weight of salt in 95 parts by weight of distilled water.

The salt solution specific gravity was checked; it was in the range of 1.023 to 1.037 utilizing the measured temperature and density of the salt solution as shown in Figure 509.1 of Military Standard MIL-STD-810A.

The salt solution was adjusted to a pH range of 6.5 to 7.2 at $95 \pm 2 - 4^{\circ}\text{F}$ and collected by the method specified by Method 509.1 of Military Standard MIL-STD-810A.

The test chamber temperature was adjusted in the exposure zone to $95 \pm 2 - 4^{\circ}\text{F}$. The salt fog conditions maintained in all parts of the exposure zone were such that a clean fog collecting receptacle placed at any point in the exposure zone would collect from 0.5 to 3 milliliters of solution per hour for each 80 square centimeters of horizontal collecting area based on an average test of at least 16 hours.



REPORT NO. 41062-1

PAGE NO. 10

GOODYEAR LABORATORIES / TESTING DIVISION HUNTSVILLE FACILITY

5.0 REQUIREMENTS, PROCEDURES, AND RESULTS (Continued)

5.3 Salt Fog Test (Continued)

5.3.2 Procedures (Continued)

The test specimen was exposed to the above Salt Fog Test for a period of at least 48 hours.

Upon completion of the Salt Fog Test, a photograph of the test specimen was taken.

The Goodyear Representative performed a post Functional Test.

5.3.3 Results

A visual examination of the test specimen revealed no visual evidence of damage or degradation as a result of the Salt Fog Test.

A photograph of the Salt Fog Test setup is shown in Photograph 3 of this report.

The test data are presented in Appendix I of this report.

The Functional Test data were retained by the customer representative.

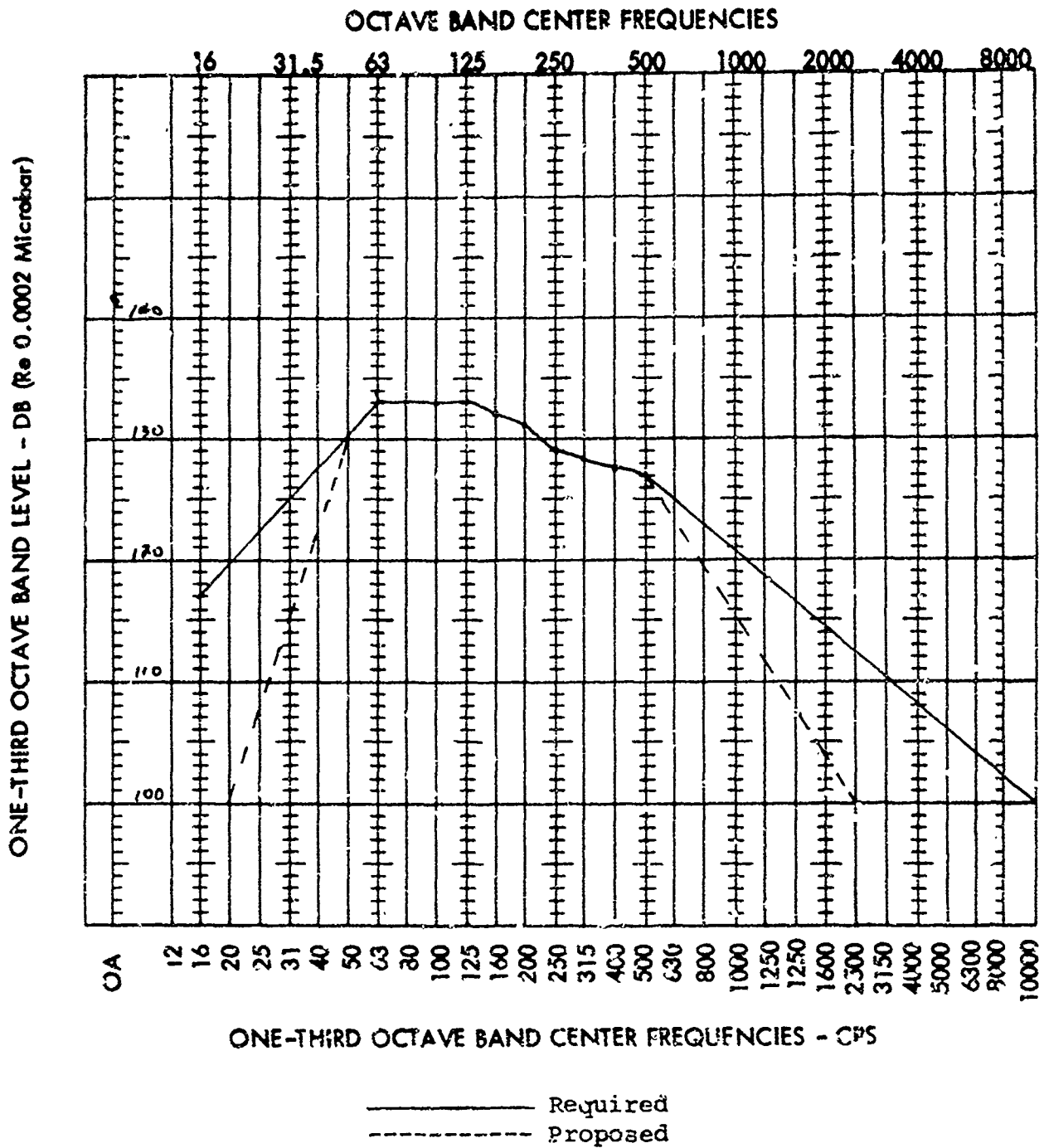


Figure 70

ACOUSTIC TEST SPECTRUM

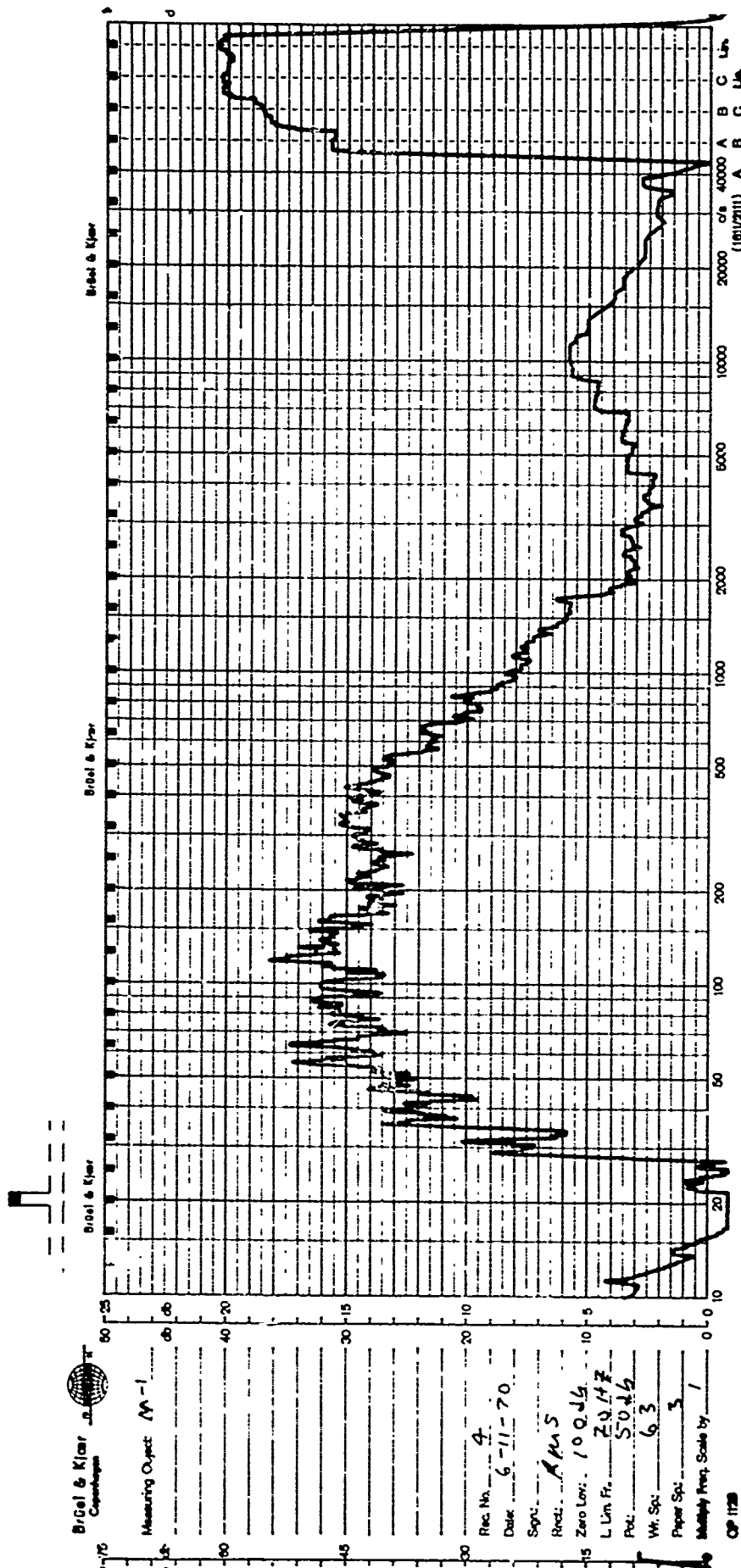


Figure 74
ACOUSTIC SPECTRUM PLOT
Rec. No. 4 - Microphone 1

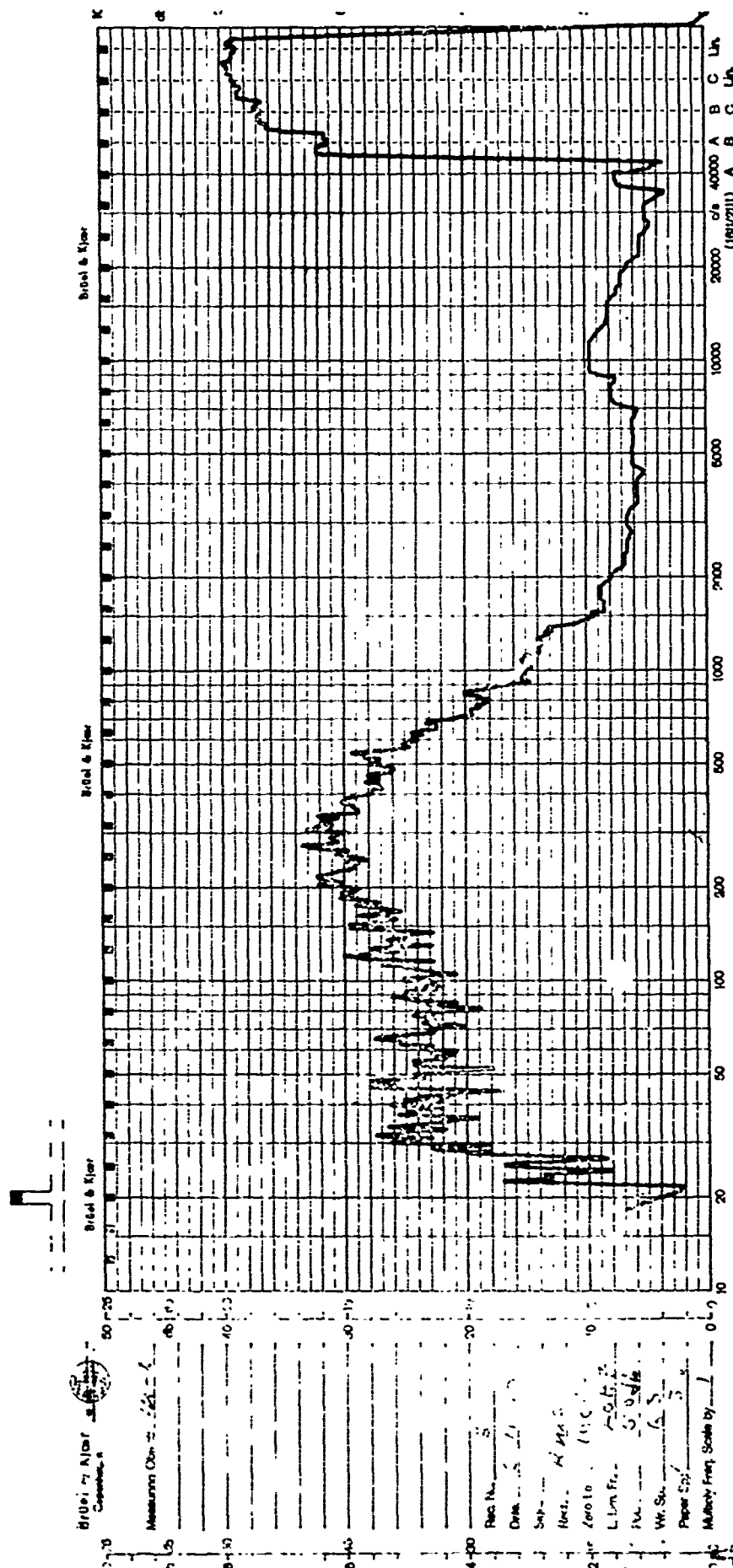


Figure 75
ACOUSTIC SPECTRUM PLOT
Rec. No. 5 - Microphone 2

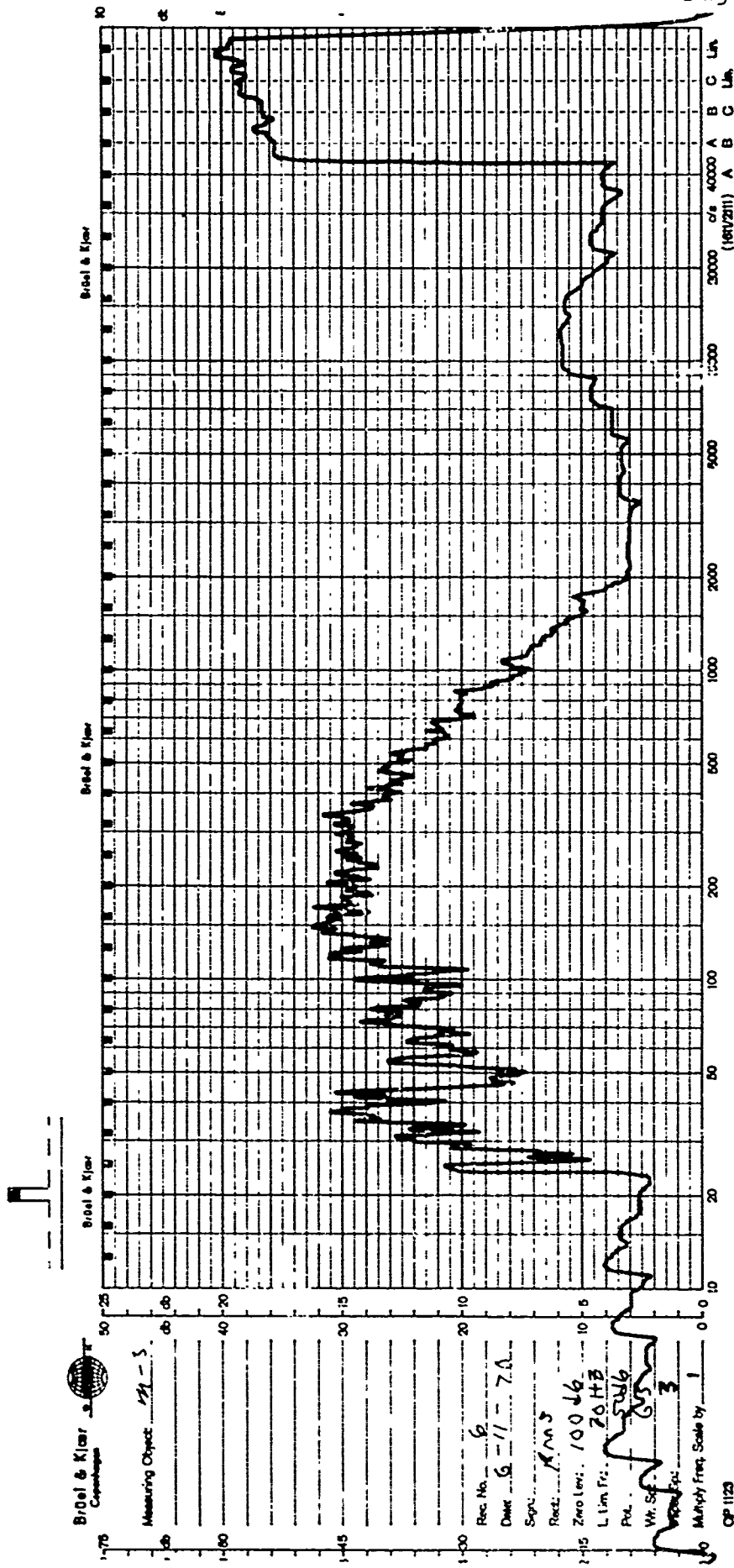
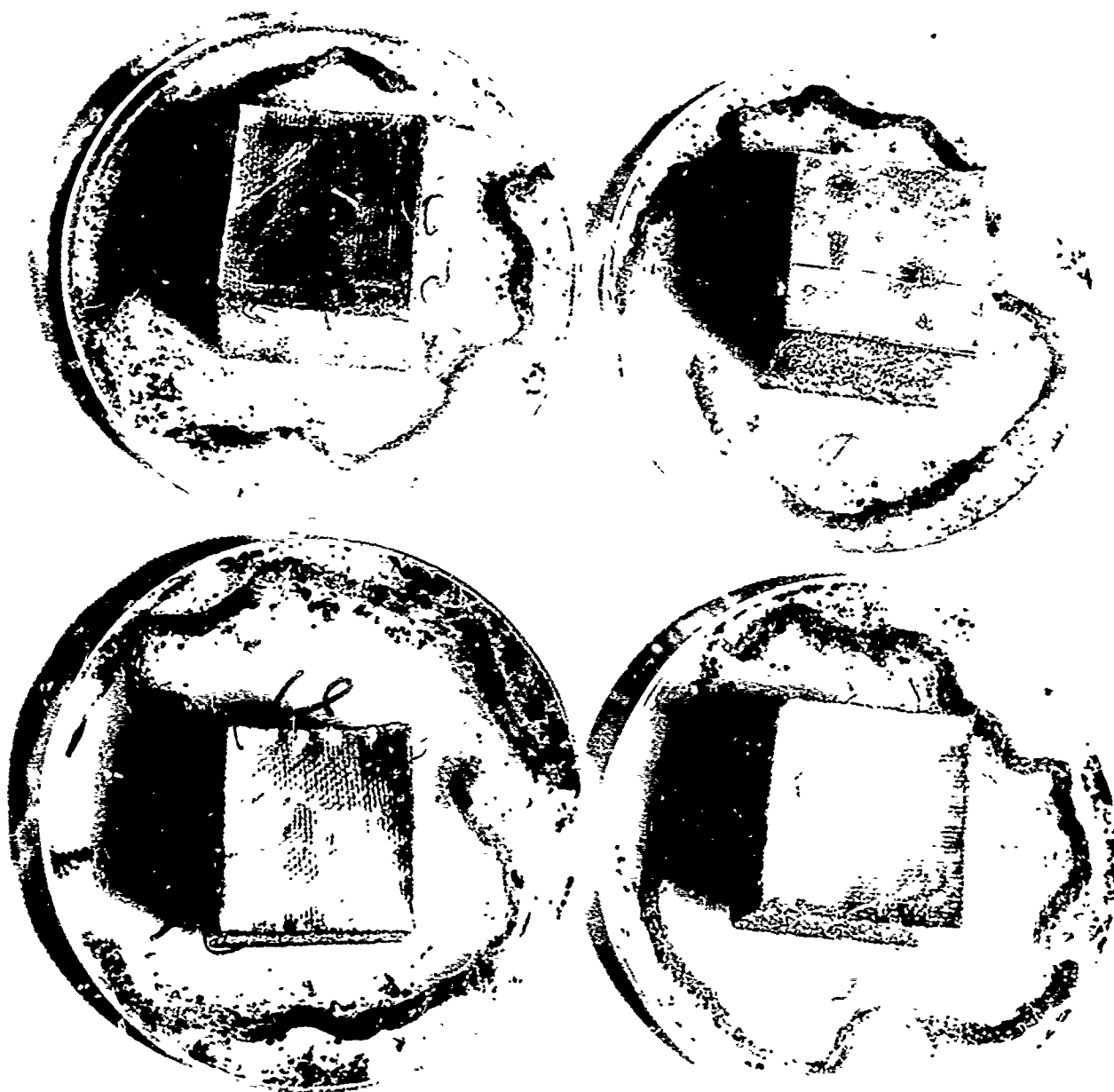
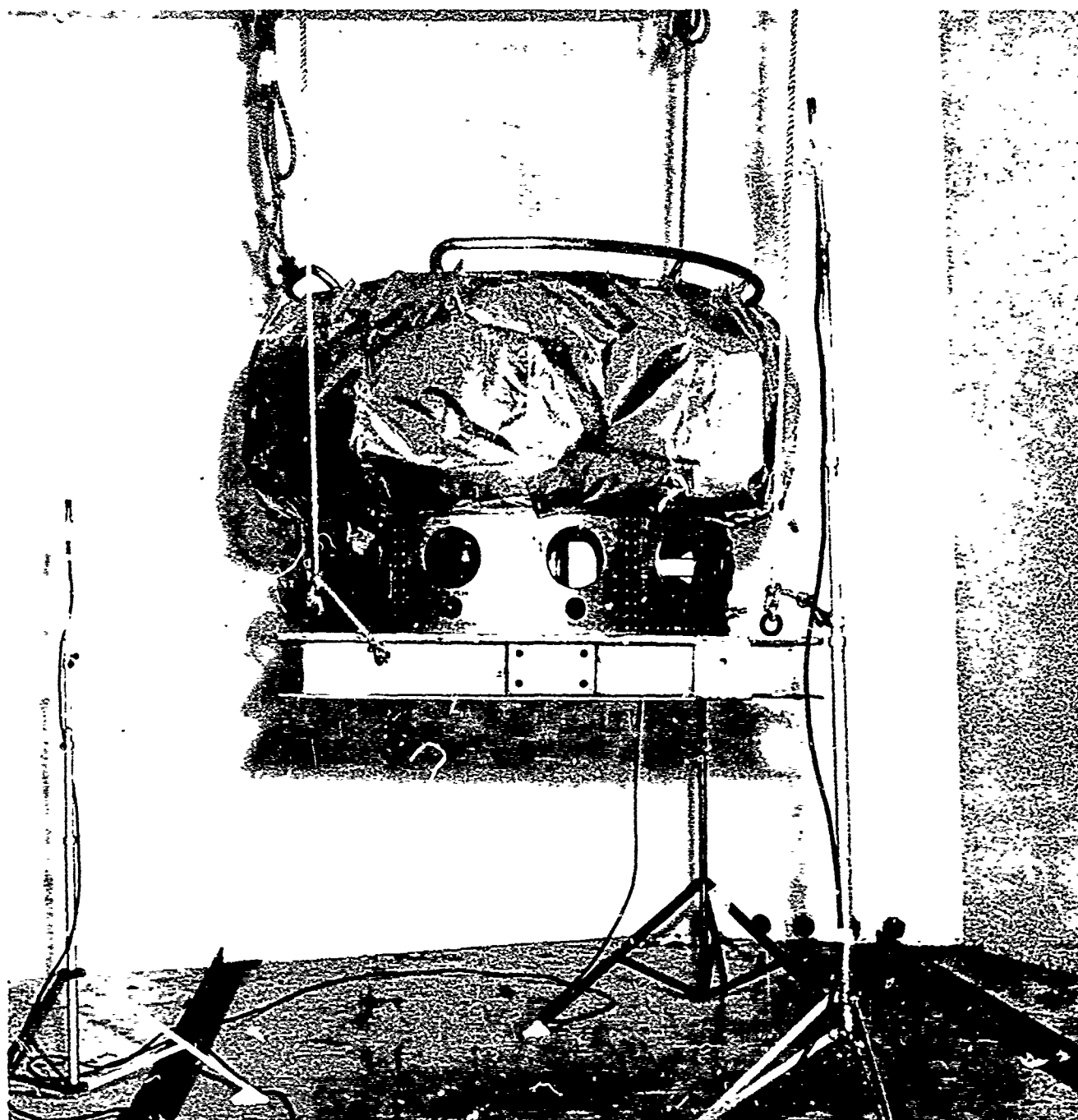


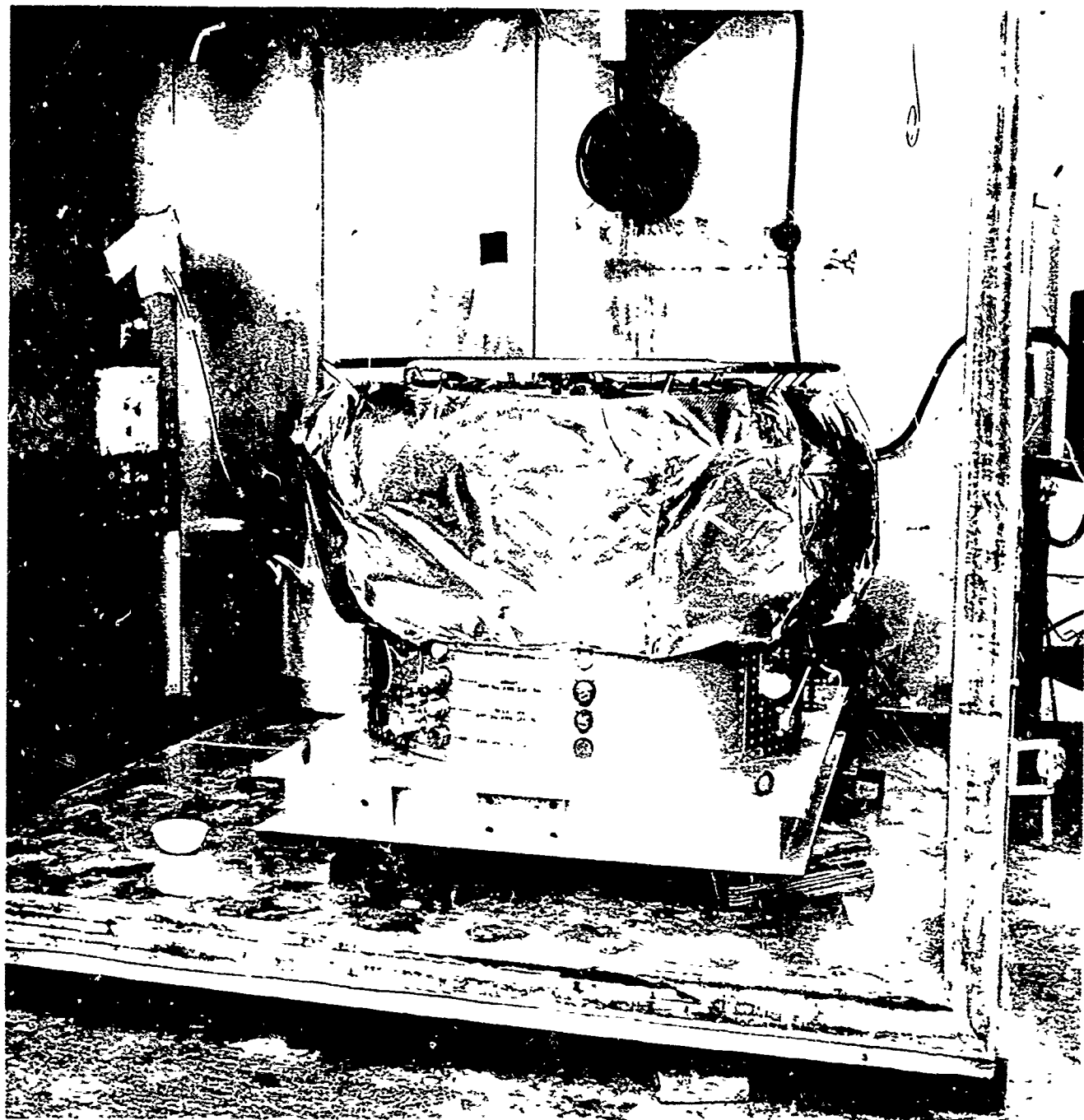
Figure 76
ACOUSTIC SPECTRUM PLOT
Rec. No. 6 - Microphone 3

REPORT NO. _____

DATE _____







REPORT NO. 41062-1

PAGE NO. 21

WYLL LABORATORIES TESTING DIVISION, HUNTSVILLE FACILITY

APPENDIX I
TEST DATA
AND
TEST EQUIPMENT LISTS

DATA SHEET



WYLE LABORATORIES

Customer Goodyear AerospaceJob. No. 41062Part No. D-21Report No. 41062-1Spec. WLTP 41062Date 3-14-68Para. 9.4Amb. Temp. 75°FS/N 1Photo YESTest Med. FUNGUSSpecimen Temp. N/ASpecimen Girlent (27)Test Equipment. 1. See Equipment Sheet 2.

3. _____	4. _____	5. _____
6. _____	7. _____	8. _____
9. _____	10. _____	11. _____
12. _____	13. _____	14. _____
15. _____	16. _____	17. _____
18. _____	19. _____	20. _____

Test Title: Fungus

Description of Test: Two (27) samples 1 1/4 inches square were cut from each of the two (2) test specimens. The four (4) samples were then inoculated with approximately 0.3 ml each of a Composite Spore Suspension prepared from the following fungi: Aspergillus niger, Aspergillus flavus and Trichoderma T-1. The samples were then placed in the center of individual petri dishes which contained harden agar. Eight (8) strands of cotton twine were then inoculated with the spore suspension and two (2) strands were placed in each of the petri dishes approximately 1.0 inch from the specimen.

The petri dishes were then placed in a mold chamber which had been previously cooled to 86° ± 3.6°F with a relative

Specimen Filled _____

Specimen Passed YesNOD Written NoTested By John S. Ford Date: 3-28-68

Witness _____ Date: _____

Signed By _____ of W

Approved _____

DATA SHEET

WYLE LABORATORIES

Specimen AirlockPart No. D-21S/N 1Job No. 41062Report No. 41062-1Date 3-14-68Test Title Fungus

Description of Test (Continued): humidity of 95 ± 5 percent. The specimens were subjected to these conditions for a period of 14 days. Upon completion of this period the specimens were removed from the chamber. A visual inspection revealed that the fungus was growing on the cotton twine, but there was no evidence of growth on the specimens.

JD 3-28-68Sheet No. II of III(P)

DATA SHEET

WYLE LABORATORIES

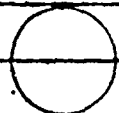
Specimen AIRLOCITJob No. 41062-03Part No. D-21Report No. 41062-1S/N 1Date 6-11-70Test Title ACOUSTIC, REVERBERATION.

Description of Test:

THE TEST SPECIMEN WAS SUSPENDED IN THE CENTER OF THE 1500³ FT REVERBERATION FACILITY. THREE MICROPHONES WERE USED TO MEASURE THE SOUND FIELD. THEY WERE LOCATED AT DIFFERENT POSITIONS AROUND THE SPECIMEN BUT ALL WERE EIGHTEEN (18) INCHES FROM THE SPECIMEN. M-1 WAS ON THE CENTER LINE OF THE SPECIMEN WHICH WAS 47 INCHES FROM THE FLOOR. M-2 WAS 36 INCHES FROM THE FLOOR, AND M-3 WAS 68 INCHES FROM THE FLOOR. (SEE SKETCH)

A FUNCTIONAL TEST AS WELL AS PHOTOGRAPHS WERE MADE BEFORE AND AFTER THE ACOUSTIC TEST. TOTAL TEST TIME AT A LEVEL OF 140.5 dB WAS 9 MINUTES AND 57 SECONDS. NO FAILURE WAS INDICATED. TEMP. = 78 DEG. F, R.H. = 67%.

M-2



M-1



SOUND

M-3



W. J. Hall & Son
6-11-70



DATA SHEET

Customer GoodmanSpecimen BlackPart No. Q-31Spec. WLTPPara. WLTP Par. 9.0S/N 1GSI YesAmb. Temp. 75°FPhoto YesTest Med. Salt SolutionSpecimen Temp. N/A

WYLE LABORATORIES

Job No. 41062Report No. 41062-1Start Date 6-15-70Test Title Salt Fog

The specimen was placed in a Salt Fog chamber. A 5 percent salt solution was then prepared by dissolving 5 parts by weight of salt in 95 parts by weight of distilled water. The pH and specific gravity of the solution was 7.1 and 1.035 respectively. The chamber ambient temperature was increased to 75°F and the salt solution atomizer was adjusted to produce 0.5 milliliters of solution per hour in the test area. The specimen was exposed to this condition for four (4) hours. Upon completion of this period the specimen was visually inspected. There was no apparent specimen degradation resulting from the test performed. Upon completion of the inspection the specimen was removed from the chamber and a functional test was performed by the Goodman Representative. All data was recorded and retained by same. At the conclusion of the functional test the specimen was rinsed with tap water.

Specimen Failed _____

Specimen Passed _____

NDD Written NoneTested By John Todd Date: 6-15-70

Witness _____ Date: _____

Sheet No. I of IIApproved Ch. B. R.

INSTRUMENTATION EQUIPMENT SHEET



INSTRUMENTATION

DATE 3-28-69

108 NO. 41062

TEST AREA ~~Examination~~ 226

TECHNICIAN ~~James Z. Zadd~~

CUSTOMER Goodbar Residence TYPE TEST Exposure

TEST TYPE TEST

542845

[illegible]

Report No. 41062-1
Page No. 26

INSTRUMENT TEST ENGINEER

ENGINEER *W. B. B. B. B.*
Sheet No. *III* of *III*

CHECKED & RECEIVED BY:

Marshall Lindsay

WYLE LABORATORIES, INC.

JOE NO. 41067 -03

TEST AREA 1800' FT FACILITY

CUSTOMER GOODYEAR HEAD

ACUSTIC, REVERBERANT

Page No. 27

[illegible]

INSTRUMENT TEST ENGINEER

CHECKED & RECEIVED BY

Marshall County

INSTRUMENTATION

WATERBURY, CT.

DATE 1-18-73 JOB NO. 44263 TREAT AREA 2

JOB NO. 41262

TPA P-APCA

TEST AREA

TECHNICIAN Frank T. Adell CUSTOMER Goodfellow TYPE TEST 5211-52

CUSTOMER Goodys

TYPE TEST 58715-2

[illegible]

Page No. 28

INSTRUMENT TEST ENGINEER

APPENDIX X

ILLUSTRATIONS AND TABLES EXTRACTED FROM AEDC-TR-70-262

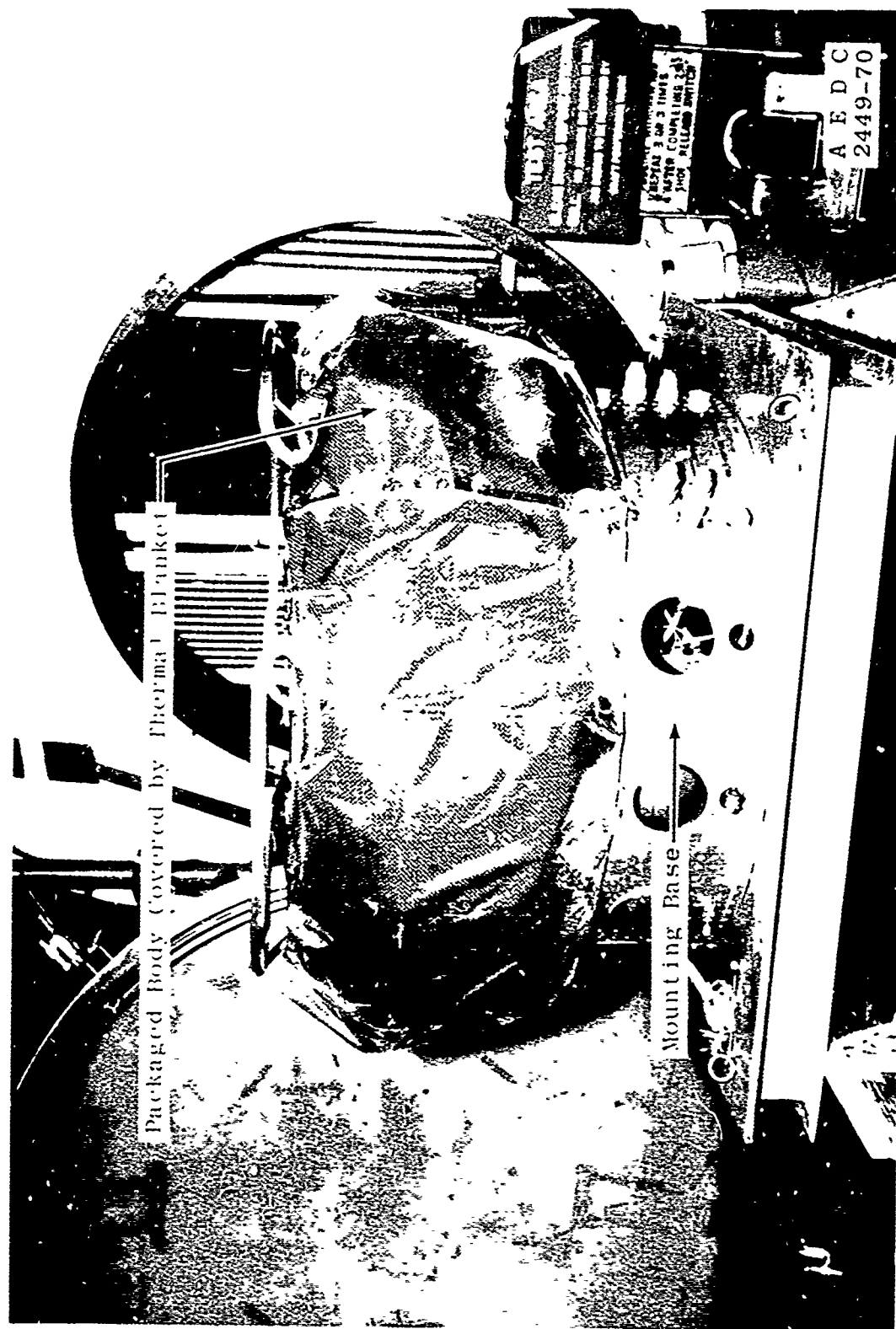


Figure 77. Packaged D-21 Airlock

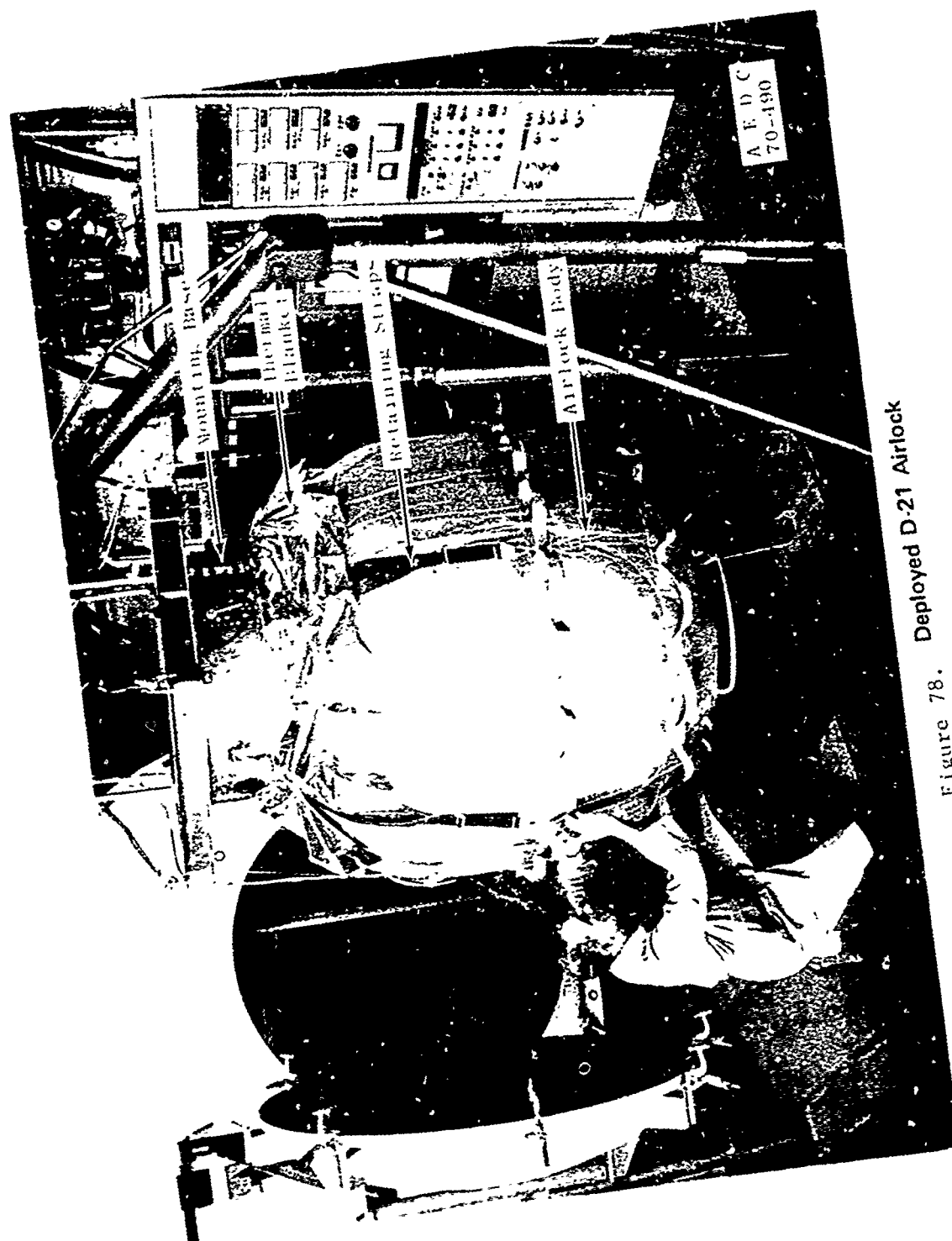


Figure 78. Deployed D-21 Airlock

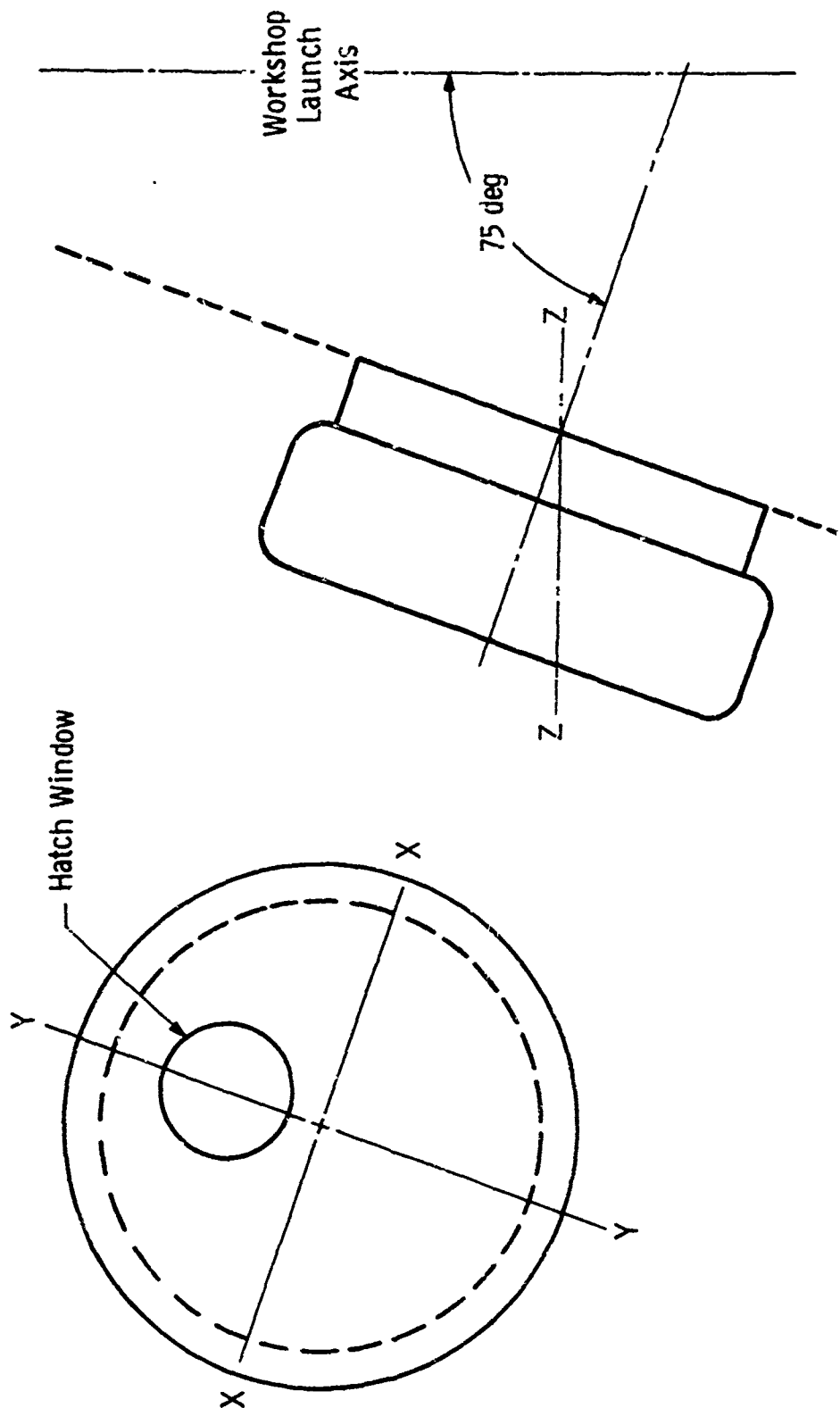


Figure 79. Airlock Axes Orientation

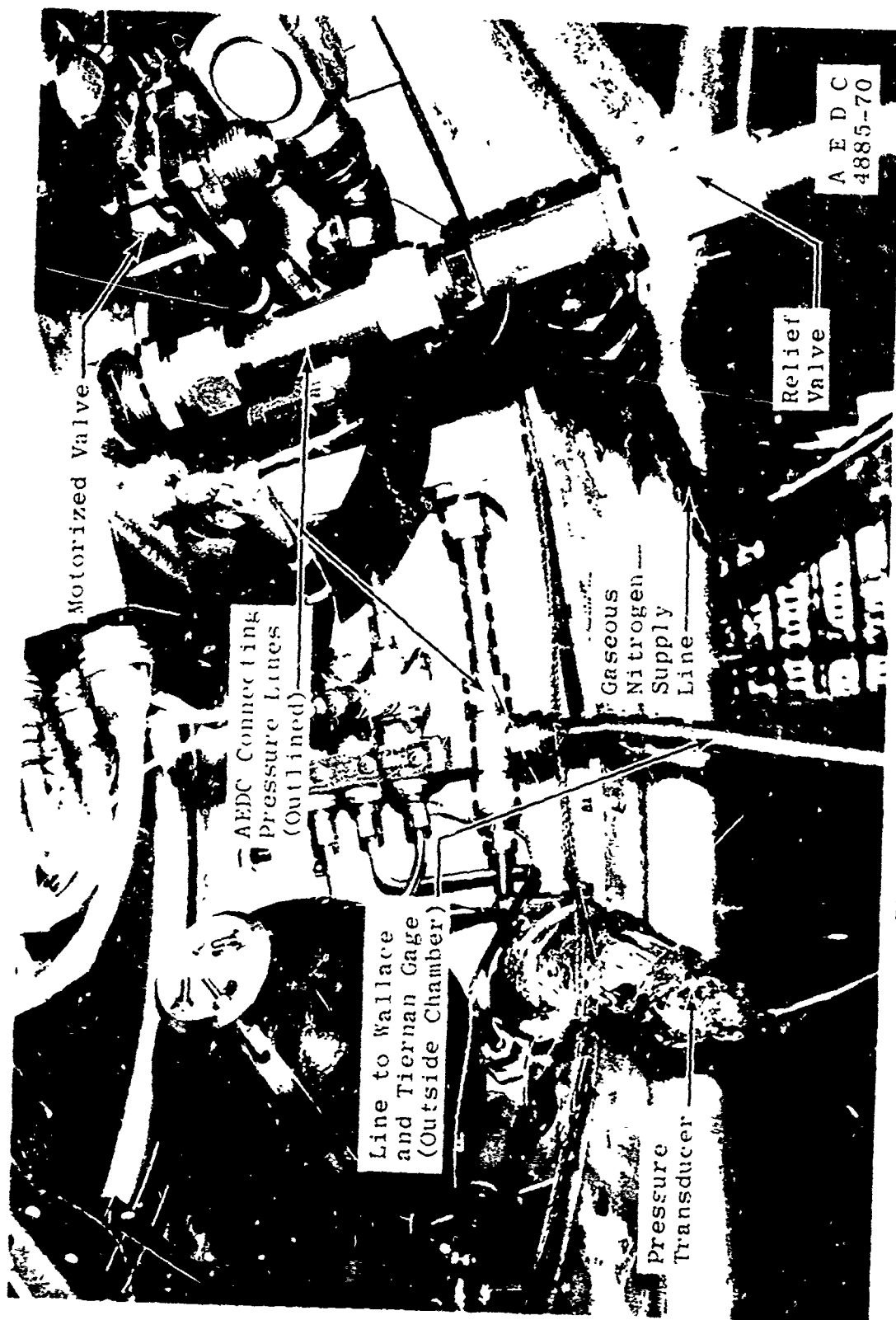


Figure 80. Airlock Pressure System

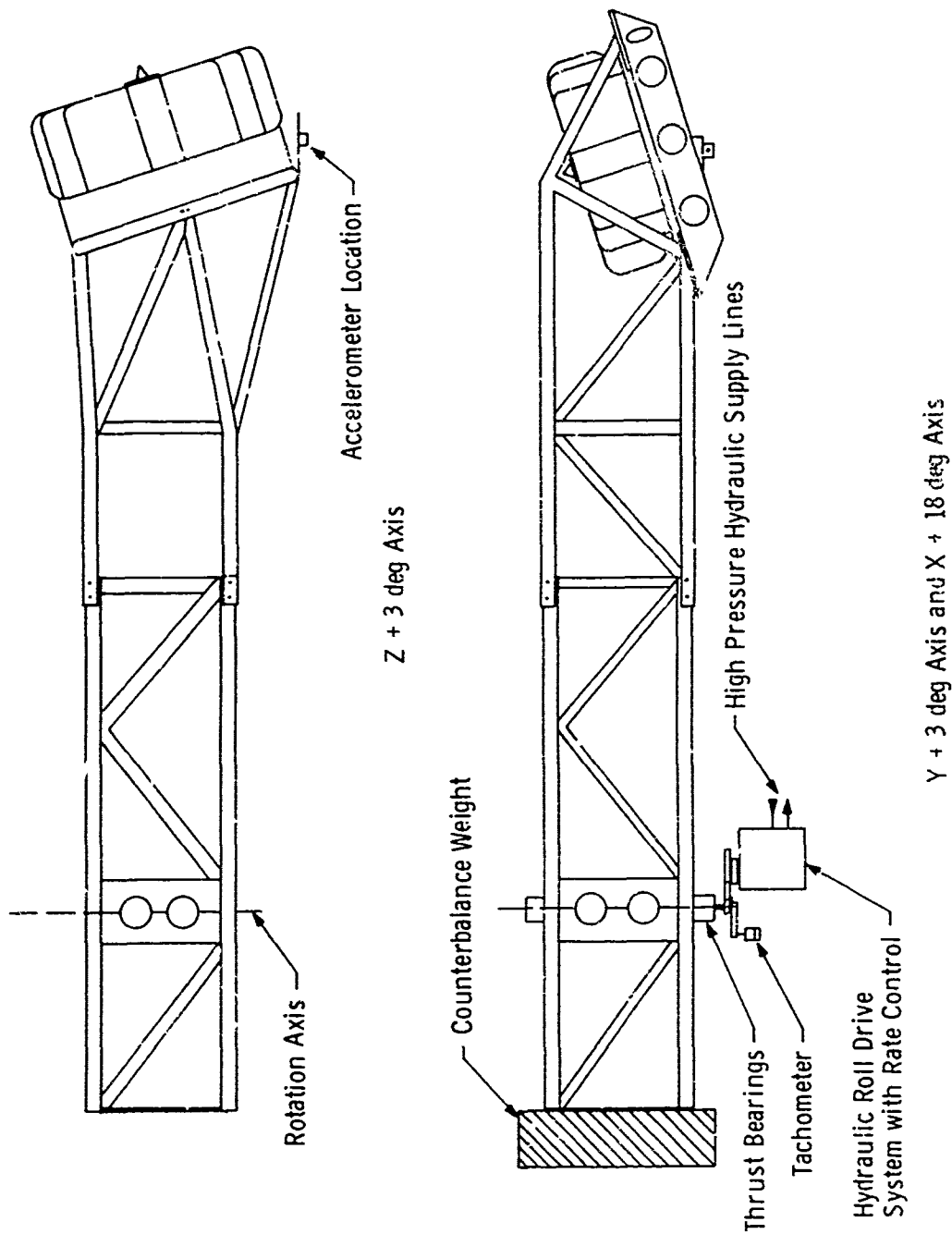


Figure 31. Centrifuge Schematic

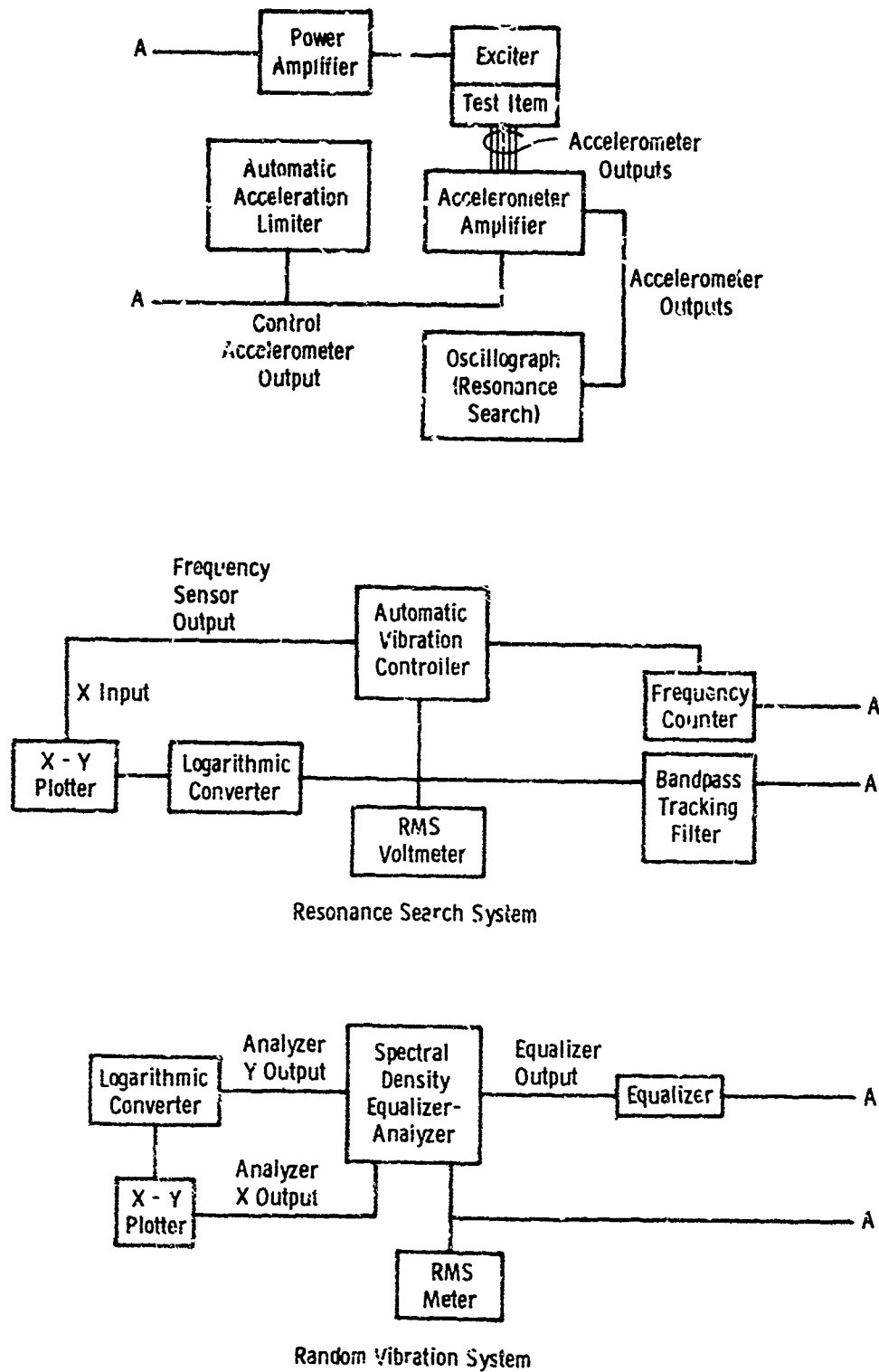


Figure 82. Vibration System Schematic

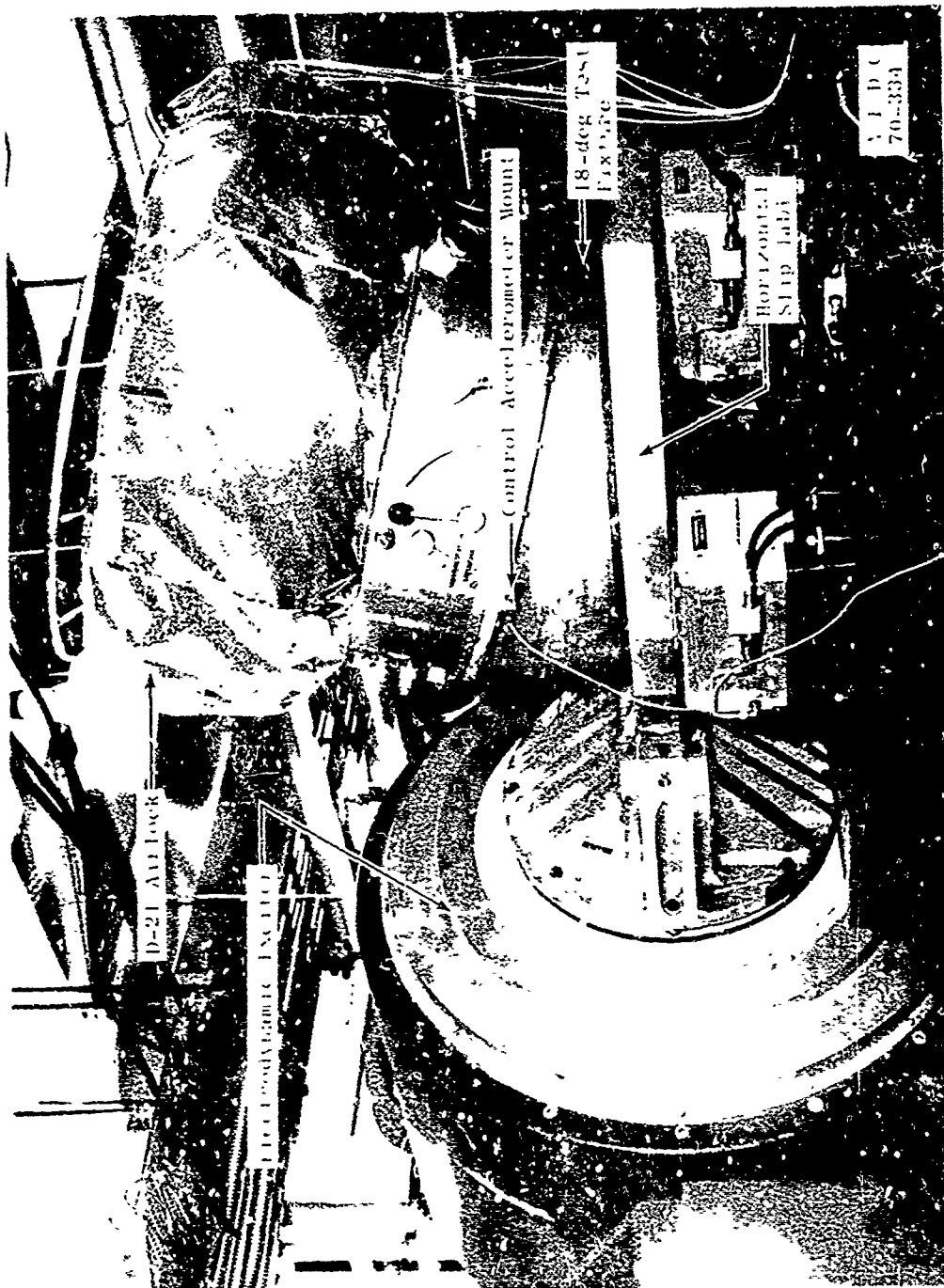


Figure 83. Vibration Equipment

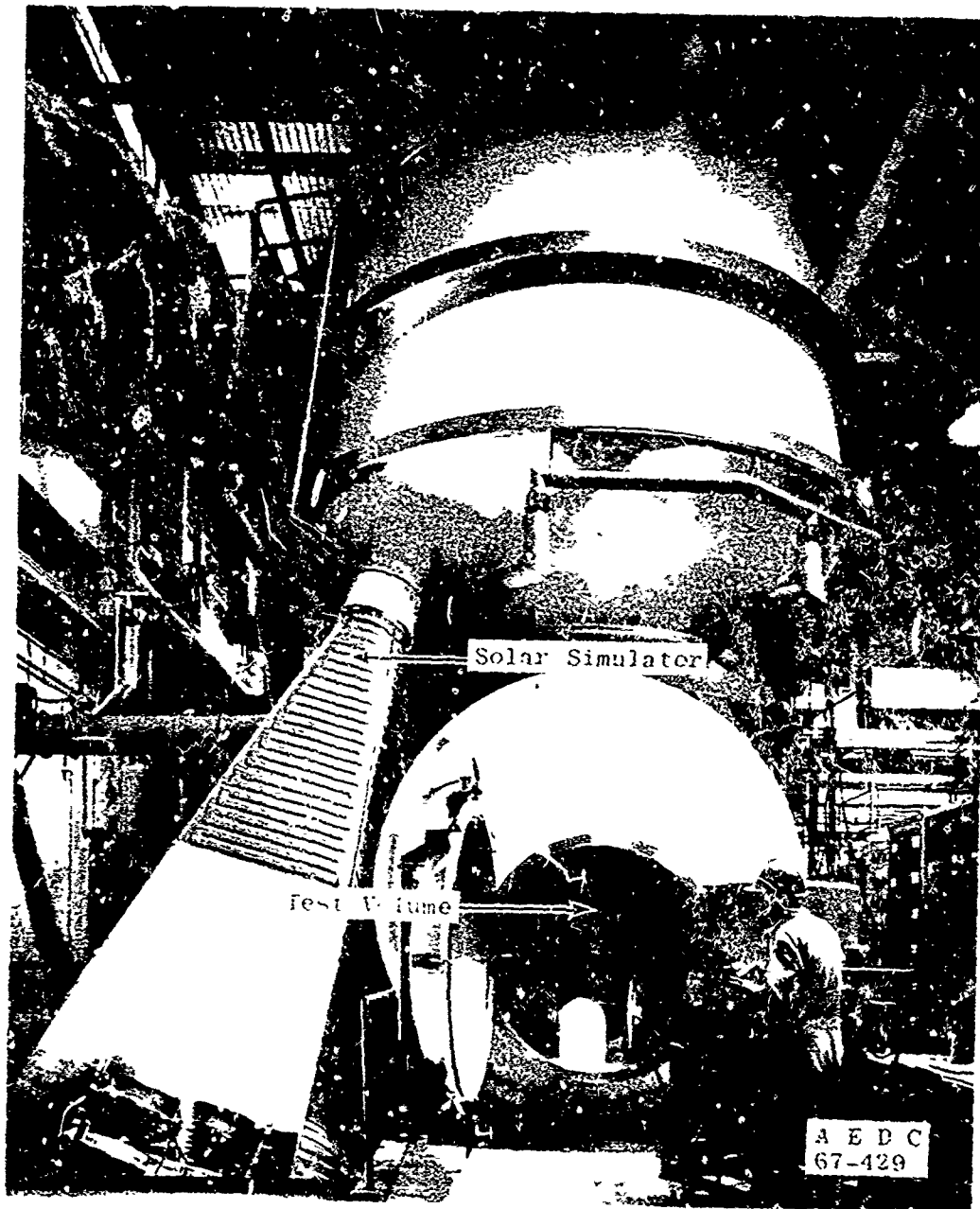


Figure 94. Aerospace Research Chamber (12V)

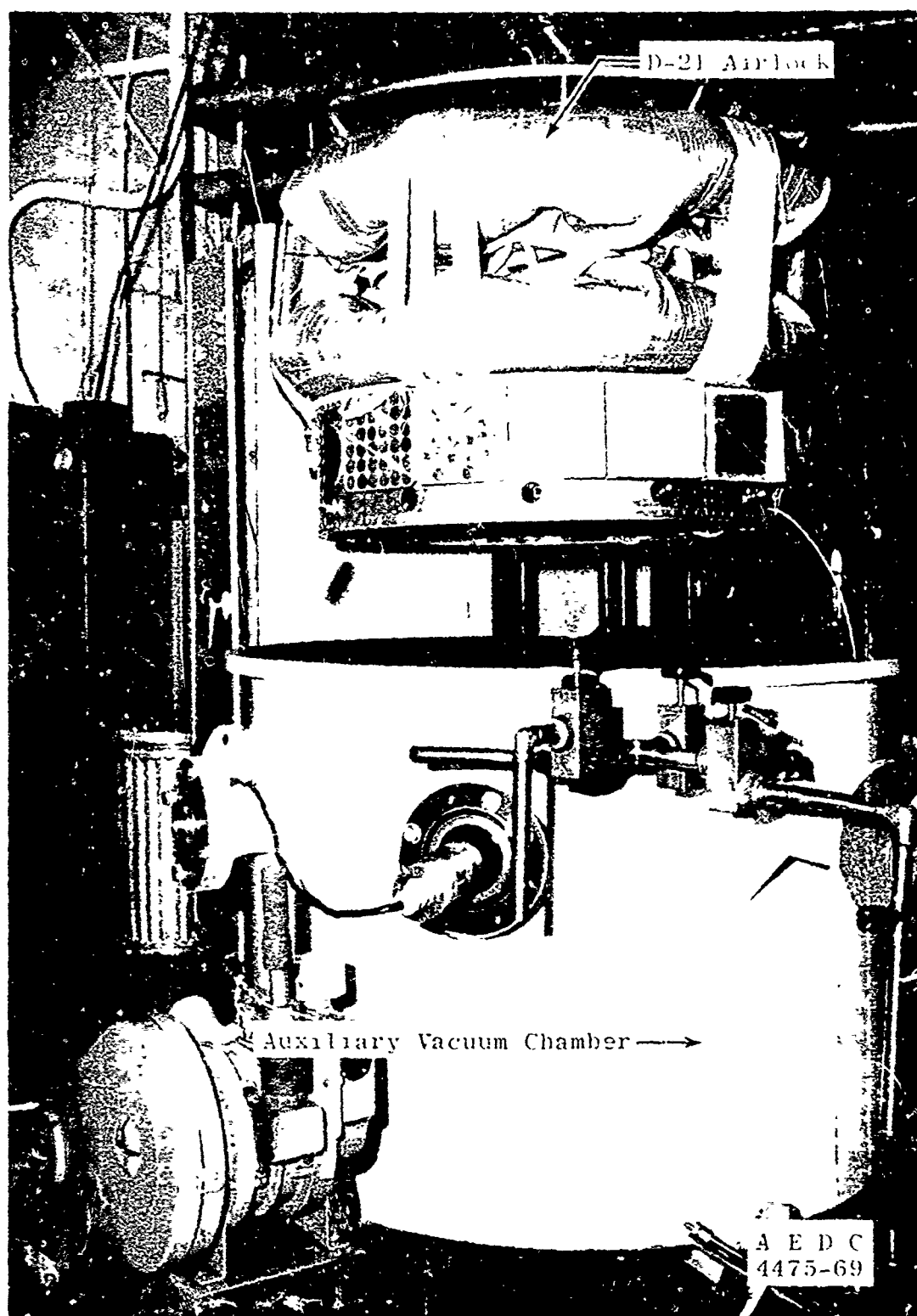


FIGURE 85. Auxiliary Vacuum Chamber

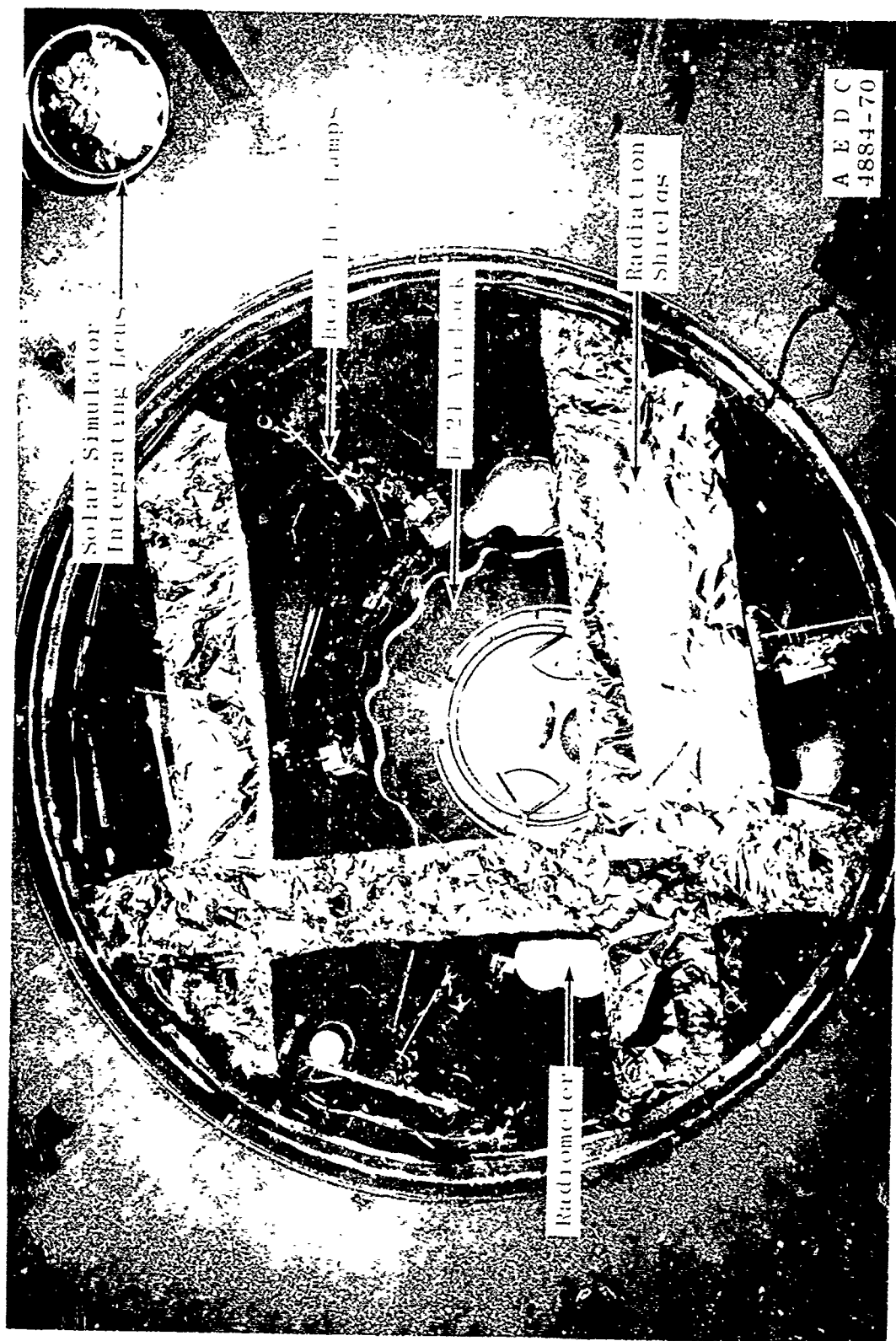


Figure 86. Solar Shield

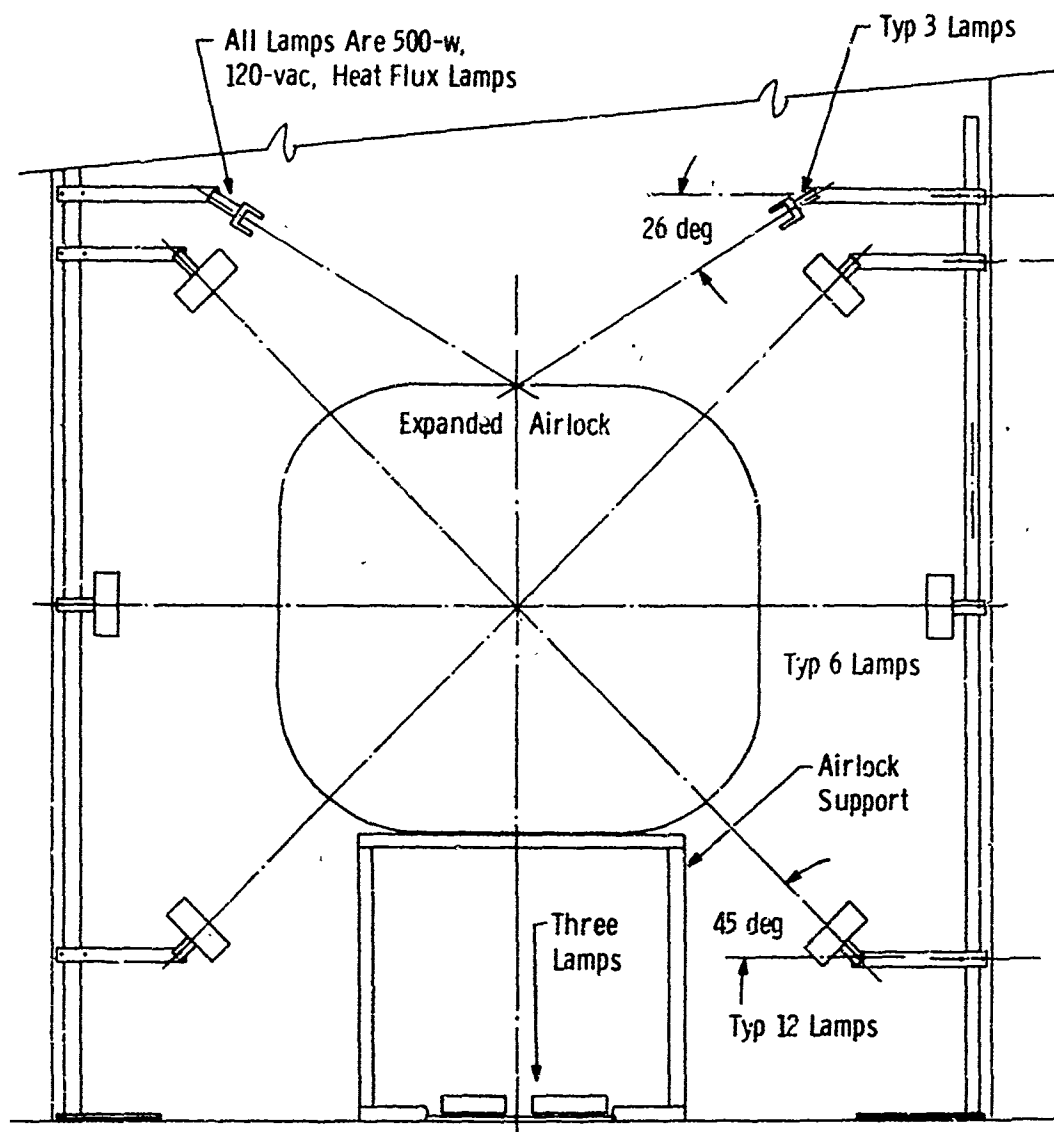
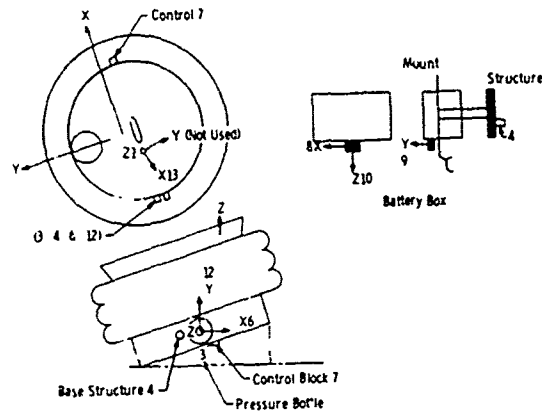
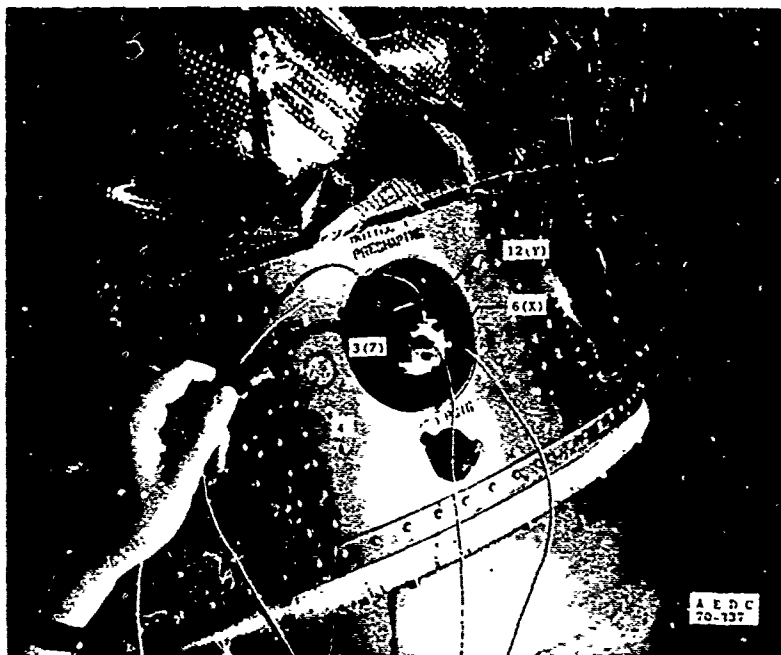


Figure 87. Heat Flux Schematic

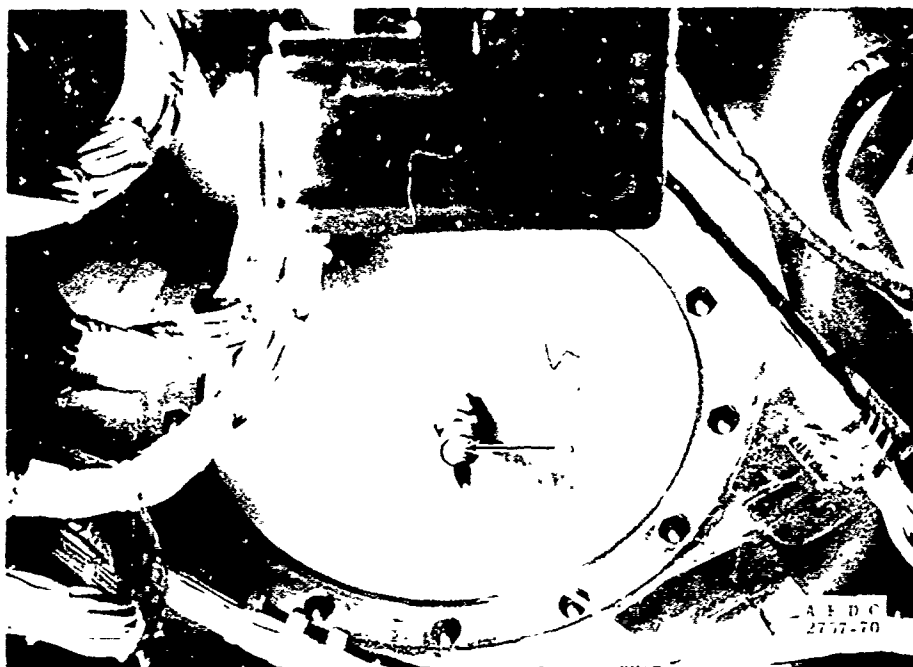
<u>Photograph</u>	<u>Oscillograph</u>	<u>Location</u>	<u>Axis</u>	<u>Accelerometer</u>
Fig. 12 f	1	Match	Z	i-40274 Triaxial
Fig. 12 e	2	Instrument Box		i-31822
Fig. 12 d	3	Pressure Bottle	Z	i-40271 Triaxial
Fig. 12 b	4	Base Structure		i-40290
Fig. 12 c	5	Base Pressure Bulkhead		i-40259
Fig. 12 b	6	Pressure Bottle	X	i-40271 Triaxial
Fig. 7	7	Control		i-40258
Fig. 12 d	8	Battery Box	X	i-40272 Triaxial
Fig. 12 d	9	Battery Box	Y	i-40272 Triaxial
Fig. 12 d	10	Battery Box	Z	i-40272 Triaxial
Fig. 12 b	12	Pressure Bottle	Y	i-40271 Triaxial
Fig. 12 f	13	Match	X	i-40274 Triaxial



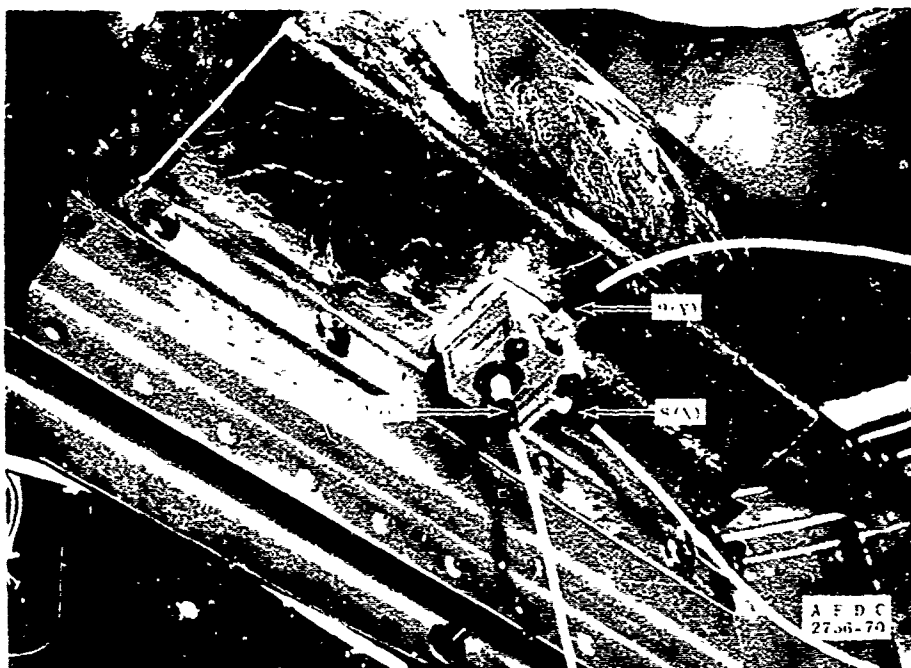
a. Schematic



b. Base Structure and Pressure Bottle
Figure 88. Accelerometer Location

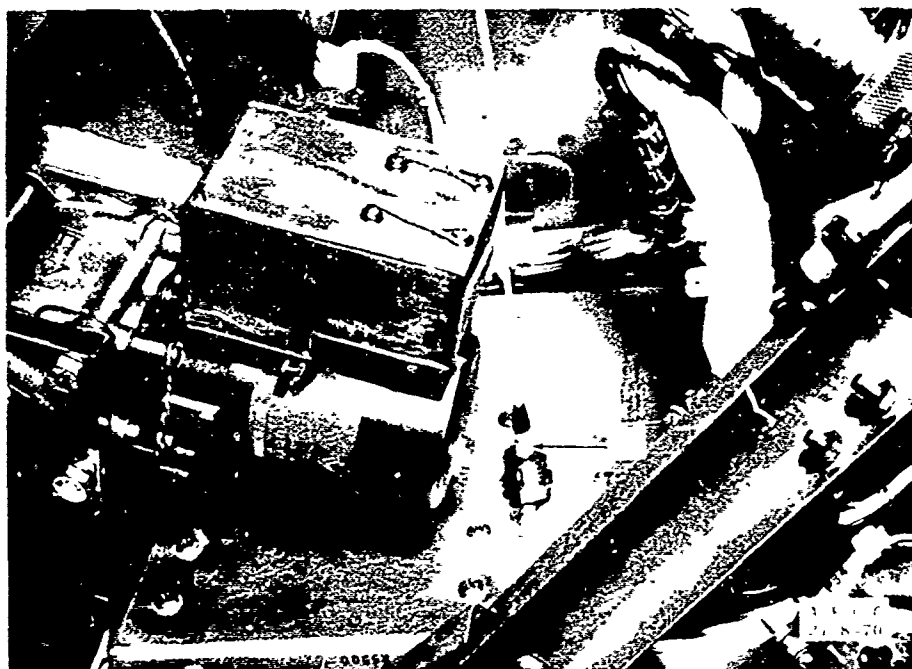


c. Base Pressure Bulkhead

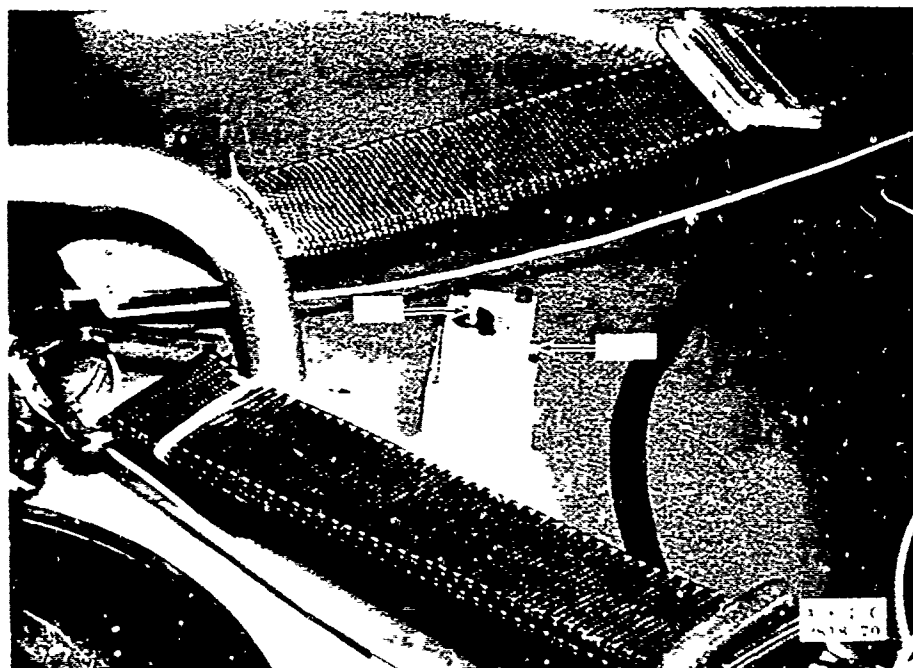


d. Battery Box

Figure 88. Continued



e. Instrument Box



f. Hatch
g. Concluded

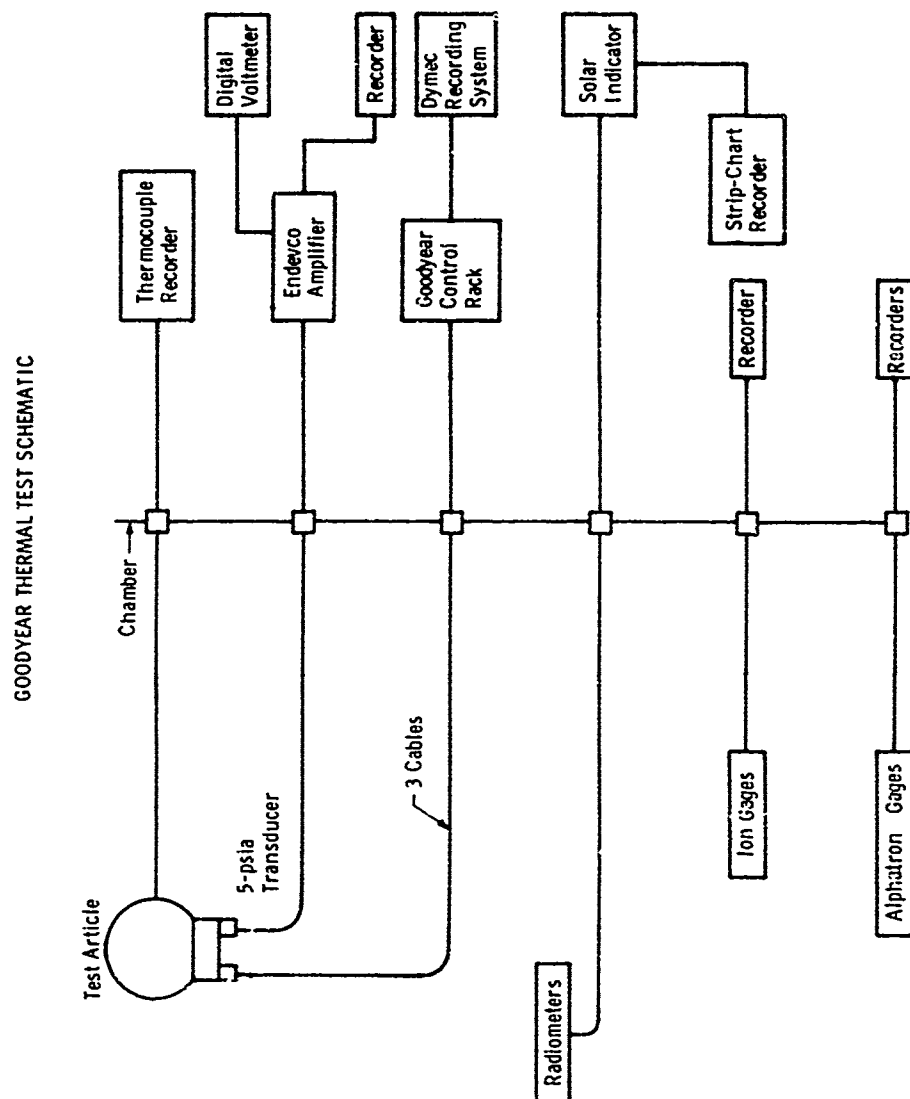


Figure 89. Vacuum Test Instrument Schematic

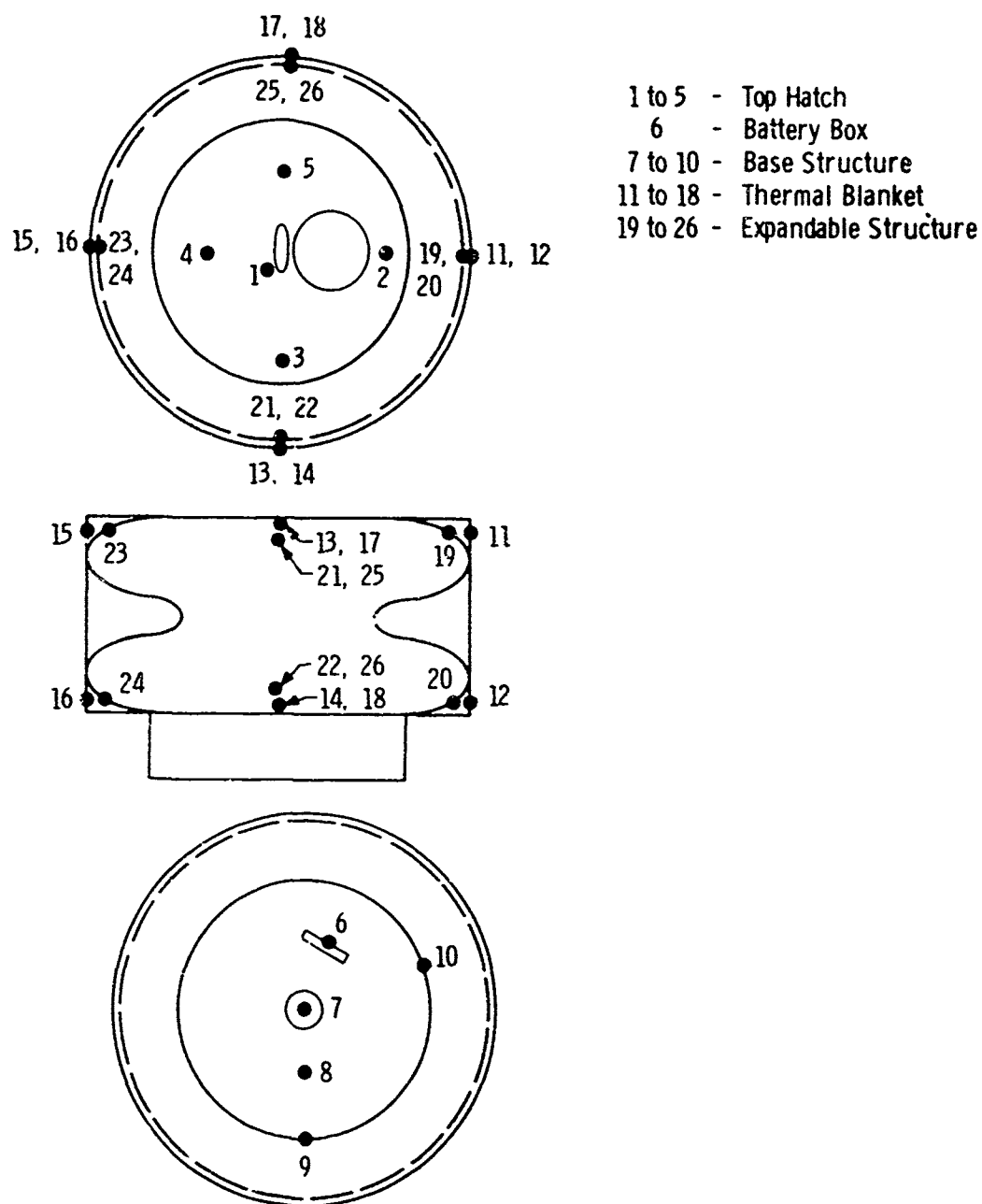


Figure 90. Deployment Thermocouple Location

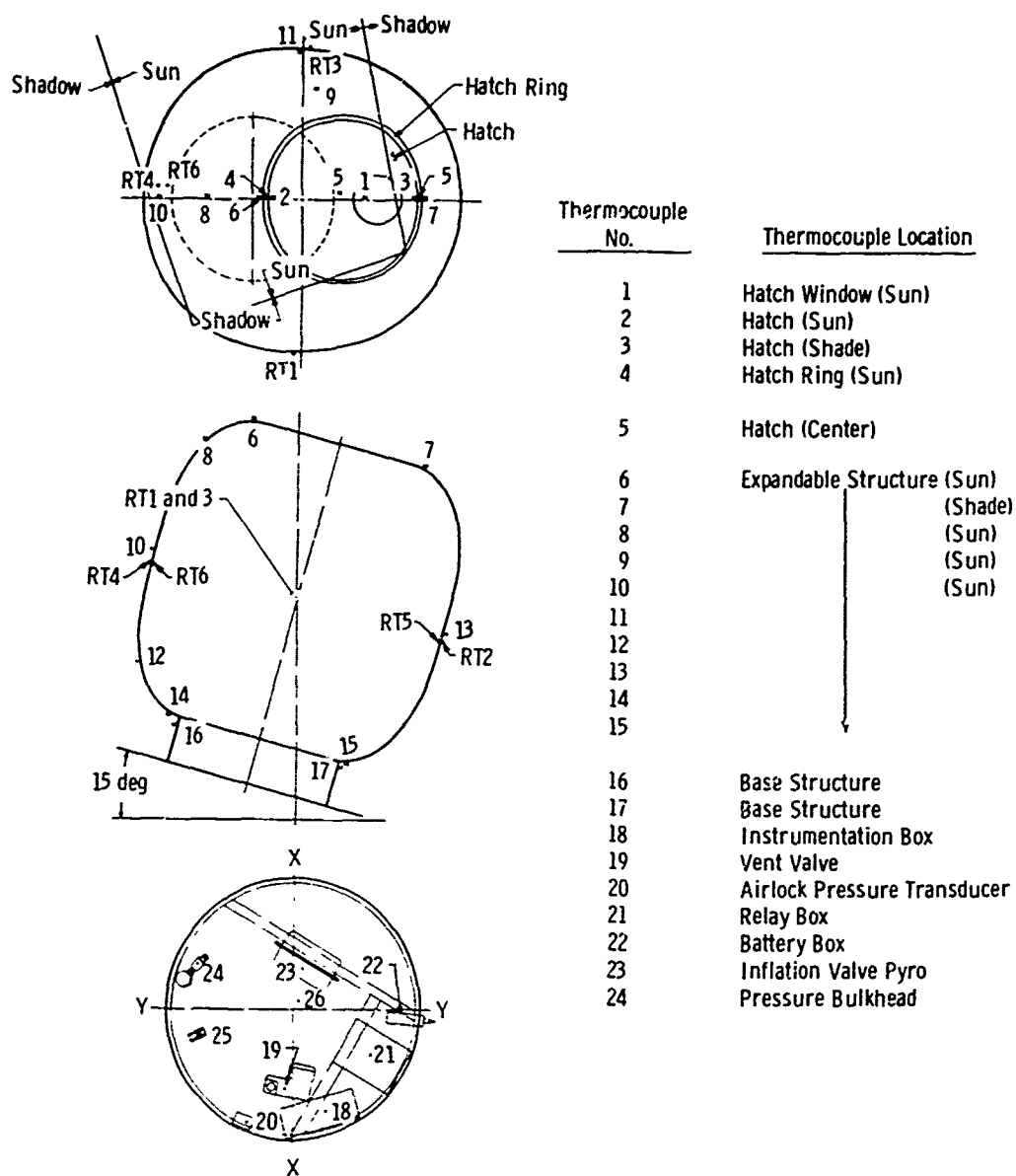


Figure 91. Vacuum Environment Thermocouple Location

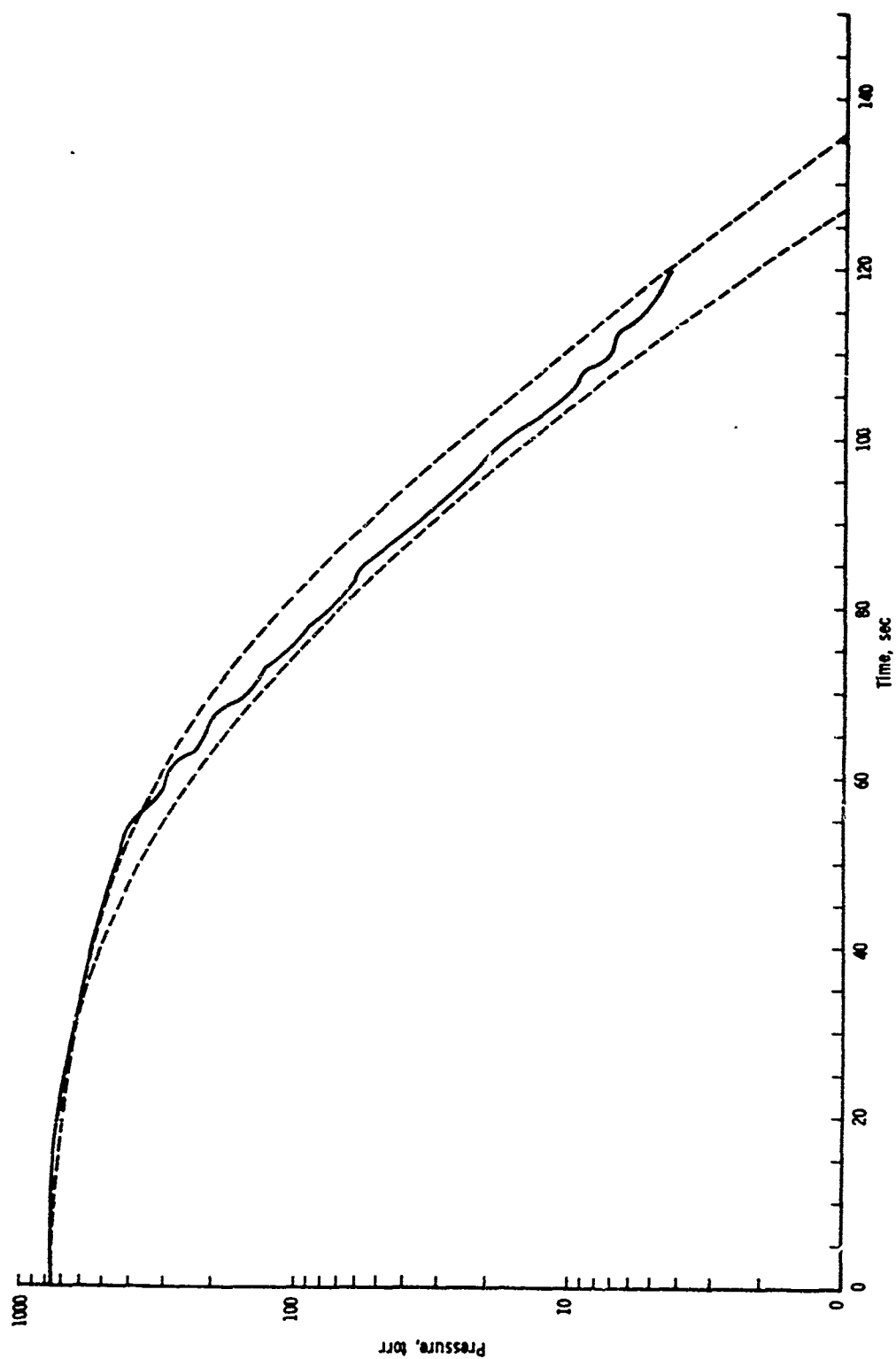


Figure 92. Launch Pressure Simulation

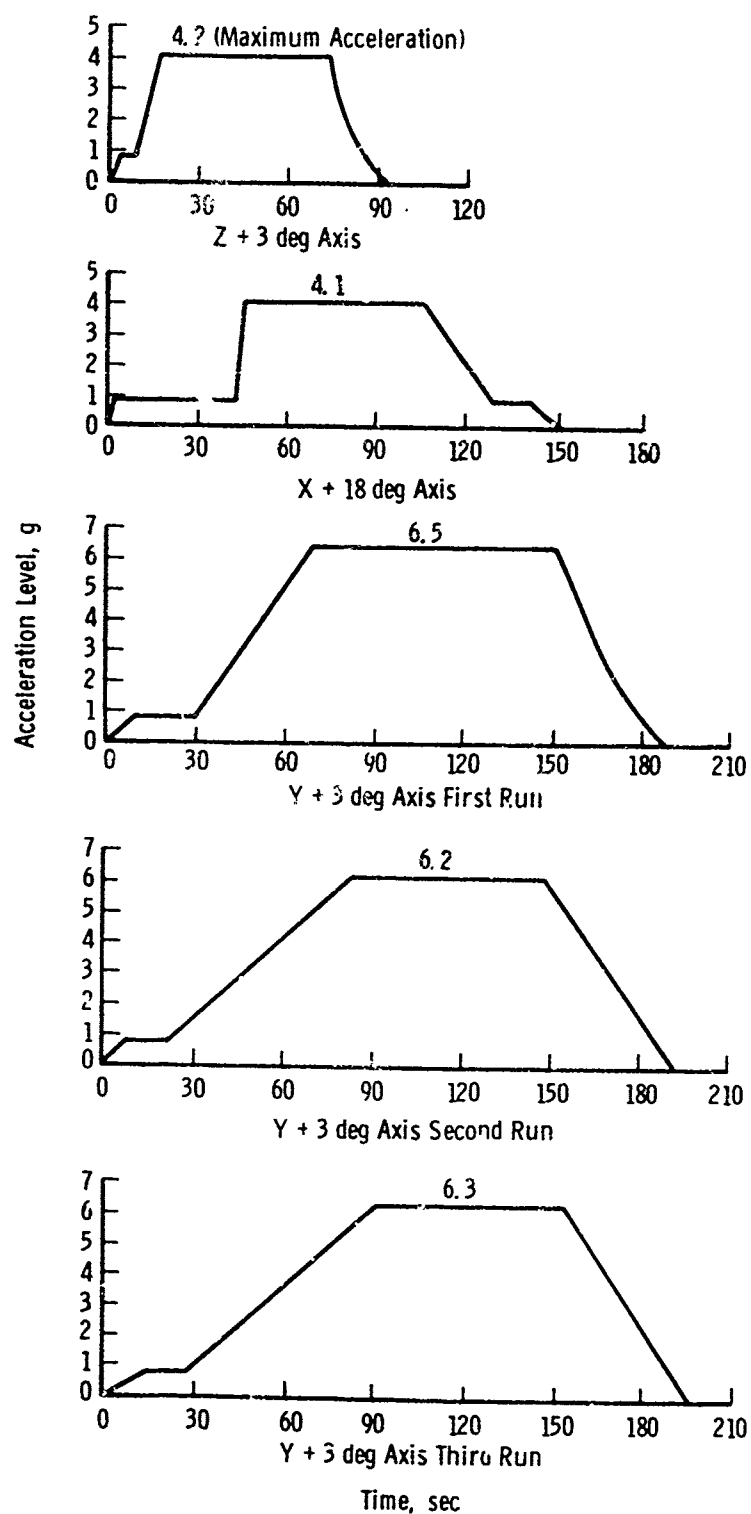


Figure 93. Acceleration versus Time



Figure 94. Thermal Blanket Separation

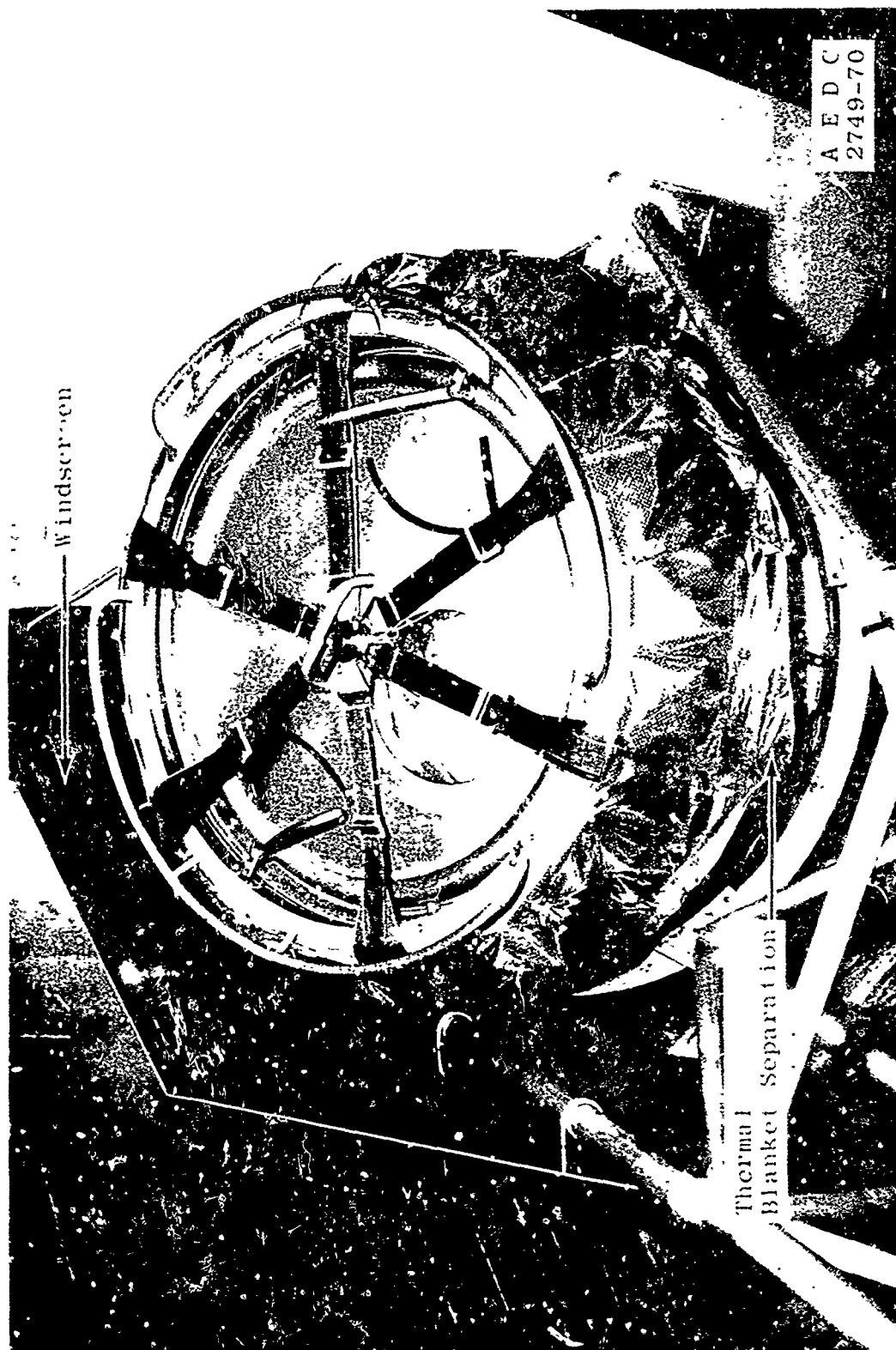


Figure 95. Acceleration Windscreen

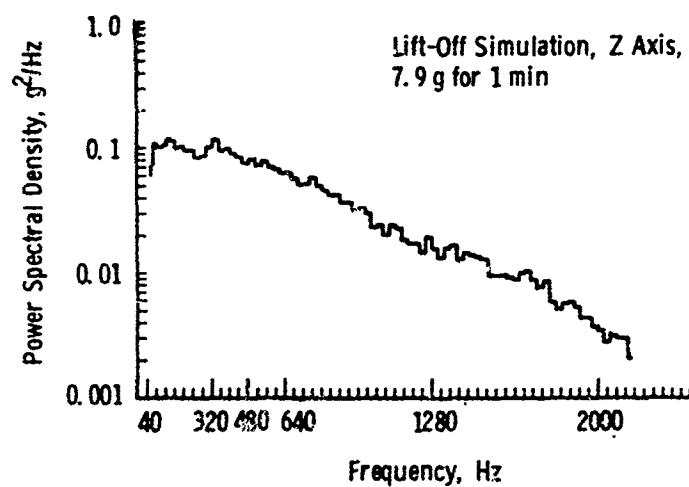
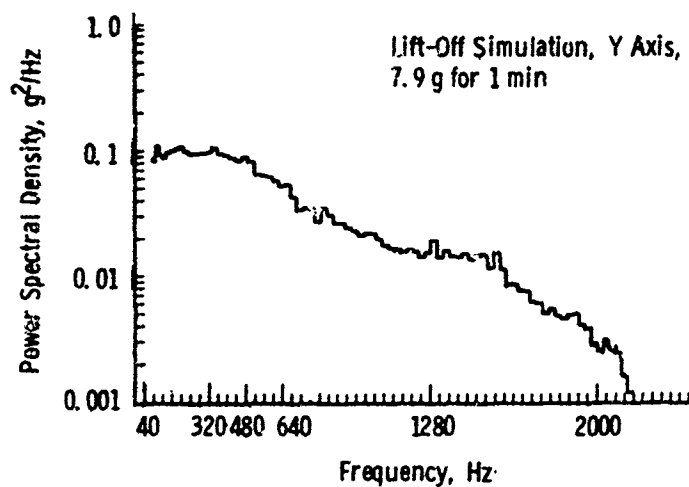
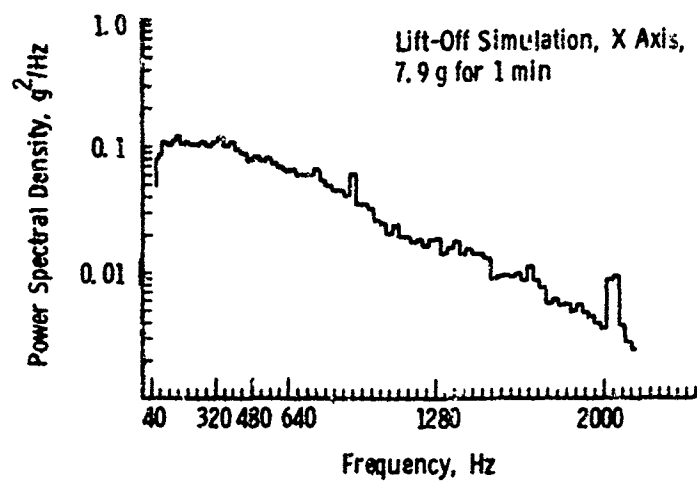


Figure 96. Vibration Spectrum

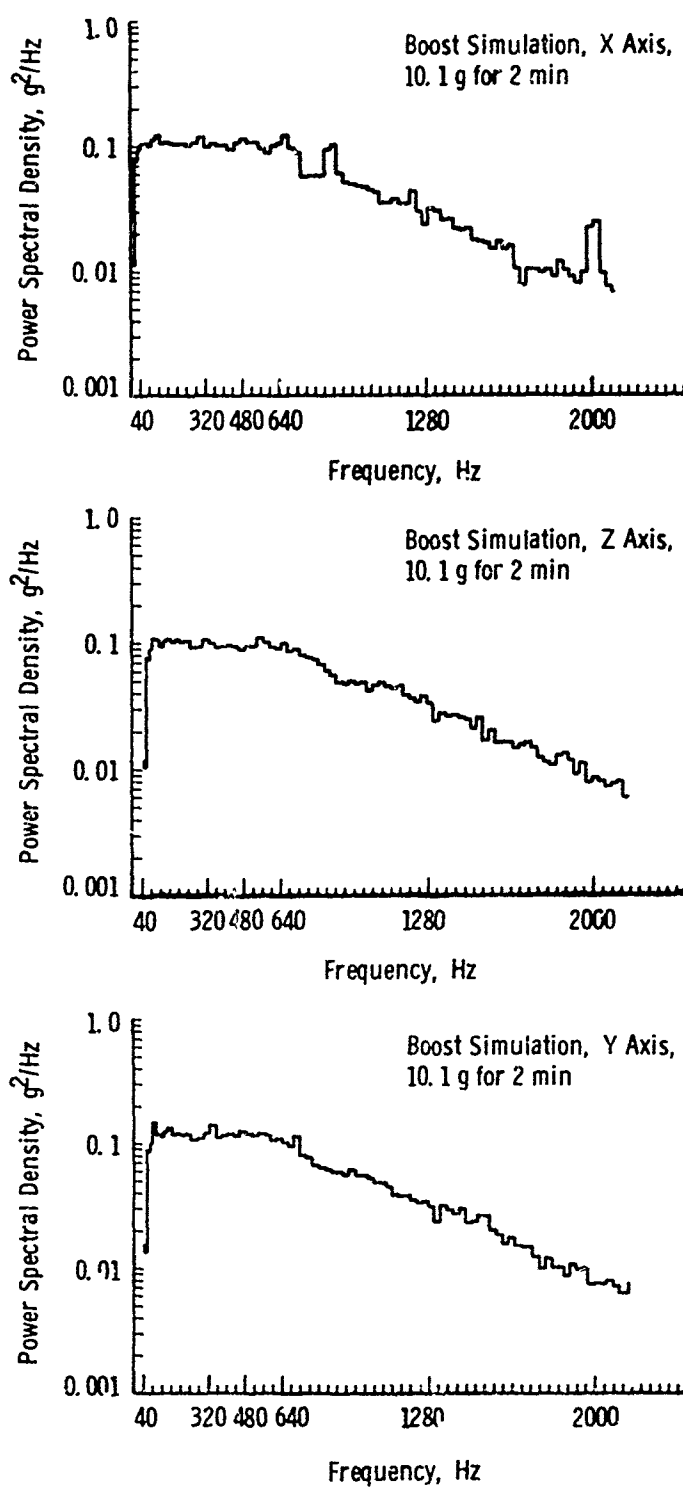


Figure 96. Concluded

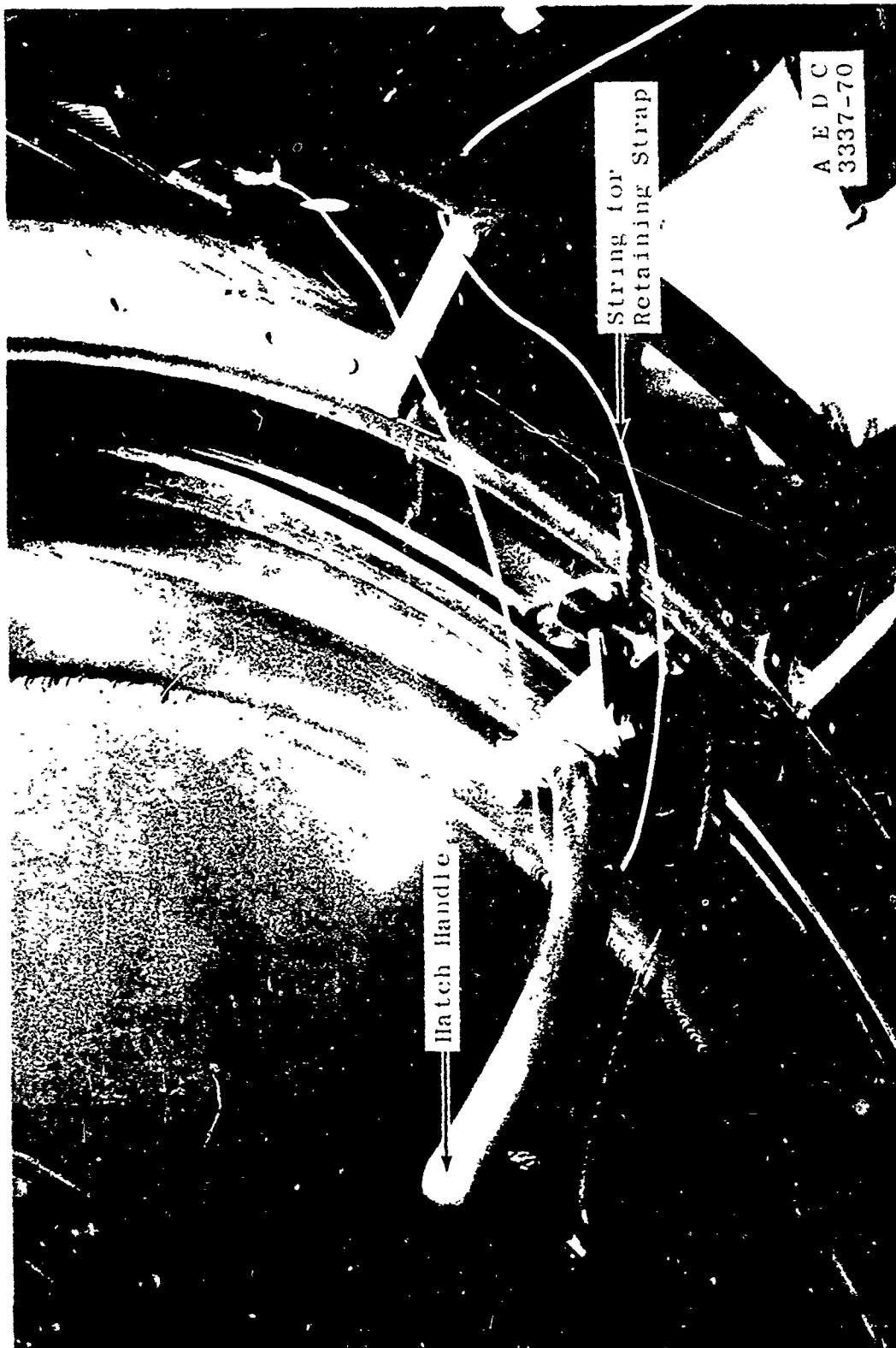


Figure 97. Deployment String Snag



Figure 98. Deployment Surface Scratch



Figure 99. Blister from Photographic Light



Figure 100. Solar Damage

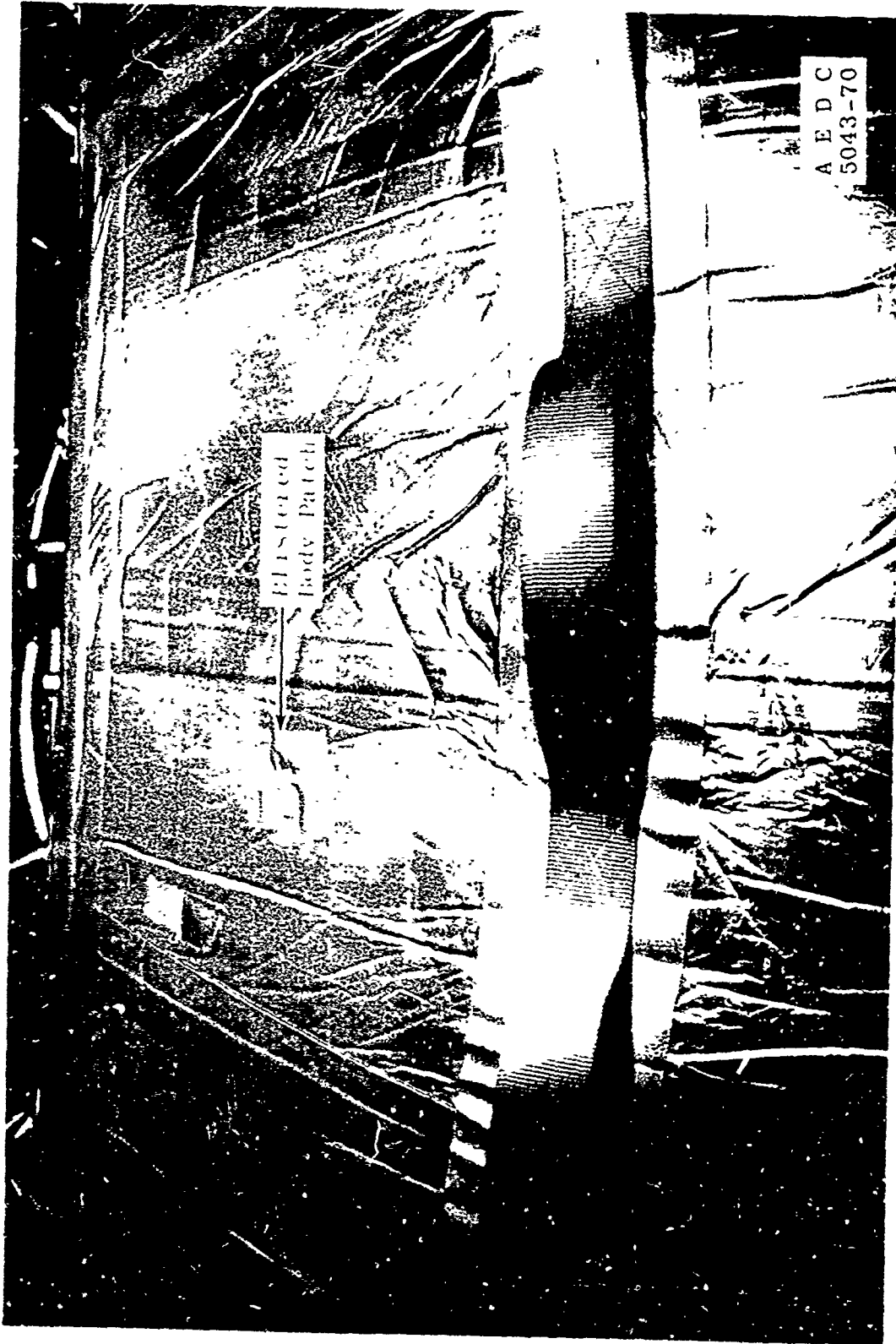


Figure 101. Solar Damage

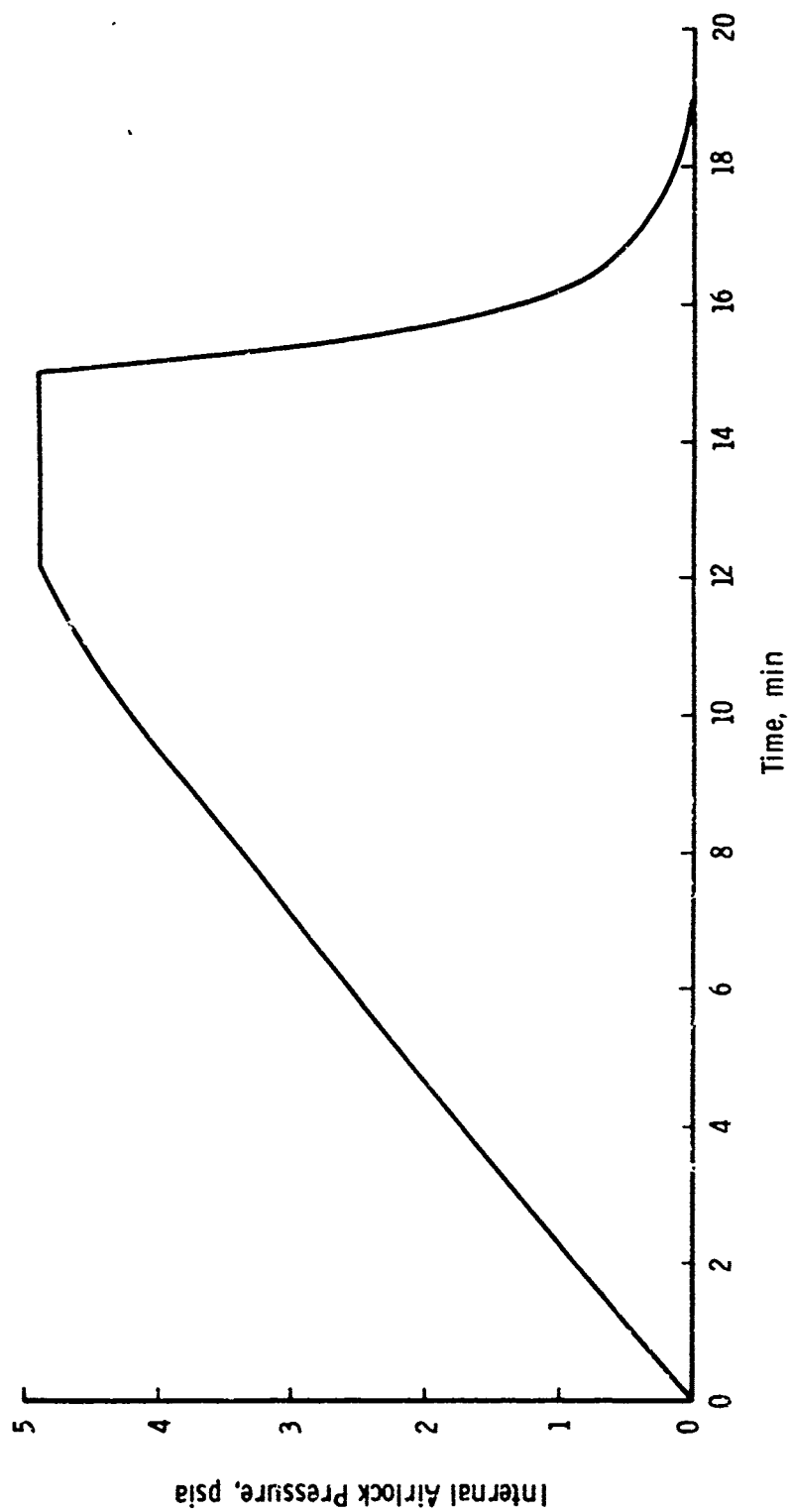


Figure 102. Typical Internal Airlock Pressure Cycle

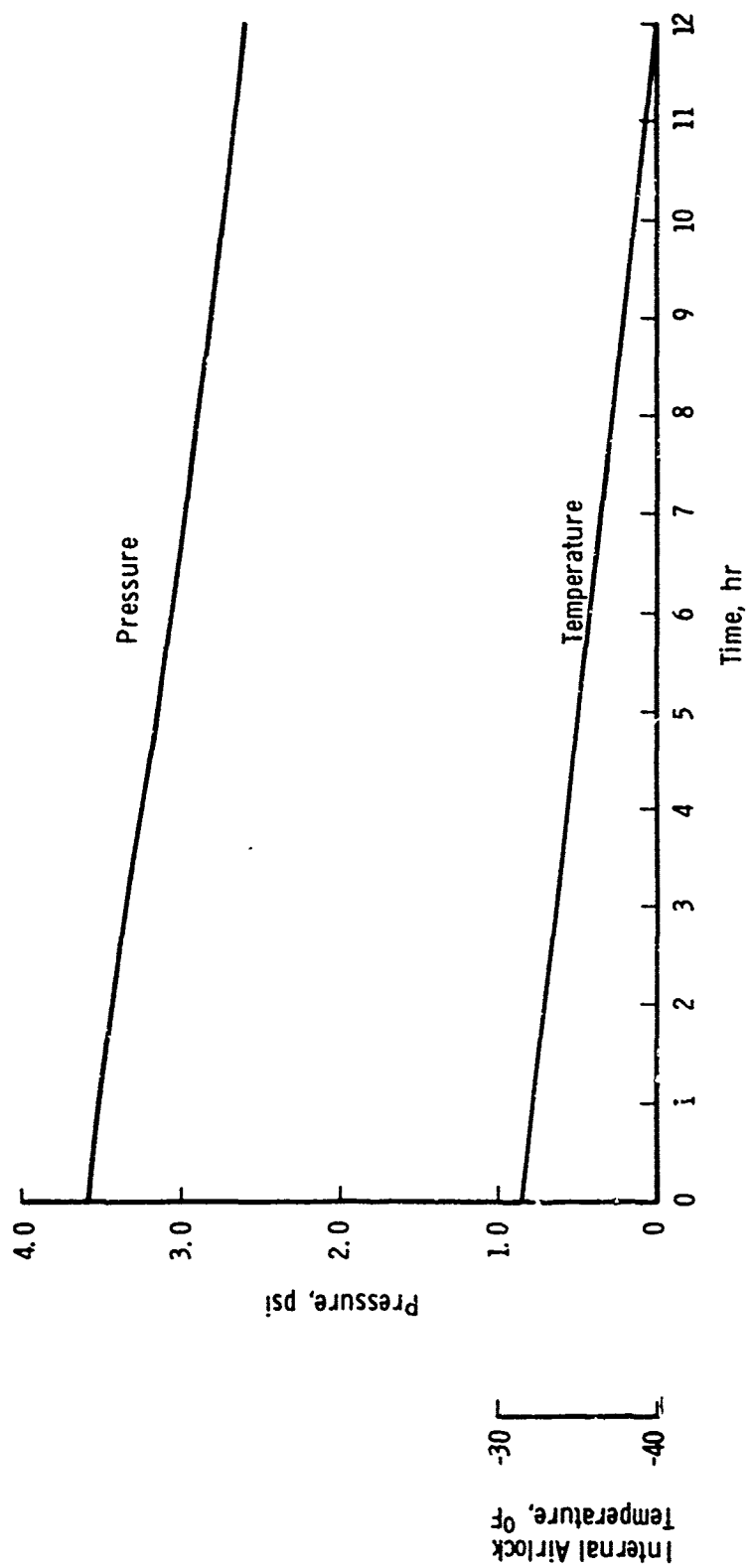


Figure 103. Pressure Degradation during 12-Hour Leak Test

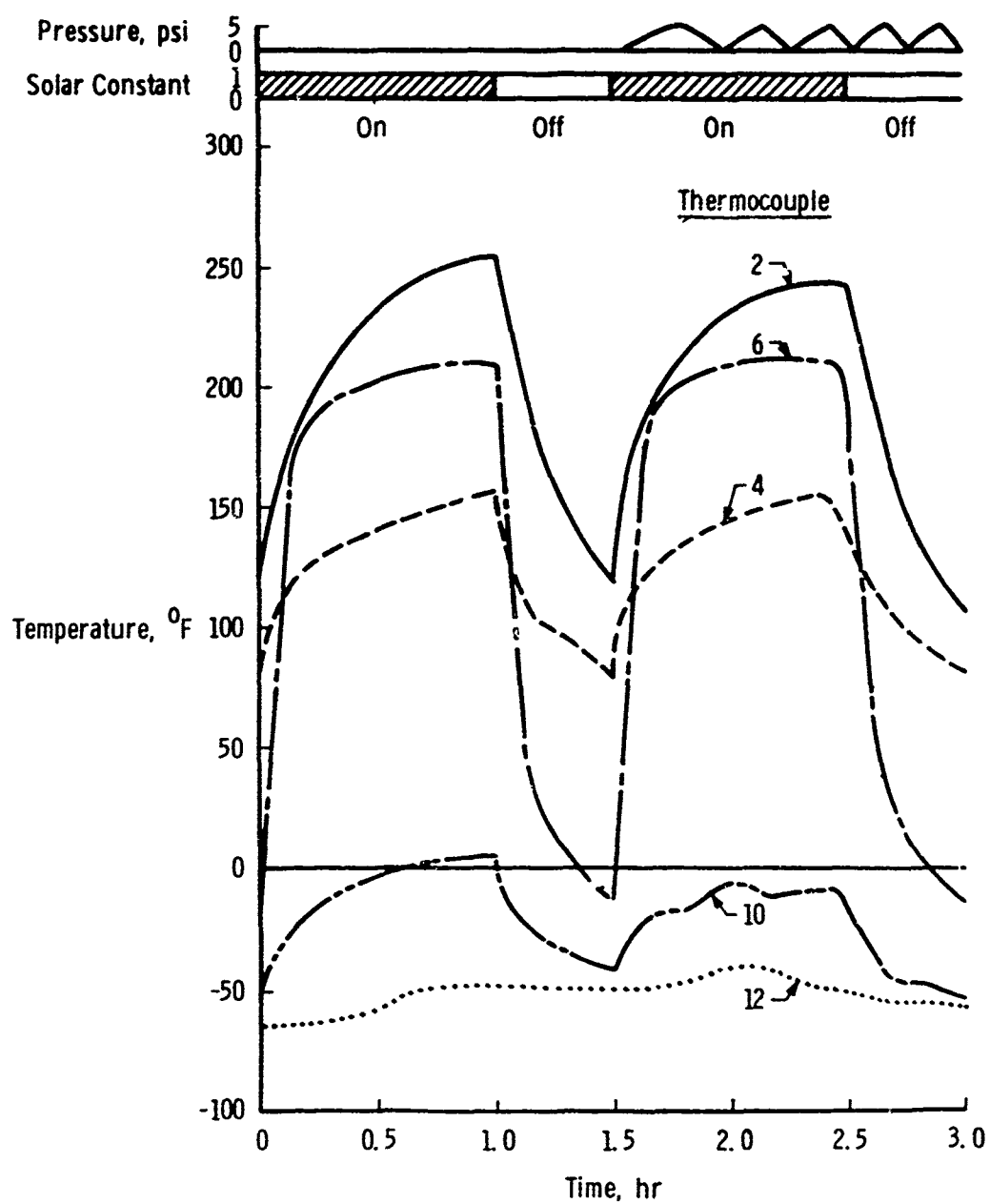


Figure 104. Temperature Change during Solar and Pressure Changes

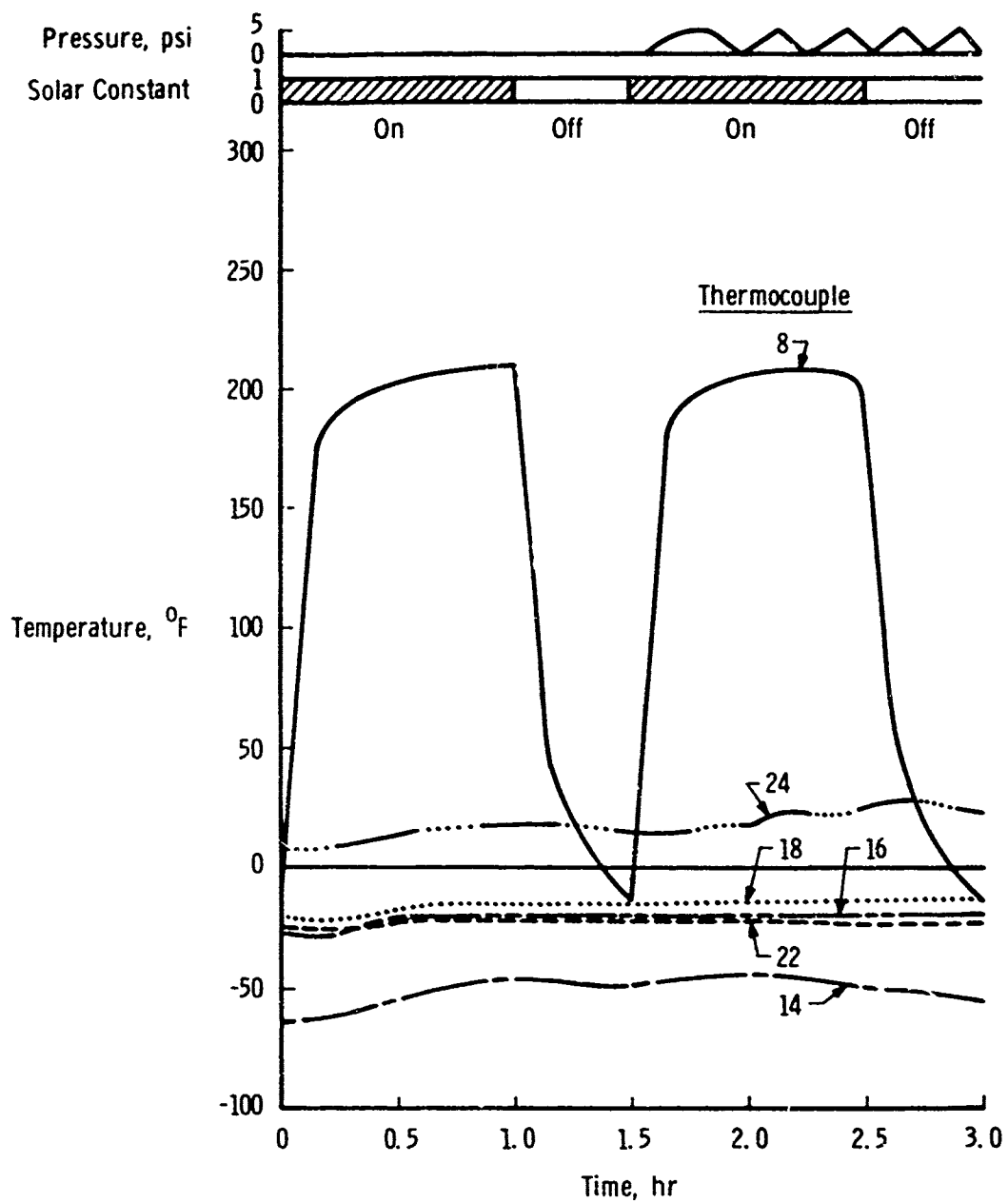


Figure 104. Continued

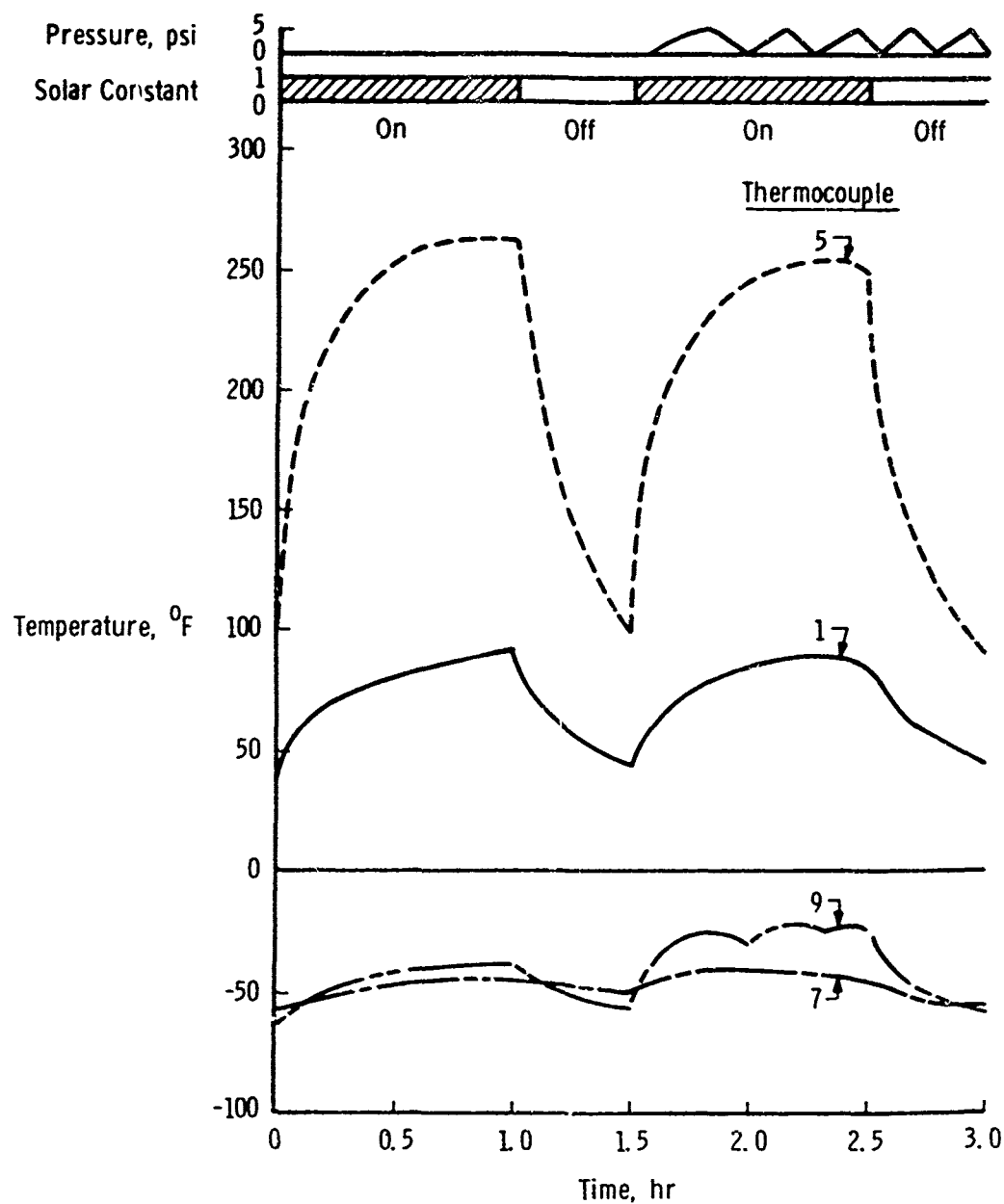


Figure 104. Continued

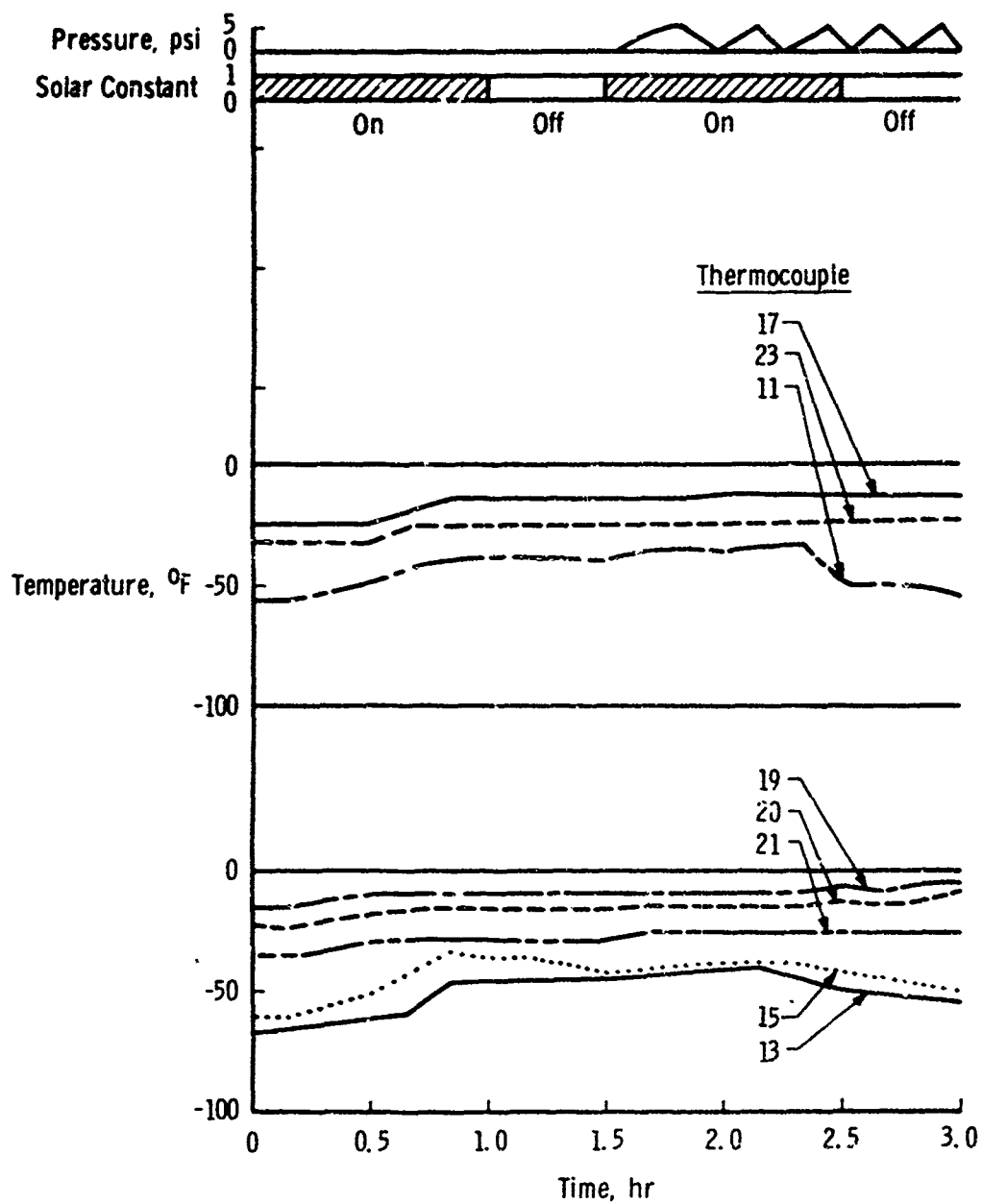


Figure 104. Concluded

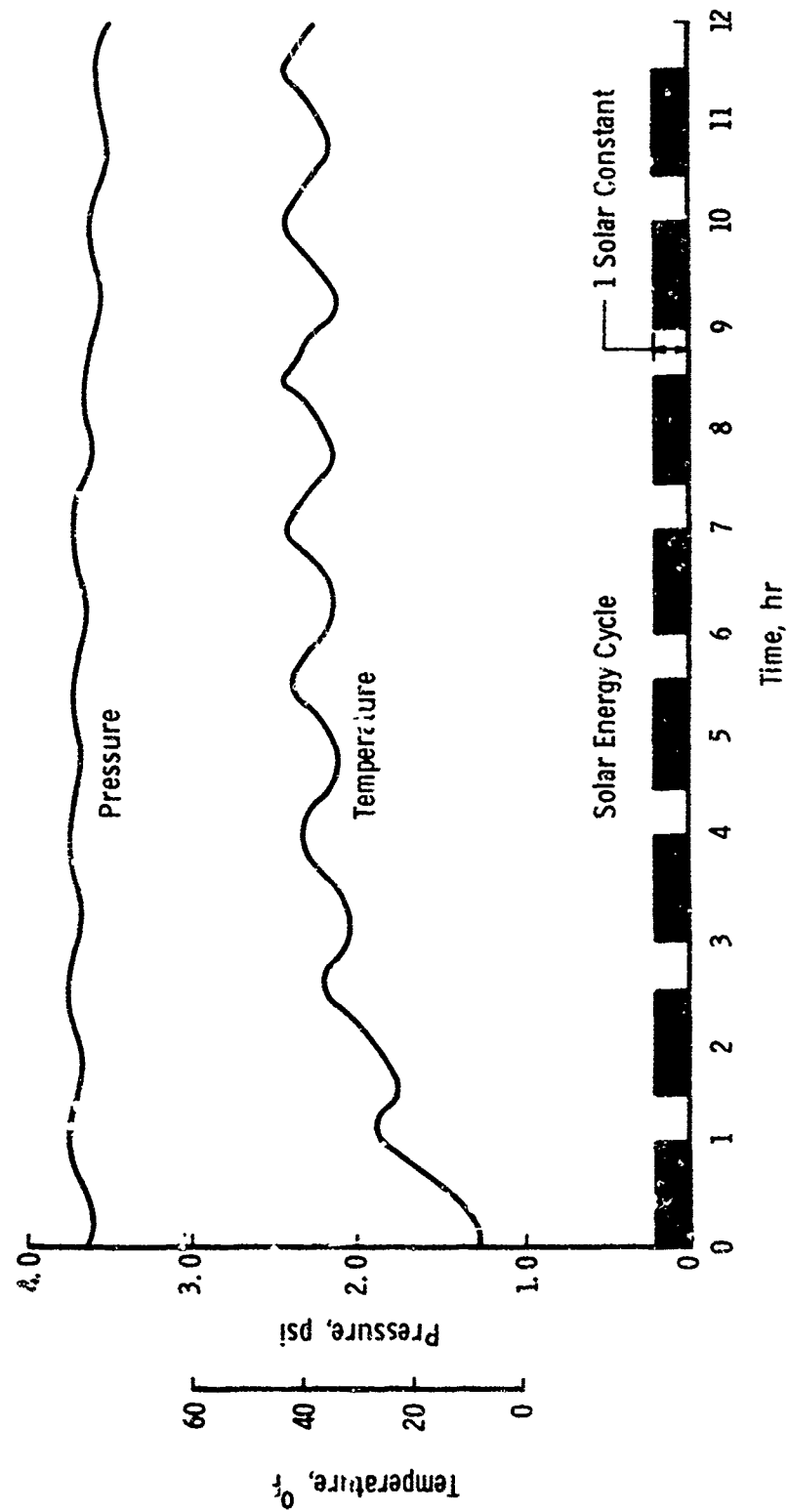


Figure 105. Pressure during Solar Leak Test

TABLE VII
RESONANCE VIBRATION RESPONSE

Channel	Location	Input Force		Resonant Force	
		Frequency, Hz	Magnitude, g	Magnitude, g	Ratio to Input, g
Y Axis April 3, 1970					
10	Battery Z	34	0.675	7.8	11.5
8	Battery X	44	0.60	4.65	7.8
9	Battery Y	81	0.645	4.5	7.0
2	Instrument Box	120	0.645	7.95	12.3
8	Battery X	116	0.60	2.55	4.3
8	Battery X	135	0.545	3.00	4.7
2	Instrument Box	215	0.72	5.25	7.2
2	Instrument Box	235	0.645	7.20	11.2
2	Instrument Box	325	0.60	3.75	6.3
4	Base Structure	395	0.60	3.75	6.3
2	Instrument Box	410	0.60	5.55	9.3
4	Base Structure	580	0.60	3.3	5.5
4	Base Structure	600	0.60	3.6	6.0
4	Base Structure	660	0.60	5.7	9.5
4	Base Structure	750	0.60	9.15	15.3
4	Base Structure	750	0.555	10.5	18.9
4	Base Structure	930	0.555	8.25	14.9
2	Instrument Box	1310	0.54	4.05	7.5
X Axis April 7, 1970					
9	Battery Y	41	0.795	9.45	11.9
8	Battery X	41	0.795	3.0	3.78
4	Base Structure	41	0.785	2.7	3.4
2	Instrument Box	41	0.785	3.3	4.15
9	Battery Y	75	0.75	10.0	13.35
2	Instrument Box	84	0.75	5.4	7.2
8	Battery X	84	0.75	2.4	3.2
2	Instrumentation	84	0.75	10.2	13.6
2	Instrumentation	103	0.75	8.7	11.6
4	Base Structure	103	0.75	8.4	11.2
9	Battery Y	103	0.75	2.55	3.4
8	Battery X	103	0.75	5.25	7.5
2	Instrument Box	182/193	0.72	12.9	17.95
2	Instrument Box	410	0.72	4.05	5.64
4	Base Structure	530	0.72	3.6	5.0
4	Base Structure	700	0.72	4.2	5.84
4	Base Structure	800	0.72	3.75	5.21
Z Axis April 8, 1970					
10	Battery Z	25.5	0.84	18.9	22.5
9	Battery Y	73	0.75	8.4	11.2
4	Base Structure	95	0.75	2.4	3.2
4	Base Structure	148	0.72	7.2	10.0
12	Pressure Battery (Vertical)	148	0.72	2.7	3.75
3	Pressure Battery (Horizontal and Normal)	175/185	0.75	2.85	3.8
4	Base Structure	175/185	0.75	1.8	2.4
5	Pressure Bulkhead	175/185	0.75	3.0	4.0
6	Pressure Battery (Horizontal and Normal)	175/185	0.75	3.9	5.2
12	Pressure Battery (Vertical)	175/185	0.75	4.2	5.6
5	Pressure Bulkhead	335	0.72	4.8	6.68

TABLE VIII
COLD ENVIRONMENT TEST*

Thermocouple No.	Cold Soak		Pressure Cycle		Leak Test	
	5/25/70 1000	5/25/70 2200	5/26/70 1730	5/27/70 0540	5/28/70 1000	5/28/70 2200
	Start	End	Start	End	Start	End
1		-46	-10	-36	-22	-36
2		-33	8	-32	-21	-33
3		-44	Open	Open	-27	-32
4		-34	2	-36	-21	-35
5		-34	5	-32	-20	-33
6		-19	-19	-41	-16	-37
7		-74	-55	-75	-45	-67
8		-24	-25	-45	-21	-41
9		-74	-71	-50	-37	-66
10		-75	-66	-60	-65	-63
11		-25	-68	-37	-39	-27
12		-76	-71	-68	-68	-63
13		-65	-57	-70	-60	-62
14		-56	-71	-60	-67	-65
15		-57	-50	-59	-64	-62
16		-42	4	-63	-43	-54
17		-41	2	-63	-44	-53
18		-27	17	-50	-27	-38
19		-43	12	-62	-43	-55
20		-31	11	-52	-36	-46
21		-42	8	-68	-42	-55
22		-28	33	-65	-20	-51
23		-43	10	-33	-45	-56
24		-37	12	-53	-39	-50

Ambient Room Temperature

*No Solar Heating

TABLE IX
SOLAR CYCLE DATA

Thermocouple Elapsed Time, min		Airlock Temperature, °F																	Solar		Off
		0	5	10	15	20	25	30	35	40	45	50	55	60	65	70	75	80			
1	3	26	38	44	49	50	57	61	63	67	71	73	75	53	43	39	35	32	28		
2	42	77	118	145	164	178	193	203	211	217	223	227	232	188	157	135	120	108	99		
3	30	29	43	54	65	72	84	93	100	107	113	118	123	124	115	126	120	107	92		
4	13	61	75	84	91	91	103	109	112	118	123	126	130	88	76	70	65	60	56		
5	37	106	150	150	193	206	218	227	233	240	245	249	253	176	143	122	109	98	88		
6	-15	167	199	197	201	202	206	206	206	209	210	211	211	72	29	7	-4	-12	-17		
7	-59	-61	-55	-55	-54	-57	-51	-53	-53	-52	-51	-50	-50	-53	-59	-59	-60	-60	-59		
8	-15	144	179	189	195	196	200	202	202	205	205	206	206	78	35	12	-1	-10	-17		
9	-65	-61	-53	-51	-49	-50	-47	-45	-45	-44	-43	-42	-42	-49	-57	-60	-63	-64	-65		
10	-55	-31	-20	-15	-9	-9	-6	-4	-3	-2	-1	0	-1	-27	-43	-50	-53	-55	-57		
11	-51	-55	-68	-71	-63	-63	-57	-54	-55	-55	-54	-54	-54	-54	-59	-59	-59	-58	-57		
12	-64	-67	-66	-67	-64	-65	-64	-63	-62	-61	-61	-60	-59	-60	-65	-65	-66	-66	-66		
13	-64	-67	-66	-66	-65	-67	-66	-66	-65	-65	-65	-64	-64	-64	-69	-68	-68	-68	-68		
14	-58	-60	-59	-60	-63	-59	-57	-57	-57	-56	-56	-55	-55	-56	-62	-62	-61	-62	-62		
15	-59	-61	-60	-59	-62	-57	-55	-54	-53	-52	-51	-50	-50	-50	-55	-56	-56	-57	-57		
16	7	4	3	3	2	0	0	-1	-1	-2	-3	-2	-4	-4	-9	-10	-10	-10	-11		
17	5	2	3	3	1	1	2	1	1	0	0	0	-1	-2	-7	-8	9	-10	-10		
18	21	17	17	17	11	14	13	12	11	10	10	9	9	7	2	2	1	0	0		
19	15	12	11	10	6	7	7	6	5	4	3	3	3	2	-3	-3	-4	-5	-5		
20	15	12	11	10	6	7	7	6	5	5	3	3	3	-5	-3	-3	-4	-5	-5		
21	11	8	6	6	2	3	3	2	1	0	-2	-1	-2	-8	-9	-9	-10	-11	-11		
22	40	38	36	35	32	3	33	32	31	31	29	29	28	23	22	22	21	20	19		
23	11	9	7	6	3	4	3	2	1	1	-1	-1	-2	-8	-8	-8	-9	-10	-10		
24	15	13	12	12	9	11	11	11	12	12	12	12	13	9	8	8	9	8	7		
		On																	Off		

TABLE IX (Continued)

Elapsed Time, min		Airlock Temperature, °F																Solar	
		95	100	105	110	115	120	125	130	135	140	145	150	155	160	165	170		
Thermocouple	1	54	62	65	68	68	73	77	79	82	83	84	85	64	58	53	44	40	39
	2	154	182	197	207	214	224	234	238	241	243	245	247	201	175	155	131	120	112
	3	92	99	105	119	123	120	128	133	136	139	182	145	143	137	152	126	115	111
	4	103	112	117	121	123	128	134	137	140	143	144	147	105	96	90	80	75	72
	5	183	210	222	232	238	247	256	258	259	262	263	264	185	157	138	117	107	100
	6	178	196	203	206	207	210	215	211	211	212	210	210	72	35	16	-3	-10	-13
	7	-56	-52	-51	-50	-54	-51	-49	-49	-48	-48	-47	-46	-49	-50	-50	-55	-55	-53
	8	167	188	197	201	202	205	208	207	207	208	206	206	78	41	21	0	-8	-13
	9	-55	-48	-46	-45	-48	-44	-42	-42	-40	-40	-39	-39	-46	-50	-52	-57	-60	-58
	10	-23	-12	-9	-6	-7	-3	0	0	1	1	2	2	-26	-36	-42	-50	-52	-51
	11	-56	53	-54	-53	-56	-53	-52	-51	-51	-50	-50	-49	-50	-50	-50	-54	-54	-51
	12	63	-61	-62	-60	-63	-60	-58	-57	-57	-57	-55	-55	-55	-56	-57	-62	-62	-60
	13	-66	-64	-63	-63	-67	-64	-63	-62	-62	-61	-60	-60	-60	-60	-60	-64	-64	-62
	14	-58	-57	-56	-55	-59	-56	-55	-54	-54	-53	-52	-52	-53	-54	-54	-58	-68	-57
	15	-58	-55	-55	-54	-56	-52	-51	-50	-49	-48	-47	-46	-47	-47	-48	-54	-54	-53
	16	-10	-9	-9	-9	-13	-11	-11	-11	-11	-11	-12	-12	-12	-12	-12	-16	-16	-14
	17	-9	-8	-8	-7	-10	-8	-8	-8	-8	-8	-8	-7	-8	-8	-8	-9	-13	-14
	18	1	1	1	1	-3	-1	-2	-4	-3	-3	-3	-3	-3	-3	-4	-9	-8	-7
	19	-4	-3	-3	-3	-7	-4	-5	-5	-5	-5	-5	-5	-5	-5	-6	-5	-10	-9
	20	-4	-3	-4	-4	-7	-6	-6	-7	-7	-7	-6	-7	-7	-7	-7	-7	-12	-11
	21	-10	-9	-9	-10	-13	-12	-12	-13	-14	-14	-13	-14	-14	-15	-15	-19	-19	-17
	22	20	21	20	20	16	18	16	17	16	15	15	15	15	13	13	12	6	8
	23	-9	-9	-9	-9	-13	-11	-12	-12	-13	-12	-13	-13	-13	-13	-13	-14	-18	-17
	24	9	10	10	11	8	11	13	13	13	14	15	15	15	16	15	15	11	12
		On																Off	

TABLE IX (Concluded)

Elapsed Time, min Thermocouple		Airlock Temperature, °F																			
		185	190	195	200	205	210	215	220	225	230	235	240	245	250	255	260	265	270		
Solar	1	60	65	69	70	72	75	77	79	80	82	83	84	63	57	52	47	43	39		
	2	150	179	199	209	218	227	232	236	239	242	243	245	201	175	155	137	125	113		
	3	148	172	197	213	221	227	231	235	238	242	243	245	146	139	132	125	117	110		
	4	113	120	123	125	128	133	136	138	141	143	145	148	106	97	91	85	79	73		
	5	173	206	223	232	238	245	250	253	256	258	260	262	184	155	136	121	110	99		
	6	153	187	196	199	201	204	204	204	205	205	205	206	70	32	12	0	-8	-14		
	7	-50	-50	-49	-51	-51	-50	-50	-50	-50	-49	-49	-49	-50	-52	-53	-52	-53	-54		
	8	144	180	191	194	197	200	201	201	201	202	201	202	203	76	38	18	3	-7	-14	
	9	-51	-47	-45	-47	-47	-45	-45	-44	-43	-43	-42	-42	-42	-48	-52	-55	-57	-59	-60	
	10	-24	-13	-9	-8	-7	-4	-4	-3	-3	-2	-2	-2	-2	-28	-38	-44	-48	-51	-54	
	11	-50	-50	-50	-54	-54	-53	-54	-53	-53	-53	-53	-53	-52	-52	-52	-53	-53	-53	-54	
	12	-59	-59	-59	-62	-62	-61	-61	-60	-60	-60	-59	-58	-58	-59	-60	-60	-61	-61	-62	
	13	-61	-62	-62	-65	-65	-64	-65	-64	-64	-64	-64	-63	-63	-62	-63	-63	-63	-63	-63	
	14	-55	-55	-55	-57	-57	-57	-57	-57	-56	-56	-56	-56	-55	-56	-57	-57	-57	-58	-57	
	15	-53	-54	-54	-56	-55	-54	-54	-52	-51	-50	-50	-50	-49	-50	-50	-51	-53	-54	-55	
	16	-14	-14	-15	-18	-18	-18	-19	-19	-19	-19	-19	-19	-19	-19	-19	-19	-20	-20	-20	
	17	-12	-12	-12	-14	-14	-14	-14	-14	-14	-14	-14	-14	-14	-14	-14	-15	-17	-17	-17	
	18	-7	-7	-8	-10	-11	-11	-12	-12	-12	-12	-12	-12	-12	-12	-13	-13	-14	-14	-14	
	19	-8	-7	-8	-10	-11	-10	-11	-11	-11	-11	-11	-11	-11	-11	-11	-11	-11	-11	-11	
	20	-9	-10	-10	-13	-14	-13	-14	-14	-14	-14	-14	-14	-15	-15	-15	-15	-15	-15	-15	
	21	-13	-17	-13	-21	-22	-22	-22	-22	-22	-23	-23	-23	-23	-24	-24	-24	-25	-25	-25	
	22	8	8	7	3	3	3	2	2	1	0	0	0	-1	-1	-2	-2	-3	-4	-4	
	23	-16	-17	-17	-20	-21	-20	-21	-21	-21	-22	-22	-22	-22	-22	-23	-23	-23	-23	-23	
	24	12	13	13	10	5	11	10	11	11	11	12	13	13	13	13	13	13	12	11	
		On																		Off	

APPENDIX XI

ENGINEERING REPORTS OF DEPLOYMENT
VERIFICATION TESTS PERFORMED AT GAC

ENGINEERING REPORTS OF DEPLOYMENT
VERIFICATION TESTS PERFORMED AT GAC

Initial deployment tests of the airlock at low temperature disclosed an unsatisfactory condition.

In the end analysis, it became necessary to verify whether the locking of the folded material was caused by the low temperature effect on the materials or a result of long-term storage in a packaged state.

The engineering memoranda in this appendix cover the deployment testing of an airlock which had remained in a packaged state for 9 months, followed by a low temperature deployment test of an airlock with modifications added to cure the low temperature problem.

ENGINEERING MEMORANDUM

23 September 1969
SP-7099

Subject: D-21 Airlock Experiment Vacuum Chamber Deployment
Failure Analysis Report

Reference: (a) SP-7087 dated 4 September 1969 - Thermal Analysis -
Effect of Apollo Telescope Mount on D-21 Airlock
Location

INTRODUCTION AND SUMMARY

The initial deployment test in the vacuum chamber at Arnold Engineering Development Center (AEDC) resulted in some damage to the expandable structure. The deployment was intermittent and final expansion step was rather sudden.

The primary reason for the erratic deployment is attributed to low temperature effects on the materials, compounded by an excessive pressure rise prior to full preshaping of the structure.

A review of all pertinent factors indicates that the environmental test procedures should be revised to more realistically simulate the orbital space environment as well as some design improvements to the airlock.

For design improvement, it is planned to add a thermal insulation blanket to the packaged state of the airlock and to revise the pressurization system to a much slower flow rate from a limited supply container. The thermal environment values are being revised in the Qualification Test Procedures to reflect the thermal analysis results.

TEST DESCRIPTION

The deployment test was conducted using the Qualification Test Unit (GAC Serial No. 1). The airlock was installed in the Mark I vacuum chamber on 17 June 1969 and pump down was started. The following day, the LN₂ cold wall cool down was started at 11:30 a.m. and deployment was initiated at 5:45 p.m. At the time of deployment, a test thermocouple located on the exterior of the hatch read -85° F, and the temperature sensors built into the airlock expandable structure were

reading +28° F to +42° F. The test was intended to be conducted at a temperature -65° F. Internal airlock pressure readings were recorded during deployment and are presented as Figure 106.

Movies were taken of the airlock deployment and correlated to the pressure recordings (Figure 107).

ANALYSIS OF DATA

Based on the above temperature readings, it was theorized that the exposed expandable structure must have reached -85° F or even colder. The difference in temperatures at the various locations could be attributed to the fact that all airlock temperature sensors are packaged well into the interior of the folded material in the launch configuration. This assumption is further supported by subsequent thermal analysis. The micrometeoroid barrier is a good insulator and will keep the interior of the airlock fairly warm for extended cold soak periods. The exterior will chill down quite rapidly and this is what apparently occurred during the vacuum chamber test. It is therefore reasonable to assume that the outer inch or so of exposed expandable structure was as low as -85° F.

Movies taken of the airlock deployment were analyzed by comparing framing speeds against pressure rise recordings. Results are correlated on Figure 106. The sudden deployment event corresponds to the sharp drop in pressure at approximately 6.0 seconds after start.

From the above evidence, it appears that at least a portion of the expandable structure was in a "semi-frozen" state at the time of deployment. An excessive pressure rise occurred with the airlock restricted to approximately 30 percent of its expanded volume by the trapped folds of material. This pressure finally produced enough force to unwrap the folds but at this point the conversion of pneumatic potential energy to kinetic energy occurred so rapidly that damage to the structure was incurred in the unfolding process.

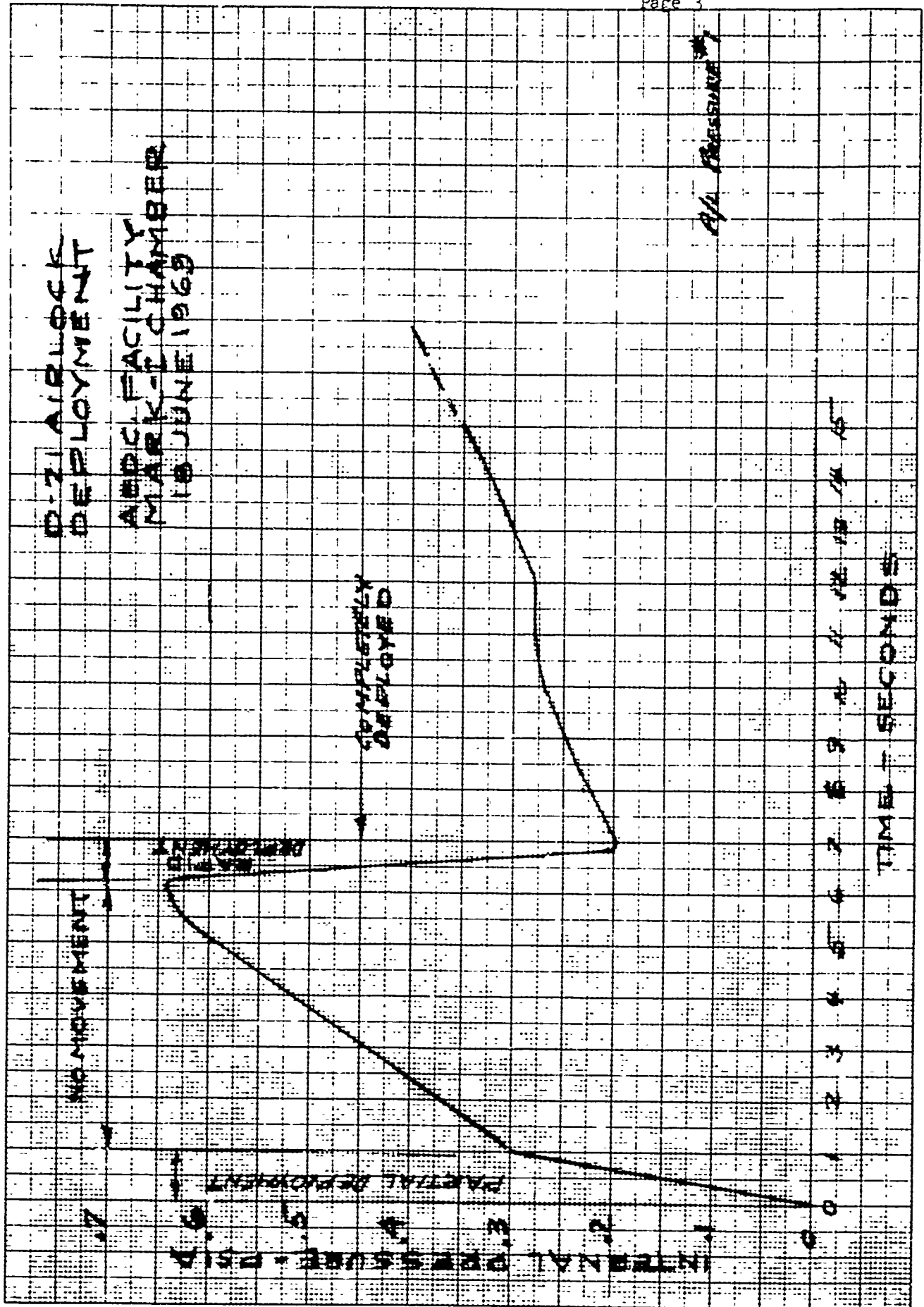


Figure 106



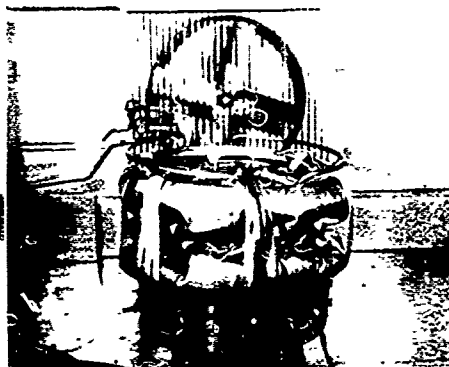
TEST CHAMBER



PACKAGED



PARTIALLY DEPLOYED



HARNESS RELEASED



PARTIALLY DEPLOYED



FULLY DEPLOYED

Inspection of the airlock disclosed failure of the filament wound structure in two areas, several areas of delamination of the bladder from the filament wound cage, and a number of rips in the outer cover and micrometeoroid barrier. A typical rupture of the outer surface is shown on Figure 108.

SUBSTANTIATION TESTS:

General

In order to add confidence to the accuracy of the above analysis, it was decided to conduct additional low temperature material tests and conduct a deployment test in a vacuum chamber at room temperature.

Low Temperature Material Tests

The results of low temperature tests on the micrometeoroid barrier disclosed an unexpected effect. This data is shown on Figure 109. Originally, the design had been based on 1.0 pcf polyurethane foam for this layer and low temperature verification tests of flexibility had been carried out on composite sections of the airlock structure. Flexibility had been maintained well below -65°F and this temperature was specified for environmental qualification testing. Subsequently, fire retardant characteristics were added to the material requirements as a result of the Apollo fire. At the time, the only polyurethane foam which met the new "self-extinguishing in air" requirement was available only in 2.0 pcf density. An erroneous assumption was made that the low temperature characteristics would be reasonably close to that of the 1 pcf foam. As can be seen from Figure 109, the 2.0 pcf foam is approximately 15 times stiffer in compression modulus at -65°F , whereas the difference is insignificant at room temperature. There appears to be an abrupt change in the stiffness characteristics at -20°F to -25°F .

Sections of the expandable structure using both 1.0 pcf and 2.0 pcf foam were cold soaked to varying temperatures as low as -100°F in the folded state. These were then manually unfolded to determine the degree of stiffness in a qualitative sense. The 1.0 pcf foam section was obviously less stiff at any temperature. Although the



Figure 108. Typical Tear of Outer Cover Caused by Low Temperature
Deployment

DATE _____
REV DATE _____
REV DATE _____

GOODYEAR AEROSPACE
CORPORATION
AKRON 15, OHIO

SP-7099
PAGE Page 6
CODE IDENT NO 25500

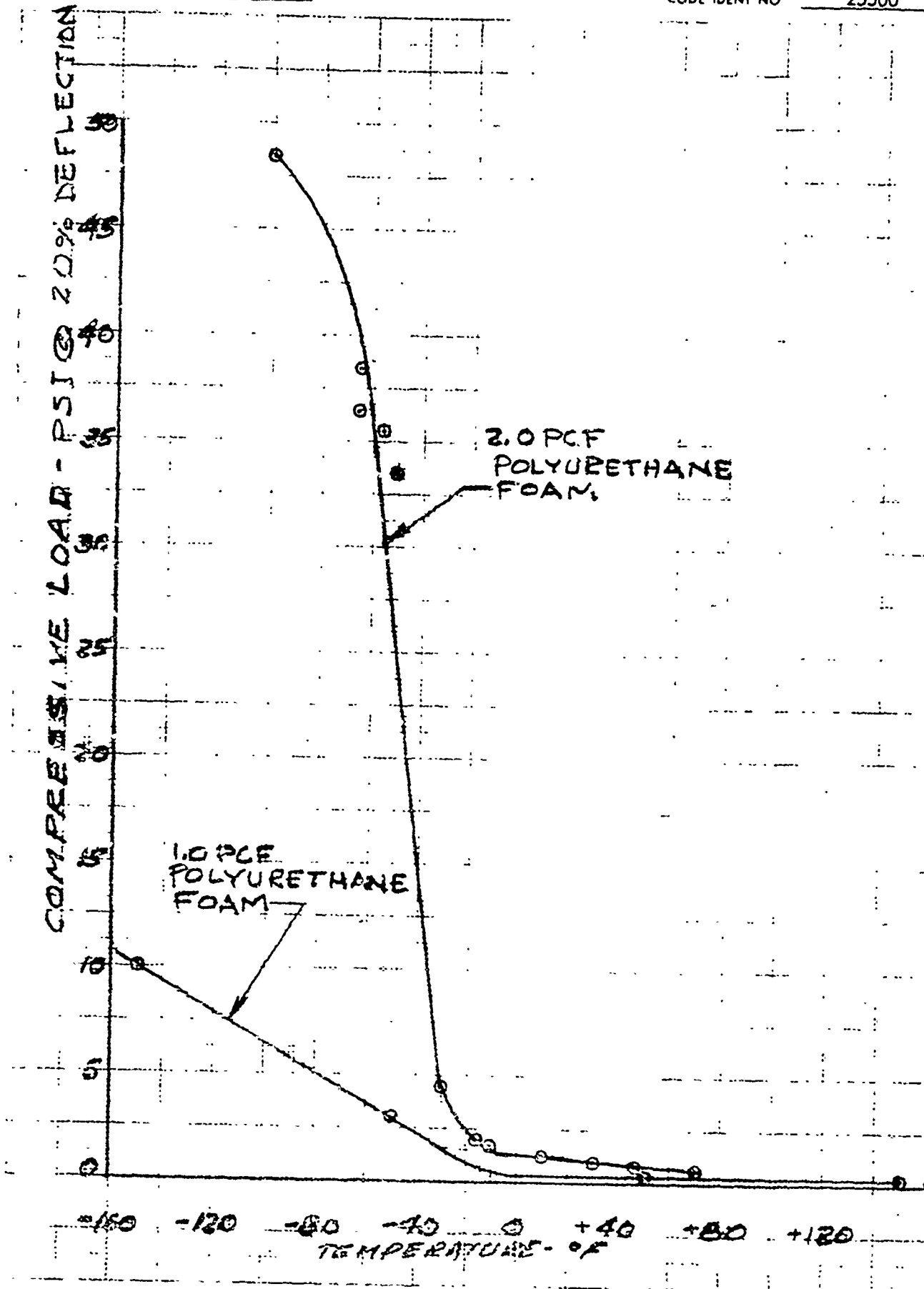


Figure 109

2.0 pcf foam section did exhibit considerable stiffness increase below -20° F, it did not become brittle or crack under manual manipulation.

Deployment Verification Test

It was considered important to establish whether the locking of the folded material was a result of the low temperature effect on the material or a result of long-term storage in the packaged condition. The crew training unit was selected as the proper test article to determine this. This unit had remained in a packaged state since delivery to Wright Field in October 1968. (Approximately 9 months storage)

The unit was returned to GAC and was tested in the vacuum chamber, 23 June 1969.

A special pressurization system as shown on Figure 110 was connected to the inflation manifold. The reason was to duplicate the design flow discharge rate but to reduce the total capacity of the system to reduce risk of damage if hang up occurred during deployment. A standby system of regulated N_2 was also connected. This system is used to maintain shape during the repressurization of the vacuum chamber.

The unit was also deployed vertically upwards instead of downwards as was the case at AEDC in order to eliminate the benefit of gravity aiding the unfolding of the material. The unit was successfully deployed at a chamber pressure of .02 psia and room temperature. The pressure rise data is shown on Figure 111 together with photographs of the deployment sequence.

The deployment under either room temperature or low temperature environment shows a characteristic pressure peak part way through the deployment cycle. However, this peak for the room temperature case is only one-sixth the value of that for the low temperature deployment. The deployment is also considerably slower with no pronounced hangup of the packaging folds.

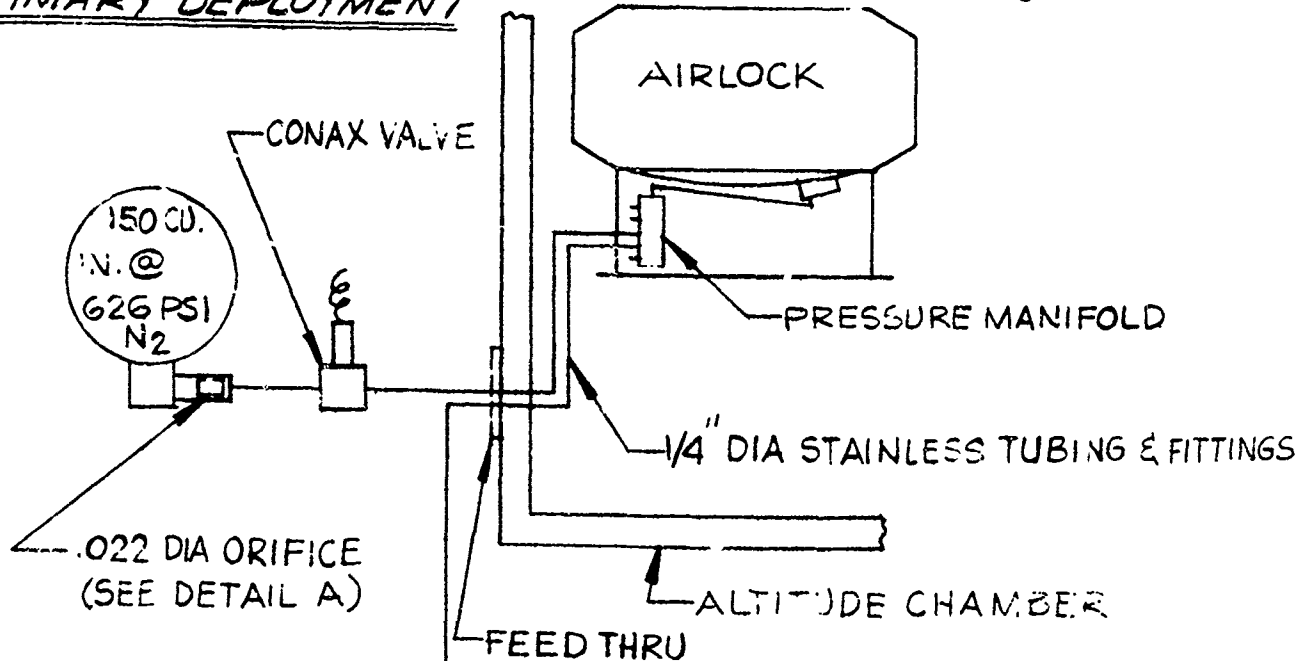
CONCLUSIONS

1. The results of the room temperature deployment test definitely establish low temperature as the primary cause for the unsatisfactory deployment at AEDC.

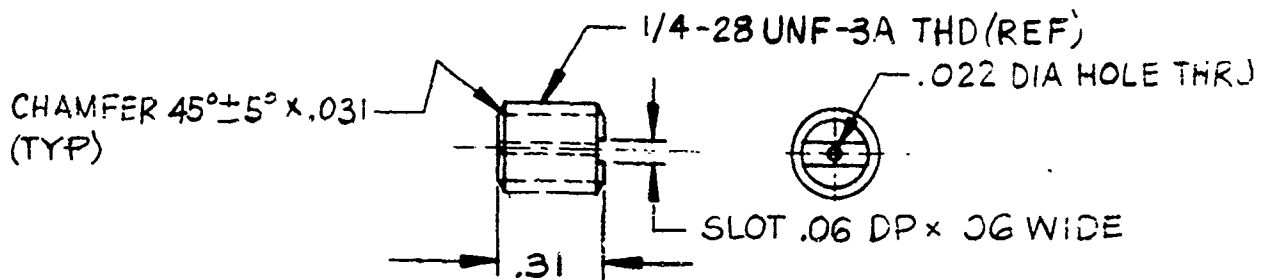
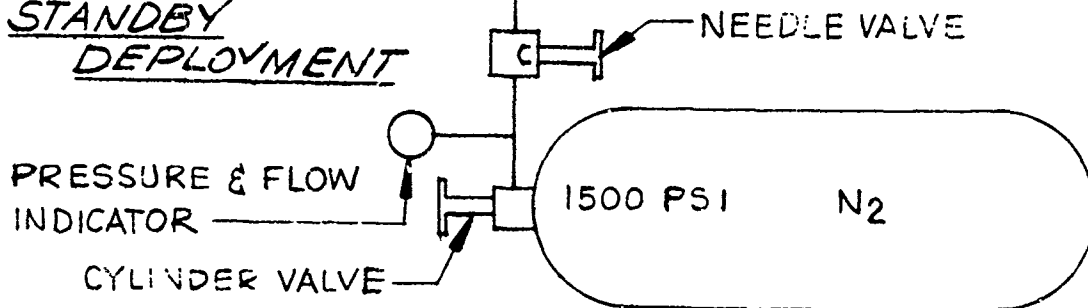
DEPLOYMENT TEST SCHEMATIC

SP-7099
Page 8

PRIMARY DEPLOYMENT



STANDBY DEPLOYMENT



MAKE FROM AN4C-4A BOLT
DETAIL A

Figure 110

DATE _____
 REV DATE _____
 REV DATE _____

GOODYEAR AEROSPACE
 CORPORATION
 AKRON, OHIO

SP-7099
 PAGE Page 9
 CODE IDENT NO 25500

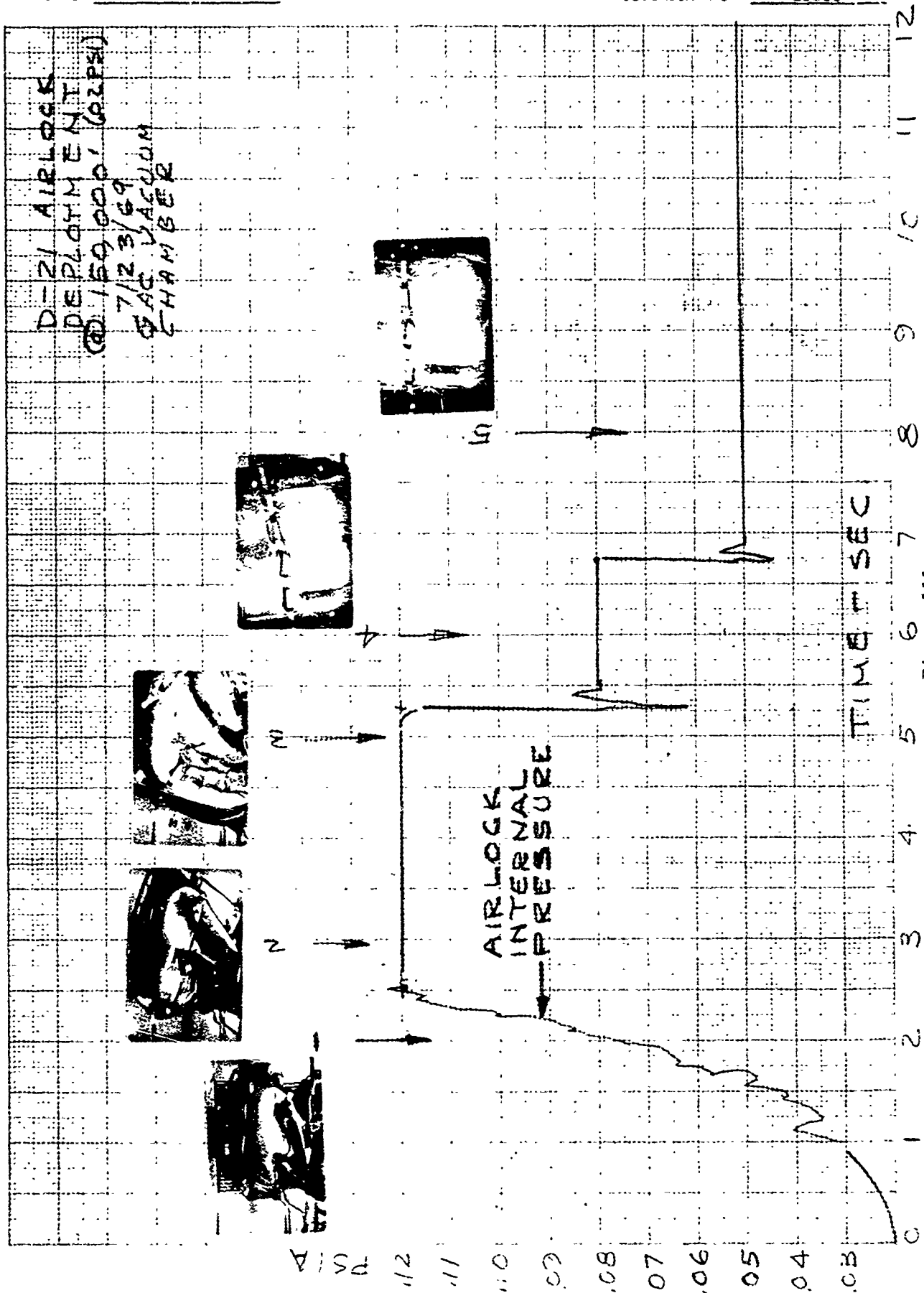


Figure 111

2. Low temperature materials tests establish -20° F as the minimum temperature at which deployment should be attempted with the current airlock structure. (This temperature limitation does not apply after deployment.)
3. A reduction in initial flow rate of the inflation gas could be of some benefit to minimize intermittent deployment effects.

REMEDIAL ACTION BEING TAKEN

1. The airlock in the packaged shape will incorporate a multilayer insulation cover over the expandable structure to maintain orbital temperatures at time of deployment warmer than -20° F. (The thermal blanket effect was analyzed and reported in Reference a.)
2. The airlock pressurization system will be modified to provide a preshaping cycle with a reduced flow rate from a low capacity gas supply. The new system is shown schematically on Figure 112 and the pressure flow characteristics on Figure 113.
3. Additional test thermocouples will be added to the airlock exterior surface which will more accurately establish the expandable structure temperature during deployment tests.
4. The deployment test will be repeated in the GAC vacuum chamber with the airlock cooled to -20° F.

**D-21 AIRLOCK
MODIFIED INFLATION & PRESSURIZATION SYSTEM
SCHEMATIC**

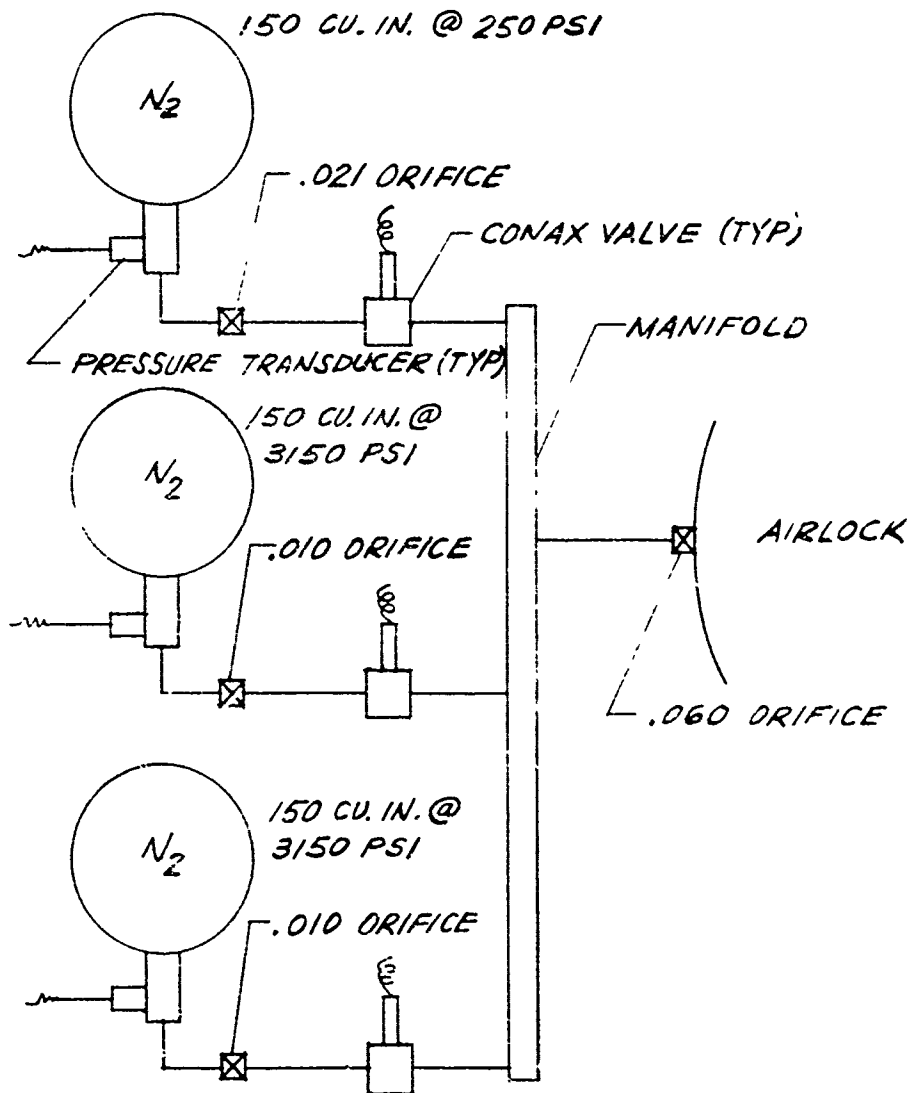
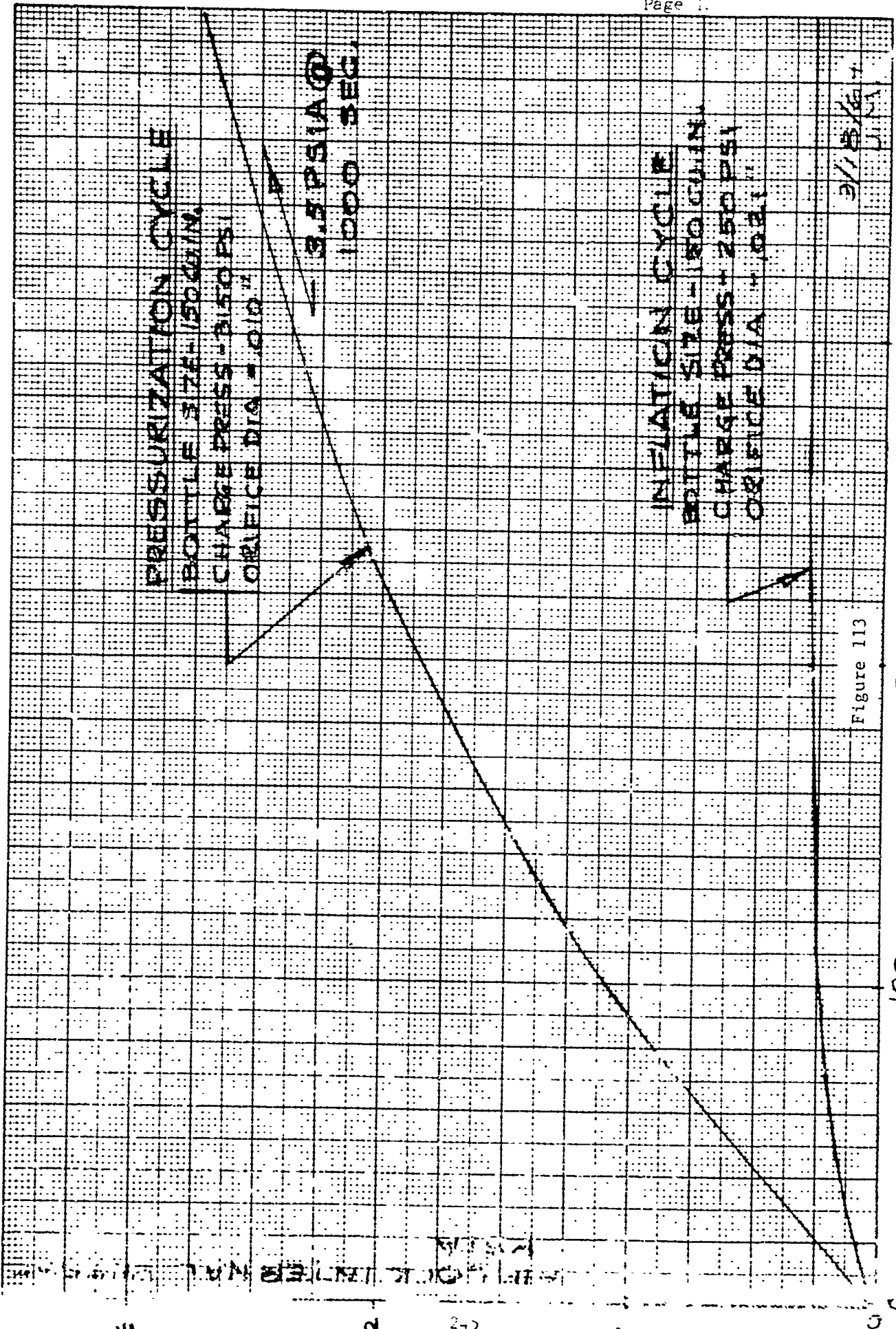


Figure 112



TIME AFTER START-SECONDS

100

200

300

400

ENGINEERING MEMORANDUM

1 January 1970
SP-7232

Subject: DO21 Airlock Vacuum Chamber Low Temperature
Deployment Test

Attachment: (a) Environmental Qualification Test Procedure
GER-13088 Rev. C, Page 63a dated September 1969

(b) DTI GA597-30 - Expandable Airlock Deployment Test
Plan dated 10 December 1969

PURPOSE

The purpose of the low temperature low pressure deployment test is to demonstrate satisfactory operation of the airlock deployment system under these conditions.

TEST PROCEDURE

The test procedure which was followed is defined in attachment (a). This procedure is essentially identical to that specified in attachment (b) except that the altitude during the test was 150,000 ft instead of 200,000 ft. It is considered that this slight difference in pressure is insignificant in this particular test.

TEST EQUIPMENT

The following test equipment was used to perform the test.

<u>Item</u>	<u>Model</u>	<u>Serial No.</u>
1. Digital Voltmeter	NLS MOD451	AF 80092
2. Power Supply	KEPCO-MOD SC 32-15A	GA38-710-479-7-1 S/N C30194
3. Igniter Circuit Test	ALINCO MOD 101-5BFC	GFE 15
4. Manometer	MERIAM MOD A203	L1157 S/N 56751
5. OSC Power Supply	CEC Type 2-1054	N003598 S/N 14042
6. Carrier Amp	CEC Type 1-113B	L35-1085 S/N 22137

<u>Item</u>	<u>Model</u>	SP-7232 <u>Serial No.</u>
7. Carrier Amp	CEC Type 1-113B	435-1084 S/N 134B610
8. Recorder	Azar LN 69809	L-5478 S/N B-64-48342-1-1
9. Recorder	Azar LN 69809	G1306 S/N A-60-4849-5
10. Recorder	Azar LN 69809	G1384 S/N B-64-58602-1-1
11. Recorder	Honeywell MOD 15305846-24-02-1 -000-015-10-168	S/N X5-R 12150
12. Pressure Transducer	KP-15	20443
13. 16 MM Motion Picture Camera		
14. American Research Test Chamber (-100°F to +400°F Temp Range, Atmospheric to 250,000 Ft. Alt.)		

TEST SETUP

The test setup and instrumentation are shown schematically in Figures 114 and 115. Figure 113 shows the location of the airlock integral temperature sensors which were read out on the digital voltmeter.

TEST SEQUENCE

The airlock unit was installed in the vacuum chamber and the instrumentation checked out by 4:30 PM on December 11, 1969. The chamber was set for -10°F and left for an overnight temperature soak. At 6:15 AM on December 12, 1969, the chamber was set to -25°F and by 10:00 AM the temperatures were in the range of -15°F to -25°F. The chamber was then pumped down. The initial deployment attempt was aborted when the restraint harness did not respond by falling away as expected after release of the retaining mechanism. During repressurization of the chamber, the struts did fall away without any other disturbance. Investigation of the harness release hardware did not disclose

TEST SEQUENCE (Continued)

any defects in the parts, so it was theorized that the straps did not have any residual tension due to lack of resilience in the airlock at the low temperature condition. However, as a precautionary measure the retaining collar clearance was increased by .005 in. to eliminate any possibility of a hangup due to foreign particle binding. (This design change has been released effective on all units.)

By 2:40 PM the collar had been reworked and the temperatures again stabilized to -20°F. By 3:15 PM, the chamber had been pumped down to .02 psia, and the deployment was successfully accomplished. Movies of the sequence were taken through the chamber viewing port.

The airlock was subsequently inspected and found to be in satisfactory condition.

TEST DATA

The airlock internal pressure time history is plotted on Figure 117. A sequence of photographs shows the airlock in various states of deployment on this same plot.

Figure 118 shows the preshaping pressurization bottle pressure versus time.

Figure 119 records the external thermocouple time history during deployment.

The data taken from the integral airlock thermistors located as shown on Figure 116 is listed below.

Four of these are on the outside surface of the airlock and two on the inside surface. When the unit is packaged, these are folded well into the interior of the expandable structure.

INTERNAL TEMPERATURES AT TIME OF DEPLOYMENT

<u>Location</u>	<u>°F</u>
T-1	-5
T-2	-7
T-3	-11
T-4	-10
T-5	+20
T-6	+20

PREPARED BY <i>R. J. Seidels D/ACC</i>	GOODYEAR AEROSPACE CORPORATION	DTI NO. <i>GA597-30</i>
CHECKED BY <i>[Signature]</i>		TYPE _____
APPROVED BY <i>[Signature]</i>	DEVELOPMENTAL TEST INSTRUCTIONS	DATE <i>10 December 1969</i>
DATE REVISED _____		

EXPANDABLE AIRLOCK DEPLOYMENT TEST PLAN

The purpose of the expandable airlock deployment test is to demonstrate deployment sequence of the unit at low temperature (-20 to -25°F) and low pressure (150,000 ft.). The test unit will be the Crew Training Unit (Serial No. 1)

CAUTION: Test unit must be handled with white gloves.

During the test the following data is to be recorded:

A. Temperatures

1. 6 existing thermistors on unit
- *2. 3 outside of thermal blanket
- *3. 3 inside of thermal blanket on airlock outer cover
4. 1 on hatch
5. 1 on base structure
6. 1 on battery

* Locate in pairs, one inside, one outside

B. Pressures

1. Chamber pressure
2. Airlock internal pressure transducer
3. Bottle pressure transducer
4. Airlock internal pressure (some means other than unit transducer)

C. Motion Pictures - Wide angle lens is required Camera speed to be 64 fps

The low pressure bottle is to contain an 0.021 inch orifice and is to be charged to 250 psi.

The unit is to be cold soaked at -25° F until all thermocouples generally reach -20° F, at which time pumpdown will commence. During the cold soak the battery heaters will be off. Prior to pump-down the battery heaters will be turned "ON" and left on for the remainder of the test.

13.0 LOW PRESSURE AND LOW TEMPERATURE DEPLOYMENT

13.1 Purpose

The purpose of the low pressure and low temperature deployment test is to demonstrate satisfactory operation of the deployment mechanism under these conditions.

13.2 Test Equipment

The following equipment or equivalent will be used for the performance of the deployment test:

- (1) American Research Test Chamber

Temperature Range	-100° F to +400° F
Pressure	Atmospheric to 250,000 ft.
Relative Humidity	20 to 95%
Calibration Period	3 months
- (2) Two (2) Azar strip chart recorders

Calibration Period	3 months
--------------------	----------
- (3) Two (2) Brown Multi-Channel Temperature recorders

Calibration Period	3 months
--------------------	----------
- (4) One (1) 16 mm motion picture camera

13.3 Test Setup and Procedure

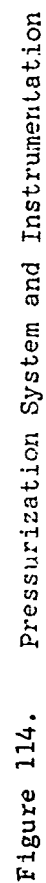
The expandable airlock will be instrumented with approximately sixteen thermocouples on the expandable structure and the thermal blanket. The unit will then be packaged and placed in the American Research test chamber. The NASA Airlock Simulator (checkout set) will be connected to the airlock with the output of the two low pressure transducers being recorded on two Azar strip chart recorders. The thermocouples will be connected to the Brown multi-channel temperature recorders.

The temperature in the test chamber will be reduced to -20° F and allowed to stabilize. After stabilization of the temperature has occurred the pressure in the chamber will be reduced to 200,000 feet. During pumpdown the electrical vent valve will be open.

When 200,000-foot altitude is reached the vent valve will be closed. The recorders and the motion picture camera, setup to record the deployment sequence, will be started. The restraint straps will then be released. After release of the restraint straps, the deployment pressure bottle squib will be fired.

13.4 Acceptance Criteria

Upon completion of the deployment test, the airlock must not show any indications of deterioration of materials or construction.



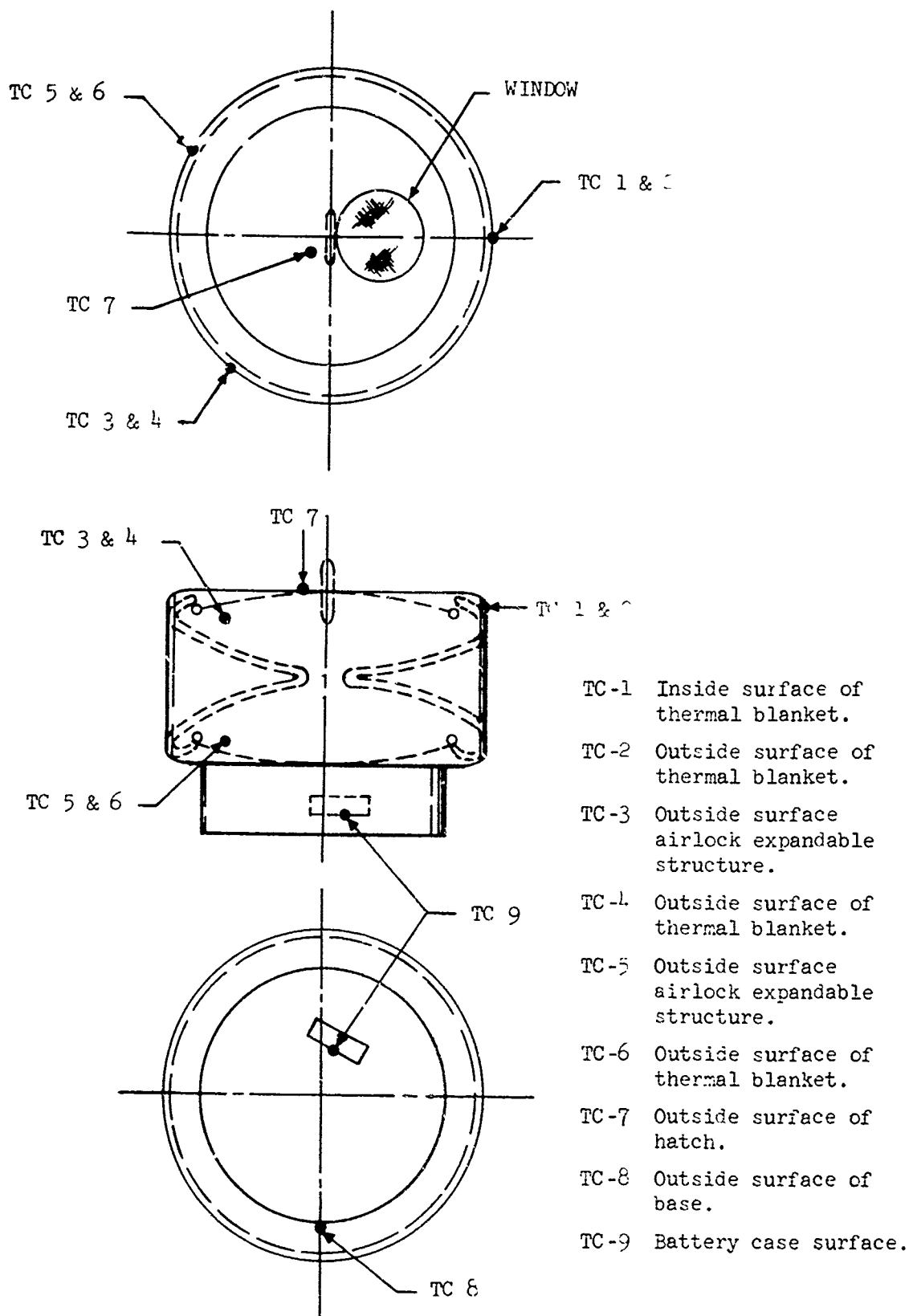


Figure 115. Thermocouple Location - Special Test Thermocouples

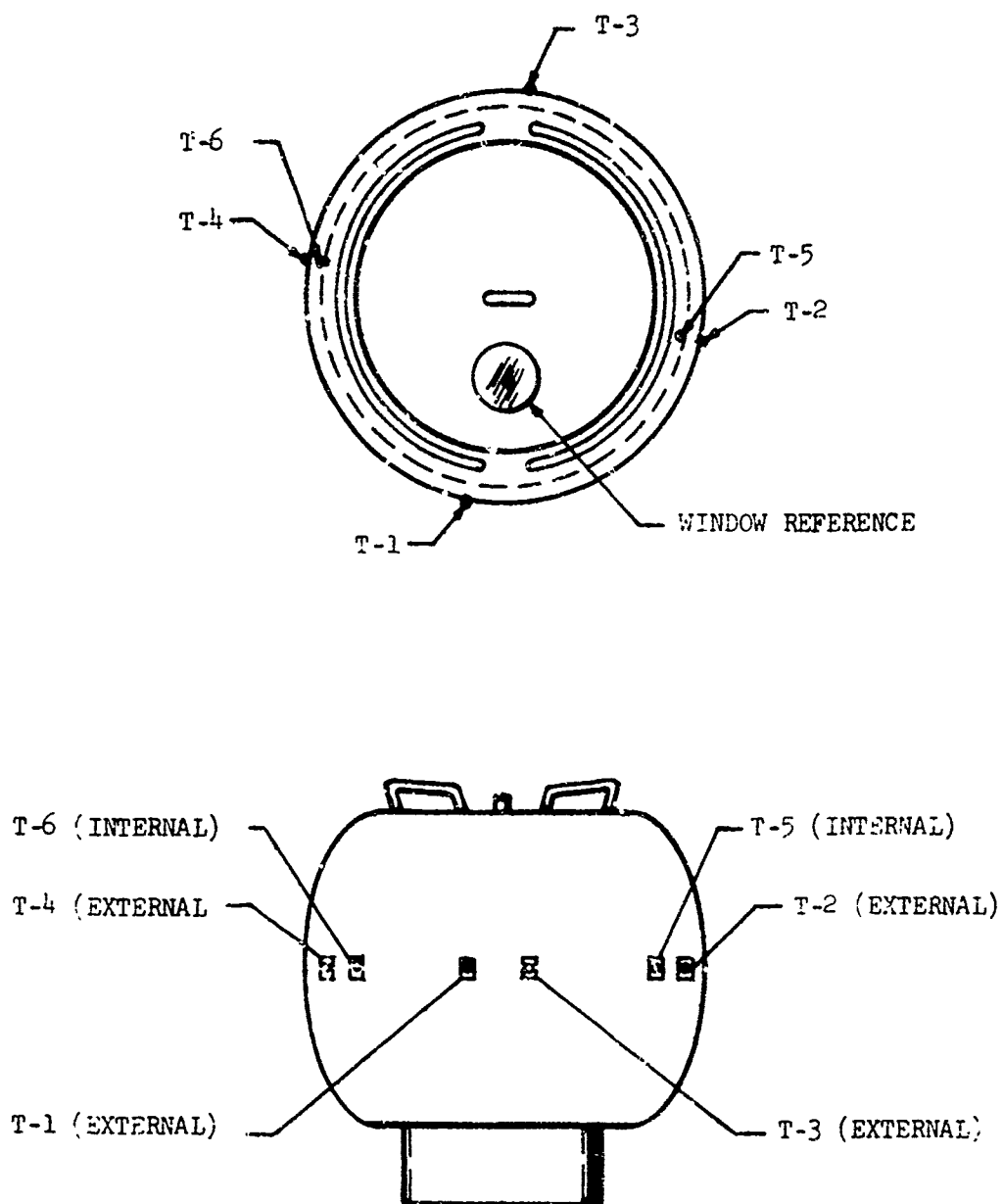


Figure 116. Airlock Integral Temperature Sensors

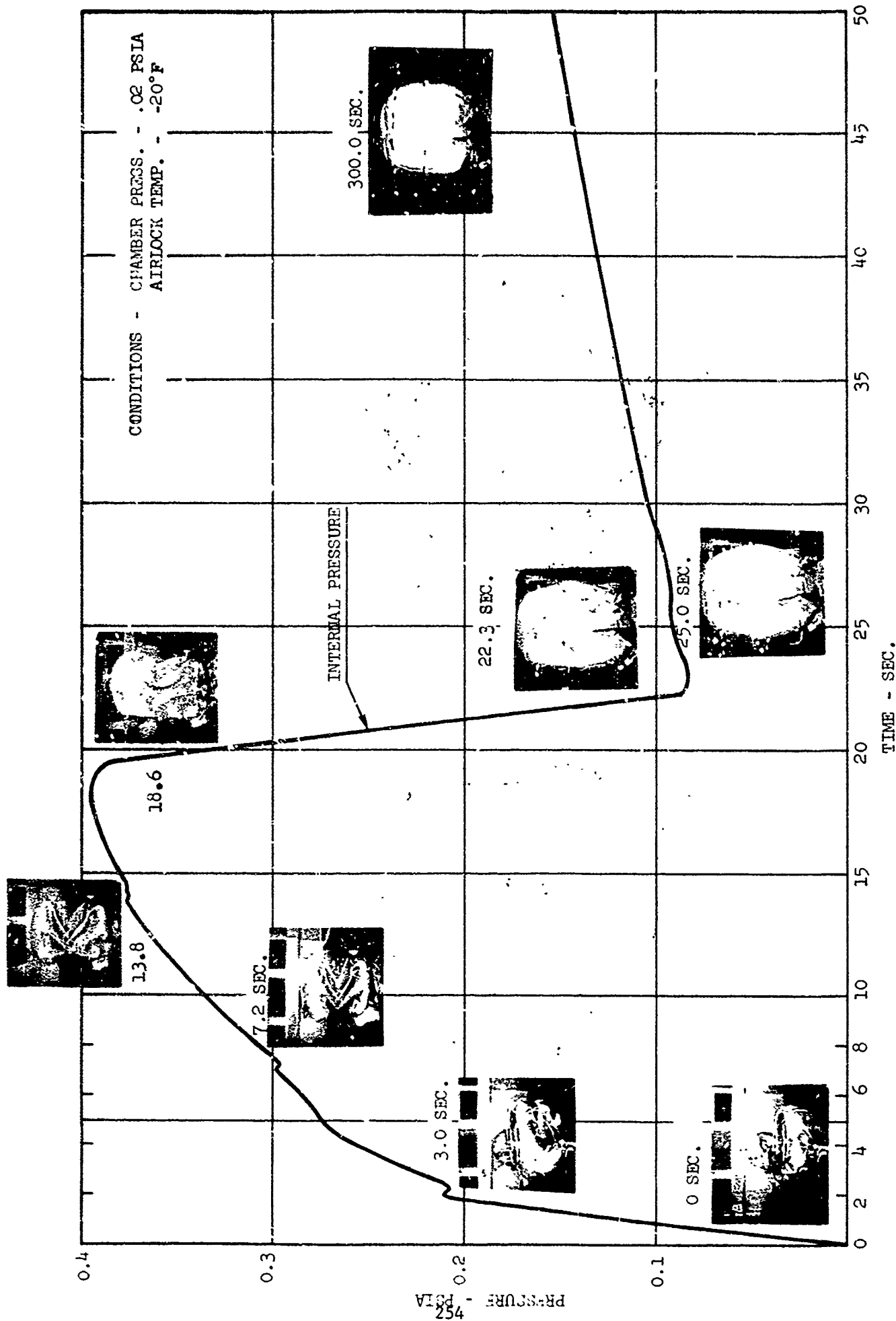


Figure 117. D021 Airlock Deployment

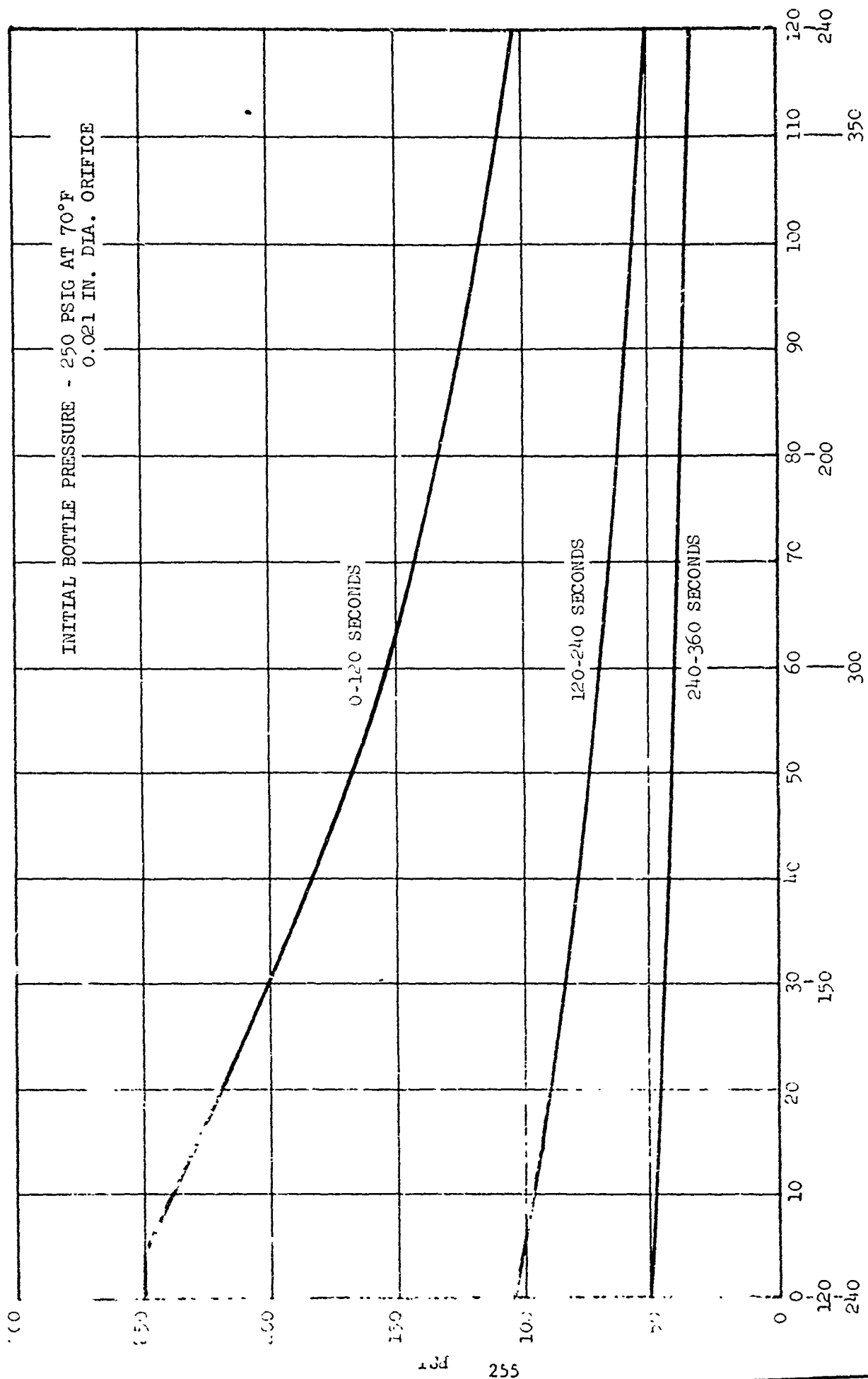


Figure 118. Low Temperature Vacuum Chamber Deployment -
Internal Pressure of Preshaping Bottle

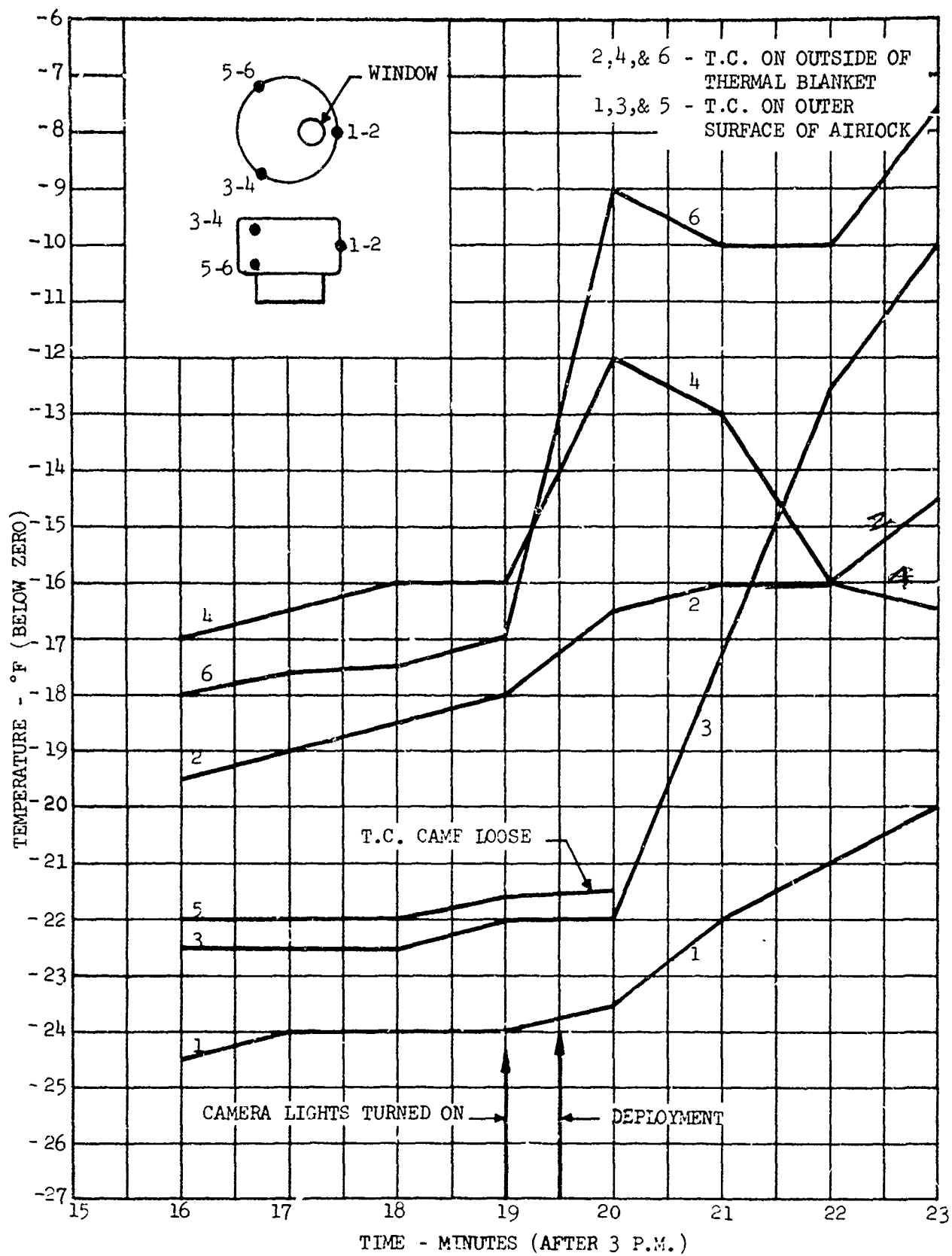


Figure 119. D-21 Airlock Low Temperature Vacuum Chamber Deployment

APPENDIX XII

DO21/DO24 VIBRATION TEST REQUIREMENTS

GOODYEAR AEROSPACE

CORPORATION

AKRON, OHIO 44315

18 September 1970

In Reply Please Refer
To: SP-7534 ✓

Mr. E. O. Walker PM-SL-DP
National Aeronautics & Space Administration
George C. Marshall Space Flight Center
Huntsville, Alabama 35812

Subject: DO21/DO24 Vibration Test Requirements

Enclosure: (A) McDonnell-Douglas Astronautics Company
Preliminary Interface Revision Notice (PIRN)-
ED-02 to ICD13:12011 dated 2 September 1970
(Pages 5 and 6 only) - 3 copies

(B) SM-9780, GAC Stress Department Memo
dated September 11, 1970 - 3 copies

Reference: (a) GER-13088, Rev. D -DO21 Environmental Qualification
Test Procedure, dated March 1970

(b) GER-14845 - DO21/DO24 Environmental Qualification
Test Spec. for Material Samples

(c) GER-14830 - DO21/DO24 Environmental Qualification
Test Procedure for Material Samples

Dear Mr. Walker:

The vibration environments defined by MDAC in Enclosure (A) PIRN were compared with the actual DO21 vibration Qualification Test as performed per Reference (a) and also with the vibration spectrum as defined in Reference (b) for the DO21/DO24 Material Samples and Material Return Container. Enclosure (B) presents an evaluation of the severity of these vibration environments as imposed on the structural characteristics of both the DO21 and DO24 experiments.

This analysis indicates that the vibration test as defined in Reference (b) and successfully performed at AEDC on the DO21 Airlock Qualification Test Unit is considered to indicate adequate structural integrity of the airlock experiment to also withstand the Enclosure (A) vibration spectrum.

Page 2
SP-7534

The analysis shows similar results for the D024 experiment, but this test has not been performed pending availability of test hardware. Therefore, References (b) and (c) will be revised to incorporate the new data and the testing conducted accordingly.

The enclosed data are forwarded to the NASA Skylab Program Office for review and substantiation of GAC's opinion that the vibration test already performed on the Qualification Test Unit need not be repeated to the new values specified on Page 5 of Enclosure (A).

Very truly yours,

GOODYEAR AEROSPACE CORPORATION


L. Manning

LM/emg

cc: F. W. Forbes - With Enclosures

PRELIMINARY
INTERFERENCE REVISION NOTICE CONTINUATION SHEET

LEV	AFFECTED ICD	REV	IRN NO.	IRN REV.	SHEET
B	13M12011				5 OF 6

DESCRIPTION:

HOW CONDITION (Page 12)

Figure 3.2-1

VIBRATION AND SHOCK DESIGN ENVIRONMENT FOR HARDWARE MOUNTED ON THE AM TRUSS

Vehicle Dynamics Criteria

Flight Axis (3-40 Hz at 3 oct/min)

- 3 - 7 Hz at 0.52 inches double amplitude displacement
- 7 - 15 Hz at 1.3 g's peak
- 15 - 20 Hz at 0.11 inches double amplitude displacement
- 20 - 40 Hz at 2.3 g's peak

Lateral Axes (2-20 Hz at 3 oct/min)

- 2 - 10 Hz at 0.14 g's peak
- 10 - 20 Hz at 0.035 g's peak

High Level Random Criteria (1 min/axis)

- 20 Hz at 0.017 g²/Hz
- 20 - 60 Hz at +9 dB/oct
- 60 - 130 Hz at 0.45 g²/Hz
- 130 - 185 Hz at -9 dB/oct
- 185 - 800 Hz at 0.15 g²/Hz
- 800 - 2000 Hz at -9 dB/oct
- 2000 Hz at 0.010 g²/Hz

Composite = 14.0 gms

Low Level Random Criteria (4 min/axis)

- 20 Hz at 0.012 g²/Hz
- 20 - 60 Hz at +9 dB/oct
- 60 - 130 Hz at 0.34 g²/Hz
- 130 - 185 Hz at -9 dB/oct
- 185 - 800 Hz at 0.12 g²/Hz
- 800 - 2000 Hz at -9 dB/oct
- 2000 Hz at 0.0074 g²/Hz

Composite = 11.8 gms

Pyrotechnic Shock Spectrum

- 10 Hz at 4.7 g's peak
- 10 - 800 Hz at +3.0 dB/oct
- 800 - 3000 Hz at 1240 g's peak
- 3000 - 10000 Hz at -7.0 dB/oct
- 10000 Hz at 290 g's peak

INTERFA REVISION NOTICE CONTINUATION SHEET

LEV	AFFECTED ICD	REV	IRN NO	IRN REV.	SHEET
B	13M12011				6 OF 6

DESCRIPTION:

NEW CONDITION (Page 13)

Figure 3.2-2

VIBRATION AND SHOCK DESIGN ENVIRONMENT FOR HARDWARE MOUNTED ON THE DA TRUSS

Vehicle Dynamics Criteria

Flight Axis (3-50 Hz at 3 oct/min)

- 3 - 6.5 Hz at 0.50 inches double amplitude displacement
- 6.5 - 25 Hz at 1.1 g's peak
- 25 - 50 Hz at 2.8 g's peak

Lateral Axes (2-20 Hz at 3 oct/min)

- 2 - 10 Hz at 0.10 inches double amplitude displacement
- 10 - 20 Hz at 0.035 g's peak

Lift-Off Random Vibration Criteria (1 min/axis)

- 20 - 35 Hz at 0.10 g^2/Hz
 - 35 - 100 Hz at -12 dB/oct
 - 100 - 850 Hz at 0.0022 g^2/Hz
 - 850 - 2000 Hz at -6 dB/oct
 - 2000 Hz at 0.00042 g^2/Hz
- Composite = 2.3 grms

Post Random Vibration Criteria (2 min/axis)

- 20 - 35 Hz at 0.036 g^2/Hz
 - 35 - 50 Hz at -12 dB/oct
 - 50 - 1000 Hz at 0.01 g^2/Hz
 - 1000 - 2000 Hz at -6 dB/oct
 - 2000 Hz at 0.0025 g^2/Hz
- Composite = 3.9 grms

Pyrotechnic Shock Criteria

- 10 Hz at 0.7 g's peak
- 10 - 1000 Hz at +7.7 dB/oct
- 1000 - 4000 Hz at 24.0 g's peak
- 4000 - 10000 Hz at -7.0 dB/oct
- 10000 Hz at 84 g's peak

MEMORANDUM

September 11, 1970
SM 9780

To: L. Manning
Project Engineer of Airlock
Dept. 453G

From: J. E. Rice
Section Head Vibrations
Dept. 456G

Enclosure: Houmard's Analysis and PSD Requirements

Subject: Consequence of Change in Vibration Qualification
Levels for Airlock and/or Samples

The new requirements should not require retesting of the airlock or samples. This conclusion is based on the following facts:

The random specifications were compared and the new requirements are superposed in broken lines on the old requirements. From Figure 120, it can be seen that the input for the 6 x 6 inch samples is increased from 60 to 120 Hz, but is reduced markedly from 180 to 900 Hz. These small samples will not be affected by the low frequency change but will receive a significantly smaller input at the high end. The overall g rms is reduced from 21 to 14 and most of this is due to reduction in input from 180-900 Hz. The consequence of the change is to reduce the response of the samples.

The changes in the sine wave input for the samples increases the input from 1 g to 2.3 g's in the frequency range from 15-40 Hz but the new requirement cuts off at 40 Hz. Since the sample natural frequencies are probably higher than 40 Hz, the small increase in g level is insignificant.

For the deployment assembly the changes in random vibration requirements are shown on Figure 121. In addition to the new requirement shown in broken lines, a series of vertical lines will be noted at various frequencies. These are the values of the natural frequencies of the D021 components such as the battery box and pressure bottles. The associated Q's are also included. These numbers were obtained from test records of the 1 g tests at the Arnold test facility.

The random levels of the new requirement are significantly less than the random levels already experienced at Arnold.

September 11, 1970
SM 9780

The new sine-wave requirements increase from 1 g to 2.8 g's from 25 to 50 Hz along the flight axis. The battery box has natural frequencies at 34 Hz with a $Q = 12$ and at 41 Hz with a $Q = 12$. The response levels of the battery box along the flight axis will be $(2.8)(12) = 33.6$ g's if the Q does not change; however, almost without exception the Q level will reduce as the g level increases with objects mounted as the battery box is mounted.

For conservatism it will be assumed that the Q level will not be reduced so an output of 33.6 g's will be maintained.

A stress analysis was performed using an input of 54 g's which represented the 3 sigma value from random noise plus 6 g's of acceleration.

Even with an input of 54 g's there is a safety factor of 50 percent based on critical buckling so an input of 33.6 g's is not a problem.

The stress analysis is enclosed.

J. E. Rice
Vibration & Acoustics
Structural Analysis Department

JER/mw

--- ORIGINAL LIFT- F RANDOM VIBRATION CRITERIA 'A' (1 MIN/AXIS)

- 20 - 20 HZ @ $0.060 \text{ g}^2/\text{HZ}$
- 20 - 150 HZ @ $+3 \text{ dB/oct}$
- 150 - 360 HZ @ $0.45 \text{ g}^2/\text{HZ}$ COMPOSITE = 16.1 Grms
- 360 - 2000 HZ @ -6 dB/oct
- 2000 HZ @ $0.015 \text{ g}^2/\text{HZ}$

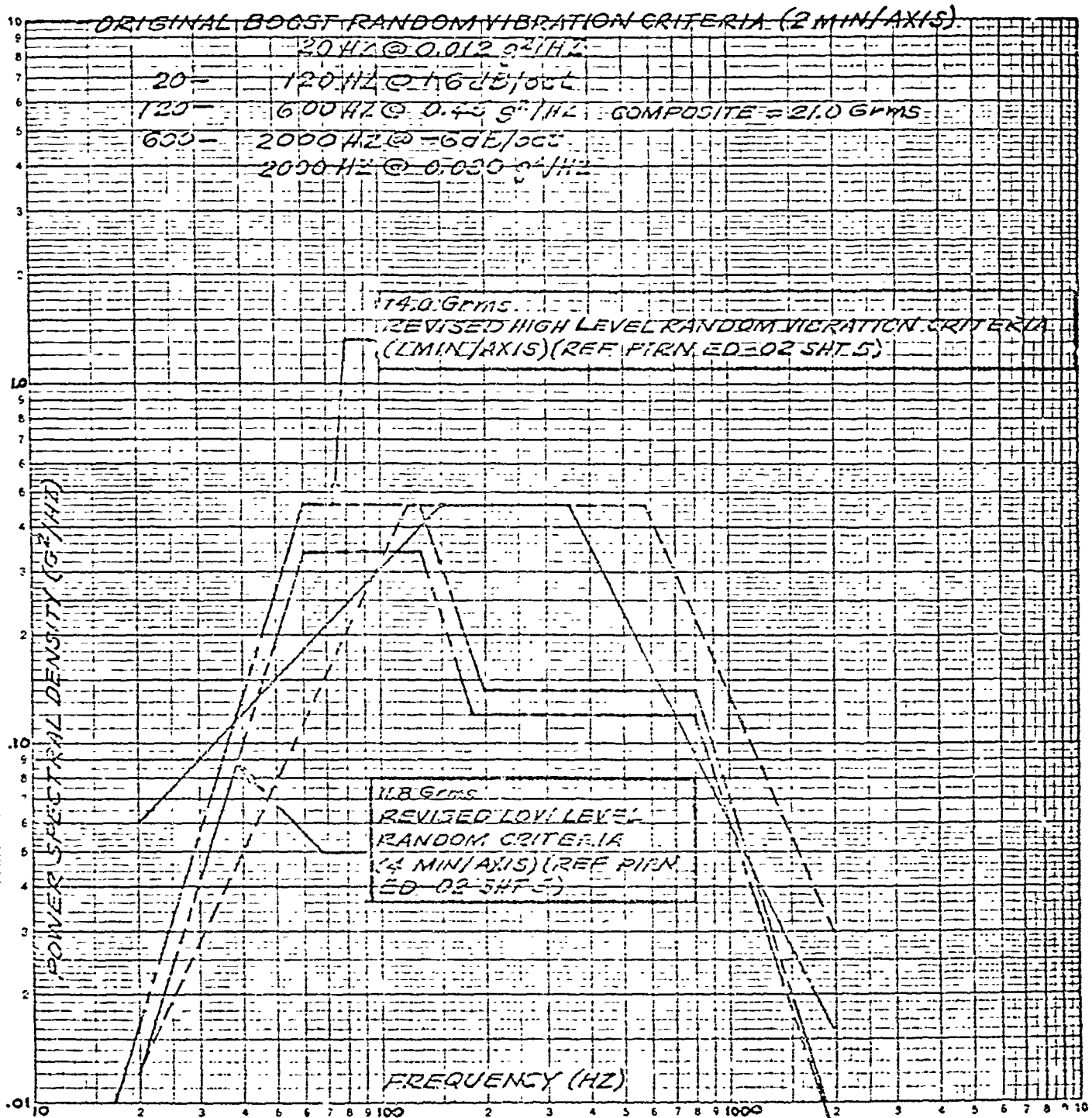


FIGURE 120- MATERIALS SAMPLES & RETURN CONTAINER
VIBRATION TEST CRITERIA

PSD REQUIREMENTS

Enclosure to SM9780

--- ORIGINAL LIFT-OFF RANDOM VIBRATION CRI. RIA (1 MIN/AXIS)

- 20HZ @ 0.060 g²/HZ
- 20 - 33HZ @ +3dB/oct
- 33 - 360HZ @ 0.10 g²/HZ
- 360 - 2000HZ @ -6dB/oct
- 2000HZ @ 0.0034 g²/HZ
- COMPOSITE = 7.9 Grms

--- ORIGINAL BOOST RANDOM VIBRATION CRITERIA (2 MIN/AXIS)

- 20HZ @ 0.012 g²/HZ
- 20 - 57HZ @ +6dB/oct
- 57 - 600HZ @ 0.10 g²/HZ
- 600 - 2000HZ @ -6dB/oct
- 2000HZ @ 0.0059 g²/HZ
- COMPOSITE = 10.1 Grms

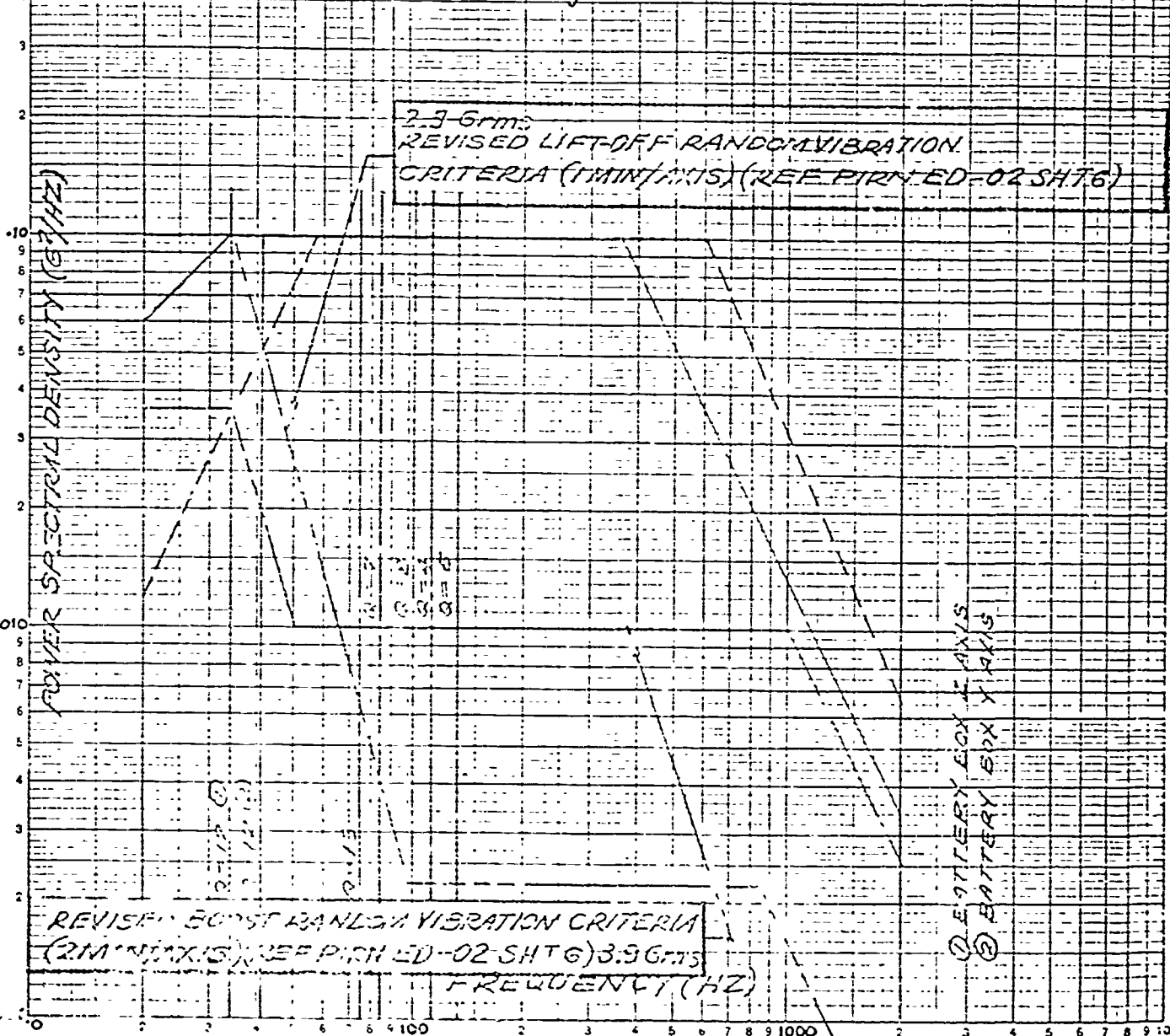


FIGURE 21-AIRLOCK EXPERIMENT VIBRATION PROFILE

D-021 Airlock

STRESS ANALYSIS OF BATTERY BOX SUPPORT CHANNELS

TOTAL BOX WT. $\sim W_b = 8^{\#}$
LD. FACTORS:
 $n_x = 126$
 $n_y = 48$
 $n_z = 40$
VIBRATION 6
ACCELERATION 4

[MAT'L \sim 2024-T3 ALCLAD

$F_{tu} = 59 \text{ ksi}$

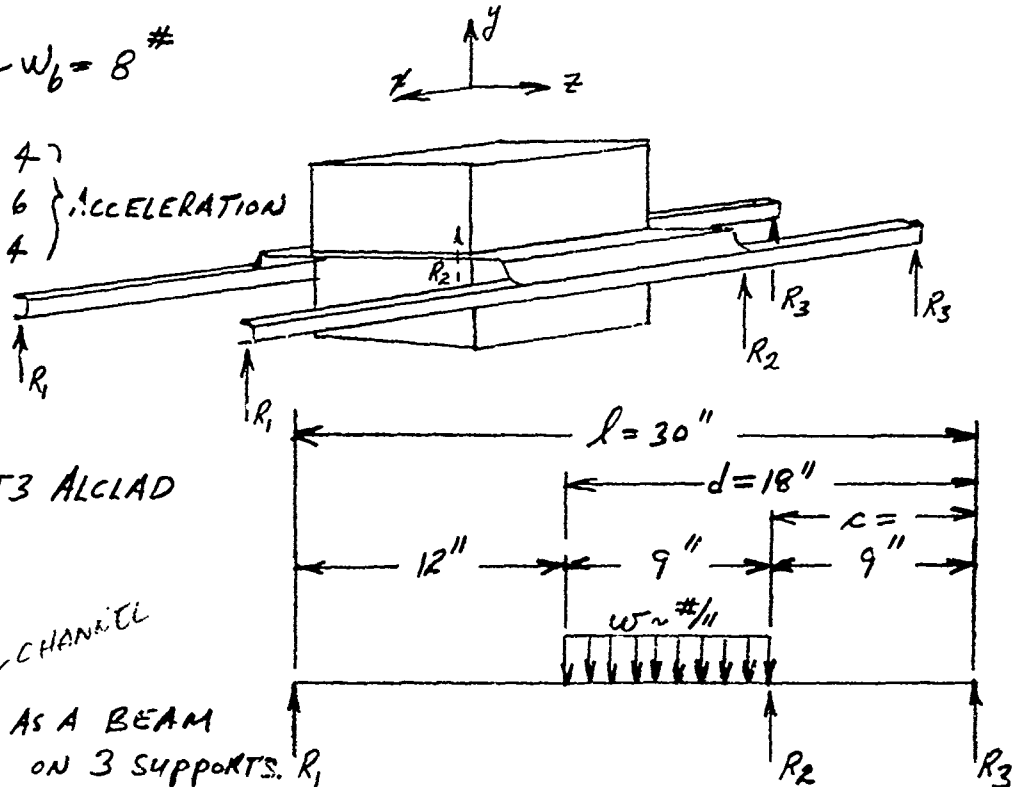
$F_{ty} = 39 \text{ ksi}$

$F_{su} = 38 \text{ ksi}$

CHANNEL

CONSIDER EACH [AS A BEAM

LOADED AS SHOWN ON 3 SUPPORTS. R_1



FIXED END MOMENT AT THE 2nd SUPPORT: *

$$M_{F2} = \frac{w}{2l^2} \left[\frac{l^2(d^2 - c^2)}{2} - \frac{d^4 - c^4}{4} \right] = \frac{w}{1800} \left[(450)(243) - \frac{1}{4}(104976 - 6561) \right]$$

$$= 47w$$

FOR SIMPLE SUPPORTS AT R_1 & R_3 , THE MOMENT OVER THE 2nd SUPPORT IS,

$$M_2 = \left(1 - \frac{c}{l}\right) M_{F2} = \left(1 - \frac{9}{30}\right) 47w = 32.9w$$

$$\text{Now, } w = \frac{n_y W_b}{2(d-c)} = \frac{(48+6)(8)}{2(9)} = 24^{\#/\text{ft}} \quad (\text{ON EACH [})$$

$$(d-c)w = 216^{\#}$$

$$\therefore M_2 = (32.9)(24) = 789.6^{\text{in}\cdot\text{lb}}$$

* TIMOSHENKO, S., "ELEMENTS OF STRENGTH OF MATERIALS", 1940

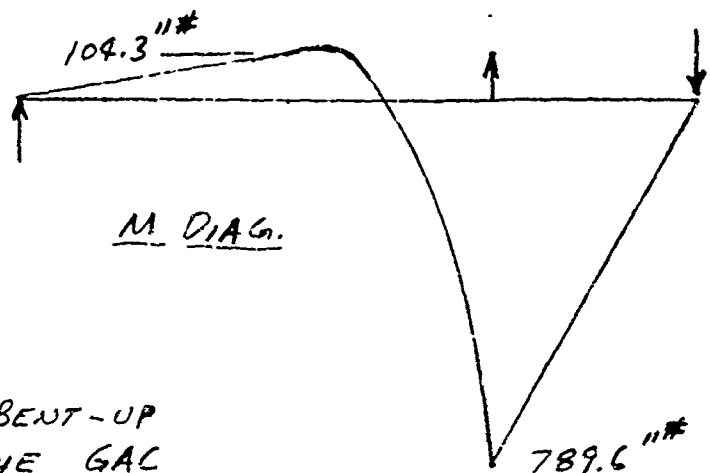
$$R_1 = \frac{(4.5)(216) - 789.6}{21} = \underline{8.69}^{\#} \quad R_3 = -\frac{789.6}{9} = \underline{-87.73}^{\#}$$

$$R_2 = \frac{1}{21} [(12+4.5)(216) + (30)(87.73)] = \frac{3564 + 2632}{21} = \underline{295.0}^{\#}$$

CHECK: $\Sigma R = 216$,

$$\begin{array}{r} 295 \\ + 8.69 \\ \hline 303.69 \\ - 87.73 \\ \hline 215.96 \approx 216 \quad \checkmark \end{array}$$

$$M_{MAX} = M_2 = \underline{789.6}^{\#}$$



STRESS & BUCKLING CHECKS:

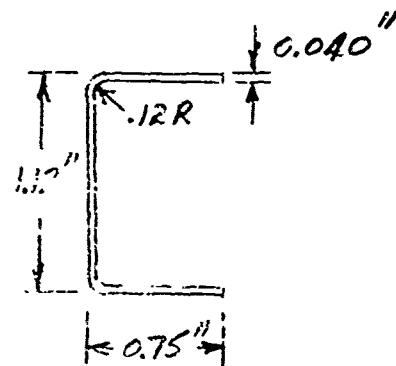
SECTION PROPERTIES OF THE BENT-UP CHANNEL PER PG. 5.6013 OF THE GAL STRUCTURES MANUAL:

$$I/C = \underline{0.040}^{\#3}$$

$$f_b = \pm \frac{Mc}{I} = \pm \frac{789.6}{0.04} = \underline{\pm 19,740}^{\#/\#^2}$$

$$\therefore \frac{F_{tu}}{F_b} = \frac{57}{19740} = \underline{3\%}$$

$$\frac{F_{tu}}{F_b} = \frac{39}{19740} = \underline{2\%}$$



THE CRITICAL LOCAL BUCKLING STRESS IS GIVEN
PER, BRUHN, E.F., "ANALYSIS AND DESIGN OF FLIGHT VEHICLE
STRUCTURES," 1965 - pg. C6.3.

$$\sigma_{CR} = \frac{k_w \pi^2 E}{12(1-\mu^2)} \left(\frac{t_w}{b_w} \right)^2$$

where, from FIG. C6.4 of this reference, $k_w = 1.9$
for, $b_f/b_w = \frac{0.75-0.02}{1.12-0.04} = 0.676$

for Aluminum, $E = 10.7 \times 10^6$ psi
 $\mu = 0.33$; $1-\mu^2 = 0.8911$

$$\therefore \sigma_{CR} = \frac{1.9 \pi^2 10.7 \times 10^6}{12 \times 0.8911} \left(\frac{0.04}{1.12-0.04} \right)^2 = \underline{25750} \text{ #/in}^2$$

$$\therefore \frac{\sigma_{CR}}{f_b} = \frac{25.75}{19.74} = \underline{1.3}$$

J. P. Hernandez 0/456
SEPT. 11, 1970

REFERENCES

1. NASA Specification - RS003M00003 - Performance and Design Integration Requirements for the Cluster System/Apollo Applications Program - General Requirements for
2. NASA Specification 50M02442 dated 1 March 1971, ATM Material Control for Contamination Due to Outgassing.
3. CD-13M12011 - Airlock Module to D021 Expandable Airlock Technology Experiment Mechanical Interface Control Document
4. Goodyear Engineering Report - GER-11676 S/24 - Development of Materials and Materials Application Concepts for Joint Use as Cryogenic Insulation and Micrometeorite Bumpers - dated 30 June 1960.
5. NASA Specification MSC-A-D-66-3 Rev. A, dated 5 June 1967, Procedures and Requirements for the Evaluation of Spacecraft Nonmetallic Materials
6. Air Force Test Report - AEDC-TR-69-14 - Simulated Micrometeoroid Impact Testing on a Composite Expandable Structure for Spacecraft Airlock Application, William H. Corden, April 1969
7. Goodyear Engineering Report - GER-13124-21 - D021 Expandable Airlock Experiment Quarterly Progress Report No. 7 Dated 1 January 1969
8. Air Force Test Report - AEDC-TR-70-262 - Expandable Airlock Environmental Tests, B. A. Busch, December 1970